Synthesis and Characterization of Mussel Adhesive Peptides

Dissertation
zur Erlangung des Doktorgrades
der Naturwissenschaften
(Dr.rer.nat)

dem
Fachbereich Chemie
der Philipps-Universität Marburg
vorgelegt von

Manjeet Vinayakrao Deshmukh

aus Nanded (Indien)

Marburg (Lahn) 2005

vom Fachbereich Chemie
der Philipps-Universität Marburg als Dissertation
am 10/05/2005 angenommen

Erstgutachter: Prof. Dr. Armin Geyer
Zweitgutachter: Prof. Dr. Thomas Schrader

Tag der Disputation: 19/05/2005

dedicated to my parents.....

गुणसुमनें मी वेचीयली या भावें ।
कीं तिने सुगंधा घ्यावें ।।
जरि उद्धरणी व्यय न तिच्या हो साचा ।
हा व्यर्थ भार विद्येचा ।।
स्वा. वि. दा. सावरकर

I have picked flowers of virtues
for her to fragrance
I have gained this knowledge
for her to flourish

- Veer Vinayak Damodar Savarkar
(in his poem addressed to mother India).

Acknowledgements

This research work was carried out at Department of chemistry, Universität Regensburg, Germany from Nov'2002 to Mar'2004 and at Department of Chemistry, Phillips Universität Marburg, Germany, from Apr'2004 until Apr'2005, under the supervision of Prof. Dr. Armin Geyer.

I am grateful to Prof. Dr. Armin Geyer for his support, earnest guidance, cordial nature, and parental care. His innovative ideas and guidance made me appreciate his inborn capabilities as a leading international scientist and a teacher. Because of his jovial and friendly nature, my association with him is a great endeavor.

I am also indebted to my group members for their constant help and support with academic, personal, and administrative problems. Only due to their helping hands, I am able to finish my work nicely. They maintained friendly atmosphere in the lab and we have together spent happy time. My greatest memento is their friendship, as I have enjoyed my stay in Germany thoroughly just because of their support.

I am thankful to Rolf Hörger for valuable discussions, constant help regarding administrative and personal problems.

I thank to Markus Pfitzenmaier for discussions on different NMR and chemical problems and I am also thankful to him for hot coffee breaks with equally hot discussions about girls.

I appreciate Dominik Kohr for his continuous help, valuable discussions, and suggestions regarding analytical part.

I am thankful to Harald Seger for discussions about chemistry and for many late evening rides back home.

I thank Ralph Wieneke for the help regarding practical students and protocols.

I also express my gratitude to Dr. Frank Noll for numerous discussions, critical remarks, and valuable advice on the AFM measurement and analysis.

I express my thanks to Susanne Schellenberg for her help to tackle administration problems in easy and quick ways and to Michael Marsch for his help regarding computers in an efficient way.

In addition, my thanks to Katja Kräling for her help for solid phase peptide synthesis reactions and to Cordula Braun, Sonja Eckhardt, Mariam Lauz, and Steffen Loh for the friendly atmosphere.

As well, I remember Dr. Karoly Agoston, Dr. Daniela Fischer, and Dr. Peter Tremmel for valuable discussions, recommendations, and suggestions.

My sincere appreciation for my association with Dr. H. B. Borate, Dr. P. R. Rajamohanan, and Latha Shivdasan (all from NCL, Pune, India) for their help, encouragement and support during my early scientific phase.

The biggest support came from my parents (Sharayu and Vinayak Deshmukh). I am greatly indebted to them. Also thanks to my brother (Dr. Mandar Deshmukh) and my sister-in-law (Mrunal Deshmukh). They were my first mentors and without all their help in many difficult situations, I would have not been able to accomplish this thesis.

Marburg, April 2005 Manjeet V. Deshmukh

Contents

ACKNOWLEDGEMENTS V
CONTENTS VII
ABSTRACT XV
ZUSAMMENFASSUNG XVII
ABBREVIATIONS XIX

1. PREAMBLE 1

2. INTRODUCTION 4

2.1. Peptides and Proteins 4

2.2. Nonprotein Amino Acids 6

2.3. Strategies for Peptide Synthesis 7

2.4. Structural Elements of Proteins and Peptides 10
2.4.1. Helices 12
2.4.2. β-Strands and Sheets 13
2.4.3. Turns 15
2.4.4. Structural Motifs 16

3. MUSSEL ADHESIVE PROTEINS 18

3.1. Byssus Adhesive Plaque 18

3.2. *Mytilus Edulis* Adhesive Proteins 21
3.2.1. *Mytilus Edulis* Adhesive Proteins -1 (*mefp*-1) 21
3.2.2. Possible Applications of *mefp*-1 26
3.2.3. *Mytilus Edulis* Adhesive Protein-2 (*mefp*-2) 27
3.2.4. *Mytilus Edulis* Adhesive Protein-3 (*mefp*-3) 27
3.2.5. *Mytilus Edulis* Adhesive Protein-4 (*mefp*-4) 29
3.2.6. *Mytilus Edulis* Adhesive Protein-5 (*mefp*-5) 29

3.3. Role of DOPA in Mussel Adhesive Proteins 30

3.4. Availability of *Mytilus Edulis* Adhesive Proteins - 1 to 5 34

3.5. Dipeptide Building Blocks 35
3.5.1. 7-thiaindolizidiene Amino Acid and Bicyclic Thiaindolizidiene 36
3.5.2. Epimerization of Thiazabicycloalkane Amino Acids 38
3.5.3. Iminium Ion Cyclization 39

3.6. Polymerization of Amino Acids 42

3.7. Synthetic Polymers 43

4. ADHESIVE PEPTIDES AND COPOLYMERS: SYNTHESIS 47

4.1. Synthesis of Dipeptide Building Blocks 47
4.1.1. Boc-and Fmoc-protected dipeptide building blocks 48
4.1.2. Saponification Reaction 52

4.2. Synthesis of Peptides in Solution 54
4.2.1. Synthesis of Tetrapeptide 54
4.2.2. Synthesis of Tetrapeptide (Lys-Bic-Tyr) 55
4.2.3. Synthesis of Tetrapeptide (DOPA-Bic-Tyr) 56
4.2.4. Synthesis of Tetrapeptide (Boc-Bic-DOPA-Tyr-OMe) 57
4.2.5. Synthesis of Tetrapeptide (Lys-DOPA-Tyr) 58
4.2.6. Synthesis of Dipeptide (Lys(2-Cl-Z)-Tyr) 59

4.3. Oligomerization reactions 59
4.3.1. Poly Amino Acids: Synthetic Methods, Isolation and Purification 60
4.3.2. Oligomerization of Dipeptide Building Blocks 63
4.3.3. Oligomerization of L-Tyrosine 67
4.3.4. Oligomerization of L-DOPA 68
4.3.5. Oligomerization of L-Lysine 70

4.4. Copolymerization Reaction 72
4.4.1. Copolymerization of Tripeptide (Bic-Tyr) 74
4.4.2. Copolymerization of Dipeptide (Lys(2-Cl-Z)-Tyr) 76
4.4.3. Copolymerization of (Lys(Z)-Bic-Tyr) 77

5. ADHESIVE PEPTIDES AND COPOLYMERS: CHARACTERIZATION 79

5.1. Structural Characterization and Molecular Size of Synthesized Peptides 80

5.1.1. Compound **6** (Fmoc-Bic-COOMe) 80
5.1.2. Compound **7** (NH_2-Bic-COOH) 81
5.1.3. Compound **9** (Fmoc-Bic-COOH) 83
5.1.4. Compound **16** (Lys-Bic-Tyr) 85
5.1.5. Compound **18** (NH_2-DOPA-Bic-Tyr-OMe) 86
5.1.6. Compound **23** (Lys-DOPA-Tyr-OMe) 87
5.1.7. Oligopeptides: poly-Tyr 89
5.1.8. Oligopeptides: poly-DOPA 89
5.1.9. Oligopeptides: poly-Lys(Z) 90
5.1.10. Oligopeptides: poly-Bic 92
5.1.11. Co-polymers: poly-Bic-Tyr 94
5.1.12. Co-polymers: poly-Lys(2-Cl-Z)-Tyr 96
5.1.13. Co-polymers: poly-Lys(Z)-Bic-Tyr 98
5.1.14. Co-polymers: poly-Lys-Bic-Tyr 100
5.1.15. Comparison of Molecular Weights of Compounds 101

5.2. Techniques Used for Testing Adhesive Properties 102
5.2.1. Diffusion Ordered Spectroscopy 102
5.2.2. Synthesis of Silicon Beads 103
5.2.3. Atomic Force Microscopy 103

5.3. Adhesiveness of Synthesized Peptides 105
5.3.1. DOSY of Lys-Bic-Tyr, Lys-DOPA-Tyr-OMe and DOPA-Bic-Tyr-OMe 105
5.3.2. DOSY of poly-Bic-Tyr 108
5.3.3. DOSY of poly-Lys(Z)-Bic-Tyr and poly-Lys-Bic-Tyr 110
5.3.4. AFM Studies of poly-Bic-Tyr 113
5.3.5. AFM Studies of poly-Lys(Z)-Bic-Tyr 115
5.3.6. AFM Studies of poly-Lys-Bic-Tyr 116

6. SUMMARY AND CONCLUSIONS 118

7. EXPERIMENTAL SECTION 120

7.1. Compound 1: 9a(R)H-5-oxo-(6S,7S,8S,9R)-tetrahydroxy-octahydro-thiazolo-[3,2-a] azepin-3R-carboxilic acid-methyl ester. 120
7.1.1. Procedure 120

7.1.2. Analytical Data 121

7.2. Compound 2: 9a(R)H-5oxo-(6S)-trifluoromethansulfonyloxy-(7S,8S,9R)-trihydroxy-octahydro-thiazolo [3,2-a]azepin-3R-carboxilic acid-methyl ester. 121

7.2.1. Procedure 121

7.2.2. Analytical Data 121

7.3. Compound 3: 9a(R)H-(6S)-azido-5-oxo-(7R,8S,9R)-trihydroxy-octahydro-thiazolo [3, 2-a]azepin-3R-carboxilic acid-methylester. 122

7.3.1. Procedure 122

7.3.2. Analytical Data 122

7.4. Compound 4: 9a(R)H-(6S)-amino-5-oxo-(7R,8S,9R)-trihydroxy-octahydro-thiazolo[3,2-a]azepine-3R-carboxilic acid-methylester. 123

7.4.1. Procedure 123

7.4.2. Analytical Data 123

7.5. Compound 5: 9a(R)H-(6S)-tert-butyooxycarbonylamino-5-oxo-(7R,8S,9R)-trihydroxy-octahydro-thiazolo [3,2,-a]azepin-3R-carboxilic acid-methylester 124

7.5.1. Procedure 124

7.5.2. Analytical Data 124

7.6. Compound 6: 9a(R)H-(6S)-Fmoc-amino-5-oxo-(7R,8S,9R)-trihydroxy-octahydro-thiazolo [3,2-a]azepin-3R-carboxilic acid-methylester. 125

7.6.1. Procedure 125

7.6.2. Analytical Data 125

7.7. Compound 7: 9a(R)H-(6S)-amino-5-oxo-(7R,8S,9R)-trihydroxy-octahydro-thiazolo [3,2,a]azepin-3R-pottasium salt of carboxylic acid. 126

7.7.1. Procedure 126

7.7.2. Analytical Data 126

7.8. Compound 8: 9a(R)H-(6S)-tetra-butyloxycarbonylamino-5-oxo-(7R,8S,9R)-trihydroxy-octahydro-thiazolo [3,2-a]azepin-3R-carboxilicacid 127

7.8.1. Procedure 127

7.8.2. Analytical Data 127

7.9. Compound 9: 9a(R)H-(6S)-Fmoc-amino-5-oxo-(7R,8S,9R)-trihydroxy-octahydro-thiazolo [3,2-a]azepin-3R-carboxilic acid 128
7.9.1. Procedure 128
7.9.2. Analytical Data 128

7.10. Compound 10: Boc-Bic-Tyr-OMe 129
7.10.1. Procedure 129
7.10.2. Analytical Data 129

7.11. Compound 11: Bic-Tyr-OMe 130
7.11.1. Procedure 130
7.11.2. Analytical Data 130

7.12. Compound 12: Bic-Tyr 131
7.12.1. Procedure 131
7.12.2. Analytical Data 131

7.13. Compound 13: Boc-Lys(Z)-Bic-Tyr-OMe 132
7.13.1. Procedure 132
7.13.2. Analytical Data 132

7.14. Compound 14: Boc-Lys(Z)-bic-Tyr 133
7.14.1. Procedure 133
7.14.2. Analytical Data 133

7.15. Compound 15: Lys(Z)-Bic-Tyr 134
7.15.1. Procedure 134
7.15.2. Analytical Data 134

7.16. Compound 16: Lys-Bic-Tyr 135
7.16.1. Procedure 135
7.16.2. Analytical Data 135

7.17. Compound 17: Boc-DOPA-Bic-Tyr-OMe 136
7.17.1. Procedure 136
7.17.2. Analytical Data 136

7.18. Compound 18: DOPA-BiC-Tyr-OMe 137
7.18.1. Procedure 137

7.18.2. Analytical Data 137

7.19. Compound 19: Boc-DOPA-Tyr-OMe 138

7.19.1. Procedure 138

7.19.2. Analytical Data 138

7.20. Compound 20: DOPA-Tyr-OMe 139

7.20.1. Procedure 139

7.20.2. Analytical Data 139

7.21. Compound 21: Boc-Bic-DOPA-Tyr-OMe 140

7.21.1. Procedure 140

7.21.2. Analytical Data 140

7.22. Compound 22: Boc-Lys(Z)-DOPA-Tyr-OMe 141

7.22.1. Procedure 141

7.22.2. Analytical Data 142

7.23. Compound 23: Lys(Z)-DOPA-Tyr-OMe 142

7.23.1. Procedure 142

7.23.2. Analytical Data 143

7.24. Compound 24: Lys-DOPA-Tyr-OMe 143

7.24.1. Procedure 143

7.24.2. Analytical Data 144

7.25. Compound 25: Boc-Lys(2-Cl-Z)-Tyr-OMe 144

7.25.1. Procedure 144

7.25.2. Analytical Data 145

7.26. Compound 26: Boc-Lys(2-Cl-Z)-Tyr 145

7.26.1. Procedure 145

7.26.2. Analytical Data 146

7.27. Compound 27: Lys(2-Cl-Z)-Tyr 146

7.27.1. Procedure 146

7.27.2. Analytical Data 146

7.28. Compound 28: Poly-Bic 147

7.28.1. Procedure 147
7.28.2. Analytical Data 148

7.29. Compound 29: Poly-Bic 148
7.29.1. Procedure 149
7.29.2. Analytical Data 149

7.30. Compound 30: Poly-Tyr 149
7.30.1. Procedure 149
7.30.2. Analytical Data 150

7.31. Compound 31: Poly-DOPA 150
7.31.1. Procedure 150
7.31.2. Analytical Data 150

7.32. Compound 32: Poly-Lys(Z) 151
7.32.1. Procedure 151
7.32.2. Analytical Data 151

7.33. Compound 33: Poly-Lys 152
7.33.1. Procedure 152
7.33.2. Analytical Data 152

7.34. Compound 34: Poly-Bic-Tyr 152
7.34.1. Procedure 153
7.34.2. Analytical Data 153

7.35. Compound 35: Lys(2-Cl-Z)-Tyr 154
7.35.1. Procedure 154
7.35.2. Analytical Data 154

7.36. Compound 36: Poly-Lys(Z)-Bic-Tyr 155
7.36.1. Procedure 155
7.36.2. Analytical Data 156

7.37. Compound 37: Poly-Lys-Bic-Tyr 156
7.37.1. Procedure 156
7.37.2. Analytical Data 156

7.38. Compound 38: Saponification Reaction 157

7.38.1. Procedure 157

7.38.2. Analytical Data 157

8. REFERENCES 159

Abstract

Mussels, marine organisms, attach to underwater surfaces by making a byssus, which is an extra-corporeal bundle of tiny tendons attached distally to a foreign surface and proximally by insertion of the root into the byssal retractor muscles. The interaction exterior of byssus and marine surface is an adhesive plaque that contains different proportion of five *mytilus edulis adhesive proteins* (*mefp*-1 to 5). Relatively high contains of Lys, L-3,4-dihydroxyphenylalanine (DOPA), *trans*-4-hydroxyproline, and *trans*-2,3-*cis*-3,4-dihydroxyproline formulates MAPs as an adhesive protein. Derivation of synthetic bio-adhesives from MAPs have been limited due to fairly unsuccessful synthesize adhesive polypeptides and poor yield in extraction from biological source.

In this study, syntheses of mussel adhesive protein analogues have been performed. Several oligomers and polymers were synthesized with the comibation of bicyclic dipeptide building blocks, DOPA, Lys and Tyr. Use of bicyclic dipeptide building block has advantage over use of Hyp and Ser as former is expensive and latter needs side chain protection. Molecular structure, mass and size of these polymers were characterized using various techniques like NMR, MALDI, and GPC. The adhesive properties of these polymers were tested using diffusion ordered spectroscopy (DOSY) NMR experiment and AFM spectroscopy. Results obtained using AFM shows adhesion of poly-Lys-Bic-Tyr to graphite surface. These results open up a wide area in which finely tuned adhesive synthetic bio-polymers can be synthesized.

Zusammenfassung

Muscheln, marine Organismen, heften sich unter Wasser an Oberflächen durch einen Byssus an. Diese extrakorporalen Fibrillen aus winzigen Sehnen heften sich in der Ferne an fremde Oberflächen, deren Wurzeln mit der Insertion in den byssalen Retraktor der Muscheln enden. Die Wechselwirkung außerhalb des Byssus und an marinen Oberflächen kommt durch eine marine Plaque zustande, die aus „Muschel-adhäsiven Proteinen“ (MAPs) bestehen. Es wurden fünf unterschiedliche MAPs entdeckt, von denen mytilus edulis adhäsiv Protein- 1 (*mefp*-1) im größten Umfang untersucht wurde. *Mefp*-1 besteht aus sich wiederholenden Decapeptiden, von denen jedes Decapeptid aus zwei Lys, ein bis zwei L-3,4-Dihydroxyphenylalanin-Resten (DOPA), ein bis zwei Resten *trans*-4-Hydroxyprolin und ein Rest *trans*-2,3-*cis*-3,4-Dihydroxyprolin bestehen. Diese spezielle Umgebung aus Lys-, DOPA- und Hyp-Resten macht *mefp-1* zu einem adhäsiven Protein, das wissenschaftliche Aufmerksamkeit auf sich gezogen hat als eine Vorlage für künstlich erzeugbare Bioadhäsiva. Versuche zur Synthese von adhäsiven Polypeptiden sind bisher ohne Erfolg. Ein limitierender Faktor ist die geringe Ausbeute bei der Extraktion dieser Proteine aus natürlichen Quellen.

In dieser Arbeit wurden verschiedene synthetische Oligomere und Polymere hergestellt, die aus Amionosäuren-Analoga und Dipeptid-Blöcken bestehen. Die molekularen Strukturen, Massen und Ausmaße dieser Polymere wurden durch verschieden Techniken, wie NMR, MALDI und GPC charakterisiert. Die adhäsiven Eigenschaften der Polymere wurden durch DOSY-NMR-Experimente und AFM-Spektroskopy getestet. Die Ergebnisse der AFM-Aufnahmen zeigen adhäsive Eigenschaften von poly-Lys-Bic-Tyr an Graphit-Oberflächen. Diese Ergebnisse öffnen ein weites Feld mit denen abgestimmte künstliche Biopolymere mit adhäsiven Eigenschaften synthetisiert werden können.

Abbreviations

Ala, alanine;
ADTN, 2-amino-6,7-dihydroxy-1,2,3,4-tetrahydronaphthelene;
AFM, atomic force microscopy;
AM, amplitude modulation;
Arg, arginine;
Asn, asparagine;
Asp, aspartic acid;
Bic, bicyclic dipeptide;
Boc, tert-butoxycarbonyl;
BOP, benzotriazole-1-yl-oxy-tris-(dimethylamino)-phosphonium hexafluorophosphate;
CCA, α-cyano-4-hydroxycinnamic acid;
CD, circular dichromism;
*c*DNA, complemantory deoxyribo nucleic acid;
COSY, correlated spectroscopy;
Cys, cysteine;
Da, Dalton;
DCC, dicyclohexylcarbodiimide;
DHB, 2,5-Dihydroxy benzoic acid;
diHyp, *trans*-2,3-*cis*-3,4-dihydroxyproline;
DIPEA, *N*, *N*-Diisopropylethylamine;
DIEA, diisopropylethylamine;
DMF, dimethyl formamide;
DNA, deoxyribonucleic acid;
DOPA, 3,4-dihydroxyphenylalanine;
DOSY, diffusion ordered spectroscopy;
E. coli, *Escherichia coli*;
EDC, *N*-(3-dimethylaminopropyl)-*N*′ ethylcarbodiimidhyrochloride;
EPR, electron paramagnetic resonance;
ESI-MS, electron spray ionization mass spectroscopy;
FM, frequency modulation;
Fmoc, 9-fluorenylmethyloxycarbonyl;
Gln, glutamine;
Glu, glutamic acid;

Gly, glycine;

GPa, gega Pascal;

GPC, Gel Permeation Chromatography;

HBTU, benzotriazol-1-yl-*N*-tetramethyl-uronium hexafluorophosphate;

HCTU, 1H-benzotriazolium 1-[*bis*(dimethylamino)methylene];

His, histidine;

HMQC, heteronuclear multiple quantum coherence;

HPLC, high performance liquid chromatography;

HSQC, heteronuclear single quantum coherence;

HOAt, 1-hydroxy-7-azabenzotriazole;

HOBt, 1-hydroxy 1H-benzotriazole;

Hyp, *trans*-4-hydroxyproline;

Ile, isoleucine;

IR, infra red;

kDa, kilo Dalton;

LC, liquid crystals;

LO, lysyl oxidase;

Leu, leucine;

Lys, lysine;

MAP, marine (or mussel) adhesive protein;

MALDI, matrix assisted laser desorption/ionization;

MALDI-TOF, MALDI-time of flight;

Meap, *mytilus edulis* adhesive protein;

Mefp, mytilus edulis foot protein;

Met, methionine;

MPa, mega Pascal;

MTX, methotrxate;

NBS, *N*-bromosuccinimide;

NCA, *N*-carboxyanhydride;

N-(Cbz), *N*- carbamazepine;

*n*D, *n* dimensional (*n* being any number belonging to the set of natural numbers);

nm, nano meter;

NMP, *N*-methyl-2-pyrrolidinone;

NMR, nuclear magnetic resonance;

NOESY, nuclear Overhauser enhancement spectroscopy;

OBt, *o*-bromotoluene;

ORD, optical rotary dispersion;

PAGE, polyacrylamide gel electrophoresis;

Phe, phenylalanine;

PLG, Pro-Leu-Gly-NH_2;

PPII, poly proline II;

ppm, parts per million;

Pro, proline;

PyBOP, benzotriazole-1-yl-oxy-tris-pyrrolidino-phosphonium hexafluorophosphate;

poly-DCC, *N*-Cyclohexylcarbodiimide, *N'*-methylpolystyrene;

RIPS, random incremental pulse search;

RP-HPLC, reverse phase HPLC;

RRS, resonance Raman spectroscopy;

Ser, serine;

SERS, surface enhances Raman spectroscopy;

SDS, sodium dodecyl sulphate;

Sinapinic acid, *trans*-3,5-dimethoxy-4-hydroxycinnamic acid;

SPPS, solid phase peptide synthesis;

Sta, 3-(S)-hydroxyl-4-(S)-amino-6-methylheptanoic acid (also known as stanine);

STM, scanning tunnel microscope;

TBTU, benzotriazol-1-yl-*N*-tetramethyl-uronium tetrafluoroborate;

Thr, threonine;

TES, tetraethylorthosilicate;

Trp, tryptophan;

Tyr, tyrosine;

Val, valine;

1. Preamble

Emil Fischer introduced the concept of peptides and polypeptides and presented protocols for their synthesis in the early 1900s. Although others scientists contributed in those days, most notably Theodor Curtius, the co-worker of Fischer and his colleagues stands out. The chemistry developed by Fischer and others during those early days led to the production of molecules containing as many as 18 amino acids [1, 2]. Nonetheless, the syntheses performed were difficult and limited to simple amino acids, and the progress was slow for many years. Then the discovery of an easily removable carbobenzoxy protecting group in 1932 by Bergmann and Zervus provided new impetus by opening the way to the use of polyfunctional amino acids [3]. Later, synthesis of an active peptide harmone, by du Vigneaud (1953), was a sensation in the peptide synthesis as he used solution-phase segment condensation method. The attempts to syntheses peptides further stretched by new technique called solution phase stepwise addition method developed by Bodanszky and Williams (1967). Around the same time, Bruce Merrifield made a land-marking achievement by introducing solid-phase peptide synthesis [4], for which he was awarded Nobel Prize in chemistry in 1984. Invention of solid-phase peptide synthesis (SPPS) together with the enormous improvements in liquid chromatographic techniques have changed peptide chemistry from being a specialist area in which a few research groups were active, into a field where virtually any scientist whose research leads to the need for the synthetic peptides can utilize these synthetic techniques.

In this thesis, synthesis and characterization of peptides derived from mussel adhesive proteins will be presented. These peptides are designed by mimicking the adhesive property of the mussel adhesive proteins.

Marine organisms such as mussels and barnacles attach themselves to almost any kind of underwater solid surfaces using specialized adhesive mechanism that utilizes mixture of several proteins. These proteins belong to a family of protein and are named as mussel adhesive proteins (MAPs). So far, five adhesive proteins from the blue mussel have been isolated, namely, *mytilus edulis foot protein*-1 (*mefp*-1) to *mefp*-5 [5-8]. J. H. Waite and co-workers characterized peptides from tryptic digests being the first of these families of protein [9, 10]. *Mefp*-1 protein contains high Lys and hydroxylated amino acids such as DOPA, is formed by 897 residues and has a molecular weight in the range of 115-130 kD[11, 12]. *Mefp*-1 is mainly formed by two building blocks (or domains) consisting 71 decapeptides composed of the residues Ala-Lys-Pro-Ser-Tyr-DiHyp-Hyp-Thr-Tyr-Lys and 12 hexapeptides containing Ala-Lys-Pro-Thr-Tyr-Lys with mainly random coil and partially helical conformation [13].

The efforts to develop biomedical adhesives from *mefp* proteins have been hampered largely due to difficulties associated with the isolation of proteins from biological sources. Therefore, synthetic polymers are a potential source to mimic the adhesive characteristics of MAPs. Investigations on the synthesis of adhesive peptides and adhesive polymers, with incorporation of functional components of the MAPs, were performed by several groups [7, 14-17].

This work is continuation of earlier attempts and efforts that were focused on the design and synthesis of simplified adhesive peptides and polymers that mimic adhesiveness of the MAPs. The approach used in this thesis involves the use of dipeptide building blocks. Dipeptide building blocks are polar, rigid and stabilized by extended helical conformation found in the *mefp*-1. In the course, we seek to develop new polar adhesive oligopeptides and have a comprehensive understanding of the role of hydroxylated amino acids when adhering to marine wet surfaces. Synthetic adhesive peptides also will also prove important in clarifying the principle of molecular recognition of adhesive peptides.

To begin with, chapter 2 starts with the introduction to the natural amino acids extending it further to non-protein amino acids. Introduction to the structural elements commonly found in proteins is then briefly given.

Mussels make a byssal adhesive plaque to adhere to the wet surface. In chapter 3 an in-depth discussion on mussel adhesive peptides is featured. This includes all the five known mussel adhesive proteins (*mefp*-1 to 5), their occurrence, conformational studies and biological importance. This chapter also informs about the importance of amino acid like DOPA in MAPs. The second part of this chapter discusses previous attempts to synthesize poly amino acids, which would be analogues to the MAPs′.

Chapter 4 comprises the synthesis of adhesive peptides that were designed and developed during this study. The synthesis of adhesive peptides was achieved in solution as well as in solid using Boc and Fmoc strategies. The bicyclic di-peptide building block, co-polymeric and polymeric amino acids were synthesized in an attempt to design synthetic adhesive biopolymers.

Information on the molecular structure of these peptides was gained using 2D Nuclear Magnetic Resonance Spectroscopy, whereas molecular weight was determined by MALDI-TOF, gel permission chromatography (GPC) and gel electrophoresis. The details of these characterizations are mentioned in chapter 5. In order to test adhesive property of synthesized oligomers and co-polymers, diffusion ordered spectroscopy (DOSY) and atomic force microscopy (AFM) was used. Chapter 5 has details of these studies with concluding evidences of adhesiveness of synthesized co-poymers.

Chapter 6 gives summary of the research work performed in this thesis.

The detailed experimental procedures, analytical characterization of all the synthetic molecules performed during this study are listed in chapter 7.

2. Introduction

Amino acids can be broadly divided based on the hydrophobic and hydrophilic character of its side chain. The hydrophobic amino acids include those with aliphatic side chains, such as, Ala, Val, Ile, Leu and Met, and those with aromatic side chains, such as Phy, Tyr and Trp. The hydrophilic amino acids include (i) neutral and polar side chains, such as, Ser, Thr, Asn and Gln; (ii) with acidic side chains such as Asp and Gln, and (iii) with basic side chains such as His, Lys and Arg. Ala with its small aliphatic side chain and Gly can be found in hydrophilic regions of peptides and proteins where as long alkyl chains of Lys and Arg give those residues an overall hydrophobic character with just the terminal charged group being hydrophilic. The two amino acids Cys and Pro have special properties. Cys contains a thiol to form a disulfide linkage by which peptide chains are covalently linked together to stabilize secondary or tertiary structure or to hold two different peptide chains together. Free thiols are also present in some proteins, where they often serve as ligands for metal chelation, as nucleophiles in proteolytic enzymes, such as papain or as carboxyl activators in acyl transferases. The second amino acid, Pro has specific conformational effects on the peptide or protein backbone both because of its cyclic structure and because of the alkylation of the amino group. It plays an important role in stabilizing or influencing the secondary structure of proteins [18]. All amino acids, except Gly, are chiral with an asymmetric center at α-carbon with the L absolute configuration at this center. The L does not refer to the direction of optical rotation but, rather to having the same stereo-chemical arrangement as L(-)-glyceraldehyde. In the more unambiguous Cahn-Ingold-Prelog convention, L-amino acids have the S absolute conformation (except Cys, for which this configuration is defined as R). Additionally, Thr and Ile have a second asymmetric center at the β-carbon. Thr has the R absolute configuration at the β-carbon, and it is 2-(S)-amino-3-(R) hydroxybutonic acid. Ile has the S absolute configuration at the β-carbon; it is 2-(S)-methylpentanoic acid, because of the two asymmetric centers in the molecules, for stereo isomers exist for each of these amino acids. The D-amino acid has the opposite configuration at both asymmetric centers; D-Ile is the 2-(R)-3-(R) isomer.

2.1. Peptides and Proteins

A peptide is any group of compounds consisting of two or more amino acids linked by chemical bond. A peptide can be a short segment of a larger protein, often, a completely functional molecule by itself. Use of a fragment of a parent protein (as a peptide) is frequently useful as one

has to deal with relatively small molecule. Additional advantages could be ease in handling, less chances of biodegradation and proteolysis, uncomplicated and established synthetic methods to prepare in a laboratory. Peptides found in the human body can take the function of hormones (e.g., antidiuretic hormone), can form proteins, or may have functions in the digestive process (and therefore may be found throughout the body - in the digestive tract, blood, cells and tissues).

Proteins, naturally occurring polypeptide chains, are formed by combinations of twenty naturally occurring amino acids. The choice of the amino acid and its position in the protein chain are determined by the corresponding DNA template. In a laboratory, proteins can be either over-expressed in relatively simple cells (e.g., *E.coli*, yeast cells) by adding a gene of interest in the cell or can be extracted from respective tissues of living organism (e.g., collagen, soy). Proteins have evolved in nature to perform specific functions. Known functions of proteins encompass vast array of tasks such as enzymatic activity, building up large assemblies like muscle fibers or virus particles, regulating cell functions and signal transduction. These functional properties of proteins depend upon their three-dimensional structure. Understanding functional properties of a protein can be very important to reveal its biological significance, novel drug design as well as to prepare synthetic biomaterials. Together with structural data, functional aspects of a protein can be very useful, particularly, to design a tailor-made synthetic molecule with enhanced bioactivity. Therefore, mimicked synthetic biomolecule often functions better than its parent molecule. Such approach is routinely practiced today and synthetic analogues of many important biomolecules are available for study as well as for therapeutic purpose.

The polyamide peptide backbone is also an important contributor to overall protein and peptide structures, a double-bond character is found in the carbon-nitrogen peptide bond due to the resonance structure shown in Figure 2 -1.

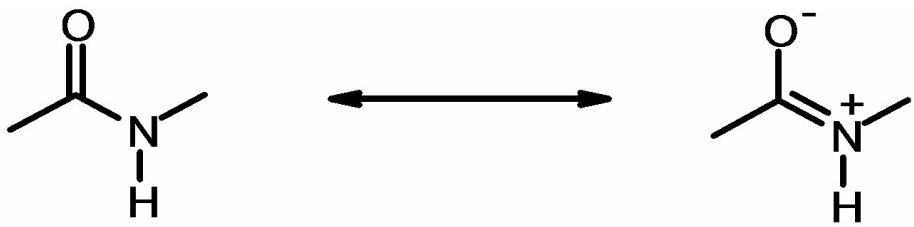

Figure 2 -1: Resonance forms of an amide bond depicting zwitter-ionic form (on the right hand side structure).

The amide bond is flat with the carbonyl carbon, oxygen, nitrogen, and amide hydrogen all lying in the same plane. No free rotation occurs about the carbon-nitrogen bond because of its partial double bond character. The torsional angle of that bond, ω, is defined by the peptide backbone

atoms C_α-CO-NH-C_α. Because of the partial double bond character, there are two rotational isomers for the peptide bond, namely, *trans* with $\omega \approx 180^\circ$ and *cis* with $\omega \approx 0^\circ$ as shown in Figure 2 -2.

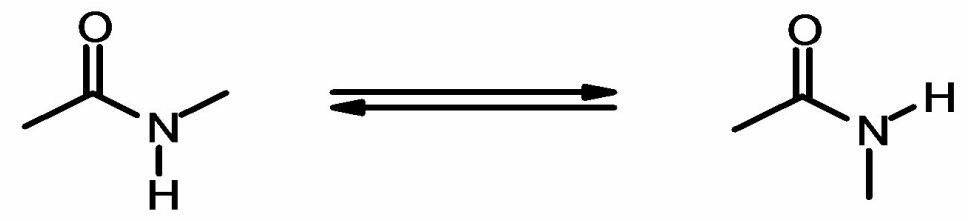

Figure 2 -2: The *cis-trans* isomerisation across peptide bond. Thick arrow indicates propagation of the peptide chain from and to connecting resides. In most of the cases a *trans* conformation is favored as it posses lowest free energy unless otherwise additional stability due to *cis* conformation.

The lower energy isomer is the *trans* peptide bond, which is commonly found for all peptide bonds not involving Pro. In the case of amide bond involving Pro, the energy of the *trans* X-Pro bond is somewhat elevated, and both the difference in energy between *cis* and *trans* isomers and the barrier to rotation is lowered. Pro containing peptides thus will often exhibit *cis-trans* isomerization along *trans* X-Pro bond. It is found that the *cis* content of X-Pro peptides generally increase when X is a bulky and hydrophobic amino acid [19].

The resonance forms of the amide bond give it one other characteristic that is extremely important in peptide and protein structure. The amide bond is quite polar and has a significant dipole moment, which makes the amide carbonyl oxygen a particularly good hydrogen-bond acceptor and the amide NH a particularly good hydrogen-bond donor. Hydrogen bonds involving the peptide backbone are an important stabilizing factor in protein secondary structures. Peptide bonds of regular secondary structures, such as helices and β-sheets are internally solvated by the hydrogen bonds hat stabilize those structures. The peptide bonds of the random coil or irregular structures, also participate in an extensive network of hydrogen bonds involving internal polar side chains, bound water molecules and backbone interactions.

2.2. Nonprotein Amino Acids

Many naturally occurring amino acids exist that are not commonly found in proteins. Some of them, like γ-aminobutyric acid, have important functions as neurotransmitters. Others like ornithine appear as intermediates in metabolic pathways and dihydroxyphenylalanine is a precursor to amino acid derivative products. These unusual amino acids can confer unusual

biological activities on peptides that contain them. Such peptides have been the basis either of biochemical tool molecules or of antibiotics, immunomodulators or antineoplastic agents that have therapeutic utility [20].

Nonprotein organic amino acids can be roughly classified into a few basic structural types. Some nonprotein organic amino acids are simply the enantiomeric D-amino acid analogue of a protein L-amino acid, e.g., D-Ala and D-Glu, which are important constituents of the proteoglycan bacterial cell wall. Other has a normal α-amino acid structure but with a novel side chain. The side chain can be a simple alkyl group such as in norvaline. Some non-protein organic amino acids deviate from the normal α-carbon, such as the aminoisobutyric acid of the ionophoretic antibiotic peptide alamethicine [21, 22]. Also, in large number of non-protein amino acids, the amino group is not on the α-carbon but at some other position in the molecule [20]. Sometimes several of these features are combined in one amino acid such as in statine [3-(S)hydroxyl-4-(S)-amino-6-methylheptanoic acid, Sta] which is the critical residue in the fungal orotease inhibitor pepstatin [23].

2.3. Strategies for Peptide Synthesis

As stated earlier (cf. Chapter 1), peptide chemistry and synthesis have gone through dramatic changes since Crutius and Emil Fischer have synthesized the first simple peptide derivatives [1, 2]. The solid phase peptide synthesis technique, developed by Merrifield in 1963 [4], substantially facilitates the practical peptide synthesis procedure. In this approach, the anchoring of the C-terminal amino acid to the insoluble support allows the use of an excess of amino acids and coupling reagents, which enables almost quantitative yields for the coupling steps of small peptides. Furthermore, after reaction, coupling and by-products can be removed by simple filtration.

The synthesis of peptides longer than two amino acids requires the tactical utility of orthogonal temporary and permanent protecting groups [24]. Amongst several approaches developed so far, the Boc-strategy [25-28] and subsequently developed Fmoc/tBu-strategy [27-30] are most prominent today. The Fmoc/t-Bu-strategy has proved to be especially practical in combination with SPPS and has been represented in Figure 2 -3.

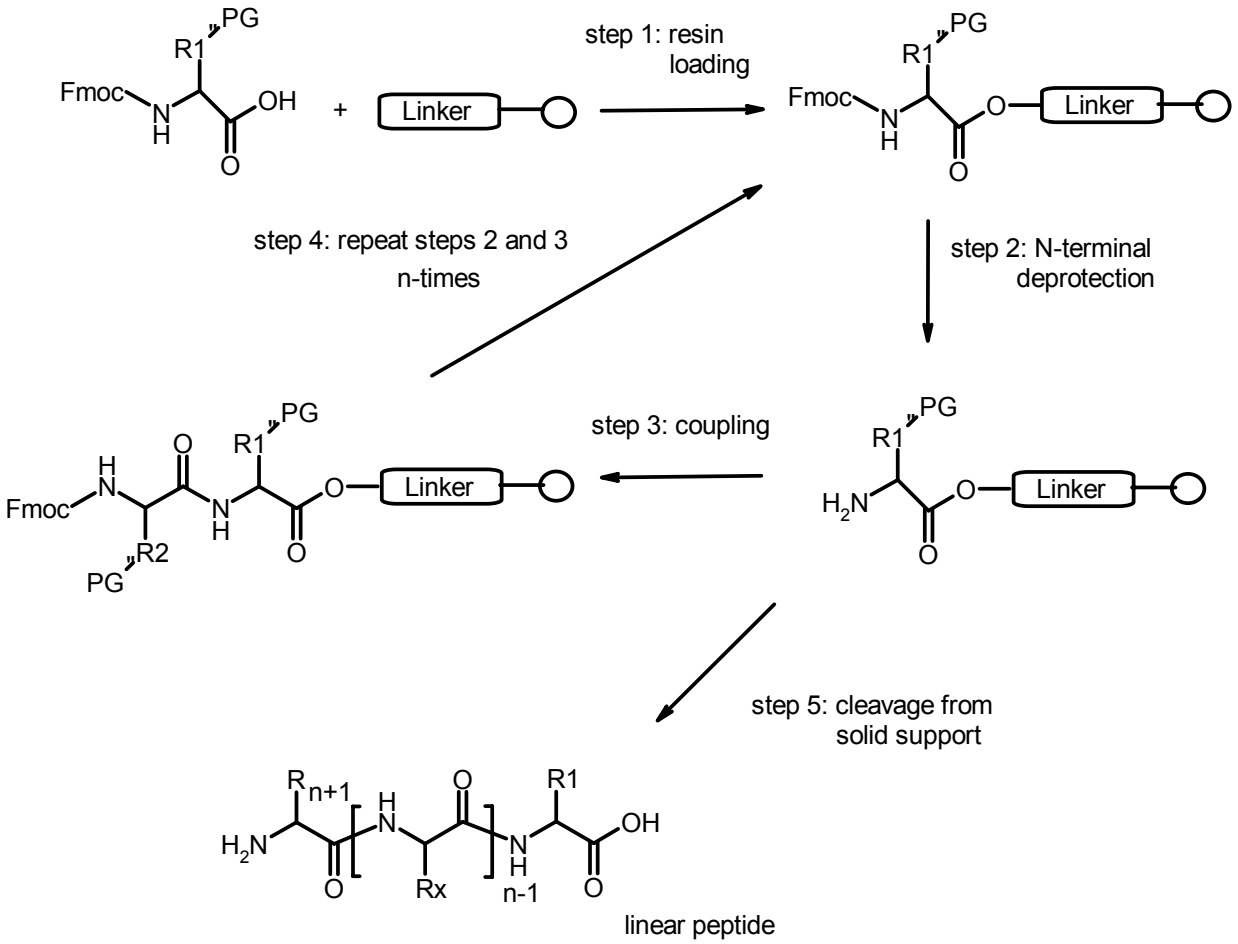

Figure 2 -3: Peptide synthesis according to the Fmoc/tBu-strategy on a solid support.

Solution phase peptide synthesis is also one of the effective synthetic methods for the preparation of small peptides and oligomers. Introduction of N^{α}-protected amino acids in solution phase synthesis normally involves *in situ* carboxyl activation of the incoming amino acid. The mechanism of peptide bond formation involves the attack of a nucleophilic α-amino group upon the activated carboxyl function of a protected amino acid or peptide segment.

Several other coupling methods such as the azide process [1], acid chlorides [31], acid fluorides [32] or nitrophenyl- and pentaflurophenyl active esters [25, 33], were developed in the course of time though the use of *in situ* activated amino acids became very popular. Suitable condensing agent such as DCC, BOP and HBTU can be employed to mediate coupling via *in situ* activation [34]. *In situ* activation reagents are widely accepted as they are easy to use, give fast reactions, even between sterically hindered amino acids and their use is generally free from side reactions.

Most are based on phophonium or iminium salts, under basic condition they convert protected amino acids to a verity of activated species. Most commonly employed BOP, PyBOP, HBTU and TBTU, generate OBt esters, and these have wide application in coupling reactions.

In comparison to other coupling reagents such as DCC, BOP couplings are essentially recemization free and exhibits superior kinetics [35, 36]. However, the use of BOP reagent in peptide synthesis is avoided since it leads to the formation of hexamethylphosphoric triamide, a respiratory toxin and possible carcinogen [37]. Chemical structure of some of these coupling reagents is given in Figure 2 -4.

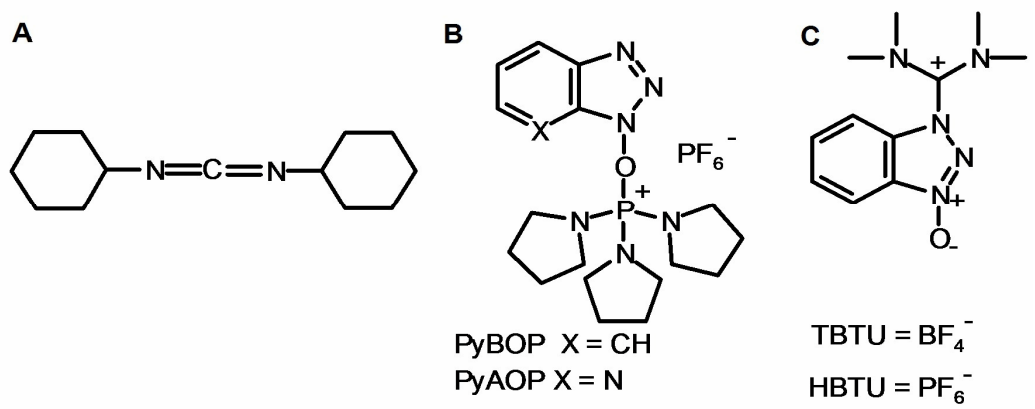

Figure 2 -4: Coupling reagents commonly used in peptide synthesis. (A) DCC; (B) PyBOP and (C) TBTU/HBTU.

Replacement of phosphorus atom in BOP by carbon atom yields, *o*-benzotriazolyl-*N*, *N*, *N'*, *N'*-tetramethyluronium hexafluorophosphate salt (HBTU), like the BOP reagent. HBTU was found to be an excellent coupling reagent for peptide synthesis in solution and solid phase. The amount of racemization of the synthesis peptides was very low and the reaction time was fast [38]. BOP can be substituted by PyBOP, which is an expensive reagent. If the reagent used excess then carboxylic acid component as this can lead to capping of the amino terminus through guanidine formation [39].

Coupling reagent which generate more reactive active ester then OBt are also accomplished. Under basic condition HCTU generate corresponding 6-ClOBt ester are more reactive than their OBt counterpart owing to the lower pKa of HOCt compared to HOBt (pKa 3.35 for Cl-HOBt and 4.60 for HOBt). HCTU was found to give superior results to PyBOP and TBTU in the synthesis of difficult peptides [40] and in hindered coupling [41].

Koenig and Geiger have led to the recommendation of 1-hydroxybenzotriazole (HOBt) as a most efficacious *in situ* additive for coupling in peptide synthesis. The active species in solution is presumably the 1-hydroxybenzotriazole ester, which is aminolyzed at a rate about 103-fold faster than *N*-hydroxysuccinimide and similar active esters because of a concerted bifunctional catalytic mechanism [42, 43]. These coupling additives are shown in Figure 2 -5.

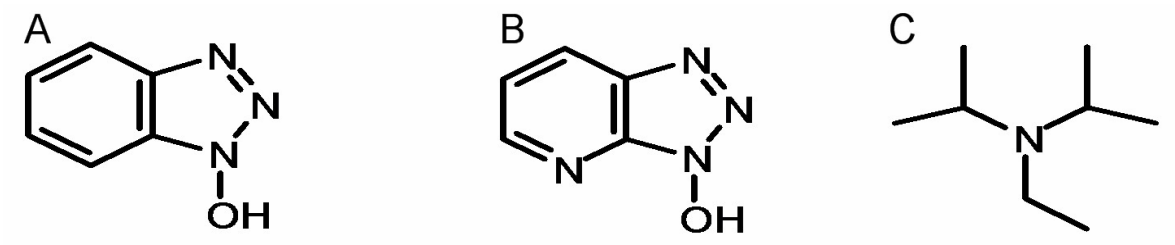

Figure 2 -5: Chemical representations of the coupling additives such as (A) HOBt, (B) HOAt and (C) DIPEA.

Upon addition of benzatrazoles HOBt and/or Cl-HOBt to the carbodimide base, coupling reagents leads to the formation of benzatrazol active esters. These esters are less reactive then the *o*-acylisourea lowering racemization of protected amino acids and avoiding the formation of other derivatives [44]. Cl-HOBt performs at least as well as HOBt [45, 46], but since it is more acidic and it is better leaving group and its active ester are more reactive than OBt ester another advantage in Cl-HOBt is that the chlorine atom stabilise the structure, making Cl-HOBt less hazards coupling reagent. HOBt and Cl-HOBt are also added to the aminium salt mediated coupling reactions with the purpose of favouring the active ester formation, thus HOBt and Cl-HOBt are used as an additive together with HBTU to suppress recimization.

2.4. Structural Elements of Proteins and Peptides

Protein (henceforth also peptide) structures are organized in several hierarchical levels of increasing structural complexity. The most basic level is the primary structure or amino acid sequence. Secondary structure is formed by the folding up of short segments of the protein chain into regular structures such as α-helices, β-sheets and turns. Tertiary structure describes how the secondary structural elements of a single protein chain interact with each other to fold into the native protein structure. Quaternary structure involves the interaction of individual protein subunits to form a multimeric complex [47].

In the design of peptides, the primary structure or sequence of a protein is readily obtainable by chemical sequence analysis of the isolated purified protein or by translation of the corresponding DNA coding sequence. Computer programs are available to analyze and compare protein primary structure [20].

Amino acid chains can fold into several types of regular structures that are stabilized by intra-chain or inter-chain hydrogen bonds in the amide backbone. Helixes and turns are formed from continuous regions of protein sequence and are stabilized by inter-chain hydrogen bonds. The

parts of a protein sequence that do not appear in helices, sheets or turns are said to be in random coil.

The conformation of the peptide backbone can be described by three torsional angles: ϕ, which is the angle defined by C(O)-N-Cα-C(O); ψ, which is defined by N-Cα-C(O)-N; and the amide torsional angle ω, these angles are shown graphically in Figure 2 -6.

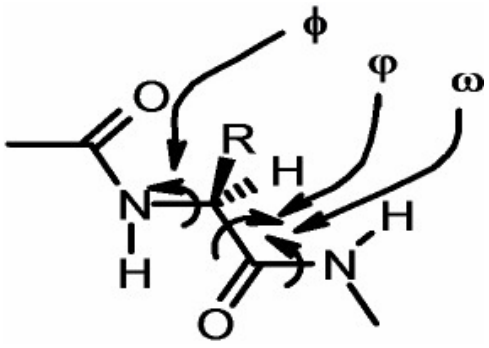

Figure 2 -6: Demonstration of the peptide backbone torsion angles, ϕ, ψ and ω. Only certain combinations of the angle ϕ and ψ are allowed, while the amide torsional angle ω remains planar. Thus information of the torsion angle can be very helpful for the structure calculation and/or prediction.

The convention in protein chemistry is that these angles are defined with respect to the peptide backbone. The angle φ is 180° when the two carbonyl carbons are *trans* to each other and the angle ψ is 180° when the two amide nitrogen are *trans* to each other as in Figure 2 -7. The angle ψ, therefore, is +180° compared to the usual chemical definition. A fully extended peptide chain, however, would have backbone torsional angles close to 180°, just like a fully extended carbon chain.

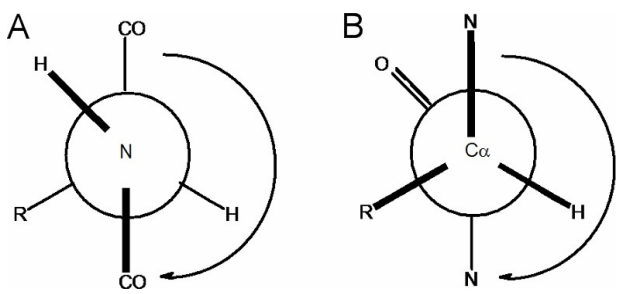

Figure 2 -7: Newman projections for the torsion angles ϕ = 180° (A) and ψ = 180° (B) in a typical extended polypeptide chain.

2.4.1. Helices

One of the common types of secondary structure in protein is the helix in which amino acid residues are wrapped around a central axis in a regular pattern. *Trans* and planar peptide bonds as well as helices can be uniquely defined by their ϕ and ψ angles. Several types of helices are found in protein structures, the α-helix being the most common. These helices and their characteristic torsional angles are listed in Table 2 -1.

Table 2 -1: Possible helical structures and their ϕ and ψ combinations.

Type of Helix	ϕ	ψ
α-helix (right-handed)	-57°	-47°
α-helix (left-handed)	57°	47°
3_{10} helix	-60°	-30°
Collagen helix	-51° -76° -45°	153° 127° 148°
Polyproline	-78°	149°

Helices are also characterized by the number of residues per turn and the hydrogen bonding pattern, specifically the number of atoms in the cyclic structure formed by the hydrogen bond. There are two most relevant helices for protein and peptides, which is defined by the screw sense of the helix. Looking down the helical axis from amino terminus to carboxyl terminus in a clockwise sense in a right handed helix, helical structures are stabilized by intra-chain hydrogen bonds in a helix, the carbonyl bonds and amide NH bonds lie parallel to the helix's axis with the carbonyls pointing downward, in the direction of the carboxyl terminal of the helix and the NHs pointing upward in the direction of the amino terminus.

In an α-helix, the carbonyl of any residue *i* is hydrogen-bonded to the amide NH of the *i*+4 residue; that is the residue four amino acids farther down along the peptide chain. In a 3_{10} helix, the carbonyl of ith residue is hydrogen bonded to the NH of *i+3* residues (see Figure 2 -8).

The helix forms a polyamide cylinder. The uniform arrangement of carbonyl and NH groups impacts a strong dipole moment to the helix, with the positive end at the amino terminus and the negative end at the carboxyl terminus. The side chains of residues are arranged radially outwards

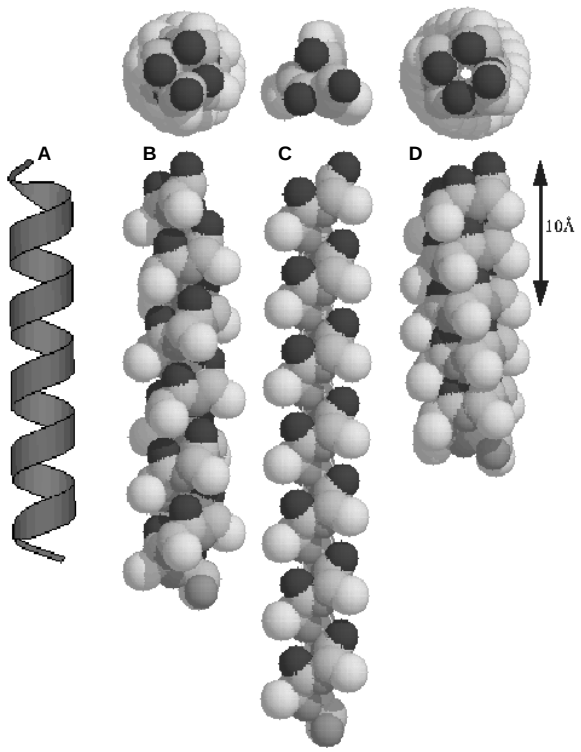

Figure 2 -8: Ribbon (A) and space fill model of helices (B, C and D). B represents a right handed α-helix with a top view. C and D represent a 3_{10} and π type of helices. Both panel C and D also shows top view of the corresponding helices (Figure reproduced from [48]).

from the helix, looking down the helix axis. Because all the backbone amide groups are involved in intra-chain hydrogen bonds, the interactions of helices with other peptide chains or small molecules occurs predominantly through side-chain interactions (hydrophobic interactions, salt bridges and hydrogen-bonding interactions and side chain interactions) and the interactions with helix dipole itself. Because of the arrangement of inter-chain hydrogen bonds, the amide bonds of the helix can be thought of as being internally solvated, resulting in the helix being more readily accommodated in a nonpolar environment, such as a lipid bilayer. The membrane-spanning regions of transmembrane proteins are generally with the axis of the helix perpendicular to the plane of the membrane [49, 50].

2.4.2. β-Strands and Sheets

Linus Pauling and Corey derived a model for the conformation of fibrous proteins known as beta-keratins [51]. In this conformation the polypeptide does not form a coil, but zigzags in a more extended conformation than the α-helix. A section of polypeptide with residues in the β-conformation is referred to as a β-strand and these strands can associate by main chain hydrogen bonding interactions to form a β sheet.

The conformation of each peptide chain is generally extended and inter-chain hydrogen bonds occur between the carbonyl oxygen and the amide NH of every other residue in the backbone. Two possible arrangements of adjacent strands occur parallel, in which each peptide strand runs in the same direction and antiparallel in which the peptide stands run in opposite directions. Both type of sheets can be found in protein structures, these two arrangements are shown in Figure 2 -9.

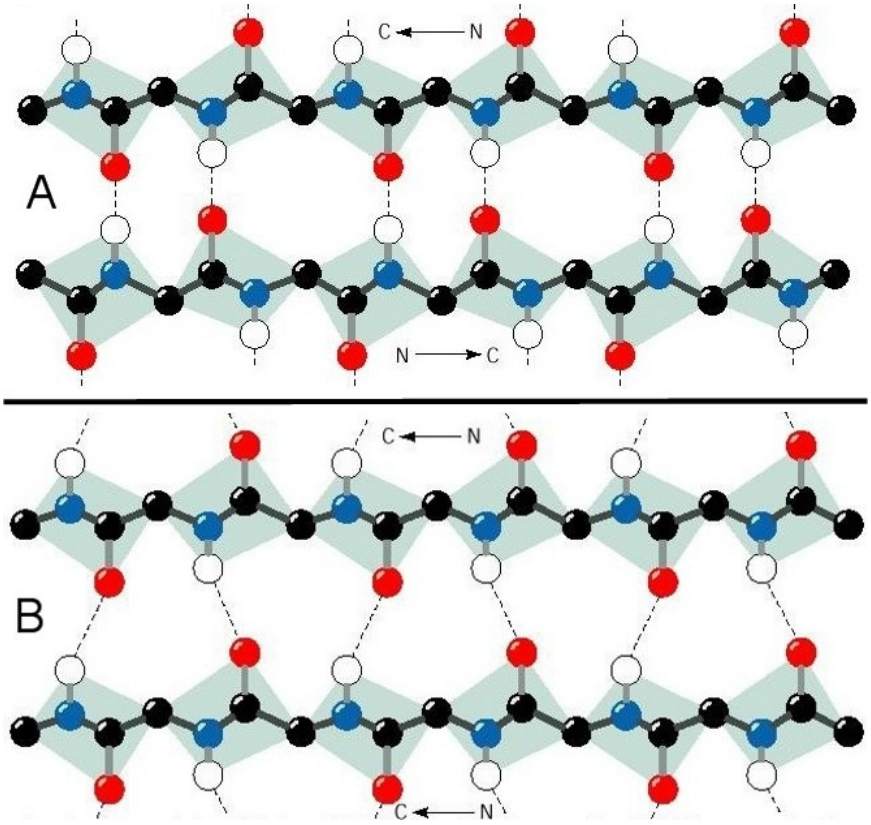

Figure 2 -9: Ball and stick representation of anti-parallel (A) and parallel (B) sheets. Black: Carbon, Blue: Nitrogen, Red: Oxygen and White: Proton (Figure adopted from [52]).

The β-structure can be thought of as forming a surface or sheet, although there is a slight twist to it because the peptide backbone is not fully extended. In contrast to the α-helical residues, amino acid residues in the β-conformation have negative ϕ angles and the ψ angles are positive. The torsional angles for β-structure are given in Table 2 -2.

Table 2 -2: Possible β-sheet structures and the allowed ϕ and ψ combinations.

Type of β-sheet	ϕ	ψ
Parallel β-sheet	-119°	113°
Antiparallel β-sheet	-139°	135°

The side chains extend roughly above and below the plane of the sheet, with every other side chain on one surface, because the inter-chain hydrogen bonds between two adjacent chains involve only every other residue and there is a possibility of larger structures forming that involve many strands. Another structural motif is that twist of the β-structure also allows sheets to fold into cylindrical structures is called as β-barrels.

2.4.3. Turns

Turns are the third type of classical secondary structures. Approximately one-third of all residues in globular proteins are contained in turns that serve to reverse the direction of the polypeptide chain.

Turns are classified by the number of residues that are involved in the regular structure; β-turns contain four amino acid residues, while γ-turns contain three residues. Each structure is stabilized by a hydrogen bond extending across the turn, in effect holding the two ends together.

The first residue of a turn is usually designated as *i*. In a β-turn, the hydrogen bond is between the carbonyl of the *i* residue and the NH of the *i+3* residue, giving the equivalent of a 10-membered ring. There may be an additional hydrogen bond between the NH of the *i* residue and the *i+3* residue, as if they were an incipient antiparallel β-structure (see Figure 2 -10).

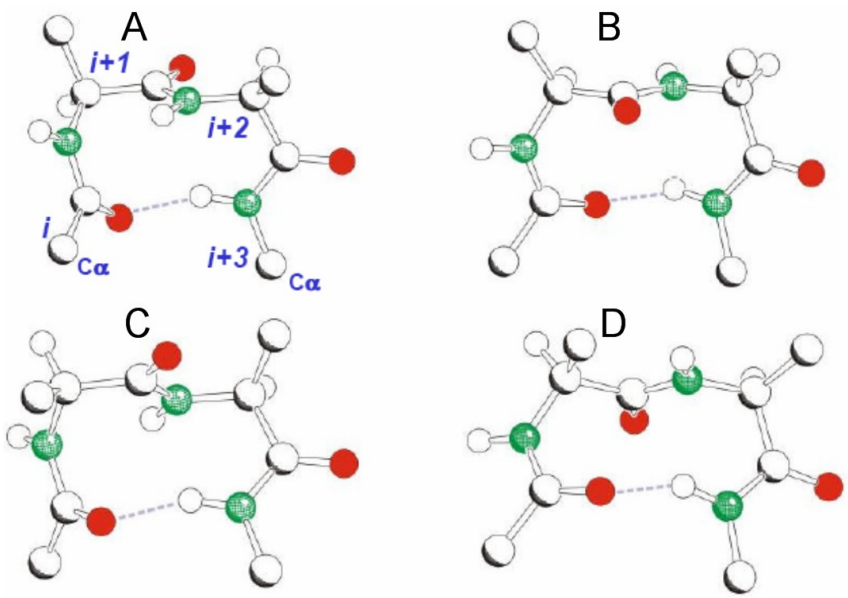

Figure 2 -10: A ball and stick representation of a β-I (A), β-II turn (B), β-I' turn (C), and β-II' turn (D). Intermolecular hydrogen bond is denoted by bond dashed lines. In panel A and B, CO_{i+1} and intermolecular hydrogen bond are below the plane whereas in latter two cases they are above the plane. Each residue is numbered starting from α_i. Atoms colours used are, carbon: big sized white; nitrogen: blue; hydrogen: small sized white; and oxygen: red.

In a γ-turn, the hydrogen bond is between the carbonyl of the *i* residue and the NH of the *i+2* residue, giving the equivalent of a seven-membered ring. Several type of β-turns are possible, the planer amide bond β and γ turns are uniquely defined by the torsional angles of the internal residues *i+1* and in the case of β-turns, *i+2*. Type III is simply a single turn of a 3_{10} helix.
The peptide backbone in a turn forms a rough plane that contains the intra-molecular hydrogen bond. In a β-turn, the amide bond between the *i+1* and *i+2* residues lies perpendicular to this plane since it is not part of the hydrogen bonding structure of the turn.
In protein, β-turns are most often found on the protein surface, where the *i+1-i+2* peptide bond can be solvated by bulk solvent. When such a turn is located in the (generally hydrophobic) interior of a protein, it is often solvated by a bound water molecule [53]. Beside the amide bond, the side chains of the *i+1* and *i+2* residues, which form the corners of the turn, are also particularly exposed. In case of small peptides such as vasopressin or somatostatin, where a turn has been postulated based on the cyclic nature of the peptide chain, the corner residues are implicated as important elements in the expression of the biological activity of the peptide [54, 55].
Side chains will adopt either a pseudo-axial or pseudo-equatorial arrangement around the cyclic hydrogen-bonded turn structure. One diagnostic criterion for the importance of a turn involves changing the chirality of a corner residue to allow the side chain to be in the more stable equatorial configuration without otherwise alternating the peptide backbone structure. Replacement of this residue with a D-amino acid should allow for equatorial placement of the side chain while the peptide backbone remains unchanged, lowering the overall free energy of that structure and making it more stable. Replacing the *i+1* residue with a Gly with no side chain should have a similar effect.
Since a turns have several unsatisfied backbone hydrogen bond donors and acceptors, they are polar, and are usually found near the surface of the protein. Pro is very common in turns, as it always has the correct ϕ angle. Gly is also very common in turns because its R group presents little steric hindrance.

2.4.4. Structural Motifs

In biological macromolecules, structural patterns are often repeated across different molecules. The introduction of the term as super-secondary structures or motifs was necessary when it became clear that certain arrangements of two or three consecutive secondary structures (α-helices or β-strands), are present in many different protein structures, even with completely different sequences.

Classic units of structural motifs include the α-α unit where two α-helices are joined by a hairpin bend changing the chain direction by 180°. Another common structural motif is β-β unit with two anti-parallel β-strands connected by a hairpin. The β-α-β motif is formed by two parallel β strands, separated by an α-helix, anti-parallel to them, with two hairpins separating the three secondary structures.

Other motifs of super-secondary structures those are commonly found are α-β-β and β-β-α units [56]. Detection of these common motifs in a new molecule can provide useful clues to the functional properties of such a molecule [47].

In addition to these structural patters, it has been also found that a protein can have repeats of a particular sequence, particularly, if the sequence is vital for the associated function. The Gly-Pro-Hyp tri-peptide repeat of collagen is well known whereas elastin contains as many 15 repeating hexapeptides and 11 pentapeptides in a run [57]. Silk fibroin has 50 repeats of a sequence that is 59-residues long. Recently the Pro-rich submaxillry protein of saliva was found to contain four repeats of a heptapeptide [58].

3. Mussel Adhesive Proteins

The tenacious holdfasts of barnacles and mussels have been long known for their hard adhesive bonds with the underwater marine surfaces. These holdfasts are protein based adhesives exhibit striking materials properties and are formed by extensive cross-linking of protein precursors [59-61]. This cross-linking approach to biomaterial synthesis is shared by glues from mussels, limpets, and kelp, cements from barnacles, oysters, and polychaete worms, coral skeletons, and skate egg shell cases [60, 61]. There is lack of a detailed picture of the bonding schemes employed for material construction in all these cases although large numbers of researchers from various areas of sciences are involved. These attempts have revealed some basic features of the organs and the adhesives. For example, mussel adhesive plaques, post-translational inclusion of 3,4-dihydroxyphenylalanine (DOPA) into the protein is indispensable for subsequent cross-linking and proper adhesion [59-61]. Other interesting properties of the mussel glues include a transition-metal-ion content (e.g., copper, iron, and zinc) [62, 63] up to 100000 times that found in open ocean waters [64].

Biomedical and commercial use of the adhesive properties of these substances have been sought by many groups [65] such as in experimental epikeroplasty and for cellular attachment [66, 67], and in the attachment of osteoblasts and epiphyseal cartilage cells to substrata [68]. The strong adhesive properties have recently inspired a proposed use for these proteins as mucoadhesives for drug delivery [69], and these substances may offer a strong alternative to substances such as chitosans [70].

However, the small yields obtained in the extraction from biological sources and difficulties in the laboratory expression made these proteins luxurious for studies. To overcome this situation many groups have been involved in mimicking the adhesive properties of MAPs into relatively simple and easy to produce synthetic polymers. As has mentioned before, our attempt here is to synthesize peptides and co-polymers of amino acids that are abundant in MAPs, and have been known to contribute adhesive properties. Further insights into synthetic schemes and strategies, however, can only be gained by fully understanding the principles of adhesion used by mussels. This chapter is devoted to this introduction.

3.1. Byssus Adhesive Plaque

Mussels attach to marine underwater surfaces by making a byssus, connective tissue peculiar to mussels. The byssus is an extra-corporeal bundle (thread) of tiny tendons attached distally to a

foreign surface and proximally by insertion of the root into the byssal retractor muscles [71]. It is deposited outside the boundaries of living tissue and contains no cells for maintenance or repair. Byssus functions in providing mussels with secure attachment to rocks and pilings. Byssus mediates contact between very soft living tissue and a very stiff inert material such as rock or ship hull.

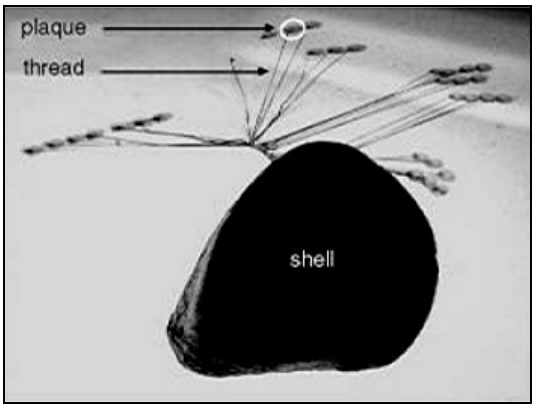

Figure 3 -1: A photograph showing mussels adhering to the glass surface (Reproduced from [72]).

Every individual mussel byssus thread represents a unit of attachment with the distal end bonded to rock and proximal end inserted into living mussel tissue (see Figure 3 -1). Each thread measures between 2 and 4 cm in length and 50 µm in diameter (in *Mytilus edulis* and *M. galloprovincialis*). These threads were dubbed 'collagenous' on the basis of fiber X-ray diffraction [73, 74], hydroxyproline content [75], amino acid composition [76-78] and shrinkage temperatures [79]. The collective evidence presents a strong case, some of the extraordinary properties of byssus are hard to reconcile with typical collagens. These include the high melting temperature, lack of banding patterns and resistance to denaturants, acids and proteases [79, 80].According to several lines of evidence, byssal threads are not uniformly collagenous throughout, i.e., the diffractive and mechanical properties typical of fibrous collagen are best reflected at the stiff distal end of the fibrous collagen are best reflected at the stiff distal end of the thread, whilst the more extensible or elastic proximal end seems to be disordered [81, 82]. This has lead to the suggestion that protein gradients including a collagen gradient occur along the length of each byssal thread [81, 83].

Byssal threads are assembled by the mussel foot from granular precursors in a rapid process resembling polymer injection-molding [84]. When a new thread needs to be made, fiber-containing granules are released from large holocrine glands and conducted through ciliated ducts into the ventral groove of the foot, which serves as the mold. There they coalesce into a thread that is

shaped, and possibly oriented, by peristalsis in the groove. Before being disengaged from the groove, the thread is sized by a protective coating [84].

Scanning electron microscopy and biomechanical studies have established that it is much more than a tether but represents a mechanically graded fiber that is significantly stiffer at the distal end where it joins to the attachment plaque than at the proximal end where it joins to living tissue (see Figure 3 -2). The stiffness in tension at the distal end is 500 MPa in *M. galloprovincialis*, whereas at the proximal end it is only 50 MPa [71]. This ten fold reduction in the distal to proximal direction does not adequately compensate for the remaining mismatches with the rock (25 GPa) or the byssal retractor muscles (0.2 MPa). These can be addressed by additional adaptations vested in the plaque and stem structures [85].

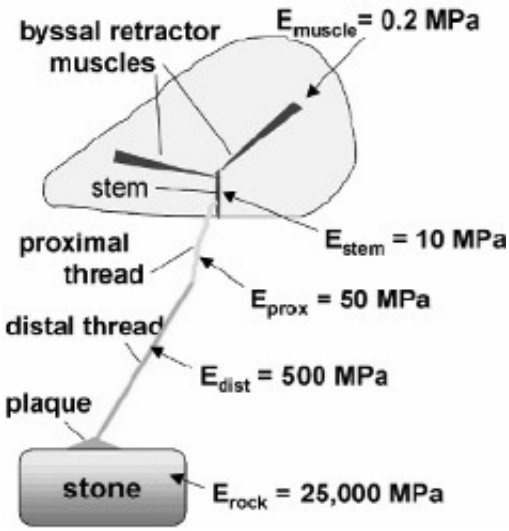

Figure 3 -2: Schematic mussel on the half-shell with one byssal thread showing the incremental steps in stiffness, Ei, from the retractor muscles to the rock. Note the 10-fold decrease in stiffness between the distal and proximal portions of the thread (Reproduced from [86]).

The disparity between the mechanically graded mussel byssal thread and *Anaphe* cocoon silk (spider dragline) may reflect differences in the processing of the two tissues. In the latter case the stiffness is even but still high (10 GPa). Silk is spun from a pair of ampullate glands containing polymer liquid crystals (LC) [87] whereas byssal threads are reaction-injection molded in the mussel foot from mixture of polymer LCs exuded from at least a dozen different pores [84]. The process of generating a solid structure from the molded LCs might be driven by covalent cross-linking and intermolecular metal ligand bridges.

High degree of cross-linking in byssal threads made it insoluble in any extraction method. Fortunately, pepsin digestion does not deter the native triple helical structure of the collagen

domain allowing PreCOL- D, P and NG* collagenous remnants to be compared from each thread segment [88]. These investigations concluded that the distribution of the preCOL-D and -P domains along the thread axis in the byssal threads [85]. PreCOL-D decreases from distal to proximal, whereas preCOL-P, which starts beyond midlength, increases from midlength to proximal.

In addition to ProCOL-P and -D, Ptmp-1 is also found in byssal proteins which is distributed as gradient and increases towards the proximal end of the thread [89]. Ptmp-1 is a protein with two *von Willebrand* type-A domain repeats. In contrast, Gly-, Tyr- and Asn -rich protein dtmp-1 is concentrated towards the distal end. Both of these proteins are present at concentrations of < 10% those of the preCOLs and appear to serve as a matrix between the preCOL fibers.

A thin protective protein coating, dubbed *mefp-1* (*mytilus edulis foot protein* -1), protects the threads from abrasion by sand as well as degradation by bacteria and other microorganisms. The presence of *mefp*-1 to *mefp*-5 is also located at the end of each thread, in an adhesive plaque, allowing plaque to anchor to wet solid surfaces [6].

3.2. Mytilus Edulis Adhesive Proteins

3.2.1. Mytilus Edulis Adhesive Proteins -1 (mefp-1)

Mytilus edulis adhesive protein-1 has a molecular weight of 115 kDa based on mass spectroscopy [11] and of 130 kDa on the basis of gel chromatography [12]. *Mefp*-1 protein is mainly built from two building blocks 71 deca-peptides composed of the residues Ala^1-Lys^2-Pro^3-Ser^4-Tyr^5-Pro^6-Pro^7-Thr^8-Tyr^9-Lys^{10} and 12 hexa-peptides containing Ala^1-Lys^2-Pro^3-Thr^4-Tyr^5-Lys^6 as shown in Figure 3 -3.

The deca-pepetide part contains three post-translation modifications. First being at the 6th residue in which a Pro converts to dihydroxyproline, second at the 7th position where a Pro gets modified into a hydroxyproline. The third modification which more important, as we will see in the following sections, leading to a conversion of Tyr to 3,4-dihydroxyphenylalanine or DOPA. Tyr at the 5th position in the hexa-peptide also gets modified into DOPA. These hydroxylated amino acids constitute the strikingly high percentage of *mefp*-1 protein.

---

* PreCOL is a block copolymer that contains a central collagen domain, which occupies roughly half of the preCOL. Its other domains are the N- and C-terminal His-rich domains (HIS), the flanking domains, and an acidic motif. The collagen domains are highly homologous in the three known variants, preCOL-P, -D, and -NG in which the postscripts P, D and NG denote proximal distal and non-graded respectively.

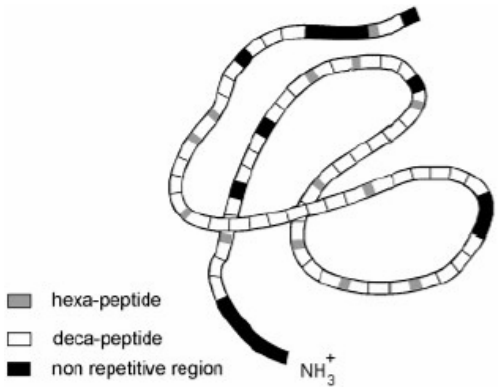

Figure 3 -3: The location of the deca- and hexapeptide on the backbone of mefp-1 based on DNA analysis (Reproduced from [11]).

Like the deca and hexa peptide the N-terminus non-repetitive domain is hydrophobic and rich in Lys residues. Between different populations of mussels, the composition of the decapeptide itself remains roughly the same. The presence and location of the Tyr and/or DOPA and Lys in this sequence is completely invariant.

The origin of hydroxyproline and DOPA in *mefp*-1 is difficult to explain with the exception of post translational enzymatic hydroxylation. In the pioneering study, Henkens and co-workers characterized the enzyme modifications of 20 repeats of the original peptide sequence (Ala-Lys-Pro-Ser-Tyr-Pro-Pro-Thr-Tyr-Lys) using mushroom *tyrosinase*. It has been long known that mushroom *tyrosinase* can introduce site-directed modifications. It catalyzes both the hydroxylation of monophenols such as Tyr, including protein tyrosyl groups and oxidative dehydrogenation of *o*-diphenols [90]. In the presence of high concentrations of ascorbate the reaction can be limited to hydroxylation as the *o*-quinone is reduced back to the *o*-diphenols by ascorbate. Mushroom *tyrosinase* oxidizes Tyr-26 in the β-chain of insulin at the rate 13 times faster than Tyr-16 which is thought to be buried [91]. Henkens and co-worker suggest that there are two tyrosyl reactivities in the 20-mer analogue of the polyphenolic protein. These vary in their rate of hydroxylation by a factor of about 20. The sequence of the hydroxylated peptide derived from the 20-mer by trypsinization indicated that Tyr-9 is almost completely converted to DOPA by *tyrosinase*, while Tyr-5 is only marginally modified in the peptides. Perhaps Tyr-9 is the more accessible of the two in the folded structure. This pattern of hydroxylation is similar to that of the natural (wild-type) protein, expect that the levels of Tyr-5 to DOPA conversion at 3h in the 20-mer are somewhat lower that those in polyphenolic protein.

Although hydroxyproline is erroneously assumed to be unique to collagenous proteins, in the polyphenolic protein most or all of the hydroxyproline remains associated with the Gly-deficient

collagenase-resistant fragment. The collagenase labile moiety may contain a collagen-like domain such as that in *torpedo acetylcholinesterase* [92] and *alvrolar glycoprotein* [93]. Waite detected DOPA in another protein (*periostracin*) also from Mytilus, but there are no other known reports of its natural occurrence in that protein. The role of the DOPA in protein is still a matter of speculation [94]. Recent studies are worth mentioning in light of their relevance to adhesion:

a) *o*-diphenols (including DOPA) and *o*-quinones can irreversibly displace water from a surface [95].

b) *o*-diphenols are readily oxidized to *o*-quinones which undergo nucleophilic addition reaction with primary amines such as lysine via Michael addition [96].

c) Bis and tris complex of DOPA with multivalent metal ions present in the marine environment. i.e., copper, Iron, manganese and zinc [72, 97].

In order to make intimate contact with a surface, the polyphenolic protein needs first to displace water molecules from that surface whether it relies on DOPA residues to accomplish this remains to be shown. For case (b), some kind of protein cross-linking in the adhesive plaque is suggested by the insolubility of material in all but hydrolytic solvents [79].The formation of DOPA quinine is known to be catalyzed by a DOPA oxidase in the foot and byssal secretion of the mussel [98-100], DOPA-Lys cross-links have yet to be isolated, Ketamura and coworker [101] observed that, the proton of Tyr may be effective at pH 11.2. The NOESY spectrum obtained by NMR spectroscopy showed that a Lys residue lay close to a Tyr residue, within at least 5Å. Although these residues can be adjacent to each other, it is clear that their side chains are close. This means that a Lys residue and a Tyr residue can react not only between molecules but also within the molecule to form the *o*-quinone linkage after the modification of *tyrosinase*. Formation of covalent cross-links in the polyphenolic protein could serve to improve the cohesive performance of the substance.

With regards to third point, the adhesive properties of DOPA have long been speculated as to direct interactions between the catechol side chains of DOPA and the surface to which they are adsorbed. It is known that the catechol has strong binding affinity to several metal ions particularly Fe (III). The protein has the capacity to bind between 50 to 75 tightly complexed ferric ions depending on whether it adopts a tris- or bis-(catecholato) coordination mode. *Mefp-1* is applied to the byssus as a lacquer-like coating; the addition of ferric iron may render it an “iron-clad” finish and contribute to the notorious intractability of this material. In the presence of ferric iron, *mefp*-1 forms an extremely complicated macromolecular coordination of ferric ion. Notwithstanding the current study that *mefp*-1 behaves very similarly to low molecular weight catecholates like the siderophores, the protein can solubilize ferric iron even when resent in polynuclear hydrolytic species inaccessible to simple complex agents.

In previous studies, the interaction of ferreascidin, a 10 kDa DOPA glycoprotein from the blood cells of the *ascidian pyura stolonifera*, with ferric ion revealed that the protein adopts a bis (catecholato) coordination mode with possibly one Tyr ligand [102]. Subsequently, it was shown that ferreascidin binds iron (III) as novel bi-and trinuclear cluster [103].

S. W. J. Taylor found that peptides derived from *mefp*-1 bind to Fe (III) in bis- and tris-(catecholate) coordination [104]. Using spectrophotometric titrations, electron paramagnetic resonance (EPR) and resonance Raman spectroscopy, Waite and co-workers [105] studied the bis and tris complex of DOPA with multivalent metal ions present in the marine environment may also contribute to cross-linking (see section 3.3).

DOPA probably owes its existence to a protein-specific 3-*tyrosylhydroxylase*. An examination of sequences reflected an enzyme preference for Tyr in the sequence Hyp-Hyp-Thr-Tyr or Pro-Pro-Thr-Tyr, depending on the priority of hydroxylations [5]. Tyr is present almost entirely as DOPA in such sequences. Conversion to DOPA is lowered to 50% in the sequences Lys-Pro-Thr-Tyr and Lys-Pro/Hyp-Ser-Tyr. Hydroxyproline is detected as two *trans* isomers in sequences atypical of collagen. This distinguishes the polyphenolic protein along with elastin [57] and geographotoxins [106, 107] as the only known animal protein with hydroxyproline in non-collagenous sequences. The putative 4-prolylhydroxylase demonstrates specificity for the sequences Pro-Ser / Thr-Tyr and Pro-Ser / Thr-DOPA depending on the order of hydroxylation. Additional specificity is indicated by the fact that unhydroxylated Pro is never detected in the second position of the sequence Hyp-Hyp-Thr-DOPA.

From long decades several groups are trying to solve the conformation of the *mefp*-1 protein using different analytical data. Protein residues contain (Ala, Lys and DOPA) with strong α-helix potential and others (Thr, Tyr and Ser) with β-sheet propensities. The high frequency of imino acids, however, is theoretically capable of breaking either of the above conformation or imposing a poly(L-Pro) type-II helix [9]. The non-collagenous hydroxyproline rich glycoproteins from the cell walls of algae [108, 109], plants [110] and in some bacterial capsules [111] probably do have some poly(L-Pro) type-II helical structure [112].

Using model peptide obtained by *E. coli* expression system, which has the similar structure to that of the native adhesive protein from a marine mussel Kitamura and co-workers [101] studied the Circular Dichromism (CD) spectrum, which indicated that about 80% of this peptide existed in a random coil structure. The change in the CD spectrum with pH indicated that some structural or conformational changes occurred under these conditions due to electrostatic repulsion among the ions, or the shielding effect due to the ions of inorganic salts. CD studies in various solvents and at various temperatures of the glue protein and non-hydroxylated analog, which consists of 20 repeats of the peptide sequence Ala-Lys-Pro-Ser-Tyr-Pro-Pro-Thr-Tyr-Lys were obtained in the

far-UV wavelength range under a variety of condition. The spectra of the glue protein in a pH 7.0 and 0.6 M guanidine hydrochloride found to be nearly the same as the spectra of non-hydroxylated 20-mer. Since there was no noticable change in the different solutions, the effect of temperature was examined. The spectrum was found to change systematically with the mean residue ellipticity becoming more negative in the 215-230 nm region and less negative in the 200-215 nm region as the temperature was increased.

The spectral analysis was performed by least-squares fits to model data taken from Chen et. al., [113] and Bolotina [114], the result of the analysis of the protein in buffer containing NaCl and KCl at 25°C suggest that the protein is 65-75% random coil structure as well as buffer containing 6.0 M guanidine hydrochloride at 25°C did not appear to alter the structure significantly as reflected in the estimates of 71 % and 79 % for the random structure.

The non-hydroxylated 20-mer exhibited CD spectra nearly identical to those of the natural glue protein in all buffer. Consequently using 20-mer as a model and evaluated its amino acid sequence by the Chou and Fasman rules of analysis in order to correlate the predicted structure to the estimated structure obtained from the analysis of the CD spectra. For the decapeptide (Ala-Lys-Pro-Ser-Tyr-Pro-Pro-Thr-Tyr-Lys) the analysis suggest that there is little probability of formation of any β or α structures while the four-amino sequences (Lys-Pro-Ser-Tyr) and (Pro-Pro-Thr-Tyr) are sequences with a good probability for forming β turns. Chou and Fasman [115] analysis which predicts little α and β structure is supported by the analysis of the CD spectra, the presence of only 18.6 % β turn structure is detectable on the basis of the CD spectrum, the similar spectra obtained for the hydroxylated and the non-hydroxylated forms suggest that the degree of hydroxylation does little to influence secondary structure of the protein in solution [116].

Gert Frens and co-worker studied the conformational of *mefp*-1 protein under the physiological conditions [117] using dynamic light scattering instrument. They experimentally obtained a hydrodynamic radius of *mefp*-1 as 10.5 ± 1.1 nm which can be explained by two different models. *Mefp-1* on larger length scales resembles a random coil but that its decapeptide segments may have a helical appearance.

Such helical appearance of the decapeptide resulting from the Pro content would make its contour length shorter than the 3.6 nm according to the virtual chain model (9.4 times the distance between two α-atoms of a peptide chain was 0.38 nm). The approximate numbers of decapeptides contain was 90 and the segment length per decapeptide was 2.7 nm.

The condition chosen in these experiments differ significantly from each other, which makes it difficult to draw final conclusion on the native conformation of *mefp*-1.

3.2.2. Possible Applications of mefp-1

The mussel adhesive protein tends to bind to practically any surface it encounters; the researchers believe that the new compound can similarly attach to other surfaces used for medical devices, including stainless steel and plastic. Several attempts are being made to make biomedical and commercial use of the adhesive properties of these substances. The adhesive properties of certain types of biopolymer can be used to increase the residence time of orally or nasally administered drug, understanding of the molecular process underpinning such 'mucoadhesive' phenomena will help in the optimal design of delivery system. Jochen Schnurrer [69] observed that MAP impresses with an excellent mucoadhesive bonding strength compared with the hitherto golden standard of poly(acrylic acid) derivatives, such as polycarbophil. It may even be speculated that the mucoadhesion of MAP or MAP like polypeptides may still be improved by better purification or preparation methods. But it is also appears that non-oxidative conditions for manufacturing and storage of MAP-based drug delivery systems will be necessary to fully exploit its mucoadhesiveness, which may be a certain disadvantage compared with other mucoadhesive polymers. Also the mucoadhesion interaction of *mefp*-1 protein has been studied by S. E. Harding [118] despite this impressive demonstration *mefp*-1 would be of limited practical use since protein-based mucoadhesives would be rapidly eaten away by the enzymes of the digestive tract, sedimenting at 7000 s also represents too strong an interaction with little opportunity for control. However, this provides the stepping stone for consideration of the use of polycationic polysaccharides that are not attacked by the digestive system and can be readily manipulated to control the extent of complexation.

MAP has seen recent interest in the biomedical community as a tissue adhesive. The protein has also been used in experimental epikeroplasty in laboratory animals, The preliminary study indicates a potential adjunctive role for MAP in epikeratoplasty, On the basis of clinical examinations and histopathologic studies J. B. Robin and co-workers [66] observed that there is no untoward effects of the adhesive on the donor lenticules or host keratotomics corneal tissue. This study marked the first *in vivo* use of this material in adhering ophthalmic tissue planes and as an adhesive agent to increase cellular attachment to substrate.

So far, this compound has not undergone animal or human testing, nevertheless, if all goes well in future studies the compound could be used in medical devices in coming years. The compound could be used as bone glue as well as tooth coating to prevent dental plaque, which is caused by bacterial infection. Also it could be used in the shipping industry as an environmentally friendly alternative to toxic antifouling coatings currently used on boats to protect against mussels, barnacles and related organism.

3.2.3. Mytilus Edulis Adhesive Protein-2 (mefp-2)

Mefp-2 is a second major DOPA protein of the blue mussel and it appears to be a structural component exclusively of the plaque, contributing up to 25% of plaque protein [6]. It is Cys rich, tendemly repetitive 45 kD protein. It is multi-domain protein, with short, acidic, DOPA containing N-and C-terminal regions and a large central domain constrained by quasi-periodic internal disulphide bridges to compact conformation resistant to proteolytic degradation [119]. The peptide motifs of *mefp*-2 are quite unlike those of any other known structure are premature, because in tendemly repetitive proteins, the correct order of short peptide motifs over an entire protein cannot be deduced by standard peptide mapping techniques, and it is debatable whether all members of the heterogeneous *mefp*-2 family share identical subsets of motifs, Nevertheless the sequence of *mefp*-2 contains Pro and/or Gly rich segments that alternate with sequences containing none of these β-turn associated residues, and it is therefore consistent with conformational models, such as the β-meander postulated for certain Gly and Tyr rich *Schistosoma* eggshell protein [119].

The composition of *mefp*-2, incorporating Cys and DOPA, implies some role involving the stabilization of the plaque matrix by covalent disulphide and quinine derived cross-links. *Mefp*-2 can from oligomeric aggregates that might be stabilized by rearrangement of disulphide bonds to form inter-molecular cross-links. If *mefp*-2 indeed constitutes 25% of plaque protein, then it would incorporate 90% of the plaque Cys residues and thus would be virtually its own sole potential disulphide cross-link partner. The DOPA residues might then serve to cross-link the resulting disulphide-linked *mefp*-2 homopolymer to other protein component of the plaque [6].

Consideration of the amino acids composition of *mefp*-1 and 2 and of the terminal adhesive plaques of byssal threads suggests that *mefp*-2 makes up about 25% of plaque protein, whereas *mefp*-1 content is about 5%. *Mefp-2* has minimal sequence homology with known structural proteins and may have a properly folded structure in the plaque matrix.

3.2.4. Mytilus Edulis Adhesive Protein-3 (mefp-3)

Mytilus edulis adhesive protein-3 (*mefp*-3) is a small (6 kDa), non-repetitive protein. *Mefp-3* resembles to other byssal precursor proteins in basicity and DOPA content. Specific variants of the *mefp*-3 family may be preferentially deposited onto glass, stainless steel and polyethylene. Mass spectrometry with time-of-flight suggests that *mefp*-3 is the only detectable protein family near the plaque-substrate interface [120]. It is also Arg rich and many of these residues are modified to 4-hydroxy-L-arginine. At least 10 electophoretic variants of *mefp*-3 can be detected in

individual mussels. Only one of these has been completely sequence, is known as variant F [120]. 4-Hydroxyarginine has been previously detected only as a free amino acid in the seeds of vetch, lentils and in tissues of sea anemones and sea cucumbers, but never as a part of the primary structure of proteins neither its function nor the reason for its incomplete conversion from Arg in *mefp*-3 are known at this time.

DOPA suggests some interaction between hydroxyarginine and DOPA, hydrogen bonding that blocks enzyme access to the peptide bond (see Figure 3 -4). Four HO-Arg-DOPA pairs exist in *mefp*-3. Like DOPA, Arg and presumably its hydroxylated derivative is also an asset for the molecular interactions indispensable for adhesion [121].

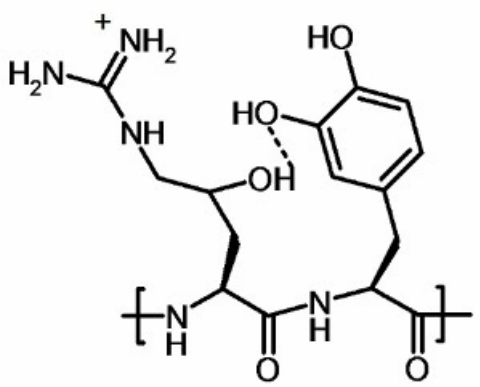

Figure 3 -4: The intermolecular H-bond between DOPA and hydroxyarginine suggesting that this conformation might protect the underlying peptide bond from trypsin attack.

DOPA engages in H-bonding, metal complexation, π-π and π-cation interactions. Hydroxyl-Arg is capable of forming six H bonds as well as π-π and coulombic interaction, such functionality is well adapted for organometallic complex [105, 122] on metal and mineral surfaces; π-π and π-cation interaction are strongly suggested on aromatic surfaces [123]. Arg can be a hydrogen donor in as many as 5 hydrogen bonds in which the acceptors are usually backbone carbonyl groups [124]. It is also involved in planar parallel stacking with aromatics that does not impede the hydrogen bonding capacity of Arg [125], for these reasons perhaps Arg rich proteins bind polyphenols avidly and are rather readily insolubilized by them [126].

Seven additional sequences of *mefp*-3 are predicted from *c*DNA clones [127]. In contrast to other mussel adhesive proteins such as *mefp*-1 and 2, which have large number of highly conserved, tendemly repeated peptide motifs, the function of *mefp*-3 in byssal adhesion is unknown [121].

3.2.5. Mytilus Edulis Adhesive Protein-4 (mefp-4)

The *mefp*-4 protein belongs to this family of proteins with a mass of 70-80 kDa. All have a common N terminus and contain elevated levels of G, R, and H. It has been assumed that *mefp*-4 is located in the bulk adhesive of the plaque. Occurrence of the DOPA in this protein is 5 mole% [120].

3.2.6. Mytilus Edulis Adhesive Protein-5 (mefp-5)

Mytilus edulis adhesive protein-5 (*mefp*-5) is an adhesive protein derived from the foot of the common mussel, *Mytilus edulis*, and deposited into the byssal attachment pads [7]. Purification and primary structure of *mefp*-5 was determined by peptide mapping and *c*DNA sequencing. The protein is 74 residues long and has a mass of about 9500 Da. *Mefp*-5 composition shows a strong bias for non-aromatic amino acids, Lys and Gly represent 65 mol% of the composition. More than a third of all the residues in the protein are post translationally modified by hydroxylation or phosphorylation. The conversion of Tyr to DOPA and serine to *o*-phosphoserine accounts for the hydroxylation and phosporylation [7].

At over one in every four amino acid, contains the highest level of DOPA have been found in *mefp*-5. DOPA and the abundance of basic residue are reminiscent of other characterized byssal precursors particularly *mefp*-3, but detection of a significant number of phosphoserine residues distinguishes it. Seven or eight Ser residues in *mefp*-5 are phosphorylated. The precise location of the non-phosphorylated Ser is unknown [128]. *Mefp*-5 joins a growing number of phosphorylated extracellular proteins with a structural role. These include salivary statherins, osteopontins, dentin phosphoryns, epidermal precursor profilaggrin and certain protein from mollusk shells. In most of these, the phosphoserines are presumed to have been shown to bind calcium and a mineral surface [129, 130]. This closely matches similar sequences in statherin, β-casein and osteopontin that are mineral and calcium ion-binding.

Recent studies with synthetic DOPA-containing random copolymers have revealed that high concentrations of DOPA are critical for wet adhesion. Perhaps the high mol % of DOPA in the precursors, *mefp*-3 and 5 is an adaptation to their interfacial role. DOPA is not the only functionality exploited for adhesion. Phosphoserine would be an ideal modification for adhesion to that substrate, to which DOPA-rich proteins shows only moderate binding [131, 132].

3.3. Role of DOPA in Mussel Adhesive Proteins

One of the defining characteristics of MAPs is the presence of L-3,4-dihydroxyphenylalanine (DOPA), an amino acid that is formed upon posttranslational modification of Tyr [133]. Recent studies suggest that DOPA is primarily responsible for the exceptional adhesives characteristics of MAPs [132, 134]. DOPA group has a double role in marine adhesion, it is important for both the cohesive and adhesive properties of the mussel's adhesive. The adhesive properties of DOPA have long been speculated as being due primarily to direct interactions between the catechol side chains of DOPA and the surfaces to which they are adsorbed. As mentioned earlier, the high content of transition metal content in the mussel adhesives is also surprising [97]. UV/Vis absorption spectroscopic studies with the DOPA containing peptide models Ac-Ala-DOPA-Thr-Pro-$CONH_2$ (AdopaTP) and Ac-Asn-DOPA-Arg-Gly-$CONH_2$ (NdopaRG) [135] showed strong binding of the DOPA catechol-like side chain to Fe^{III}, but no interaction with Cu^{II}, Zn^{II}, or any other divalent transition-metal ion [72].

Catecholato iron (III) complex are widely distributed in biological systems in which at least three functional categories of these compounds are distinguishable. The first and best characterized examples are the siderophores, low molecular weight catecholamides, which are secreted by bacteria to selectively sequester iron [136]. The second consists of enzymes with ferric ion-containing active sites that bind low molecular weight catecholes either as substrates, e.g., *catechol dioxygenases* [137] or as products e.g., *tyrosine 3-monooxygenases*, [138] or as inhibitors with useful spectroscopic properties, e.g., *soybean lipoxygenases* [139]. A third emerging area is the coordination chemistry of high molecular weight proteins and peptides with catecholic functional groups present in the primary structure as peptidyl (3,4-dihydroxyphenyl)-L-Ala (DOPA). Examples of peptidyl-DOPA come from both artificial systems such as radiation- or radical-damaged proteins [140, 141] or mutant recombinant *ribonucleotide reductase* [142] and natural systems in which DOPA is formed as a post-translational modification of Tyr.

Certain marine invertebrates produce DOPA containing proteins which are believed to fulfill a range of functions including adhesion, sclerotization, wound repair, etc. Perhaps many of these functions result from properties attributable to the tendency of DOPA residues to oxidize and cross-link in a process known a squinone tenning [61]. Presence of high concentration of metal ions in the proximity of these proteins both intracellular (such as in ascidian blood cells) and extracellular (as in mussel byssus) implicates them as non-covalent cross-linking agents. This is particularly true of iron (III), which forms catechol complexes of exceptionally high stability.

Iron (III) binding to the DOPA-containing *mefp*-1 has been studied by J. H. Waite and co-worker using spectrophotometric titration, electron paramagnetic resonance (EPR) and resonance Raman

spectroscopy [105]. According to those studies, at pH 7.0, purple (λ_{max} = 548 nm) and pink (λ_{max} = 500 nm) forms of the iron-protein complex existed. The pink form was favored at high DOPA:Fe ratios and the purple was at low DOPA:Fe ratios. Resonance Raman spectroscopy of these two forms demonstrated that the chromophores were ferric catecholate complexes. EPR spectra of both forms of the protein measured at the same iron concentration reveal a resonance ($g \approx 4.3$) of approximately four times the intensity in the spectrum of the pink, complex competed with that of the purple form. On the basis of the evidence, a model for the purple form of the ferric *mefp*-1 involving bis (catecholato) coordination of ferric ions with most of the iron (III) complexed as EPR-silent μ-oxo- or μ-hydroxo-bridged binuclear clusters was suggested. In the pink form the ferric iron is EPR-active, mononuclear and present in high-spin tris (catecholato) complex. This bis and tris-complex of DOPA with multivalent metal ions present in the marine environment also thought to contribute to cross linking of MAPs.

Jannifer M and J J. Wilker investigated role of metals in cross-linking in marine mussel adhesives and from penetration tests using metal ions [97]. There were no significant differences seen between the chloride and nitrite salt of any metal ion and the force values presented for these ions were found to be averages from both salts. A striking observation was that the protein extract containing Fe^{3+} yielded the highest resistance to penetration. The majority of metal ions tested did not bring about any curing beyond that of the water control. The level of hardening induced by Ca^{2+}, Cu^{2+}, H_2O_2 and tert-butyl hydroperoxide (BHP) were slightly greater than that of the water control but not nearly high as that found for Fe^{3+}.

Additionally, with the help of EPR and IR spectroscopic methods, J. J. Wilker provided evidence for metal-DOPA interactions in mussel adhesive plaques [72]. An adhesive film was produced by iron curing of extracted protein. In the presence of air, iron oxidized both extracted protein and peptide models to yield product that contain organic radicals. The coordination environment of iron in these studies were gained from EPR spectroscopy in which the Fe^{III} of plaques did not resemble bis[Fe(DOPA)$_2$], bonding. The adhesive film prepared by reaction of iron and protein displayed a UV spectrum similar to that of the tris[Fe(AdopaTP)$_3$] model. Only the tris[Fe(AdopaTP)$_3$] complex underwent oxidation to yield a radical upon exposure to air. Fe^{III} brings about curing of adhesive extracts more than other ions [97]. Thus, iron remains as a key reagent in protein cross-linking within adhesive cross-linking and synthesis. Therefore, it was proposed that the iron center in mussel plaques cross-links three DOPA residues as shown in Figure 3 -5.

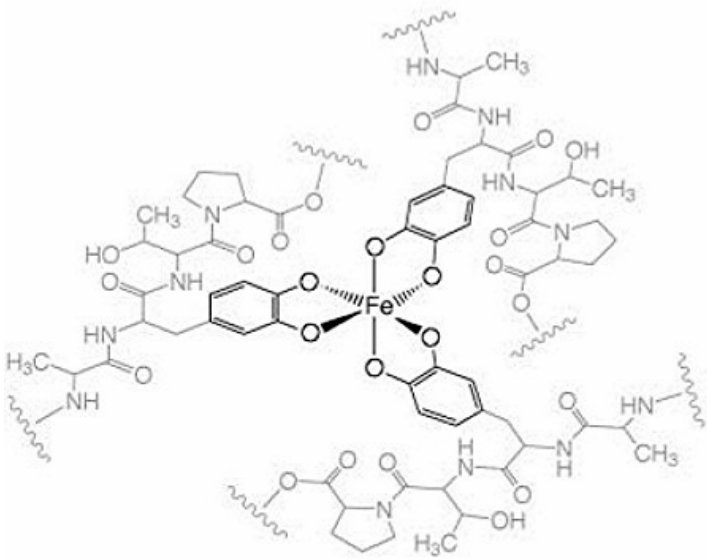

Figure 3 -5: Proposed mussel adhesive metal-protein cross-link (Adopted from [72]).

Ooka and Garrell characterized the adsorption of peptide models* of *mefp*-1 to colloidal gold using surface enhances Raman spectroscopy (SERS) [134]. According to their studies, the peptide adsorb primarily through deprotonated catecholate oxygen atoms of the DOPA residue and also interact with the surface through one or both of the primary amine group. The orientation of the DOPA residue on the gold surface in which the plane of the aromatic ring is perpendicular or tilted on the surface (not flat) and is coordinated to the metal through the catechol oxygen atoms (see Figure 3 -6).

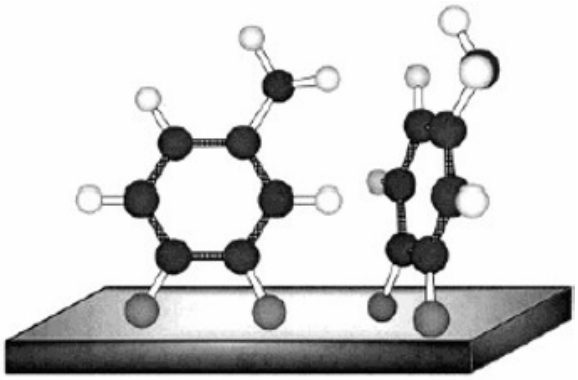

Figure 3 -6: The proposed orientation of the deprotonated DOPA side chain on gold (front and side views). Adopted from [134].

* such as Pro-Pro-Thr-DOPA-Ala which is modified sequence of second half of decapeptide of *mefp*-1.

Comparison of the SER spectra of the peptides with that of *mefp*-1 revealed that the peptides are valid methods for mussel protein adsorption on colloidal gold. Like the peptides, *mefp*-1 coordination to the gold surface through the catechol oxygen atoms of the DOPA plays a significant role in *mefp*-1 adsorption and overall adhesion.

It is known that catecholes have strong binding affinities to Fe (III), Cu (III) and Ag (III), and these results suggest that *mefp*-1 may exploit the DOPA residue to bind the metal surface other than gold.

MAPs are initially secreted as fluids that undergo an *in situ* hardening reaction and DOPA residues are also believed to participate in the intermolecular cross-linking reactions that lead to the formation of a solid adhesive plaque [143]. The cross-linking reaction are not fully understood, evidence suggests that oxidation of DOPA to DOPA-quinone or DOPA-semiquinone by *catachol oxidase* enzyme (or also by nonenzymatic means) can lead to cross-linking either with other DOPA residues by a radical mechanism or with an side chain amino group of Lys by Michael addition mechanism. Although all attempts to detect this product to date have been unsuccessful, the importance of the Michael addition in quinine chemistry has generated strong support for Lys cross-linking in MAPs [143, 144].

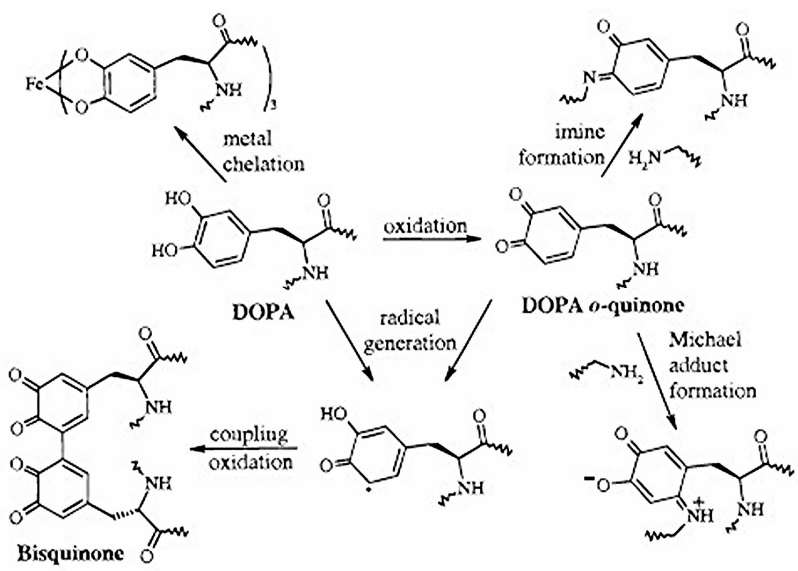

Figure 3 -7: Proposed cross-linking reaction pathways for peptidyl DOPA and DOPA o-quinone residues. (adopted from [132]).

With the help of low molecular weight DOPA model compound and mass spectroscopy, Deming and co-worker [132] recently confirmed that the catechol functionality is primarily responsible for moisture-resistant adhesion and that the oxidized *o*-quinone functionality is primarily responsible for cross-linking.

Yamamoto and co-workers [145] suggested a role of lysyl oxidase (LO) induced cross-linking of the collagenous substances responsible for the underwater adhesion of the mussel species. Using LO-mediated insolubilization reactions of the Lys-containing polypeptides, which have an elastine like composition enriched in Ala and Lys residues and the synthetic marine adhesive proteins. The insolubilization occurs in the following order (i) oxidation of the ε-amino groups of the Lys residues in the polypeptide side chains and (ii) cross-linking formation between the polypeptides. The former is the enzymatic and the latter is a chemical process. Together the result from the NBS-induced insolubilization experiments, the letter process is mainly affected by the dissociation state of the ε-amino group in the Lys residues. The collagen and elastin (tropoelastin, the soluble precursor of elastin) were that only two kinds of physiological substrates known, mainly in vertebrate [146]. The mussel byssus is composed of adhesive proteins and three kinds of collagen like proteins [147]. The LO activity exited in the mussel foot and that the mussel adhesive proteins were in fact insolubilized via the LO-catalyzed oxidation of the Lys residues. This indicated that LO is a possible candidate involved in the cross-linking of the collagenous substances responsible for the under water adhesion of the mussel species.

3.4. Availability of Mytilus Edulis Adhesive Proteins - 1 to 5

Adhesive proteins, *mefp*-1 to 5 are difficult to produce biochemically as well as it is very difficult to extract them from the biological source (i.e., marine mussels) because of poor yields. This situation makes synthetic approaches unique and demanding for accessing more quantities of these proteins. As it has been shown, certain residues like DOPA play a very important role in the adhesive properties of MAPs thus making it a plausible constituent of the synthetically prepared adhesive polymer.

Synthetic methodologies offer tailored possibilities for synthesizing adhesive proteins and one could make stable, easy to produce and probably amplified characteristic. Peptidomimetics of protein of interests offer conformationally restrained structures that can be more effective. Also, addition of hydrophobic residues and/or replacement of amide bonds results in better transport properties through cellular membranes. In addition to that isosteres, retro-inverso peptides, cyclic peptides and non-peptidomimetics all reduce the rate of degradation by peptidases and other enzymes.

Before getting into details of synthetic strategies used in this thesis, it is better to review some common building blocks as well as some earlier attempts of making these polymers. A general introduction to the polymer chemistry is also given in latter sections.

3.5. Dipeptide Building Blocks

As shown in chapter 2, β-turn is one of the important folds commonly found in peptides and proteins. Peptide analogues having a β-turn are commonly used for synthesizing longer chain of amino acids. A β-turn dipeptide building block could be effectively used for this purpose. One such common dipeptide building block is azabicycloalkane.

The general method for the synthesizing thiazabicycloalkane amino acid involves condensation of ω-formyl α-amino acid analog with a Cys derivative to provide a thiazolidine intermediate that can be treated directly under conditions to effect intramolecular *N*-acylation and furnish the bicyclic lactam (see Scheme 3 -1). Bicyclic dipeptide isosterrs like beta turn dipeptide [148, 149] contains the torsions ϕ_i and ψ_{i+1} and the side chain orientation of a dipeptide unit. The central amide bond is fixed to the *trans* orientation and βI/βII equilibrium.

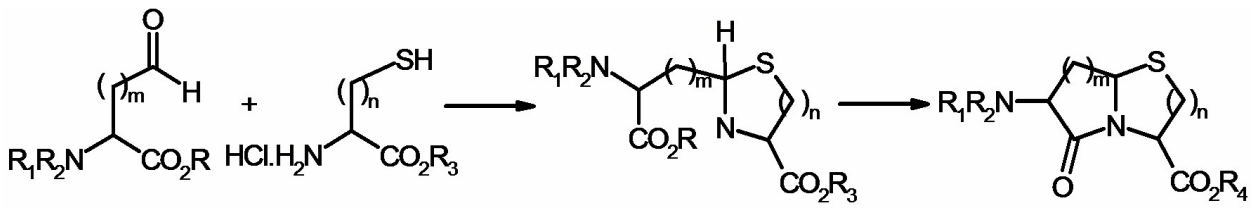

Scheme 3 -1: Commonly used strategy for the synthesis of thiazabicycloalkane amino acid analogues and the major product of this reaction. Further description of R, R_1, R_2, R_3, m and n is given in Table 3 -1.

Table 3 -1: Various combination of R, R_1, R_2, R_3, m and n and their respective product from scheme 3-1.

Sr. No.	m	n	R	R_1	R_2	R_3	R_4	Major Product
1.	1	1	Bn	H	Boc	H	Me	(2S, 5R, 7R)-**1**
2.	1	1	Bn	H	Cbz	Me	Me	(2S, 5R, 7S)-**1**
3.	1	1	Bn	H	Cbz	Me	Me	(2R, 5S, 7S)-**1**
4.	2	1	CH_2	CH_2	Cbz	H	Me	(2S, 5R, 8R)-**2**
5.	2	1	$(CH_2)_2$	TMS	Pht	Et	Et	(2R, 5S, 8S)-**2**
6.	2	1	CH2	CH_2	Cbz	Me	Me	(2R, 5S, 8S)-**2**
7.	2	1	Me	Me	Pht	H	H	(2R, 5S, 8S)-**2**
8.	2	1	CH_2	CH_2	Cbz	Me	Me	(2S, 5R, 8S)-**2**
9.	3	1	H	H	Pht	Me	Me	(2R, 5RS, 9S)-**3**
10.	3	2	H	H	Pht	Me	Me	(2S, 6S, 10S)-**4**

Yields of bicyclic products can be controlled by employing enantio pure amino acid substrates in the condensation/lactam cyclization sequence. In the case of 5,5- and 6,5-bicyclic systems, the major diastereomer that is ordinarily formed possesses the ring-junction hydrogen and the Cys derived carboxylate, on the same side of the thiazolidine ring.

The ω-formyl α-amino acids were protected to avoid intramolecular cyclization in those cases that could lead to the formation of dehydroprolines and dehydropiperidines. Although pthalimides were initially used for amino protection, *N*-(Cbz)oxazolidinones have been used more recently to protect both the amine and acid group, thereby preventing intramolecular cyclization and simultaneously active the α-carboxylate for intramolecular lactam formation [150-152]. The hydroxyl methyl group that resulted from ring opening of the *N*-(Cbz)oxazolidinone was subsequently removed under mildly alkaline conditions.

3.5.1. 7-thiaindolizidiene Amino Acid and Bicyclic Thiaindolizidiene

Nagai and co-workers had introduced the 7-thiaindolizidiene amino acid, **5** [148].

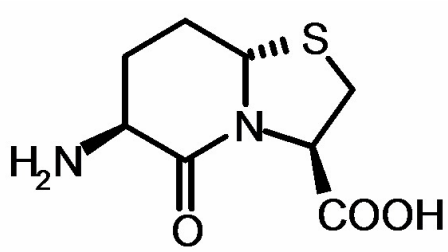

Figure 3 -8: 7-thiaindolizidiene amino acid.

It is a bicyclic dipeptide thiazolidine derivative with fixed conformation simulating that of the two central amino acid residues in type II β -turn had been synthesized **5** starting from L-Glu and L-Cys which showed super-imposable conformation of type II β-turn on that of D-Ala-L-Pro residues [148]. The thiazo[4.3.0]-alkane amino acid was stable under physiological condition and was introduced into various peptides and biologically active molecules [151, 153, 154].

R. L. Johnson and co-workers [150] studied the two compounds, **6** and **7**, containing bicyclic thiazolidine lactam constraints capable of mimicking a type-II β-turn and which are able to modulate dopamine receptors. Both peptidomimetics, **6** and **7**, found to be more effective than Pro-Leu-Gly-NH_2 (PLG) in enhancing the binding of the dopamine receptor agonist 2-amino-6,7-dihydroxy-1,2,3,4-tetrahydronapthalene (ADTN) to dopamine receptors.

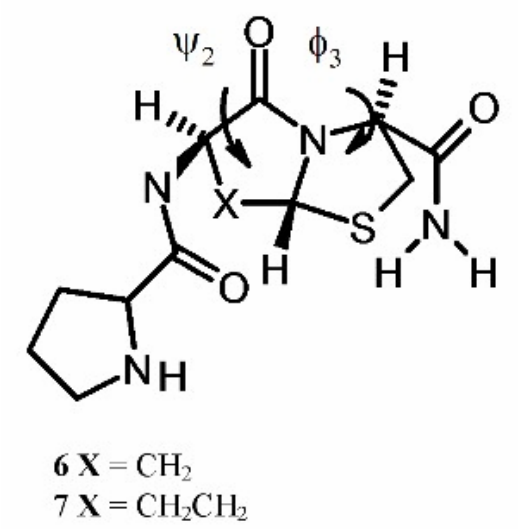

Figure 3 -9: Bicyclic thiazolidine lactams **6** and **7** as possible peptidomemetics of PLG.

Both of these bicyclic systems restrict two, ψ_2 and ϕ_3, of the four torsion angles that define a β-turn. Molecular modeling studies were carried out on the *N*-acetyl-*N*'-methylamide 5,5- and 6,5-bicyclic thiazolidine lactam model compound (see Figure 3 -10) using the random incremental pulse search (RIPS) program of Ferguson and Raber [155, 156].

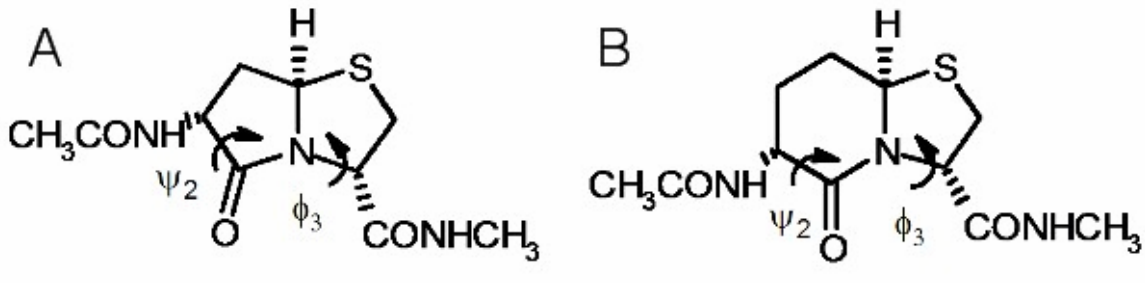

Figure 3 -10: *N*-acetyl-*N*'-methylamide. 5,5 and 6,5-bicyclic thiazolidine lactam model compounds as shown A and B respectively.

The lowest energy conformer of 5,5-bicyclic model was found to possess ψ_2 and ϕ_3 torsion angles of 109.3° and 77.4°, respectively. The ψ_2 and ϕ_3 values that were obtained for the lowest energy conformer of the 6,5-bicyclic model on the other hand, were 132.0° and 69.1°. It showed that both 5,5- and 6,5- bicyclic thiazolidine lactam ring systems restrict the ψ_2 and ϕ_3 torsion angles to values which were quite close to those of an ideal type-II β-turn ($\psi_2 = 120°$,

$\phi_3 = 80°$) [157] The most significant difference between the 5,5- and 6,5-bicyclic thiazolidine lactam was found to lay in their different ψ_2 torsion angles (109° versus 132°).

Compound **6** possesses 5,5-bicyclic system showed greater effectiveness than the peptidomimetic containing the 6,5-bicyclic systems compound **7**. The major difference between the 5,5- and 6,5-bicyclic thiazolidine lactam systems was the magnitude of the ψ_2 torsion angle, this may be a leading factor behind the difference in activity observed for **6** and **7**.

The use of thiazolizidinone amino acid **2** in conjunction with studies of different biologically active peptides had lead to several potent conformationally-constrained surrogates [148, 158, 159]. Similar antibacterial activity and CD spectra indicated that (2R, 5S, 8S)-**2** mimics the type II β-turn in gramicidin S, replacing D-Phe at the *i+1* and Pro at the *i+2* position [149, 158, 160, 161], in which thiaindolizidinone amino acid 2 had been incorporated into peptide analogs, lacking biological activity might have been resulted from mimicking an inactive conformation and from structural features that interfere with receptor recognition. NMR and computational studies of an inactive cyclic hexapeptide mimetic of tendamistat showed that (2R, 5S, 8S)-**2** adopted a conformation in which the constrained dipeptide occupied *i* and *i + 1* position rather than *i + 1* and *i + 2* position of a type II β-turn [153]. On the other hand (2R, 5S, 8S)-**2** was recently shown to adopt the desired type II β-turn, and to stabilize a bioactive geometry in a cyclic hexapeptide inhibitor of the interaction between integrin $\alpha_4\beta_1$ and the vascular cell adhesion molecule-1 [162].

3.5.2. Epimerization of Thiazabicycloalkane Amino Acids

Epimerization had been encountered during the synthesis and further transformation of 1-azaoxobicyclo [X.Y.0] alkane amino acids [150, 163].

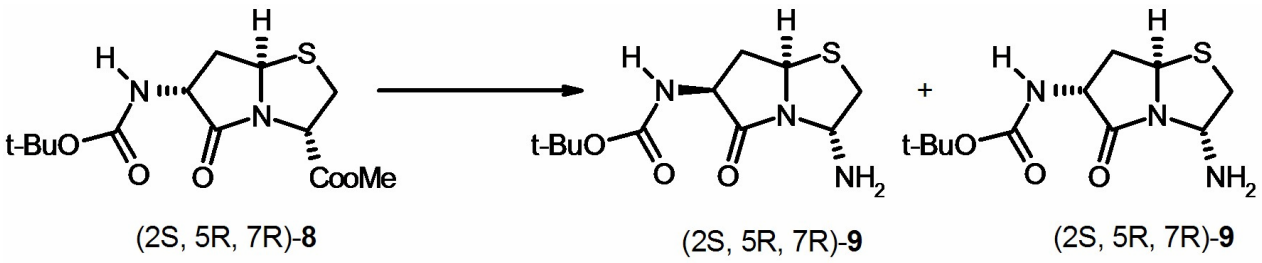

Scheme 3 -2: Conversion of (2S, 5R, 7R)-8 to (2S, 5R, 7R)-9 and (2S, 5R,7R)-9

Treatment of (2S, 5R, 7R)-N-(Boc)aminothiapyrrolizidinone methyl ester **8** with NH_3 in methanol gave a 9:1 mixture of (2S, 5R, 7R)- and (2S, 5R, 7S)-N- (Boc)amino thiapyrrolizidinone carboxamides **9** (see scheme 3-2).

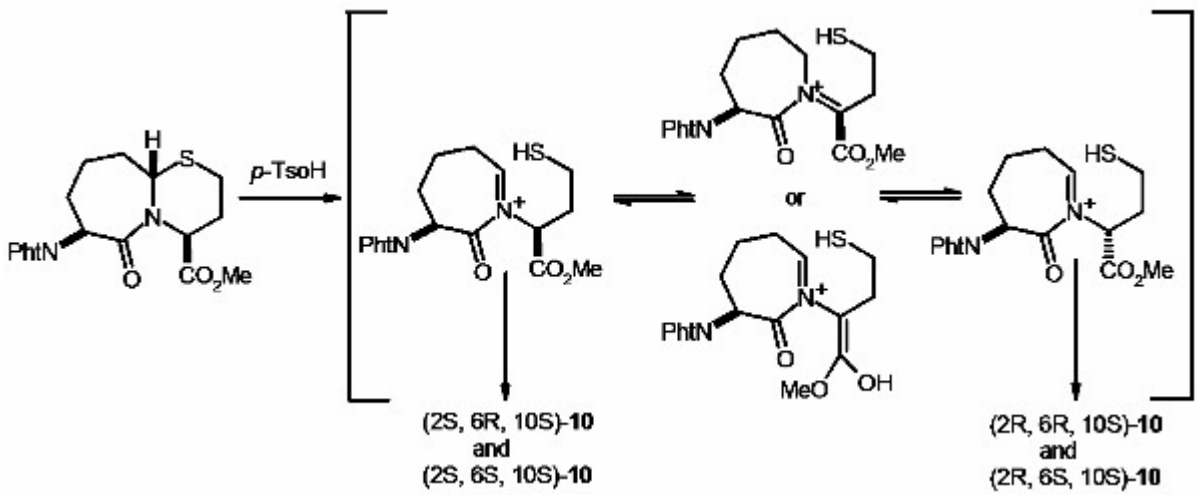

Scheme 3 -3: Synthetic scheme for preparation of thiazabicyclo[5.4.0]alkane phthalimido ester.

Whereas, during the preparation of thiazabicyclo [5.4.0] alkane phthalimido ester **10**, treatment of pure ester **10** of either (2S, 6S, 10S)-, (2R, 6S, 10S)- or (2R, 6R, 10S)- configuration with *p*-toluenesulfonic acid in benzene at reflux for 2-4 hr furnished a 10:30:<1:15 ratio of (2S, 6S, 10S)-, (2R, 6S, 10S)-, (2R, 6R, 10S)- and (2S, 6R, 10S)- diastereomers **10** as shown in scheme 3-3. The mechanism for epimerization of **10** may involve enolization of an imino ester intermediate or equilibration of iminium ion intermediates under the acidic condition [164]. Very few synthesis methods of thiazolidines based on cyclization mode are known [165].

One of the main reasons is that chiral amino thiols are not so easily available compared to chiral amino alcohols. The most easily available chiral aminothiol is Cys. This primary aminothiols forms stable NH-thazolidine through imine cyclization. This stability strongly contrasts with the stability of NH-oxazolidines that mainly exists in solution in an equilibrium with open imine form [166].

3.5.3. Iminium Ion Cyclization

Iminium ion cyclization is probably one of the most powerful methods to form nitrogen-containing heterocycles since it offers several advantages over the other possible cyclization method. Iminium ions are quite often prochiral species and thus offer the possibility of the construction of new stereogenic centers during the cyclization process. This is the important feature concerning the preparation of chiral heterocycles [165].

Condensation of D-glucorono-3,6-lactone and L-Cys methyl ester was carried out in water and pyridine (9:1) gives polyhydroxylated bicyclic thiazolidine lactam (see Figure 3 -11) probably via an acyliminium as shown in scheme 3-4.

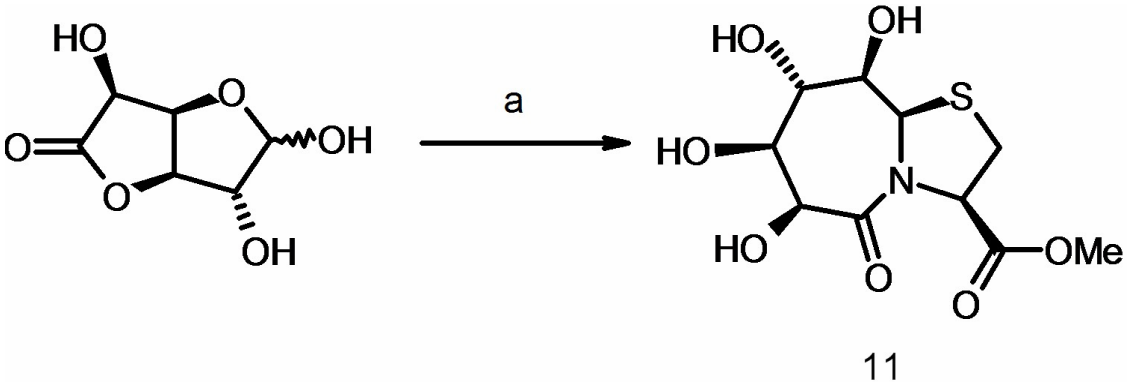

Scheme 3 -4: Synthesis of polyhydroxylated bicyclic thazolidine lactam [9a (R) H-5-oxo-(6S, 7S, 8S, 9R)-tetrahydroxy-octahydro-thiazolo-[3,2-a] azepin-3R-carboxilic acid-methyl ester]. Reagents used were (a) L-Cys methyl ester, H_2O:Py (9:1), RT.

The experimental studies showed that seven membered ring of **11** is found exclusively in the chair conformation [167]. O-6 occupies an equatorial position and O-7, O-8, and O-9 are found in axial positions. 9-OH forms a hydrogen bond with the carbonyl oxygen of the ester group and hold the exocyclic torsion (N-C3-CO-O) in a preferred conformation. This hydrogen bond is maintained in solution since all derivatives of **11** exhibits a large three bond $^3J_{9,9OH}$ coupling constant and a distinct shielding of the 9-OH. Whereas, condensation of D-glucorono-3,6-lactone and L-Cys methyl ester in water or pyridine to give thiazolidine (see Figure 3 -11) which were unable to form the aminolysis of the lactone.

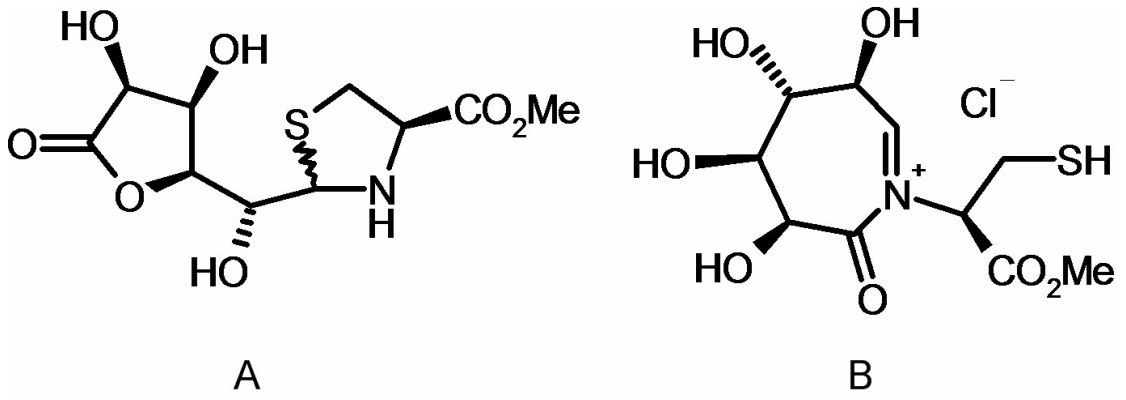

Figure 3 -11: Chemical representation of Thiazolidines (A) and *N*-acyliminium ion (B).

Introduction of amino group at α-hydroxyl group can be done in a two to three step transformation without the protection of secondary hydroxyls to get the polyhydroxylated bicyclic dipeptide building block (Bic) as shown in scheme 3-5.

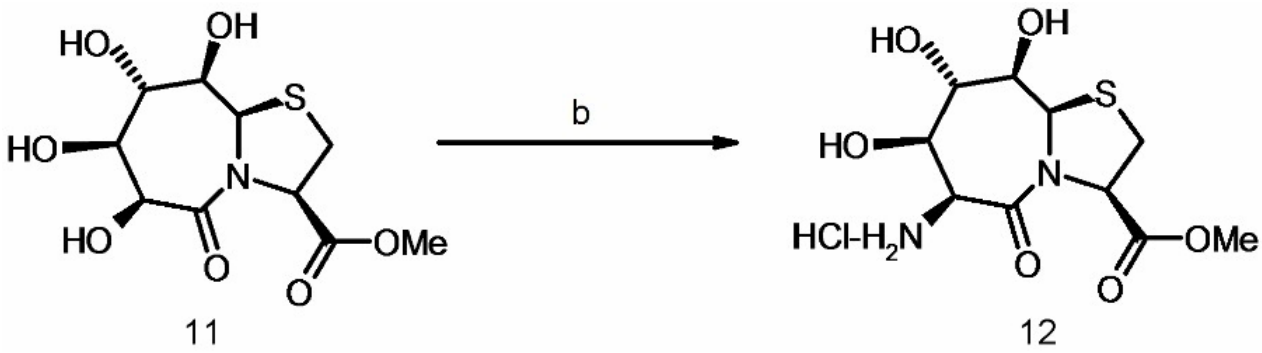

Scheme 3 -5: Conversion of **11** to **12**. Reagents used were (i) Tf_2O, Py, CH_2Cl_2 (89%); (ii) NaN_3, DMF (82%) (iii) Pd/C, MeOH (90%).

This bicyclic template orientated the amino – or carboxyl terminal peptide chains and additionally acted as a scaffold which presents extra functionalities. The seven-membered ring contained a *cis* amide bond and therefore populated a well-defined chair conformation [168].

Five stereo centers of the polyol dipeptide shown in scheme 3-5 (Compound **12**) were introduced by starting materials, the controlled by the reaction conditions [168]. The energy-minimized structural model of trimer **13** folded into a left handed helix with backbone torsions corresponding to that of the polyproline II (PPII) helix [169].

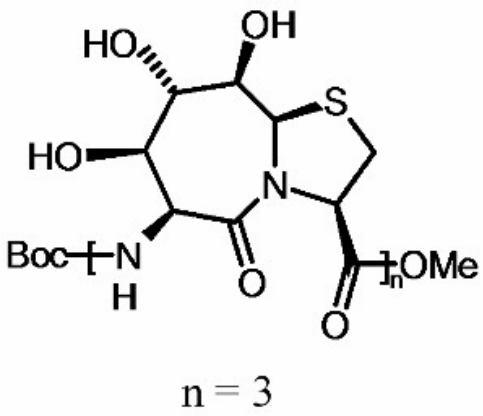

Figure 3 -12: Trimer of Boc-protected polyhydroxylated dipeptide.

One pair of ϕ and ψ torsions was found constrained within the annelated ring system to the values of -80° and 160°. The amino terminal ϕ torsion is less severely restricted to values around -90° and the carboxyl terminal ψ torsion of the bicyclic dipeptide unit is tethered by the hydrogen bond to 140°. Values which deviate from the idealized PPII torsions (-78°, 146°) uncoil the extended helix slightly towards the β-sheet conformation [169].

3.6. Polymerization of Amino Acids

Polymers are a class of colossal molecules consisting of discrete building blocks linked together to form long chains. Simple building blocks are called monomers, while building blocks that are more complicated are some times referred to as repeat unit. When only one type of monomer is present, the polymer is referred to as a homopolymer. Polyethylene- the material commonly used in plastic bags- is a homopolymer formed by polymerization of ethylene. A copolymer is formed when two of more monomers that are different are linked together. The process, by which the monomers are assembled into polymers, either chemically or biologically, is referred to as polymerization. Polymers can be either linear or branched.

Biopolymers are diverse and versatile class of materials that have potential applications in virtually all sectors of the economy. For example, they can be used as adhesives, absorbents, lubricants, soil conditioners, cosmetics, drug delivery vehicles, textiles, high-strength structural materials, and even computational switching devices. Currently many biopolymers are still in the developmental stage, but important applications are beginning to emerge in the areas of packaging, food production, and medicine. Some biopolymers can directly replace synthetically derived materials in traditional applications, whereas others possess unique properties that could open up a range of new commercial opportunities.

In general, biopolymers fall into two principal categories,

a) Polymers that are produced by biological systems such as microorganisms, plants and animals.

b) Polymers that are synthesized chemically but are derived from biological stating materials such as amino acids, sugars, natural fats or oils.

There are various types of naturally occurring biopolymers defined on the basis of the chemical structure of their monomeric units and indicates the functions hat these polymers serve in lining organisms. For example, DNA, which carries the essential genetic information of living systems, is a linear copolymer composed of four monomer nucleotides. The nucleotides are linked together along a pair of helical sugar-phosphate backbones.

Proteins also referred to as polypeptides are complex copolymers composed of up to 20 different amino acids building blocks. Proteins can contain a few hundred amino acid units or thousands of

units. Each protein has a specific chemical composition and three-dimensional shape. The amino acid building blocks are linked by amide bonds in specific sequence determined by the DNA code of the corresponding gene.

In recent years, researchers have been able to synthesize various polypeptides that are similar to natural proteins found in, for example, in biominerals such as shell or bones. Synthetic polypeptides are usually created from amino acids precursors.

Poly amino acids are an important class of synthetic polymers produced by chemical polymerization of the same amino acid building blocks found in naturally occurring proteins [170]. Poly amino acid chains are sometimes referred to as polypeptides. Approximately 20 amino acids can be found in proteins and from these basic building blocks a variety of homopolymers and complex copolymers have been synthesized. Because of the great chemical diversity of amino acid monomers-anionic, cationic, hydrophobic, polar, non-polar, thermally stable-polyamino acids can be envisioned for virtually all types of polymer application ("*Anionic*" monomers are negatively charged; "*Cationic*" monomers are positively charged).

Polymer chains consisting of Glu, Asp, Leu, and Val are the polypeptides most frequently used for biomedical purposes. Lys and Met are also important amino acid building blocks in polypeptide polymers. Glu and Asp are hydrophilic, whereas Leu and Val are hydrophobic. When these hydrophilic and hydrophobic building blocks are combined, copolymers with vastly different rates of biodegradation can be created. This allows the copolymers to be used as delivery systems for a verity of different drugs. Homopolymers and copolymers of these simple amino acids are nonimmunogenic, i.e., they do not produce an immune response when injected into animals. Polyamino acid microspheres-spheres ranging in size from 50 nm to 20 microns are currently being developed for oral drug administration [171].

In an effort to duplicate the adhesive characteristics of MAPs in synthetic polymers, several groups have investigated the synthesis of adhesive polymers by incorporation of DOPA into synthetic polymer backbones, side chains or end groups ([132]).

3.7. Synthetic Polymers

In an effect to duplicate the adhesive characteristics of MAPs in synthetic polymers, several groups have investigated the synthesis of adhesive polymers by incorporation of functional amino acids like Lys, Tyr and DOPA into synthetic polymer backbone [154, 172-175].

Yamamoto and co-workers synthesised DOPA homopolymer as well as specific sequence copolymers of DOPA with L-Lys and L-Glu using solution polymerisation of the *p*-nitrophenyl ester of the corresponding di-, tri-, and tetrapeptides [172-174, 176] and synthesis of random co-

polypeptides that contains as many as 18 different amino acids, including DOPA [177, 178]. Studies on the cross-linking and adhesive properties of these polymers were limited and adhesive properties of these polymers were limited. Initial adhesive studies were performed using iron and Al_2O_3 adhered with no oxidising agents [175]. More detailed studies focused on L-Lys/L-Tyr random copolymer and complex random copolymers using tyrosinase enzymes as the oxidising agent [154, 179]. Yamamoto and co-workers observed that the absorption spectra of Boc-L-DOPA quinine exhibited an absorption at 340 nm and a shoulder at around 270 nm and after the addition of Boc-L-Lys into same solution new band are develop at 360-365 nm due to the cross reaction was gradual. The addition of *tyrosinase* and α-*chymotrypsin* to the poly(Lys-Tyr) solution caused a rapid 275 nm spectroscopic change in seawater and turbidity formed after 4 min. After hydrolysis same sample showed absorption band at 360-365 nm, which was similar to cross-linked compound. A possible insolubilizing mechanism was thought that using oxidase enzymes *tyrosinase* was found to catalyze a successive reaction form phenol to catechol and finally to *o*-quinone in both fresh water and sea water. The oxidation reaction was found to be much faster towards Tyr than towards Tyr copolymer. α-*chymotrypsin* thought to exist in the integument and to act as a kind of activator of prephenol oxidase, randomly digests the Tyr copolymer at aromatic residues and accelerates oxidation by tyrosinase, followed by rapid precipitation due to intermolecular cross linking.

Deming and co-workers [131] prepared sequentially random water soluble co-polypeptides contains L-DOPA and L-Tyr using ring opening polymerization of α-amino acid *N*-carboxyanhydrides (NCAs) as shown in scheme 3-6.

NCAs are readily prepared from amino acids by phosgenation and can be polymerized into high molecular weight polypeptides via successive ring-opening addition reactions that liberate carbon dioxide [180].

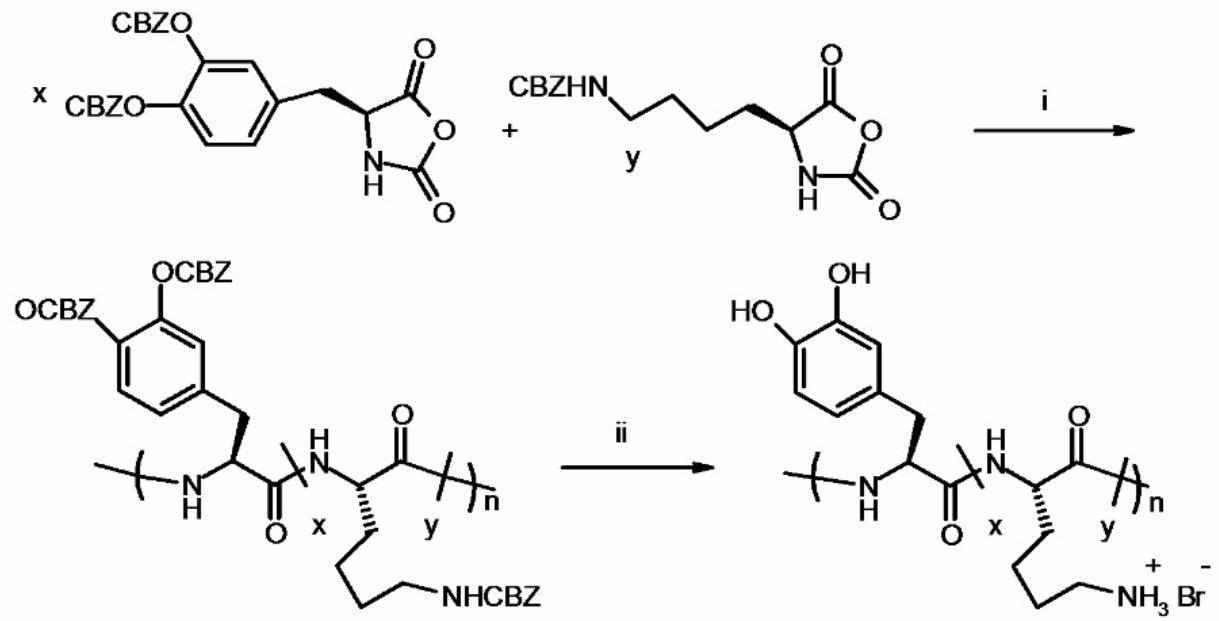

Scheme 3 -6: Synthesis of adhesive co-polypeptides using NCA monomers. Reagents used were (i) NaOtBu, THF, (ii) HBr, HOAc.

Aqueous solution of these copolymers, when mixed with a suitable oxidizing agent (e.g., O_2, mushroom tyrosinase, Fe_3^+, H_2O_2 or IO_4^-), formed cross-linked networks that were found to form moisture resistant adhesive bonds to a verity of substrates, e.g., aluminum steel, glass and plastics [131]. The plastic adherents formed the weakest adhesive bonds of all adherent studies. It is likely the relatively nonpolar surfaces displayed by the plastics provided a poor substrates displayed by the plastics provided a poor substrate for chemisorption of the polar functionalities of the polymer. The polar surface of glass provided a better substrate, nearly equivalent to the metals. Steel adherents gave adhesive bond strength that was comparable to those formed on aluminium. The major difference from aluminium was that adventitious iron oxide present on the steel surface was able to act as an efficient polymer oxidant. Consequently, no additional oxidant was necessary to obtain fast oxidation on steel adherents. In particular, it was found to be unnecessary to scrupulously clean the steel surface since a thin coating of iron oxide promoted rapid curing of the adhesive also by the variation of the oxidizing agent and pH. The kinetics of gel formation and gel strength were followed by viscosity measurement. Periodate, hydrogen peroxide and base (pH = 12) formed gels fastest, as compared to the tyrosinase and aerobic oxidation. Hydrogen peroxide and base also gave the highest cross-link densities, as estimated by solution viscosities. It appears that either basic aqueous solution or H_2O_2 would be the most efficient oxidants for the synthetic adhesive polymer.

The conformational assignment for Poly-Tyr has been widely studied using variety of physical methods including ultra-violet absorption (UV), optical rotatory dispersion (ORD), circular dichroism (CD), infra-red absorption (IR), nuclear magnetic resonance (NMR), ultra-centrifugation, calorimetric measurement, light scattering and potentiometer titration. In solvent such as aqueous sodium chloride (below pH 11.5), methanol, dimethylformamide, trimethyl phosphate[$(CH_3O)_3PO$], quinoline, water/ethanol mixed solvent, dimethyl sulphoxide (Me_2SO)/ dichloroacetic acid (DCA) mixed solvents, Me_2SO/D_2O mixed solvents and Me_2SO/ $(CH_3O)_3PO$ mixed solvents poly-Tyr assumes an α-helical conformation. In strongly basic aqueous solution or Me_2SO poly Tyr is a random coil. If the pH is lowered very slowly a transition from coil to antiparallel β-conformation is observed in water and in the prevailing aqueous region.

In the conformational study of Poly(L-Lys), Grourke and co-workers [181] observed that at 25°C un-ionized poly(L-Lys) above pH 10 is known to exist in a right-handed α-helix and ionized poly (L-Lys) is a random coil structure. During the conformational study of Poly (DOPA) and sequential polypeptides containing DOPA and Lys, Yamamoto and co-workers [176] observed that, in water or methanol-trimethyl phosphate, in the ratio 1:1 (v/v), mixed solvents unionized poly(L-DOPA) below pH 10.4 assume a right handed helical structure and ionized poly(L-DOPA) shows a random coil structure in dimethyl sulphoxide or water/ trimethyl phosphate mixed solvent above pH 11.

In case of five sequential polypeptides, containing L-Lys and L-DOPA, when Lys content is greater than 67 mol%, sequential polypeptides composed of Lys and DOPA shows a helical conformation in alkaline solution at room temperature or in alcohol rich solutions and it show β-structure above 60°C. sequential poly (L-lysyl-L-DOPA), with 50 mol% Lys content takes a β-structure, These results is similar as compare to previous result finding by Seipke et al. [182, 183]. Pierre et al. [184] and Trudelle [185]. When the DOPA content is greater than 67 mol%, sequential polypeptides assume the α-helical conformation below pH 7 at 25°C based on the CD peak position at 274-285 nm, the IR frequencies for the amide bond, the NMR α-CH chemical shifts [172] and copolymer study to conform the helical structure [186]. The conformation of poly(L-lysyl-L-Phe) [182, 183] poly (L-tyrosyl-L-Lys) [184] and poly(L-lysyl-L-DOPA) were assigned a β-structure. The only difference between the three aromatic amino acids is that Phe has no hydroxyl group; Tyr has one hydroxyl group at the 3- and 4-position in the benzene ring.

4. Adhesive Peptides and Copolymers: Synthesis

As seen in last chapter, synthetic adhesive peptides are important and methods to synthesize them in a laboratory are needed to be established. Laboratory synthesis of adhesive peptides will help to exploit adhesive characteristics as well as in understanding of their biological importance. This chapter gives details on the preparation of synthetic peptides with adhesive properties using solution as well as solid phase peptide synthetic strategies. The polymer synthesis was carried out by means of dipeptide building blocks those were described in earlier chapter.

4.1. Synthesis of Dipeptide Building Blocks

In recent years, peptide chemistry has gained enormous popularity and relevance, particularly with the emergence of unnatural analogues as components of molecules with therapeutic potential. The need to replace natural amino acids in peptides with non-protiogenic counterparts in order to obtain drug-like target molecules has stimulated a great deal of innovation on several fronts.

Several unnatural building blocks have been prepared and are in use [164, 187, 188]. These building blocks are used to exhibit favourable properties in peptide coupling protocols. Unnatural fused bi-cyclopeptide building blocks are also in use with different ring size [164], e.g., 5,6 fused 1-aza-2-oxobicycloalkane amino acid.

The heteroatom analogues in which carbon is replace by sulphur, oxygen or nitrogen, at different synthetically attainable sites are also used [149, 164]. The presence of functional group as pendant substituents on the basic ring systems or its heteroatom congeners also provides opportunities for diversification. The structure of dipeptide motif is shown in Figure 4 -1, with specific substituents on either ring with amide appendages at each end could be the ultimate objective as a drug-like molecule. Synthetic strategies for such motifs must therefore be versatile to allow the inclusion of substituents. The particular interest has been the replacement of dipeptide motif, formed by natural amino acids in peptides, with substrate with a constrained or rigidified counter part that simulates β-turn and exhibit type I and type II β-turn [189-200].

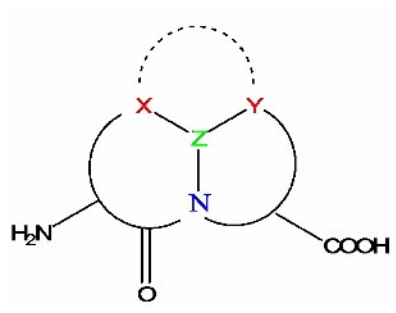

Figure 4 -1: General skeleton of a 1-azaoxobicycloalkane where as X, Y and Z can be either carbon or any heteroatom.

These properties have been established in a dipeptide building block that is polar and rigid in structure [169].

In order to synthesize simplified adhesive peptides and peptide oligomers, polyhydroxylated dipeptide building blocks were used in this work. In fact, these building blocks do not constitute Hyp and Pro, amino acids that are present in mussel adhesive peptides *mefp*-1. The advantage of using polyhydroxylated dipeptide building blocks is to avoid expensive Hyp and Ser that would need additional side chain protection during peptide synthesis. Additionally, the polyhydroxylated dipeptide building block could stabilise the extended conformations in the deca-peptide repeating units to maximise the numbers of intermolecular contacts as in fibrous peptides.

4.1.1. Boc-and Fmoc-protected dipeptide building blocks

Boc- and Fmoc- protected dipeptide building blocks are derived in 5 steps from D-glucorono-3,6-lactone and L-cysteine methyl ester, which are shown in Scheme 4 -1, Scheme 4 -2, and Scheme 4 -3. Conversion of triflate to azide with retention of configuration was a key step for the preparation of both Boc- and Fmoc- protected dipeptide building blocks (**8** and **9**).

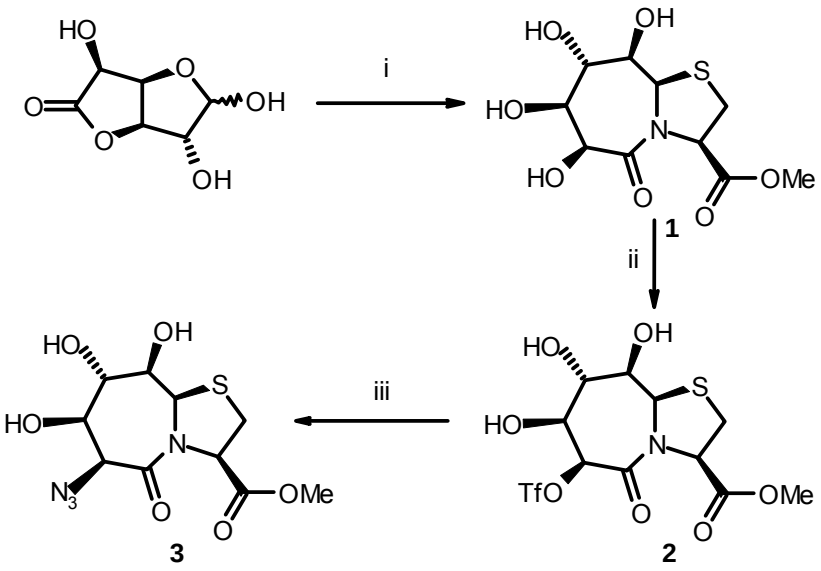

Scheme 4 -1: Synthesis of azide methyl ester **3**. Reagents used were (i) L-cysteine methyl ester, H_2O:Py (9:1), RT, 4 days, 90%. (ii) Trifilic anhydride, DCM, 89%. (iii) NaN_3, DMF, 82%.

Synthesis of azide precursor **3** has been executed earlier [169]. Simple one step condensation of D-glucorono-3,6-lactone and L-cysteine methyl ester yields bicyclic thiazoliden lactone **1** (Scheme 4 -1, step 1). The probable mechanism of this reaction possibly involves formation of an acylnimum ion shown in Figure 4 -2 [165].

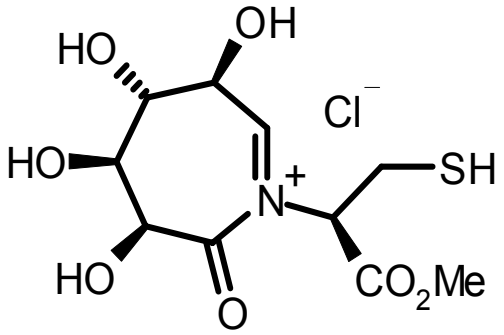

Figure 4 -2: *N*-acylnimum ion which is assumed to be formed during condensation of D-glucorono-3,6-lactone and L-cysteine methyl ester.

Selective activation of α-hydroxyl groups without protection of side chain (other hydroxyl groups) with triflate occurred using triflic anhydride at 0°C, yielding **2** (Scheme 4 -1, step 2). Thus under inversion of configuration at C6 position at 50°C in DMF the triflate ester **2** was converted to

azide **3** (Scheme 4 -1, step 3). Later, compound **3** was used for the synthesis of both Boc and Fmoc-dipeptide building blocks (Scheme 4 -2).

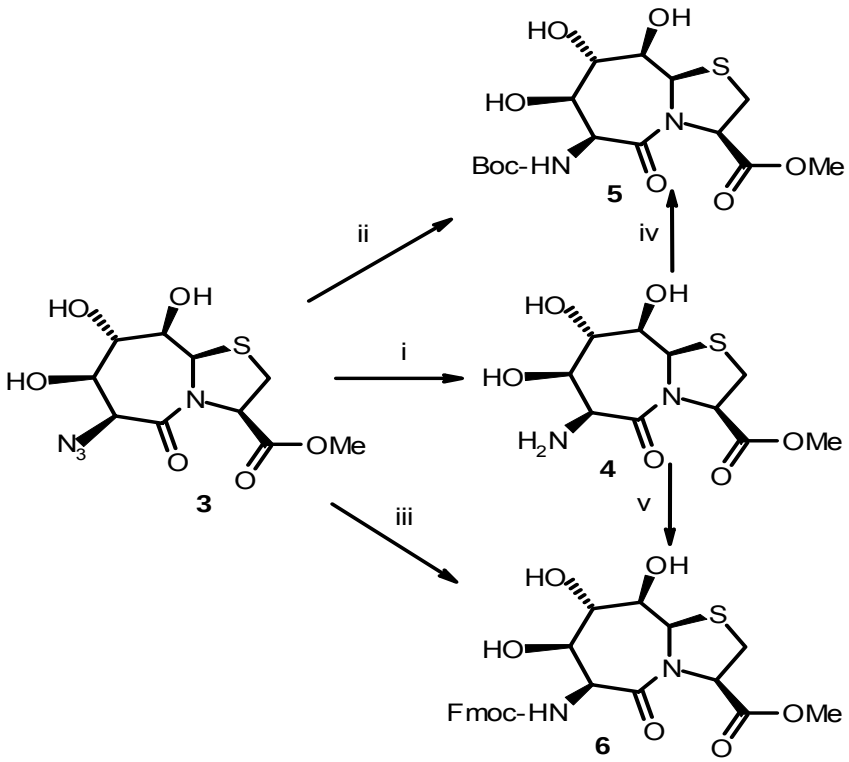

Scheme 4 -2: Synthesis of Boc and Fmoc protected methyl ester (**5** and **6**). Reagents used were (i) Pd/C, MeOH, RT, 94%. (ii) $(Boc)_2O$, Pd/C, MeOH, RT, 96%. (iii) Fmoc Succ., Pd/C, MeOH, CH_3CN, 38%, (iv) $(Boc)_2O$, Na_2CO_3, MeOH, RT, 90%. (v) Fmoc Succ., $NaHCO_3$, MeOH, CH_3CN, RT, 68%.

The azide compound **3** was reduced with hydrogen using 10% Pd/C in MeOH to yield about 94% of free amine ester **4** (Scheme 4 -1, step 1). This reaction was also performed previously with the use of H_2S for the conversion of azide ester **3** into amine ester **4** [169]. Use of rotten egg smelling H_2S as a reducing agent, was the major drawback of this reaction. Alternatively, reduction of **3** was performed using 10% Pd/C with hydrogen. The yield obtained in both cases was quantitatively similar (94 % for **3** to **4** using 10% Pd/C with hydrogen and 95% using H_2S).

Compound **4** was simultaneously protected by Boc- and Fmoc- group using $(Boc)_2O$ and Fmoc-succinimide (Scheme 4 -2, step 4 and 5). This step yielded, respectively, about 96% and 68% of Boc and Fmoc protected polyhydroxylated dipeptide building blocks **5** and **6**, respectively.

Conversion of azide **3** to Boc and Fmoc protected polyhydroxylated dipeptide building blocks **5** and **6** was also performed using one-pot synthesis. This was achieved by using $(Boc)_2O$, Pd/C, MeOH and Fmoc-succinimide, Pd/C, MeOH under hydrogen, respectively. Yields obtained for the one step conversion of **3** into Boc protected acid **5** was 96%, while that for two step

conversion of **3** to **5** (via **4**) was 94%. One pot conversion of **3** to Fmoc protected acid **6** yielded 38 %, whereas two step conversions of **3** to **6** (via **4**) yielded 68%.

Conversion of Boc and Fmoc protected dipeptide methyl ester to Boc and Fmoc protected acid yielded compounds **8** and **9** (Scheme 4 -3) which are further useful for the solution as well as solid phase peptide synthesis.

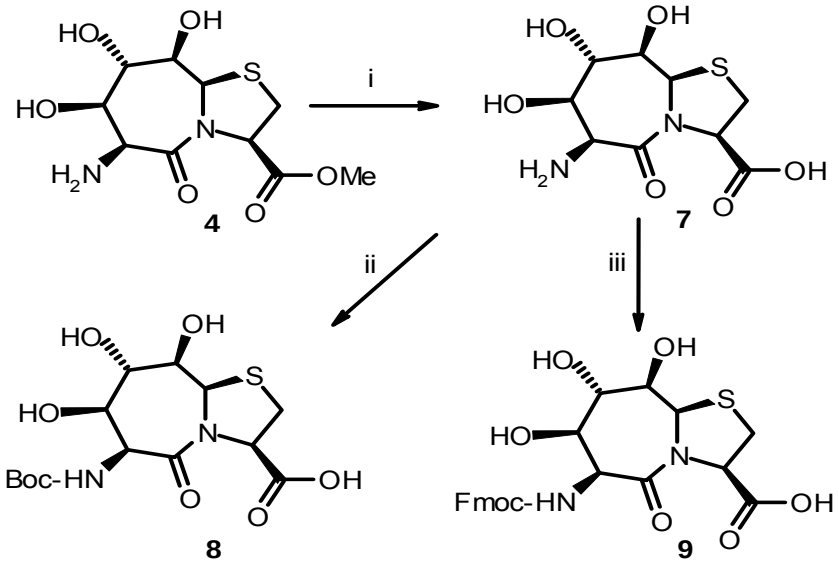

Scheme 4 -3: Synthesis of Boc- and Fmoc-protected dipeptides (**8** and **9**). Reagents used were (i) KOH, H_2O, HCl, quant. (ii) $(Boc)_2O$, Na_2CO_3, H_2O, Dioxan, 85%. (iii) Fmoc-Cl, $NaHCO_3$, H_2O, CH_3CN, 40 %.

In this reaction, the methyl ester of free amine **4** was quantitatively deprotected to **7** using 2 eq. of KOH and water. The reaction was stopped after 35 min by addition of 1eq. of 1N HCl into the reaction mixture. Choice of 35 min was based on the observation that the compound **4** was not stable under basic conditions. Reaction product was seen to undergo decomposition when it was stirred more than 35 min. Compound **7**, the amine ester, was protected by Boc and Fmoc group using $(Boc)_2O$ and Fmoc-Cl to yield, respectively, 85% and 40% of Boc and Fmoc protected polyhydroxylated dipeptide building blocks **8** and **9**.

Conversion of **6** to **9** is also feasible and was performed under acidic conditions using acetic acid and 5 M hydrochloric acid as a catalyst. This reaction yielded about 97%. Thus direct conversion of **6** to **9** yields more product than the conversion of **7** to **9**.

Compounds **8** and **9** were used as starting compounds for further peptide synthesis that was carried out using solution as well as solid phase peptide synthesis protocols. Additionally, it was observed that the Fmoc protected polyhydroxylated dipeptide **9** was stable under acidic conditions. This fact was quite helpful, particularly, for solid phase synthesis.

4.1.2. Saponification Reaction

Saponification was optimized to understand the conversion of methyl ester to the acid. This information would prove important for the preparation of suitable and easy dipeptide building block. Various bases were tested for the optimization of this transformation. A general protocol of saponification is represented in Scheme 4 -4.

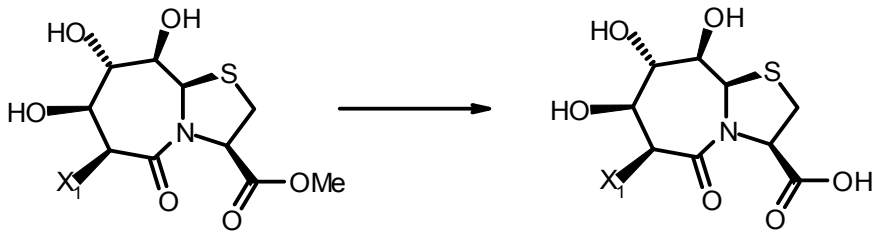

Scheme 4 -4: Saponification reaction performed to convert methyl ester to the acid. Reagents and substituents used were a) X_1 = -OH, -N_3, -NH_2, -Boc-NH. b) Bases = KOH, NaOH, LiOH.

The optimization of saponification reaction was achieved by monitoring the reaction using nuclear magnetic spectroscopy (NMR). One dimensional ^{1}H NMR gives a clean spectrum of product if the saponification reaction works. For optimization of saponification reaction, three different bases have been used, namely, KOH, NaOH, and LiOH. The choice of three different bases was driven by the fact that their basic strength is in the increasing order from KOH to LiOH. The cause for the difference in the basic strength depends on the electronegativity of the metal ion and thus is greatest for Li.

The reaction was performed by stirring the reaction mixture at room temperature for 30 min with H_2O as a solvent. It was observed that 30 min duration is optimum as decomposition of reaction products were seen when the reaction was allowed to proceed for more than 30 min (in this case 40 min). Therefore, the reaction mixture was quenched by 1eq. of 1N HCl after 30 min while using all bases.

Saponification reaction for compound **1** (Scheme 4 -1) (for X_1 = -OH) worked well using all three bases. However, the reaction product, i.e., formed acid, was difficult dissolve in organic solvents. This has limited our attempts to convert methyl ester to acid (for X_1 = OH) and thus was left out from further synthetic steps.

Saponification reaction for compound **3** (Scheme 4 -2, for X_1 = -N_3), did not work in all three bases. The probable cause of this failure could be the fact that the 6-H proton is more acidic. This

acidic proton might lead to the opening of the ring at C^6 position, thus leading to decomposition of the reaction mixture.

On the other hand, saponification reaction for compound **4,** (Scheme 4 -2, for X_1 = $-NH_2$) worked excellent, as seen in the clean one dimensional ^1H NMR spectrum of this compound. This reaction was performed in all the three bases and in each case formed product was the salt of amine and acid. This salt is stable for about 40 minutes under strong basic conditions. After 40 minutes, additional peaks were seen in the NMR spectrum arising from the decomposed product. The reaction product was also easy to purify as was purified by simple washing with 10% MEOH in $CHCl_3$. After the protection of amine through Boc-and Foc- group, the salt of amine and acid, yielded Boc- and Fmoc- protected dipeptide building blocks.

Tremmel and Geyer performed saponification reaction on the compound **5** (Scheme 4 -2, for X_1 = -NH-Boc) using only LiOH as a base [169]. The method of analysis of reaction product used by then was NMR and TLC. Additionally, this reaction was performed using previously mentioned other bases (i.e., NaOH and KOH). In our observation, results obtained using KOH and NaOH were similar with the furnished method which was performed using LiOH.

Table 4 -1: Yields obtained in saponification reaction

Sr. No.	Product	Yield
1	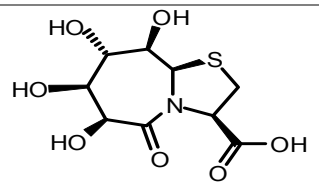	86%
2	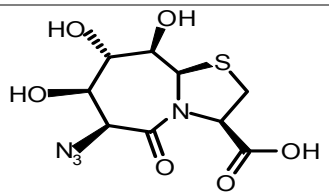	87%
3	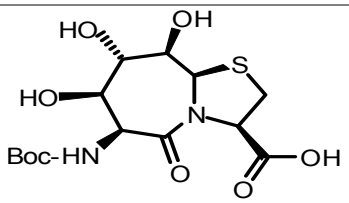	86%

It is important to mention that the reaction products obtained for compound **5** were not very pure, particularly as was observed with compound **4**. The obtained Boc- protected acid **5** was found to have impurities as seen by additional NMR signals. However, when the saponification reaction

was performed on compound **4**, followed by the protection of amine by Boc- group, resulted compound **5** was pure as seen by NMR.

This set of saponification reactions helped us in deducing that the reaction performance was best for compound **4**. The conversion of methyl ester to acid with amine at X_1 position was, clean and suitable for the preparation of Boc-and Fmoc-protected dipeptide building blocks.

4.2. Synthesis of Peptides in Solution

Solution phase peptide synthesis is one of the effective synthetic methods for the preparation of adhesive peptides. For the preparation of fibrous peptides, dipeptide building blocks were coupled with Tyr, Lys and DOPA using coupling regent HBTU, additive HOBt and DIPEA as base. The latter mentioned amino acids are essential amino acids in *mefp*-1 protein (see section 3.2.1). Using Boc-stratergy, different tetrapeptides were which details are given in following sections.

4.2.1. Synthesis of Tetrapeptide

Four different tetrapeptides were synthesized using Boc-strategy. Compound **11** was the main building block for the preparation of two tetrapeptide molecules. Synthetic scheme for the compound **11** is shown in Scheme 4 -5.

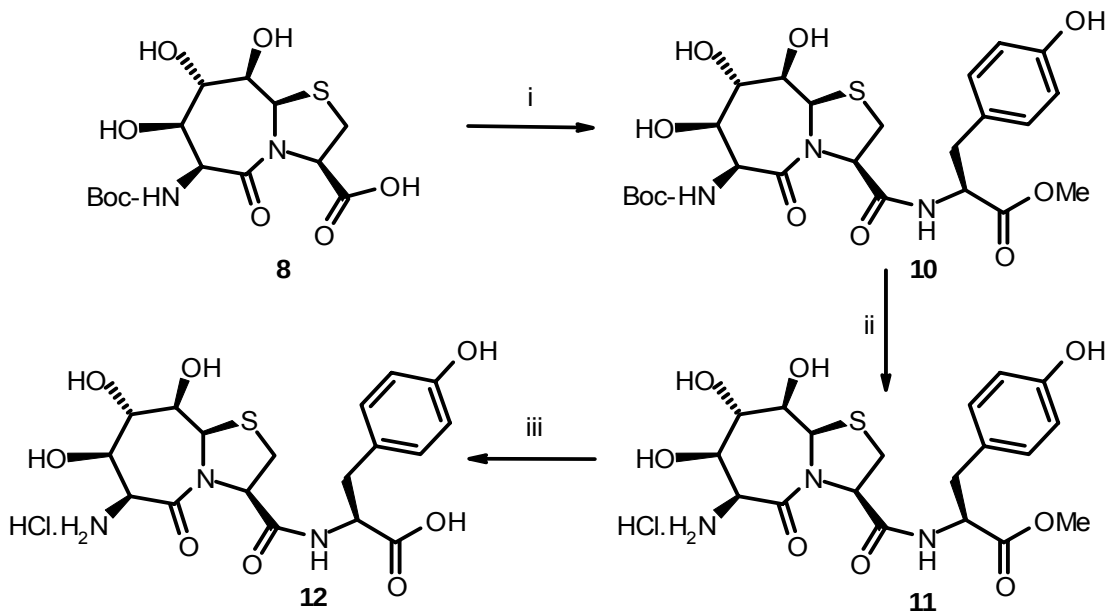

Scheme 4 -5: Synthesis of Bic-Tyr tripeptide **12**. Reagents used were (i) L-Tyr methyl ester, HOBt, HBTU, DIPEA, DMF, RT, 6h, 92%. (ii) HCl/Et_2O, RT, 1h, quant. (iii) KOH, H_2O, RT, quant.

The Boc protected polyhydroxylated dipeptide building block was coupled with L-Tyr methyl ester using the coupling reagent HBTU and additive HOBt between pH 8-9 (pH was maintained with base DIPEA), which yielded Boc-protected tetrapeptide compound **10**. Boc- group was quantitatively cleaved to **11** using HCl/Et_2O at room temperature. Compound **11** further used for the preparation of compound **18** tetrapeptides DOPA-Bic-Tyr and compound **16**, Lys-Bic-Tyr. Quantitative cleavage of methyl ester of compound **11** was carried out using 2 eq of KOH and water at room temperature, the reaction mixture was stopped after 40 minute by addition of 1 eq 1N HCl into the reaction mixture yields compound **12**, it shown in scheme 4-5. Compound **12** further used for polymerization reaction.

4.2.2. Synthesis of Tetrapeptide (Lys-Bic-Tyr)

Synthesis of Lys-Bic-Tyr tetrapeptide was performed using compound **11** (Scheme 4 -5). Coupling of compound **11** with Boc-Lys(z) was carried out using the coupling reagent HOBt and additive HBTU between pH 8-9. pH of the reaction mixture was maintained using DIPEA. The reaction mixture was stirred for 6 h which then yields Boc-protected tetrapeptide **13**.

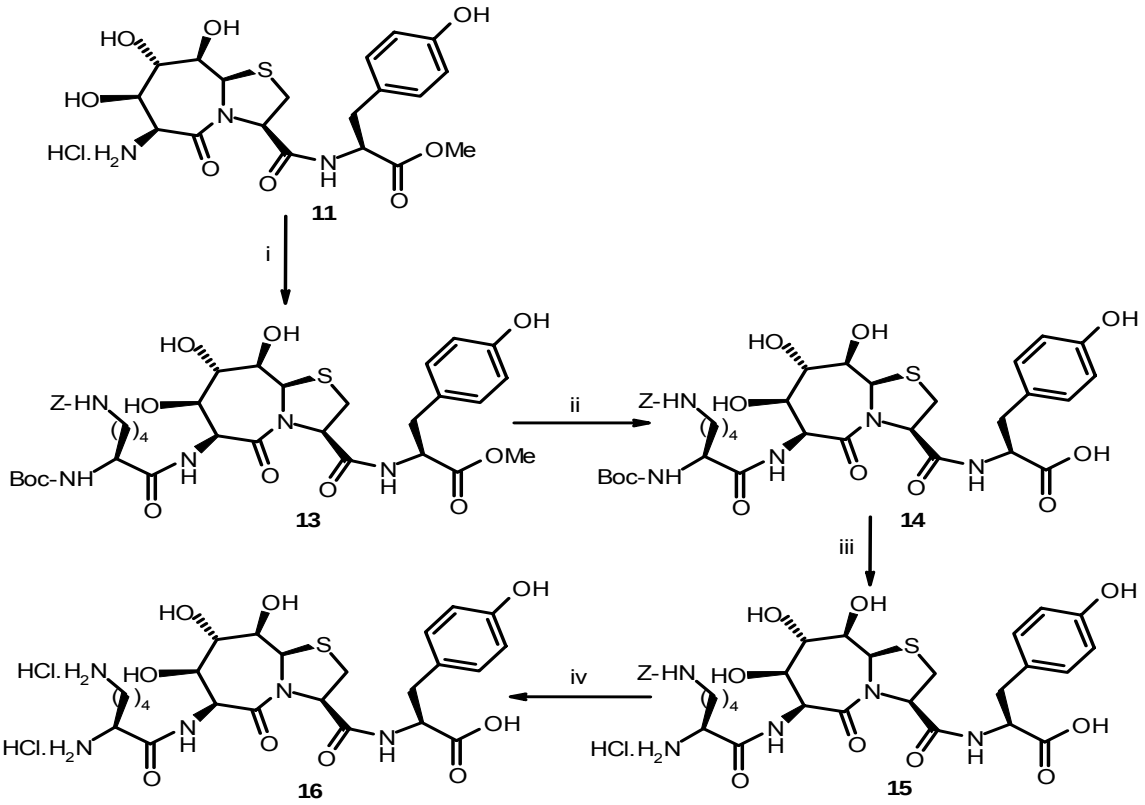

Scheme 4 -6: Synthesis of tetrapeptide **16**. Reagents used were (i) Boc-Lys(z), HOBt, HBTU, DIPEA, RT, 6h, 80%, (ii) 1N KOH, MeOH, RT, 7h,1N HCl, quant. (iii) HCl/Et_2O, RT, 40 min, quant. (iv) Pd/C, MeOH, RT, H_2 atm. quant.

Quantitative cleavage of methyl ester of compound **13** was carried out using 2 eq of KOH and water at room temperature, the reaction mixture was stopped after 40 minute by addition of 1 eq 1N HCl into the reaction mixture yielded compound **14** shown in Scheme 4 -6.

Compound **15** was obtained through quantitatively cleavage of Boc- group using HCl/Et_2O at room temperature, which was further used for polymerization reaction. The cleavage of Boc-group is normally achieved in 40 minutes. It was observed here that this time duration was ample enough to start cleavage of Z group. Further, it was observed that six hours duration was enough to cleave Boc- as well as Z group in one-pot. Deportation of Z group was carried out by hydrogen using 10% Pd/C in MeOH yielded compound **16**.

4.2.3. Synthesis of Tetrapeptide (DOPA-Bic-Tyr)

Unprotected catecholic oxygen of Boc-DOPA was used for the coupling reaction in solution phase. All the coupling reactions of the DOPA are done between pH 7 and 8. Stirring of the reaction mixture was stopped after the completion of the reaction, and the product was purified immediately using column chromatography.

Compound **11** was coupled with Boc-DOPA using the coupling reagent HOBt and additive HBTU between pH 8 and 9. pH of the reaction mixture were maintained using the base DIPEA to achieve Boc- protected tetrapeptide **17** is shown in Scheme 4 -7.

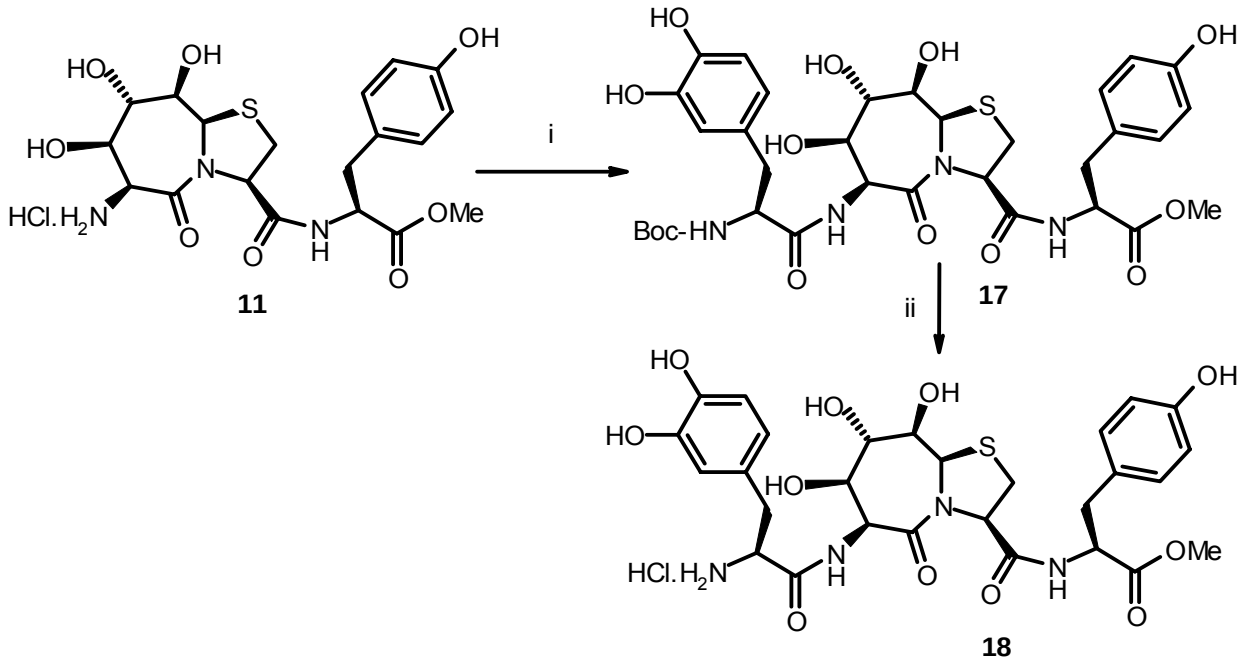

Scheme 4 -7: Synthesis of (DOPA-Bic-Tyr) tetrapeptide **18**. Reagents used were (i) Boc-DOPA, HOBt, HBTU, DIPEA, DMF, RT, 6h, 79%; (ii) HCl/Et_2O, RT, 1h, quant.

Compound **18** was prepared through quantitative deportation of compound **17** using HCl/Et_2O at room temperature.

4.2.4. Synthesis of Tetrapeptide (Boc-Bic-DOPA-Tyr-OMe)

Synthesis of Bic-DOPA-Tyr-OMe tetrapeptide was performed using compound **20**. It is main building block for the preparation of two tetrapeptides Bic-DOPA-Tyr-OMe and Lys-DOPA-Tyr-OMe and is shown in Scheme 4 -8 and Scheme 4 -9, respectively.

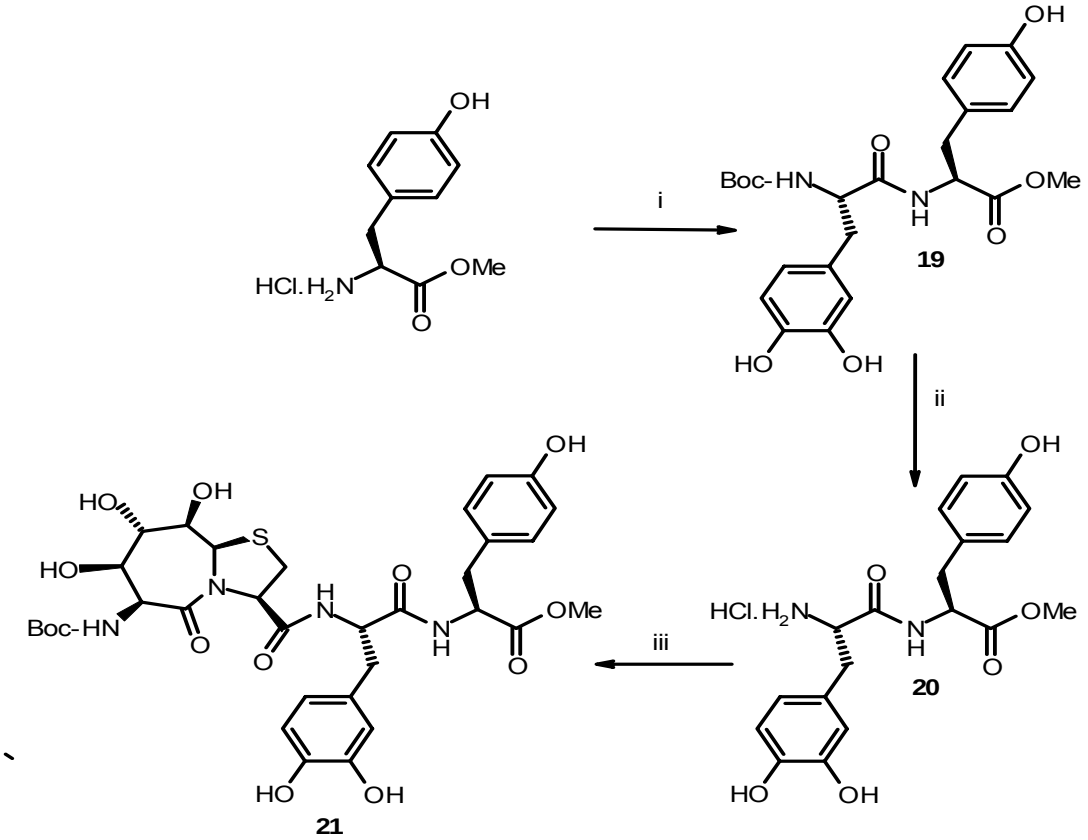

Scheme 4 -8: Synthesis of (Boc-Bic-DOPA-Tyr-OMe) tetrapeptide **21**. Reagents used were (i) Boc-DOPA, HOBt, HBTU, DIPEA, RT, 6h, 93%. (ii) HCl/Et_2O, RT, 1h, quant. (iii) Boc-Bic, HOBt, HBTU, DIPEA, DMF, RT, 6h, 80%.

Boc-protected dipeptide **19** was obtained by coupling of L-Tyr methyl ester and Boc-DOPA using additive HOBt and coupling reagent HBTU between pH 8-9. pH of the reaction mixture was maintained using DIPEA. Boc- group was quantitatively cleaved using HCl/Et_2O. Further, compound **20** was coupled with Boc-Bic using HOBt and HBTU between pH 8 to 9 to get compound **21**.

4.2.5. Synthesis of Tetrapeptide (Lys-DOPA-Tyr)

Synthesis of (Lys-DOPA-Tyr) tetrapeptide was performed using compound **20** and is shown in Scheme 4 -9.

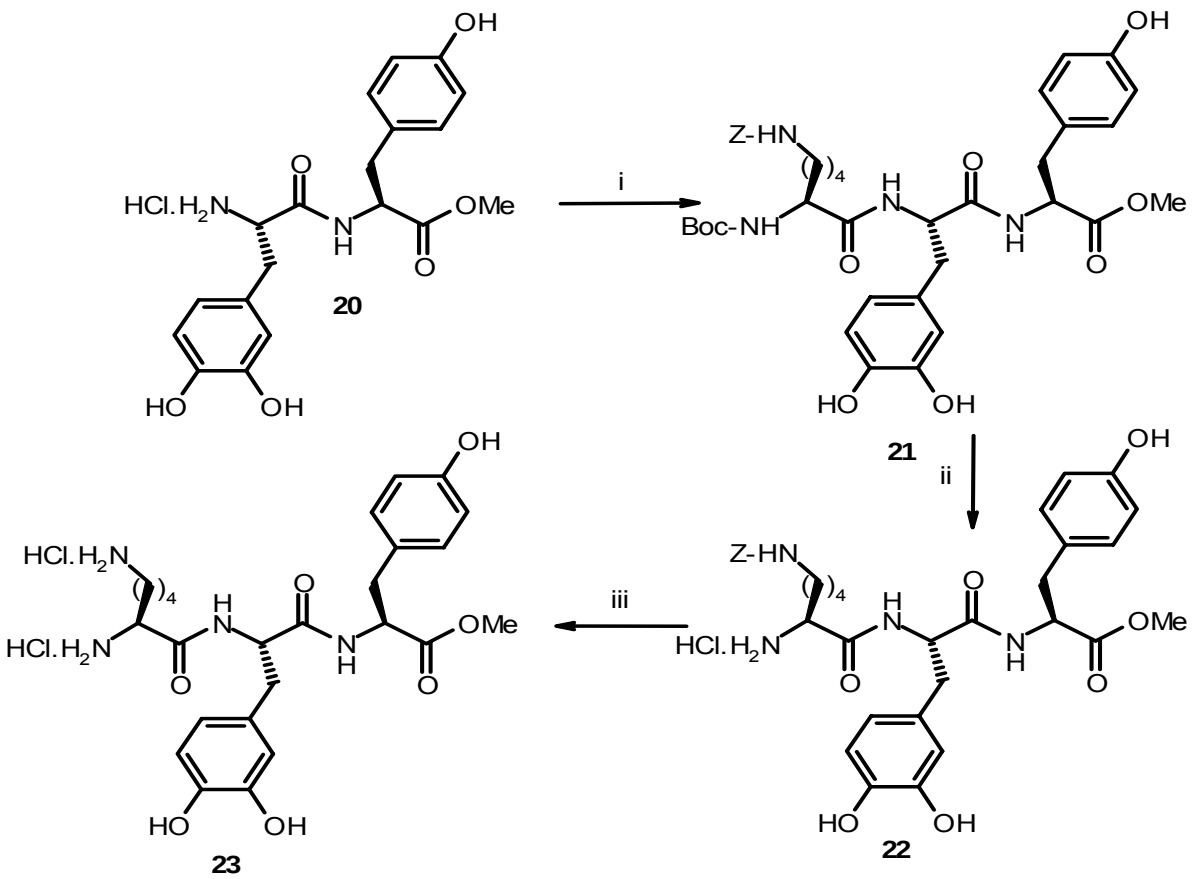

Scheme 4 -9: Synthesis of (Lys-DOPA-Tyr-OMe) tetrapeptide **23**. Reagents used were (i) Boc-Lys(Z), HOBt, HBTU, DIPEA, DMF, RT, 6h, 80%. (ii) HCl/Et_2O, RT, 40 min, quant. (iii) Pd/C, MeOH, H_2 atm, 3h, quant.

Dipeptide compound **20** was coupled with Boc-Lys (Z) using the coupling reagent HOBt and additive HBTU between pH 8-9. The pH of reaction mixture was maintained using DIPEA, yields compound **21**. Boc group was quantitative cleavaged using HCl/Et_2O at room temperature to yield compound **22**. Further, cleavage of Z group was done with hydrogen using 10% Pd/C in MeOH, to produce compound **23**.

4.2.6. Synthesis of Dipeptide (Lys(2-Cl-Z)-Tyr)

Synthesis of Lys(2-Cl-Z)-Tyr dipeptide was performed using coupling of Boc-Lys(2-Cl-Z) and L-Tyr methyl ester and shown in Scheme 4 -10.

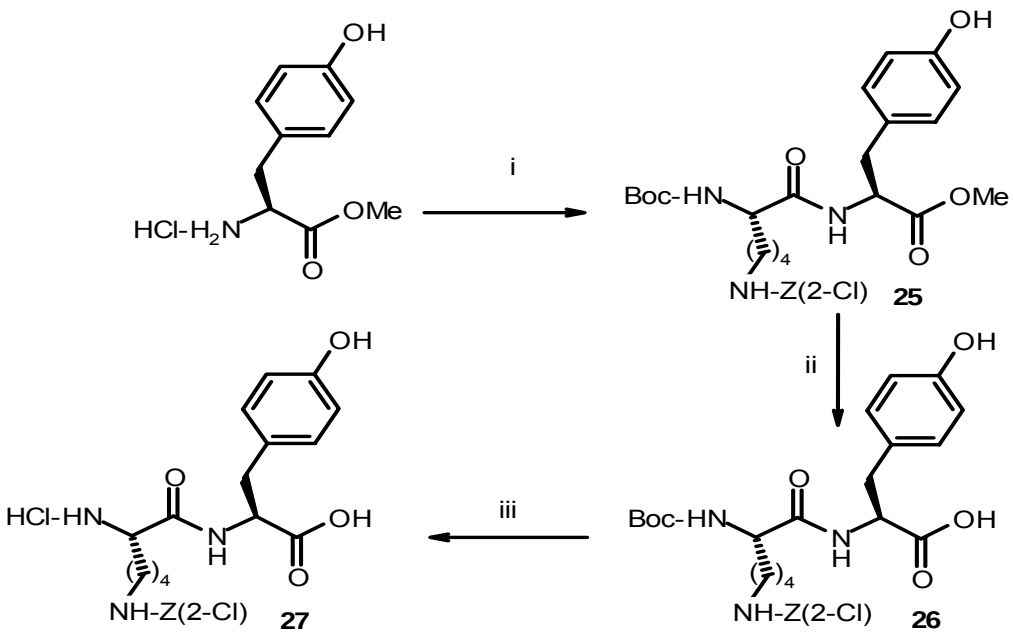

Scheme 4 -10: Synthesis of Lys (2-Cl-Z)-Tyr **27**. Reagents used were (i) Boc-Lys(2-Cl-Z), HOBt, HBTU, DIPEA, DMF, 6h, 92%. (ii) 1N KOH, MeOH, RT, quant. (iii) HCl/Et_2O, RT, quant.

Coupling of L-Tyr methyl ester with Boc-Lys (2-Cl-Z) was carried out using additive HOBt and coupling reagent HBTU between pH 8-9. DIEPA base was used to maintain pH of the reaction mixture to yield compound **25**. Methyl ester of compound **25** was quantitatively converted into free acid using 2 eq of KOH and MeOH at room temperature, the reaction mixture was stopped after 7 h by addition of 1 eq HCl into the reaction mixture to get compound **26**. Additionally, Boc-group was quantitatively cleaved using HCl/Et_2O to receive compound **27**. It further used for polymerization reaction that is described in latter sections.

4.3. Oligomerization reactions

In an effect to duplicate the adhesive characteristics of MAPs in synthetic polymers, several groups have investigated the synthesis of adhesive polymers by incorporation of Lys, Tyr and DOPA into the synthetic polymer backbone [17, 154, 177, 178, 184, 201].

As stated prior, major objective of this thesis work was to produce synthetic polymers made up of essential amino acids found in *mefp*-1.

In this work, oligomerization of L-Tyr, L-DOPA, L-Lys, and dipeptide building blocks was accomplished without protection of side groups (phenolic –OH) in the first three cases and without protection of secondary hydroxyl group in the latter case. Oligomerization reactions were carried out using poly-DCC or DCC and HOBt. Oligomerization of dipeptide building blocks as well as copolymerization of dipeptide molecules with Lys and Tyr worked effectively. Sequence of oligopeptides was characterized using MALDI-TOF mass spectrometer. Several analytical techniques, such as NMR, GPC and AFM were used to characterize these oligomers as well as to study the interaction of the molecules on different surfaces.

But before getting into performed work a short introduction on poly amino acid is presented in the following section.

4.3.1. Poly Amino Acids: Synthetic Methods, Isolation and Purification

Poly amino acids are an important class of synthetic polymers produced by chemical polymerization of the same amino acid building blocks found in naturally occurring protein [170]. Poly amino acid chains are sometimes referred to as polypeptides. Because of the great chemical diversity of amino acid monomers, anionic, cationic, hydrophobic, polar, nonpolar, thermally stable poly amino acids can be envisioned for virtually all types of polymer applications.

When hydrophilic and hydrophobic building blocks are combined, copolymers with vastly different rates of biodegradation can be created. This allows the copolymers to be used as delivery systems for a variety of different drugs. The fact that the homopolymers and copolymers of these simple amino acids are nonimmunogenic (i.e., they do not produce immune response when injected into animals) makes them particularly attractive for medical application.

Various methods have been used for the synthesis of poly-amino acids. Some of them cause racemization, while others give rise to products with low molecular weights. Certain methods are promising and may permit not only the preparation of optically active poly amino acids of a high molecular weight but, also polypeptides with a known repeating sequence of amino acids.

Several reactions leading to the stepwise synthesis of low molecular peptides [202, 203], based on the activation of either the amino or carboxyl group of reactants have been used, with slight modification, for the synthesis of poly amino acids. In such synthesis “monomers” composed of suitable amino acid or peptide derivatives, with two functional groups, were chosen, and the polymerization proceeded by a classic polycondensation reaction. In order facilitate the polycondensation, the terminal α-amino or the α-carboxyl group of the monomer is generally

activated chemically. Methods of activation used in the stepwise syntheses of peptides are discussed in a most lucid manner in the review article of Grassmann and Wunsch [203]. Some of the activation methods are as follows:

(i) A number of different derivatives of α-amino acids and peptides have been used as monomers for the preparation of poly-α-amino acids. The most suitable and commonly used are the *N*-carboxy-*α*-amino acid anhydrides (NCAs) as shown in Figure 4 -3. These NCAs readily undergo polymerization, with carbon dioxide evolution, to yield the corresponding poly-α-amino acids.

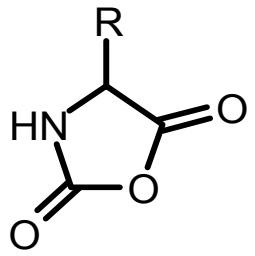

Figure 4 -3: Chemical representation of *N*-Carboxy-*α*-amino acid anhydrides.

(ii) The polymerization of peptide esters seems of particular interest since it permits the synthesis of copolymers in which the amino acid sequence reoccurs regularly.

Esters of α-amino acids and peptides generally undergo condensation reaction more readily than the free amino acids and peptides [204, 205] and normally polymerization works up to 10 to 35 residues.

(iii) Thiol ester of α-amino acids also used for the activation of carboxyl groups. Polymerization of thiol ester of amino acids in water at alkaline pH or in acetone yields copolymers with the defined sequence of amino acid. The product obtained was up to 2700 as determined by dinitrophenylation of the terminal α-amino end group [206].

(iv) Preparation of poly amino acids can also be obtiained by the polycondensation of amino acids and peptides chlorides in bulk or solution as shown in Scheme 4 -11 [207-209].

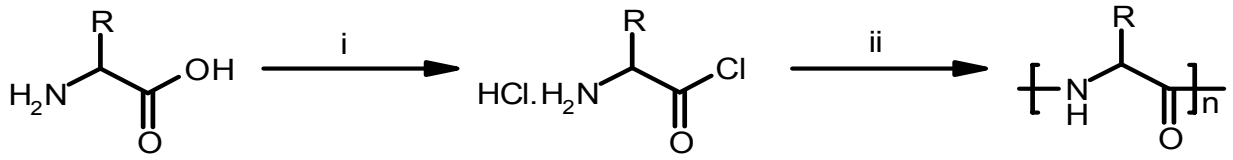

Scheme 4 -11: Poly amino acids from hydrochlorides of α-amino acids. Reagents used are (i) PCl5, CH_3COCl, and (ii) HCl.

This method has been used for synthesis of polymers of Ala, Leu, Phe, Val, β-Ala, α-amino butyric acid, Trp and Pro are reported. In these cases, the average degree of polymerization 'n' obtained was 10 to 20 which was determine by end group analysis.

(v) The formation of poly-α-amino acids from α-amino acids and peptide chlorides as well as peptide azides, containing a free α-amino group; clearly indicate that amino acid and peptide derivatives with an activated carboxyl group and a free amino group may undergoes polycondensation like any other bifuncational monomer (see Scheme 4 -12).

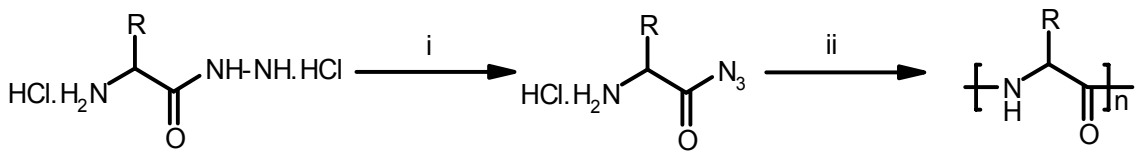

Scheme 4 -12: Poly amino acids from peptide azide. Reagents used were (i) $NaNO_2$ (ii) OH.

(vi) *N*-carbothiophenyl of many amino acids and peptide polymerization in benzene, which was accelerated by small quantities of pyridine or dioxan, gave *N*-carbothiophenyl-α-amino acids as demonstrated in Scheme 4 -13. The average molecular weight obtained in solution was in the range of 10,000 to 130,000 as measured osmometrically.

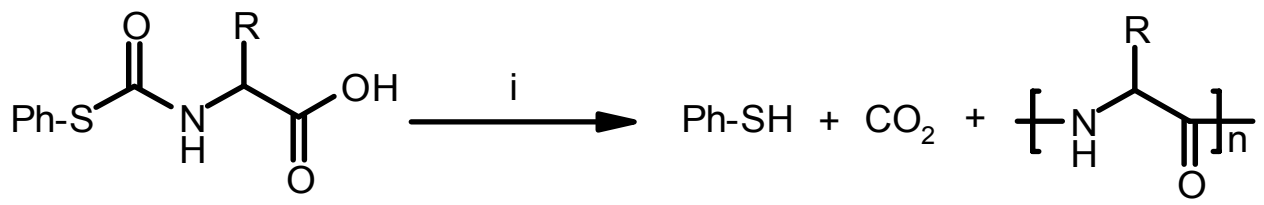

Scheme 4 -13: Polymerization from *N*-carbothiophenyl-*α*-amino acids and peptides. Reagents used were (i) Benzene:Pyridine.

(vii) Several other methods are reported for the insitu preparation of active ester using the coupling reagent EDC [210], DCC [34], α-*N*-carboxyanhydride [211], *N*-hydroxysulfosuccinimide ester [212] and *N*-hydroxysuccinimide [213, 214] have been well established.

(viii) Isolation and purification: In polymerization, mixtures leading to the formation of poly amino acids from the corresponding monomer(s), following low molecular weight compounds may appears: (a) diketopiperazines; (b) hydantoi-*N*-3-acetic acid derivatives; (c) low molecular weight peptides; (d) amino acids; and (e) unreacted monomer. Since these are, as a rule, more soluble in common organic solvents than the high molecular weight polypeptides, they are left in

solution on precipitating the polymer from the polymerization mixture. Further purification may be attained by extraction with suitable solvents or by dialysis.

Poly amino acid which has been prepared by the polymerization of the corresponding amino acid, is dissolved in a suitable solvent (e.g., dimethylformamide, acetic acid, formic acid, chloroform, or methylene chloride) and precipitated by pouring the solution into a non-solvent (e.g., water, acetone, alcohol, ether, or petroleum ether). Water soluble poly amino acids may be freed from low molecular weight impurities by dialysis and isolated by precipitation or freeze-drying. To obtain high molecular weight polypeptides in a fluffy, readily soluble form, it is advisable to lyophilize solutions of the finally purified polymers in water, dioxane, acetic acid or trifluoroacetic acid.

4.3.2. Oligomerization of Dipeptide Building Blocks

The poor receptor subtype selectivity, poor bio-stability and unfavourable absorption properties that often accompany therapeutically relevant peptides has generated a considerable amount of interest in the design of high affinity and selective peptidomimetics [215-219]. This is usually accomplished by the systematic replacement of backbone amide bonds or the incorporation of constrained elements. In a successfully designed peptidomimetic, the essential amino acid side chains of the corresponding peptide are displayed on an alternative scaffold such that the spatial orientation of the side chains corresponds to the display in the bioactive conformation of the peptide [189]. Several building blocks are synthesized which are an alternative to natural substrate [164, 187, 188]. These building blocks are used to exhibit favorable properties in peptide coupling protocols. Unnatural fused bi-cyclopeptide building blocks are also in use with different ring size [164]. The polyhydroxylated dipeptide building blocks with has polar and rigid structure which can stabilises extended helical conformation, as found in *mefp*-1, was accomplished [169]. This dipeptide features an alternative to Hyp and Ser in which former is an expensive compound and latter needs protection of side chains during coupling reaction.

In the current work, oligomerization of polyhydroxylated dipeptide building blocks that was carried out without protection of secondary hydroxyl group is described. It was accomplished with the use of coupling reagent like poly-DCC and/or DCC and additive HOBt (see Scheme 4 - 15). Copolymerization of dipeptide building blocks with Tyr and Lys were worked out effectively and are described in the subsequent sections. As stated previously, Tyr, DOPA and Lys are functional amino acids in *mefp*-1 protein.

For optimization of oligomerization reaction several coupling reagents, bases and several reaction conditions were used. MALDI-TOF MS gave information about number of oligomers obtained after oligomerization.

N-(3-dimethylaminopropyl)-*N'*-ethylcarbodiimidhydrochloride (EDC) was synthesized for the oligomerization of amino acids L-Ala and L-Gly in presence of carboxylic acid activating agent such as *N*-hydroxysuccinimide [210]. Using similar conditions oligomerization of dipeptide molecule of two different bases DIPEA and Et_3N was carried out (see Scheme 4 -14). Oligomerization worked up to n = 2. Oligomerization reaction did not work using $SOCl_2$ with base DIPEA. PyBOP was also used for oligomerization reaction using two different reaction conditions at RT and at 70°C with base DIPEA. It yielded oligomers up to n = 2.

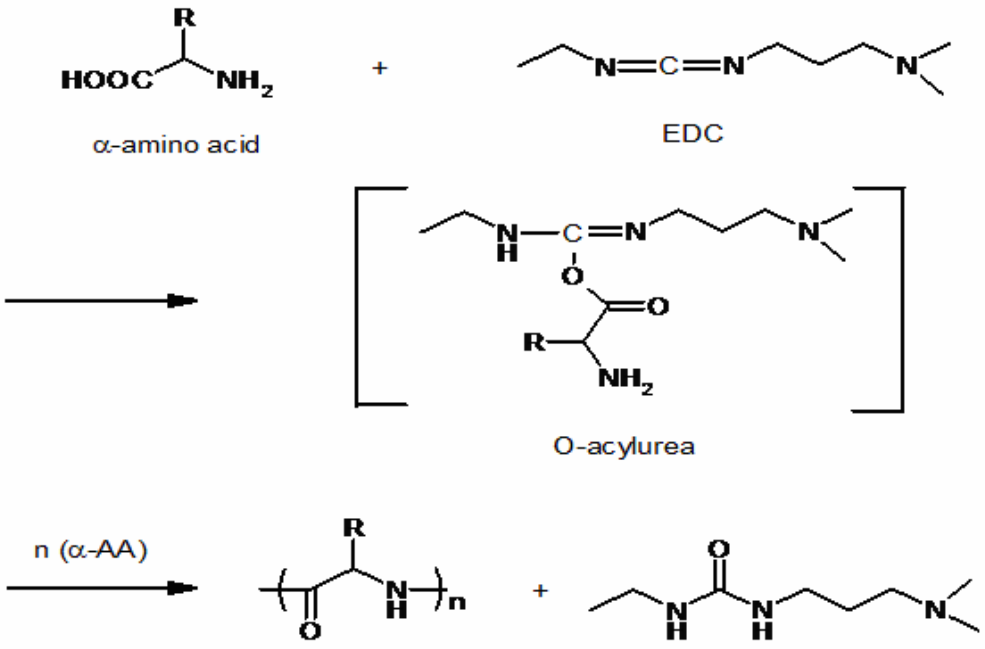

Scheme 4 -14: Oligopeptide formation of α-amino acids using EDC in two steps via formation of *o*-acylurea.

HBTU was used with two bases DIPEA and Et_3N with additive HOBt at different reaction conditions from room temperature to 100°C resulting upto n = 3 oligomers. Oligomerization using the coupling reagent DCC with bases DIPEA and Et_3N was not effectively but after the addition of HOBt, the reaction worked. Reaction mixture was stirred for 48 h with 2 eq DCC using Et_3N base and 5 eq HOBt as a additive. It gave different molecular weight oligomers in the array of n = 1 to n = 8. The same reaction also worked using poly-DCC instead of DCC. Results obtained in both cases are similar. Both coupling reagents yielded oligomers ranging from n = 1 to n = 8. Oligomerization reaction using 2 eq DCC or poly-DCC and 2 eq HOBt with base Et_3N and

solvent DFM was not very effective. In that case, oligomerization worked up to n = 1 and n = 2. Use of 5 eq HOBt instead of 2 eq HOBt helped to enhance effectiveness. The detail reaction conditions and reagents used for oligomerization reaction are mention in table Table 4 -2.

Table 4 -2: Reaction conditions and reagents which are used for oligomerization reaction

Coupling Reagents	Additives/Base/Solvent	Reaction conditions	Number of Oligomers
EDC	DMF	RT, 70°C	n = 2
EDC	DIPEA/DMF	RT, 70°C	n = 2
EDC	NHS/Et_3N/DMF or DMSO	RT, 70°C	n = 2
HBTU	HOBt/DIEA or Et_3N/DMF	RT, 0°C, 50°C, 100°C	n = 1, 2, 3 and 4
DCC	NMP/DMF	RT	n = 3.
DCC	DIEA/DMF	RT,	n = 2
PyBOP	DIEA/DMF	RT, 70°C	n = 2
$SOCl_2$	DIEA/DMF	RT	--
DCC	HOBt/DIEA or Et_3N/DMF	RT	n = 1, 2
poly-DCC or DCC	HOBt/Et_3N/DMF	RT	n = 1, 2,…., 7, 8

Both coupling reagents poly-DCC and DCC were worked for oligomerization reaction, MALDI shows series of oligomers ranging from numbers 1 to 8. After Oligomerization, 1D Proton NMR shows two new peaks at 5.89 ppm and 4.33 ppm. Further, 2D COSY NMR experiement study of oligopeptide confirmed that the proton signal at 5.89 ppm belongs to 9a-H and proton signal at 4.33 ppm was belongs to 9-H. This NMR study also helped to validate that after the polyhydroxylated dipeptide building blocks, the free caboxilic group of the terminal molecule of oligopeptide was coupled to 9-OH and formed lactone **28**. Terminal lactone of oligopeptide was quantitatively cleaved using 1N KOH in MeOH after 30 min. The reaction mixture was quenched with 1N HCl to yield compound **29** (see Scheme 4 -15).

Several matrices like sinapinic acid (*trans*-3,5-Dimethoxy-4-hydroxycinnamic acid), DHB (2,5-dihydroxybenzoic acid), CCA (α-cyano-4-hydroxycinnamic acid), PA (picolinic acid), and Caffic acid were used to optimize the MALDI spectra. Amongest these only two matrices, Caffic acid and α-cyano-4-hydroxycinnamic acid, worked effectively for the measurement of molecular

masses. A MALDI spectrum for compound 28 shows different masses ranging from 538 to 2098 Da.

Three peaks were observed for each oligomer in MALDI, which were separated by 18 Da consecutively. Thus, the difference between first and last peak was 36 Da. The origin of this discrepancy was related to the oxidation of sulpher to sulphoxide and disulphoxide as a first thought. To confirm this phenomenon, reduction of compound **28** was carried out using TFA/TMSBr/EDT by stirring the reaction mixture for 20 min. at room temperature. MALDI spectra of resulting product gaves three similar peaks with consecutive difference of 18 Da. Additionally, with the aid of NMR spectroscopy further proofs of reduction of sulpher during oligomerization were gained. However, no change in chemical shift for 2-H proton signal was observed. The peak shift would cause upon change in the chemical/electronic environment if sulpher atom oxidise to sulphoxide. This led to conclude that the additional mass arising in MALDI spectrum is due to complexation of compound with water molecule as water has a mass of 18.

After the cleavage of terminal lactone MALDI for compound **29** shows same masses with molecular weight of compounds in the range of 538 to 1838 Da (similar to compound **28**).

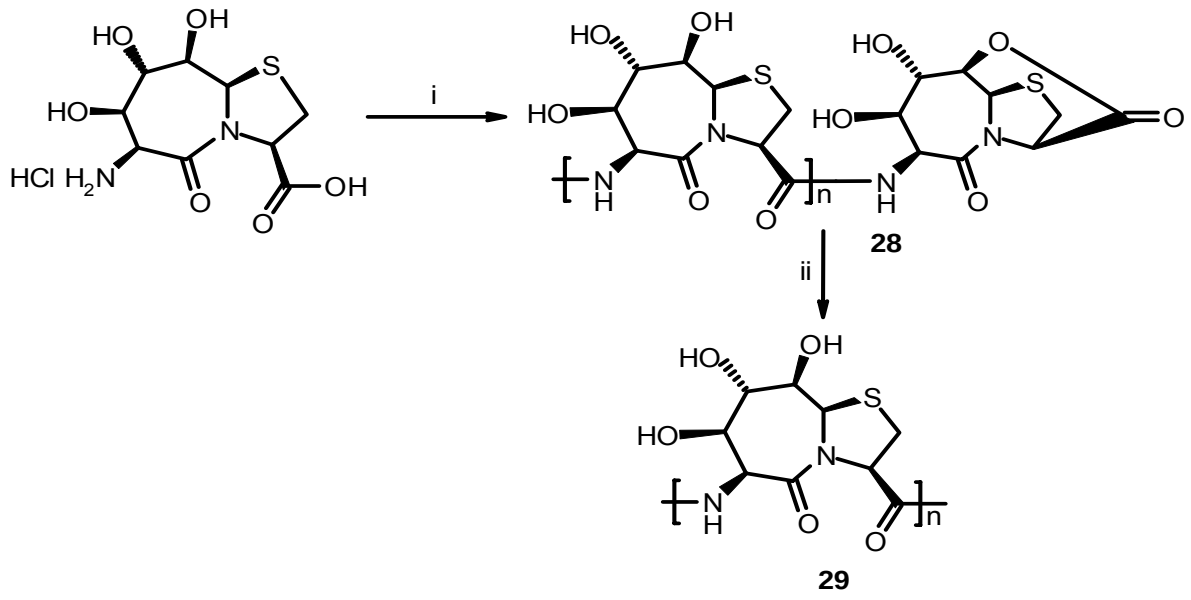

Scheme 4 -15: Oligomerization of dipeptide building blocks. Reagents: (i) poly-DCC, HOBt, Et_3N, RT, 48h, quant. or DCC, HOBt, Et_3N, 48h, quant. (ii) 1N KOH, MeOH, 1N HCl, 30 min, quant.

GPC, with polystyrene as standard, shows mixture of high molecular weight compounds masses ranging from 2962 Da to 36950 Da. These high molecular masses are deficient in MALDI-TOF

mass spectrum. HPLC also shows many signals during the retention time from 6.68 min to 14.65 min. This clearly indicates that the product had diffent oligomeric compositions.

4.3.3. Oligomerization of L-Tyrosine

Tyrosine is an important nutritional ingredient and factor for biosynthesis of the brain neurotransmitters epinephrine, norepinephrine and dopamine. Tyr has been tested on humans for increasing their endurance to anxiety and stress under fatigue. It was proven in research studies that Tyr supplementation results in increased performance over a control group [220]. Tyr was also used with Trp for treatment of cocaine abuse [221]. Astbury et. al. [222] mentioned the preparation of poly-Tyr, but no details of the synthesis or structure were given. A recemic poly-Tyr was prepared by Noguchi [223, 224], using *o*-carbomethoxy-*N*-carboxy tyrosine anhydride as the starting monomer. The synthesis of poly-L-Tyr from *o*-carbobenzoxy-L-tyrosine-NCA was described by Katchalski and Sela [225, 226] as shown in Scheme 4 -16.

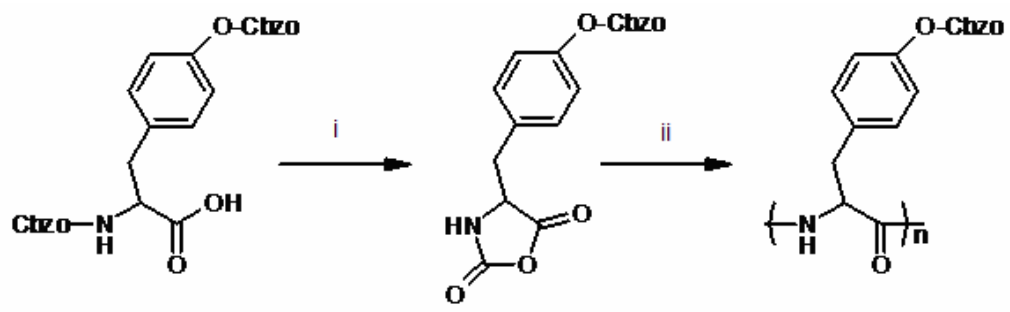

Scheme 4 -16: Oligomerization of L-Tyr as performed by Katchalski and Sela [225, 226]. Reagents: (i) PCl_5, and (ii) H_2O.

L-Tyr yielded *N,o*-dicarbobenzoxy-L-tyrosine on coupling with benzyl chloroformate between pH 9 and 10.5. *o*-Carbobenzoxy-*N*-carboxy-L-tyrosine anhydride was obtained by treatment with phosphorus pentachloride. On polymerization in bulk or in benzene solution, gave poly-*o*-carbobenzoxy-L-tyrosine with a number average degree of polymerization n = 20 to 80, as determined by amino nitrogen end group analysis. Overell and Petrow [227] repeated the synthesis of poly-L-Tyr from both the *o*-acetyl and *o*-carbobenzoxy-L-tyrosine-NCAs. The *o*-acetyl-NCA was obtained from *o*-acetyl-*N*-carbobenzoxy-L-Tyr by treatment with thionyl chloride, while the *o*-carbobenzoxy-NCA was prepared by the phogenation of *o*-carbobenzoxy-L-Tyr. Later L-Tyr derivative was formed on coupling benzyl chloroformate with copper salt of L-Tyr. The acetyl and carbobenzoxy group of poly-*o*-acetyl and poly-*o*-carbobenzoxy tyrosine respectively were

removed by means of anhydrous hydrogen bromide in glacial acetic acid. Poly-L-Tyr preparation of an average degree of polymerization n = 19 to 104.

Oligomerization of L-Tyr was synthesized by using the coupling reagent poly-DCC or DCC with additive HOBt, without protection of phenolic group. The oligomerization reaction is shown in Scheme 4 -17.

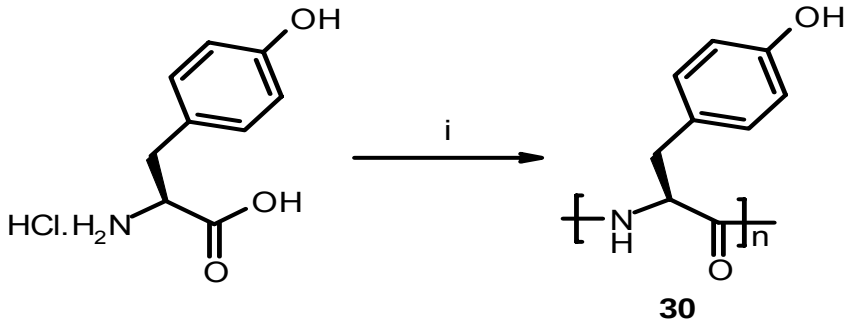

Scheme 4 -17: Synthesis of tyrosine oligomers **30**. Reagents used were (i) DCC, HOBt, DMF, RT, 48h, quant. or poly-DCC, HOBt, DMF, RT, 48h, quant.

Tyrosine oligomers was prepared using 2 eq poly-DCC (*N*-cyclohexylcarbodiimide, *N'*-methyl polystyrene) or 2 eq DCC, 5 eq HOBt and 2 eq triethylamine corresponding to amount of Tyr monomer. Dimethylformamide and triethyl amine were found to be the most suitable solvent and base, respectively. Reaction mixture was stirred for 48 h. Yield obtained in methods using poly-DCC or DCC are quantitative.

MALDI (matrices: Caffic acid and Cinnamic acid) shows different molecular masses ranging from 344 to 4256 Da. Proton magnetic resonance spectra of compound **30** shows broad signals. Threfore, 2D HMQC spectrum was used to assign the region of the signal.

4.3.4. Oligomerization of L-DOPA

3,4-dihydroxyphenylalanine (DOPA) is a naturally occurring, unusual amino acid derived from post-translational modification of Tyr, as stated earlier [228]. It has been one of the principal agent administer to patients with Parkinson's disease since 1967 [229]. Although rarely found in proteins, DOPA was detected in high yield (*ca* 10%) in marine mussel proteins [230], as well as eggshell precursor proteins of *fasciola hepatica* [231], and *schistosoma mansoni* [232]. As shown in section 3.3, the catechol functionality of DOPA residues is mainly responsible for adhesion and cross-linking of proteins. Michael reaction is one of the most frequently cited reactions of side-chain amino groups of Lys residues to a DOPA-quinone residue. The mechanism of this process is

unknown. Focus of several research groups is on DOPA to explore its exact role in mussel adhesive protein.

Our additional goal for this study was to prepare fibrous peptides using oligomerize DOPA as well as copolymerization of DOPA with bicyclic dipeptide building blocks and Lys.

Optically inactive poly(DL-β-3,4-dihydroxyphenyl-α-alanine) has been synthesized by Harwood and Cassidy [233] as shown in Scheme 4 -18.

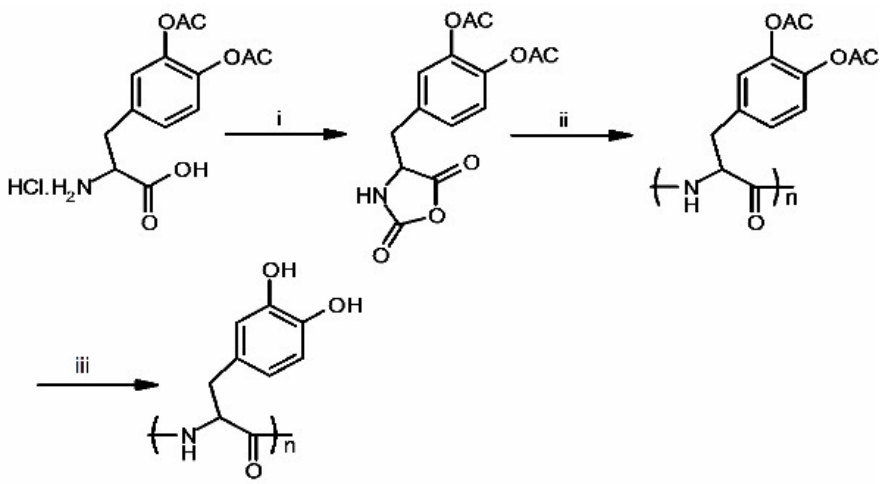

Scheme 4 -18: Synthesis of L-DOPA oligomers perfoemd by Harwood and Cassidy [233]. Reagents used were (i) $SOCl_2$, (ii) dioxane, trace NaOH, (iii) 0.4 N NaOH, 45 min, and HCl.

A solution of 4-(3,4-diacetoxybenzyl) oxazolidine-2,5-dione in dioxane was mixed with a solution of mixed sodium hydroxide in methanol dissolved in dioxane, the reaction was stirred for four days. The crud polymer was dissolved in ethyl acetate and reprecipitate by adding petroleum ether. In those studies, the molecular weight of polymer was found to be 7000 Da with the use of end group titration [234, 235].

Preparation of poly-DOPA has been already performed through polymerization of *o,o'*-dicarbobenzoxy-DOPA-*N*-carboxyanhydride. Subsequent removal of the protecting group by alcoholic sodium hydroxide or hydrogen bromide in 1:2 dioxane/glacial acetic acid mixed solvent and the oligomers was characterised by using elemental analysis. The elemental analysis showed that the oligomerization yielded n = 2 to 3.

The method adopted in this study to produce polyDOPA without protection of catechol moiety using coupling reagent poly-DCC (*N*-cyclohexylcarbodiimide, *N'*-methyl polystyrene) or DCC and HOBt as additive is shown in Scheme 4 -19. Characterization of oligopeptides was carried out using MALDI, which shows excellent fraction of alternating masses from 376 to 4672 Da.

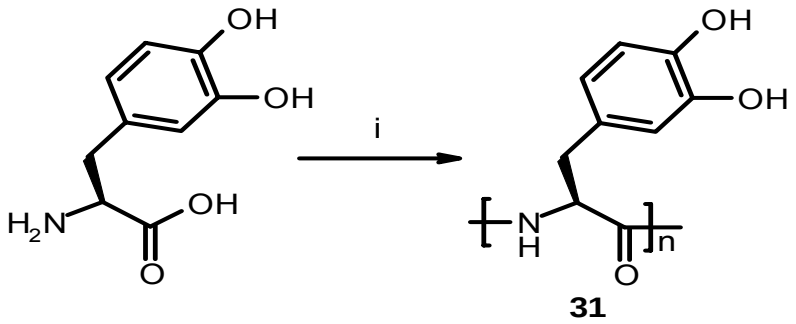

Scheme 4 -19: Synthesis of DOPA oligomers **31**. Reagents used were (i) DCC, HOBt, Et_3N, DMF, RT, 48 h, quant. or poly-DCC, HOBt, Et_3N, DMF, RT, 48 h, quant.

DOPA oligomers **31** were prepared using 2 eq poly-DCC (*N*-cyclohexylcarbodiimide, *N'*-methyl polystyrene) or 2 eq DCC and 5 eq HOBt. The pH of the reaction mixture was maintained in between 8 to 9 using triethyl amine. Dimethylformamide and triethyl amine were found to be the most suitable solvent and base, the reaction mixture were stirred for 48 h at room temperature, yield obtained using both coupling reagent was quantitative.
MALDI (matrices: Caffic acid and α-cyano-4-hydroxycinnamic acid) gives molecular weight of DOPA oligomers in the range of 376 to 4672 Da. Proton NMR spectrum of compound **31** show many broad peaks. Therefore, the spectral assignment was performed with the help of 2D HMQC spectrum (see chap 5).

4.3.5. Oligomerization of L-Lysine

Due to its polycationic property, water solubility, biodegradability and biocompatibility, poly-Lys shows multifarious application in the life sciences. In medical application, α-poly-L-Lys has been used to enhance efficacy of some interferon inducers, antiviral and antitumer agent [236, 237]. It has also been shown to improve drug transport by reducing drug resistance and to increase the efficiency of organelle fusion from hematocytes, liposomes etc. Many workers have investigated the use of α-poly-L-Lys in human drug delivery systems, especially for gene delivery. The antifolate agent methotrexate (MTX) which is one of the most widely used drugs in the treatment of human leukaemia, sarcomas and other forms of neoplastic diseases [238] Conjugation of poly-L-Lys with methotrexate increased cellular uptake and offers a new way to overcome drug resistance related to deficient transport [239, 240].
Polymerization has been carried out, in the past, using the ε-amino group of Lys had to be masked in order to prevent its participation in the polymerization and thus to insure that all the amide bonds are derived from α-amino group of the monomer followed by removal of blocking group to

yields poly-L-Lys. The synthesis of a crude poly-L-Lys preparation was described by Frankel and Katchalski [241]. In 1998, Katchalski and associates [242] described the synthesis of poly-L-Lys in detail (see Scheme 4 -20) and gave a proof of its structure.

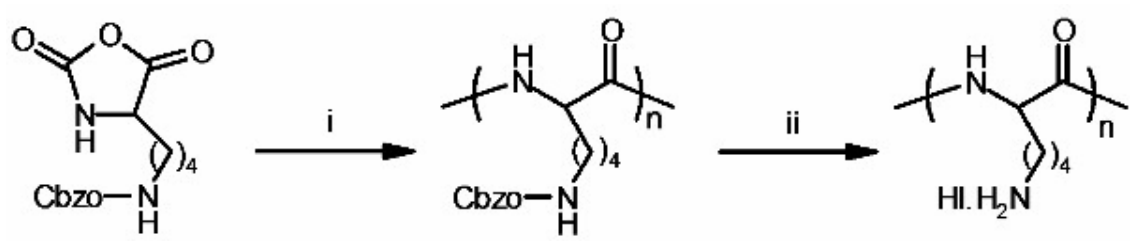

Scheme 4 -20: Synthesis of L-Lys oligomers performed by Katschalski et. al. [242]. Reagents used were (i) H_2O and (ii) PH_4I.

The method used is as: ε,*N*-Carbobenzoxy-α,*N*-carboxy-L-Lys anhydride was chosen as starting monomer and preparation of the desired polymer was carried out in bulk at a temperature of 105°C with a pressure 10^{-4} mm of Hg. The average degree of polymerization, n = 32, of the product obtained being determined by amino N end group analysis. Cleavage of carbobenzoxy group was carried out using phosphonium iodide, which shows that decarbobenzoxylation is accompanied by the formation of benzyl iodide.

Several polymerization techniques starting from monomer ε,*N*-carbobenzoxy-α,*N*-carboxy-L-Lys have been furnished, via ammonia initiation in dioxane [243], diethylamine initiation in dimethylformamide [244], and water initiation in benzene [234].

High molecular weight poly-L-Lys resulted through polymerization of ε,*N*-carbobenzyloxy-L-lysine-*N*-carboxy anhydride using dry dioxane and sodium methoxide as a base and ε,*N*-carbobenzyloxy group was removed HBr in acetic acid [245].

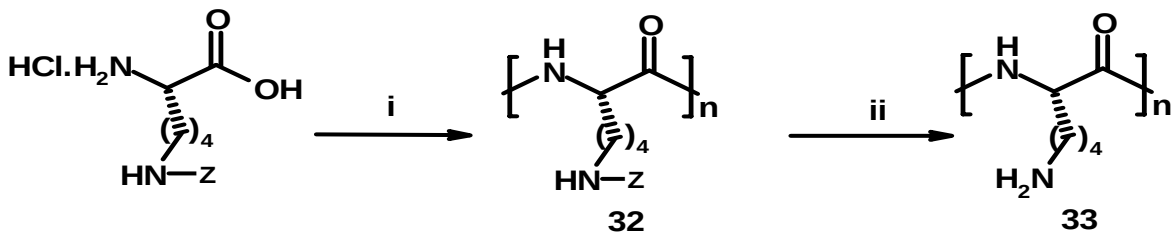

Scheme 4 -21: Synthesis of L-Lys oligomers **33**. Reagents used were (i) DCC, HOBt, Et_3N, DMF, RT, 48h, quant. or poly-DCC, HOBt, Et_3N, DMF, RT, 48h, quant. (ii) 60%TFA, 30% HBr, 20 min, quant.

In this study, the poly-L-Lys was synthesized through polymerization of ε,*N*-carbobenzyloxy-L-Lys using coupling reagent DCC or poly-DCC and additive HOBt. The oligomerization reaction is shown in Scheme 4 -21. Cleavage of *N*-carbobenzyloxy group was carried out using TFA and HBr.

Compound **32** were prepared using 2 eq poly-DCC (*N*-Cyclohexylcarbodiimide, *N'*-methylpolystyrene) or 2 eq DCC and 5 eq additives HOBt. The pH of the reaction mixture was maintained between 8 and 9 using triethyl amine. Dimethylformamide and triethyl amine were found to be the most suitable solvent and base, the reaction mixture were stirred for 48 h at room temperature, yields obtained using the coupling reagent poly-DCC or DCC are quantitative. MALDI spectra with Caffic acid and cinnamic acid as matrices worked effectively leading to molecular weight of DOPA oligomers in the range of 547 to 4498 Da.

Deprotection of Z-group was carried out using 60% TFA in DMF and 30% HBr in acetic acid. The reaction mixture was stirred for 20 min. The product was reprecipitated in cold ether to get **33**. Yield obtained was quantitative. Strong acidic nature of poly-L-Lys lead to the cleavage of molecular weight of oligomers on MALDI matrices, resulting into oligomers with an array of 147 to 1050 Da. 1D Proton NMR of compound **32** and **33** contained broad peaks which led us to utilize 2D HMQC for assigning the spectral region.

4.4. Copolymerization Reaction

The polymerization techniques available at present permit the synthesis of copolymers of α-amino acids with a random sequence, bulk copolymers as well as copolymers composed of a few amino acids with a known repeating sequence. Many of copolymers were used as a model compound in the study of the effect of different amino acid residues, on the crystallinity of peptides, their solubility properties and the backbone configuration. Some of them are used in the evaluation of the effect of neighboring amino acid residues and on the chemical and physical properties of specified functional groups present in the copolymer.

Proteins are polyampholytes and thus particular attention was given by various authors to the study of copolymers composed of basic and acidic amino acids. Akabori et. al. [246] was the first to account a synthesis of a polyampholyte composed of DL-Lys and L-Glu, using the NCAs of ε-carbobenzoxy-DL-Lys and γ-methyl-L-Glu as monomers. Later, several synthetic copolymers with a known sequence of α-amino acids have been accomplished [247]. Most of them were obtained by the polycondensation of peptide esters, peptide chloride hydrochlorides, or *N*-carbothiophenyl peptides. These methods usually yield polymers with low degree of polymerization. Several

methods of the activation of α-amino acids and peptides for the polymerizations and its isolation and purification methods are introduced in section 4.3.1.

The preparation of such polymers, especially those containing trifunctional amino acids, is certainly a challenging problem to an organic chemist. Many of the methods adopted in the past few years in peptide for the suitable synthesis of the above type of copolymers. This includes, the carbodiimide method [45, 248] and the activation of α-carboxy groups by their transformation into the *p*-nitrophenyl, *p*-nitrophenyl thiol, or cynomethyl esters [249-252].

As stated in chapter 3, natural adhesive precursor protein (i.e., *mefp*-1) has been extracted from the blue mussel, *Mytilus edilus*, spread on culture plates and oxidized with mushroom *tyrosinase*. This procedure led to the formation of an adhesive that could be used for cell attachment and growth [76]. It has also been shown to be effective as an adhesive for the bonding of wet tissue samples [253]. The adhesive protein was also found to be non-toxic; however, the toxicity of enzymatic oxidizing agent was problematic.

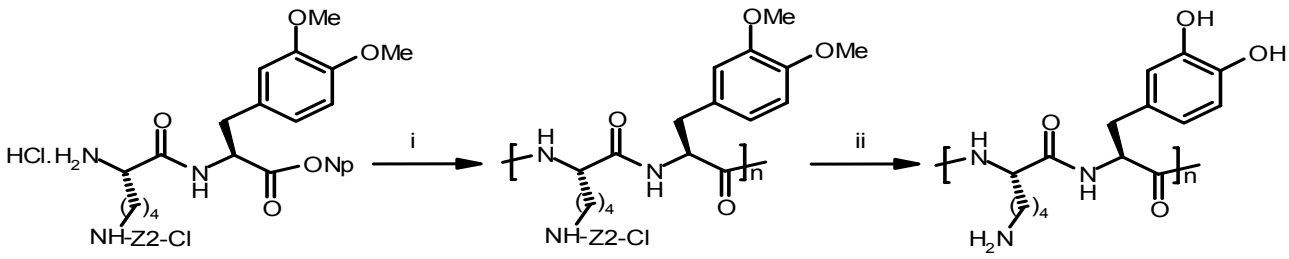

Scheme 4 -22: Preparation of sequential polypeptide poly-Lys-DOPA. Reagents used were (i) HOBt, Et_3N, DMF and (ii) BBr_3, $CHCl_3$.

Alternatively several synthetic polypeptides containing DOPA, Lys and Tyr homo-polymers as well as specific sequence copolymers of L-DOPA with L-Lys and L-Glu have been accomplished [173, 174, 176, 186].

Scheme 4 -22 and Scheme 4 -23 show the preparation of sequential polymerization of poly-Lys-DOPA and poly-Glu-DOPA.

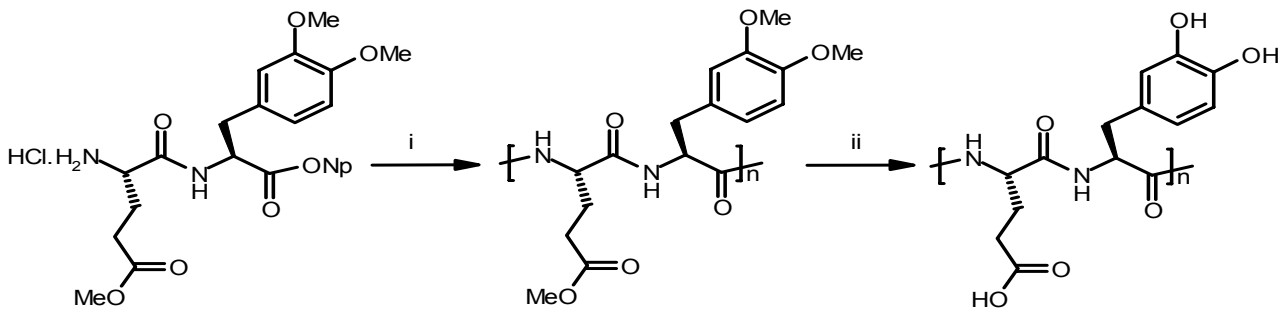

Scheme 4 -23: Preparation of sequential polypeptide. Reagents used are (i) HOBt, Et_3N, DMF and (ii) BBr_3, $CHCl_3$.

Synthesis of L-Lys/L-Tyr copolymers has been performed in the laboratory of Ikeda [154, 176]. In addition to that, synthesis of random co-polypeptides containing as many as 18 different amino acids, including DOPA was also executed [177, 178]. Adhesive studies and cross linking of these polymers were implemented using iron and Al_2O_3 adherends without any oxidizing agent [175].
More detailed studies focused on L-Lys/L-Tyr random copolymers and complex random copolymers where Tyr enzyme was used as the oxidizing agent [154, 179]. This adhesive system was studied in water and diluted sea water and was found to form adhesive bonds, although conversion of Tyr residues to DOPA was inefficient. Successful oxidation was achieved only when the polymer chains were cleaved with *chymotrypsin*.
Copolymerization of L-Tyr and L-Lys with polyhydroxylated dipeptide building blocks were carried out during study for this thesis. The copolymers were characterized for their size, structure and adhesiveness using several analytical tools.

4.4.1. Copolymerization of Tripeptide (Bic-Tyr)

The adhesive characteristic of mussel adhesive polymers have been attempted to mimic into synthetic polymers by several groups. This involves the synthetic co-polymerization of natural amino acids like Lys, Tyr and DOPA since these are functional amino acids in mussel adhesives.
Polymerization of L-Tyr was already accomplished using side chain protection groups [173].Also the ring opening random polymerization of L-Tyr-*N*-carboxyanhydride was synthesized as well as copolymerizaion of *N*-carboxyanhydide (NCA) of *o*-acetyl-L-Tyr with NCAs of L-Val and L-Gly using dioxane at 25°C with *N*-butylamine as initiator [254]. Sequential copolymerization of Tyr-Lys and Tyr-Glu and its conformational studies was as well accomplished [154, 184, 185, 255].
Synthesis of Bic-Tyr tripeptide **12** was carried out using Boc-stratergy (see Scheme 4 -5), during this study. Sequential copolymerization of tripeptide molecule without protection of hydroxyl and phenolic–OH groups was carried out using the coupling reagent HOBt, and additive HBTU. The

polymerization reaction was shown in Scheme 4 -24. The obtained product, poly Bic-Tyr, compound **34** was characterised using MALDI-TOF MS, NMR, GPC, AFM and Gel electrophoresis to resolve structure and size.

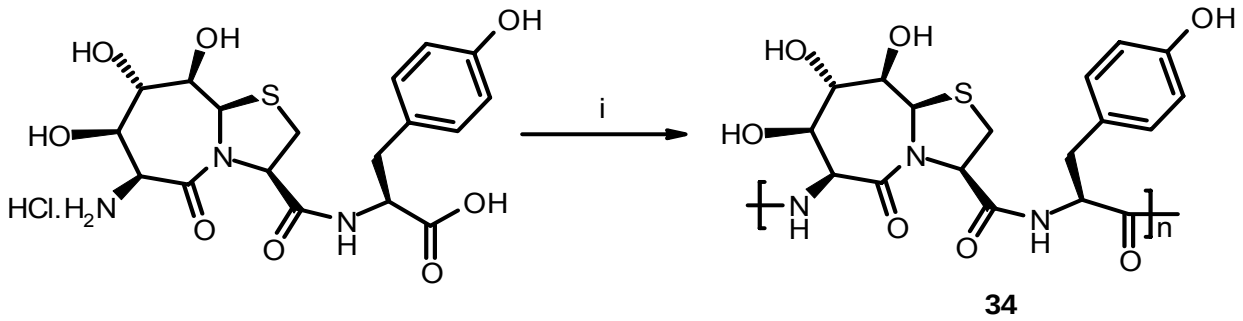

Scheme 4 -24: Synthesis of compound **34**. Reagents used were (i) DCC, HOBt, Et_3N, DMF, RT, 48 h, quant. or poly-DCC, HOBt, Et_3N, DMF, RT, 48 h, quant.

Tripeptide Bic-Tyr was copolymerized using both coupling reagents DCC and poly-DCC. Compound **34** was prepared using 2 eq poly-DCC or 2 eq DCC and 5 eq additives HOBt. The pH of the reaction mixture was maintained between 8 and 9 using triethyl amine. Dimethylformamide and triethyl amine were found to be the most suitable solvent and base. The reaction mixture was stirred for 48 h at room temperature, yields obtained using the coupling reagent poly-DCC or DCC are quantitative.

MALDI, with caffic acid and α-cyano-4-hydroxycinnamic acid as matrices, for compound **34,** shows that the reaction mixture contained different numbers of oligomers with their molecular weights ranging from 441 to 4671 Da.

GPC of compound **34** showed that the product contained a mixture of higher molecular weight compounds in the range of 1628 to 9031 Da. Polystyrene was used as a standard for the measurement of GPC.

The molecular size of oligopepties was measured using AFM on mica surface. According to these studies, compound **34** contains different molecular sizes with the average molecular particle size of the oligopeptides lying in the range of 2-4 nm.

Gel electophorasis studies showed that the molecular weight of compound **34** was less then 14.4 kDa. Marker (Amersham) ranges from 14.4 kDa to 97 kDa and compound **34** showed a single spot little below the 14.4 kDa band. This results shows similarity with GPC results although not with MALDI-TOF mass spectroscopy.

1D proton NMR spectrum showed only numerous unassignable peaks. COSY and HMQC were therefore used to assign resonances. Adhesive properties of compound **34** are tested and discussed in next chapter.

4.4.2. Copolymerization of Dipeptide (Lys(2-Cl-Z)-Tyr)

Synthetic co-polymerization of natural amino acids containing Tyr, Lys and DOPA are performed during this dissertation as these are functional amino acids in mussel adhesive proteins. Sequential polypeptides containing DOPA-Lys, Lys-Tyr, Lys-Phe were already synthesized by several other groups along with their conformational studies [154, 176].

However, these studies used side chain protected L-Lys, L-DOPA and L-Tyr for co-polymerization. Deming and co-workers had synthesiszed water soluble copolypeptides containing L-DOPA and L-Lys by ring opening polymerization of α-amino acid NCA monomers [131].

Synthesis of compound **27**, Lys(2-Cl-Z)-Tyr was carried using Boc-stratergy as shown in Scheme 4 -10. Sequential copolymerization of compound **27**, Lys (2-Cl-Z)-Tyr, without protection of Tyr phenolic group was carried out using coupling reagent HOBt and HBTU as an additive. The polymerization reaction is shown in Scheme 4 -25.

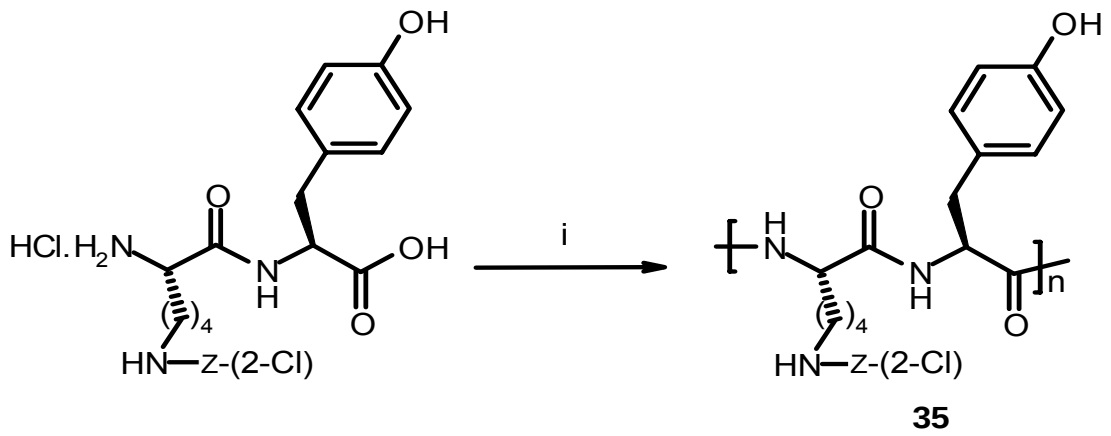

Scheme 4 -25: Synthesis of compound **35**. Reagents used were (i) DCC, HOBt, Et_3N, DMF, RT, 48 h, quant. or poly-DCC, HOBt, Et_3N, DMF, RT, 48 h, quant.

Compound **35** were prepared using 2 eq. poly-DCC or 2 eq DCC and 5 eq additives HOBt. The pH of the reaction mixture was maintained in between 8 to 9 using triethylamine. Dimethylformamide and triethyl amine were found to be the most suitable solvent and base. The

reaction mixture was stirred for 48 h at room temperature and yield obtained using both coupling reagent poly-DCC or DCC are quantitative.

MALDI-TOF MS of compound **35**, poly-Lys(2-Cl-Z)-Tyr, in caffic acid and α-cyno-4-hydroxycinnamic acid matrices gave moleculr mass in the range of 482 Da to 2323 Da.

Gel permeation chromatography (standard: Polystyrene) were showed a mixture of higher molecular weight compounds ranging from 880 to 11450 Da.

4.4.3. Copolymerization of (Lys(Z)-Bic-Tyr)

Compound **15** was prepared using Boc-stratergy as shown in Scheme 4 -6. Sequential co-polymerization of tetrapeptide Lys(Z)-Bic-Tyr without protection of secondary hydroxy group of Bic molecule and phenolic –OH of Tyr was carried out using coupling reagent HOBt and an additive HBTU. The polymerization reaction is shown in Scheme 4 -26.

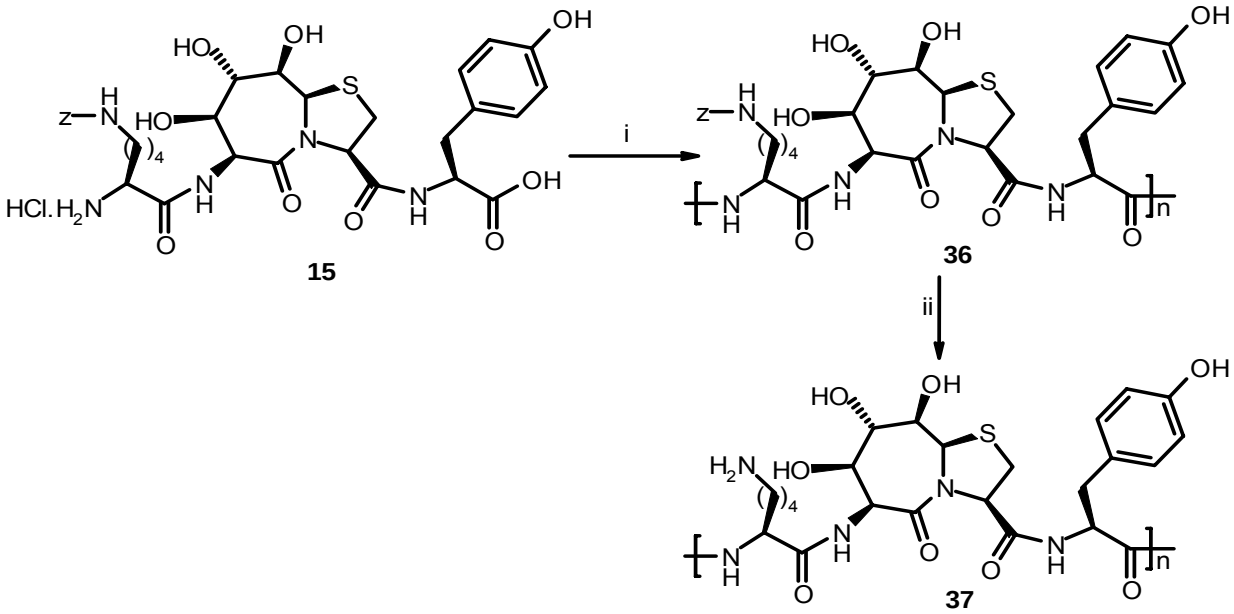

Scheme 4 -26: Synthesis of copolymer **37**. Reagents used were (i) DCC, HOBt, Et_3N, DMF, RT, 48 h, quant. or poly-DCC, HOBt, Et_3N, DMF, RT, 48 h, quant. (ii) HCl/Et_2O, 8 h, quant.

Compound **36** were prepared using 2 eq poly DCC (*N*-Cyclohexylcarbodimide, *N'*-methyl polystyrene) or 2 eq DCC and 5 eq additives HOBt. The pH of the reaction mixture was maintained in the range of 8 to 9 using triethylamine. Dimethylformamide and triethyl amine were found to be the most suitable solvent and base. The reaction mixture was stirred for 48 h at room temperature. Yield obtained using both coupling reagent poly-DCC or DCC was quantitative. was

MALDI (Caffic acid and α-cyano-4-hydroxycinnamic acid as matrices) showed a series of Lys(z)-Bic-Tyr, Compound **36**, oligomers with masses ranging from 703 Da to 2578 Da.

Gel permeation chromatography (Polystyrene standard) results for compound **36** show a mixture of higher molecular weight compounds with masses ranging from 1614 Da to 32920 Da.

Gel electrophoresis shows that the molecular weight of the compound **36** is less then 14.4 kDa, as the band runs little below marker at 14.4 kDa.

1D proton NMR spectrum showed only numerous unassignable peaks. Therefore, COSY and HMQC were used to assign.

AFM of compound **36** shows mixture of different molecular sized compounds with the average molecular size of oligomer as 3.1 nm. AFM measurement was carried out on mica surface.

Quantitatively deportation of Z-group was carried out using HCl/Et_2O. The reaction mixture was stirred for 8 h at room temperature, yields compound **37**. Deprotection of Z-group was attempted under hydrogen atmosphere using 10% Pd/C in mixture of the solvent MeOH and DMF, because the compound **36** was not soluable in MeOH.

After the deprotection Z-group compound **37** was characterized by MALDI using same matrices. It shows that molecular weight of the compounds was ranging from 569 Da to 1671 Da.

As proton NMR of compound **37** showed numerous unassignable peaks, 2D HMQC was used to analyse structure. Adhesive property of this compound has been tested and discussed in next chapter.

5. Adhesive Peptides and Copolymers: Characterization

This chapter describes characterization of compounds which were synthesized during the exploration of synthetic adhesive peptides. Analytical tools like NMR spectroscopy, MALDI-TOF mass spectroscopy, atomic force microscopy, gel permeation chromatography and gel electrophoresis were used.

^{1}H NMR was enough for structural characterization of monomeric compounds, whereas high molecular weight compounds and mixtures gave broad unassignable signals. In such cases, homo- and heteronuclear 2D NMR spectroscopy was used to gather information on structure by means of chemical shifts. As evident, 2D NMR spectroscopy has superior resolution because of introduction of the second dimension. COSY (Correlated Spectroscopy) gives correlation of protons through J couplings and HMQC (Heteronuclear Multiple Quantum Correlation) experiment correlate protons to their directly connected hetero nucleus (e.g. ^{1}H-^{13}C pair). These features of COSY and HMQC fetched attention during this study for characterization.

Matrix Assisted Laser Desorption Ionization-Mass Spectrometry (MALDI-MS) is an analytical method to determine the molecular mass of peptides and proteins in high vacuum. MALDI-TOF was used to measure molecular weights of oligopeptides and copolymers. Samples were prepared by mixing 2 µl of peptide sample with 1 µl caffic acid or 1 µl α-cyno-4-hydroxylcinnamic acid matrix solution. 1 µl of this solution was pipetted onto a metallic target probe and dried under air. The co-crystallized samples were investigated with a “Bruker FLEX III” spectrometer. Several matrices like sinapinic acid (*trans*-3,5-Dimethoxy-4-hydroxycinnamic acid), DHB (2,5-dihydroxybenzoic acid), CCA (α-cyano-4-hydroxycinnamic acid), PA (picolinic acid), Caffic acid were used to optimize the MALDI spectra. Depending on the expected molecular weight of the synthesized compound, columns were chosen while performing MALDI-TOF measurements.

In addition to MALDI-TOF mass spectroscopy, techniques like gel permeation chromatography (GPC) and gel electrophoresis on a SDS page were also used for the measurement of molecular weight (size based techniques).

GPC measurements were performed using polystyrene standards with a set of three columns with dimethylformamide as solvent (300 × 8 mm, type SDV, 10 µm from PSS) using a differential refractometer as detector at 25°C. polystyrene was used as a standard for the GPC measurements

Gel electrophoresis is a technique in which charged molecules, such as polypeptides or DNA, are separated according to physical properties as they are forced through a gel by an electrical

current [256]. Polypeptides (proteins) are commonly separated using polyacrylamide gel electrophoresis (PAGE) to characterize individual proteins in a complex sample or to examine multiple proteins within a single sample. PAGE can be used as a preparative tool to obtain a pure protein sample, or as an analytical tool to provide information on the mass, charge, purity or presence of a protein. Several forms of PAGE exist and can provide different types of information about the protein(s). Nondenaturing PAGE, also called native PAGE, separates proteins according to their mass:charge ratio. SDS-PAGE, the most widely used electrophoresis technique, separates proteins primarily by mass. In this study, the analysis of the mass of synthesized oligopepetides and copolymers samples was performed using SDS-PAGE. Samples were run on a 15% SDS-PAGE (Sodium Dodecyl Sulphate-Polyacrylamide gel electrophoresis), on a mini Biorad system at a constant current of 30 mA. The molecular weight marker from Amersham (GE Healthcare) ranging from 97 kDa to 14 kDa was used for comparison of polypeptide bands.

Characterization of adhesiveness of synthesizes compounds was done using NMR based technique, diffusion ordered spectroscopy (DOSY), and Atomic Force Microscopy (AFM). Details of both of these techniques as well as results obtained from these studies are discussed in section 5.2 and subsequent sections.

5.1. Structural Characterization and Molecular Size of Synthesized Peptides

*5.1.1. Compound **6** (Fmoc-Bic-COOMe)*

2D correlation spectrum (COSY) was used to assign chemical shifts of compound **6** (Fmoc-Bic-COOMe) (see Figure 5 -1). The aromatic proton signals belonging to Fmoc-groups appear at 7.89, 7.72, 7.41 and 7.32 ppm. Proton signal appearing at 7.20 ppm belongs to Bic-NH. COSY spectrum shows that Bic-NH is coupled with 6-H (4.86 ppm) with a coupling constant 9.06 Hz. The triplet for proton 3-H at 4.69 ppm shows a correlation with 2-H (3.30 ppm) with a coupling constant 7.68 Hz. A singlet appearing at 5.46 ppm is for proton 9a-H. Two other protons give signal at 5.68 ppm (8-OH) and 5.33 ppm (7-OH) and show a correlation with a signal at 3.81 ppm (8-H and 7-H), with a coupling constant 3.57 Hz and 4.39 Hz. Proton signal belonging to Fmoc-α & β shows at 4.25 ppm.

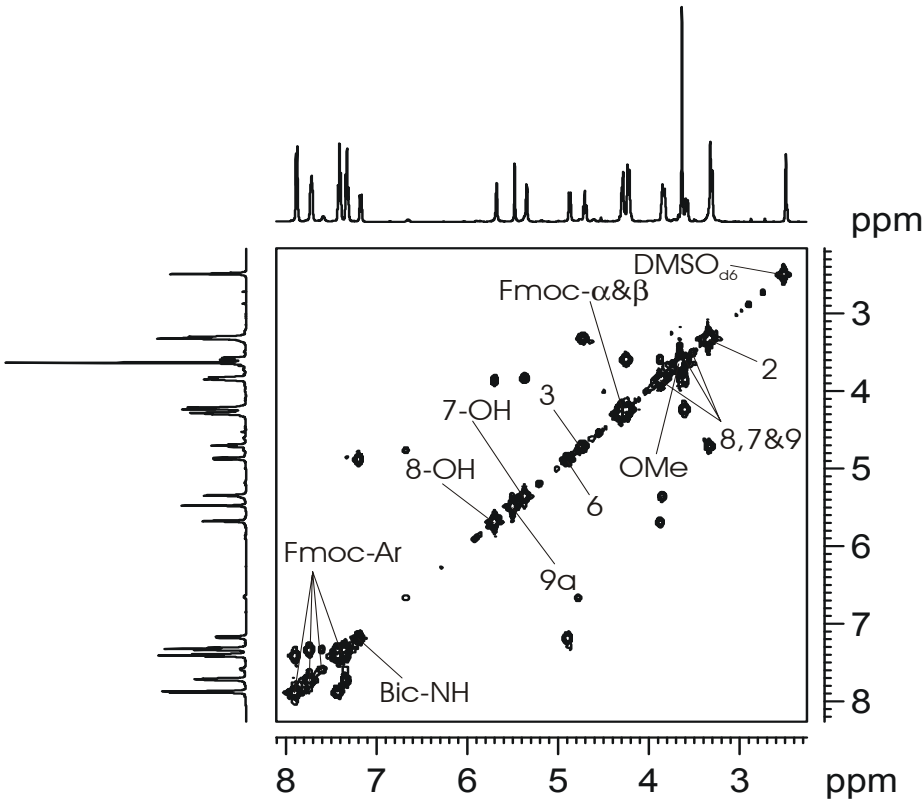

Figure 5 -1: 2D COSY spectrum of compound **6** Fmoc-Bic-COOMe (500 MHz, DMSO-d_6) along with projections. Assigned chemical shifts are shown with connecting lines.

The methyl proton shows a signal at 3.63 ppm. 9-H proton appears at 3.56 ppm with a doublet of a doublet and a correlation with 9-OH and 8-H, with a coupling constant 3.20 Hz and 8.51 Hz.

*5.1.2. Compound **7** (NH_2-Bic-COOH)*

COSY spectrum of compound **7** (NH_2-Bic-COOH) was measured in DMSO-d_6 (see Figure 5 -2). The singlet for 9a-H appears at 5.58 ppm and shows a crosspeak with 9-H proton appearing at 3.51 ppm. The 9-H proton shows a correlation with 8-H (3.82 ppm) proton with a coupling constant 3.04 Hz. Doublet of proton signal for 6-H appears at 4.53 ppm, whereas 3-H shows a triplet at 4.58 ppm. A correlation of the 3-H proton with 2-H with a coupling constant 7.0 Hz, which was appears at 3.21 ppm.

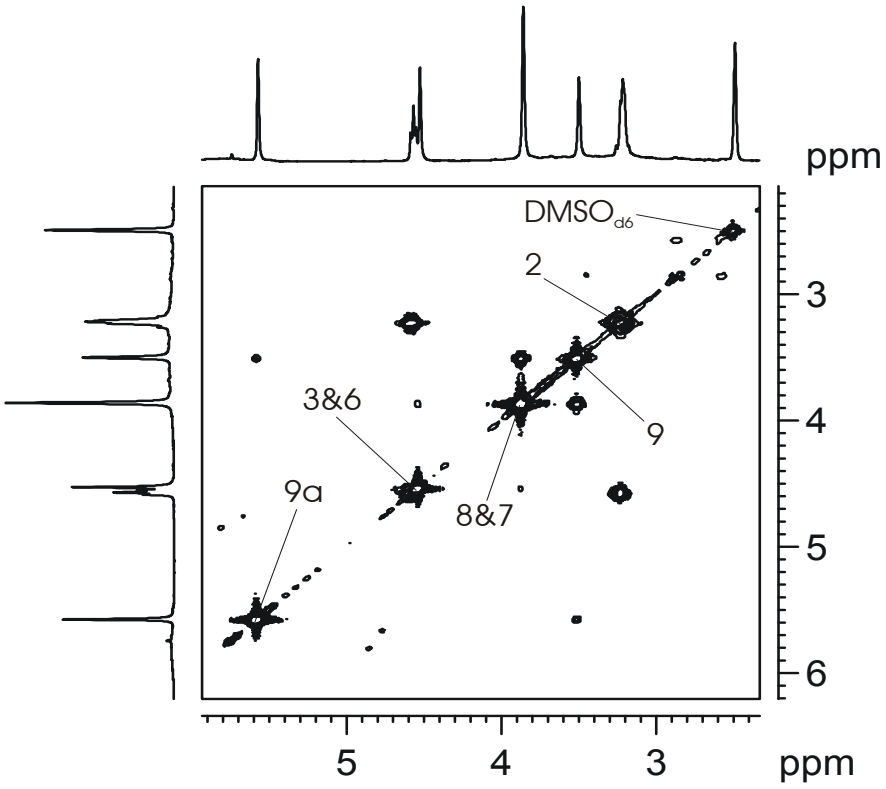

Figure 5 -2: COSY spectrum of compound **7**, NH_2-Bic-COOH (500 MHz, DMSO-d_6). Assigned chemical shifts are shown with connecting lines. Projections of both proton axes are given.

A well-resolved 2D HMQC spectrum of compound **7** is shown in Figure 5 -3. The C-9 carbon gives a signal at 75.78 ppm, whereas C-7 and C-8 carbon shows respective signals at 72.01 ppm and 71.48 ppm. The C-3 carbon appears at 66.08 ppm and C-9a carbon has shown a signal at 61.15 ppm. The carbon atom belonging to C-6 gives a signal at 53.13 ppm and C-2 carbon shows at 32.73 ppm.

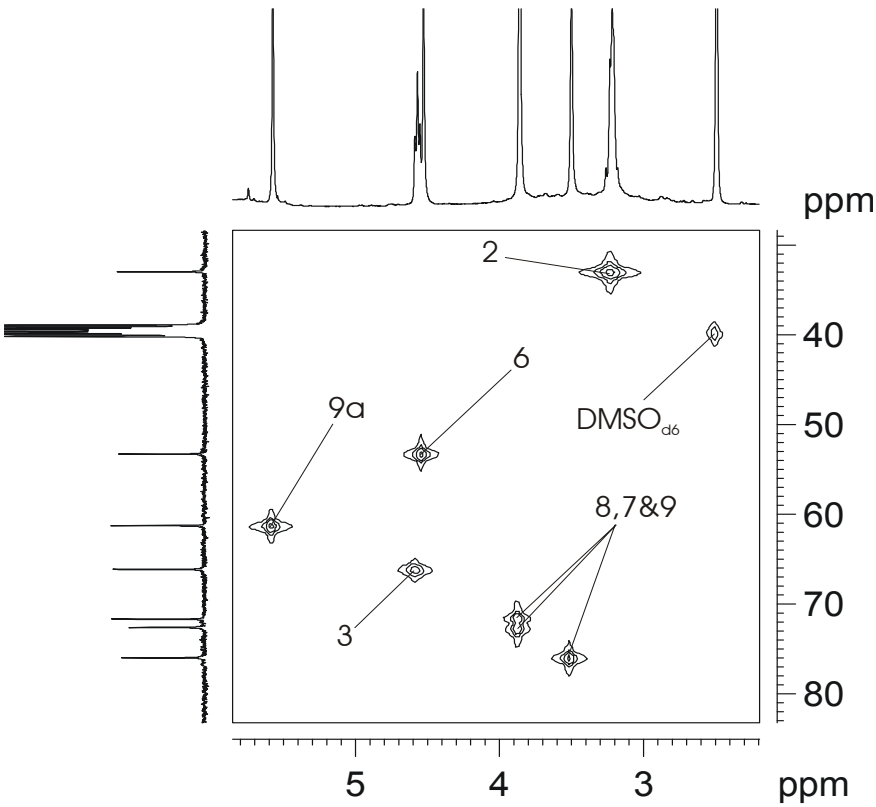

Figure 5 -3: HMQC spectrum of compound **7**, NH_2-Bic-COOH (500 MHz, DMSO-d_6) with projections of ^{1}H and ^{13}C axis. Assigned chemical shifts are marked to corresponding spin system with connecting lines.

*5.1.3. Compound **9** (Fmoc-Bic-COOH)*

2D COSY spectrum of compound **9** (Fmoc-Bic-COOH) is given in Figure 5 -4. It shows that aromatic protons of the Fmoc-protection groups appear at 7.88, 7.72, 7.40 and 7.31 ppm. A signal at 5.47 ppm corresponds to proton 9a-H and it shows a correlation with 9-H proton (at 3.37 ppm). The 9-H proton shows a correlation with 8-H at 3.81 ppm. Doublet of proton signal 6-H, appearing at 4.81 ppm, shows a correlation with Bic-NH proton with a coupling constant 7.2 Hz. α and β protons belonging to Fmoc-protected group show a multiplet at 4.24 ppm, whereas a triplet for 3-H appears at 4.65 ppm. Additionally, a correlation of 3-H proton and 2-H proton with a coupling constant 7.4 Hz, appearing at 3.30 ppm is observed.

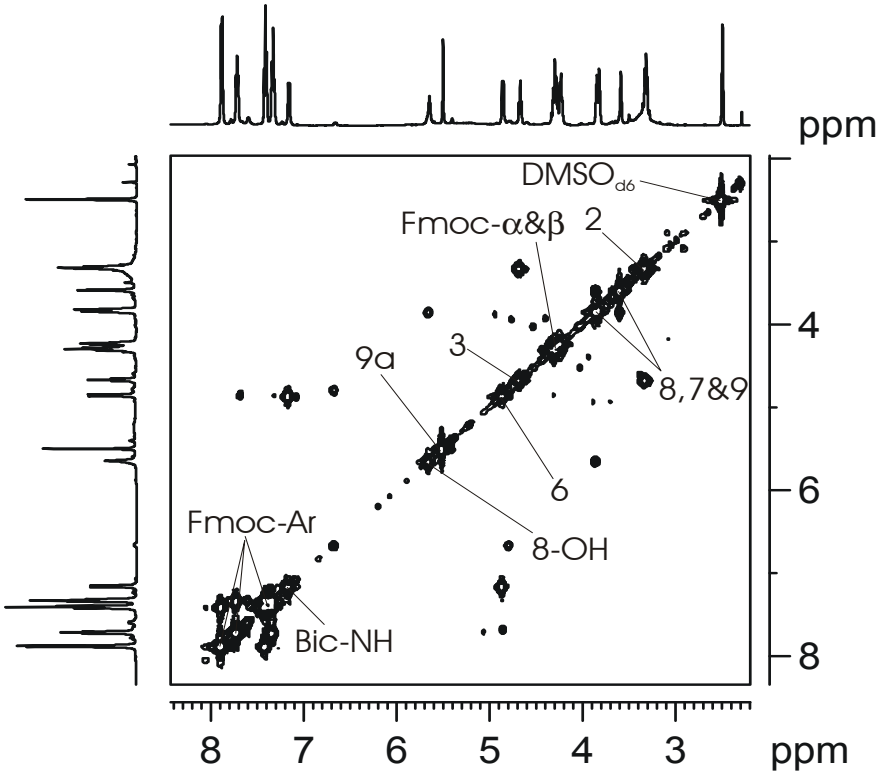

Figure 5 -4: 2D COSY spectrum and corresponding 1D projections of compound **9**, Fmoc-Bic-COOH (500 MHz, DMSO-d_6). Assigned chemical shifts are marked to corresponding spin system with connecting lines.

An HMQC spectrum of compound **9** shows a well-resolved pattern of peaks as shown in Figure 5 -5. The carbon atoms belong to aromatic Fmoc- protected group show signals at 143.68, 143.60, 140.54, 127.54, 127.54, 127.02, 125.20, 119.98 ppm. The C-9 carbon shows a signal at 76.37 ppm, whereas C-7 and C-8 carbon appears at 70.66 ppm and 74.40 ppm, respectively.

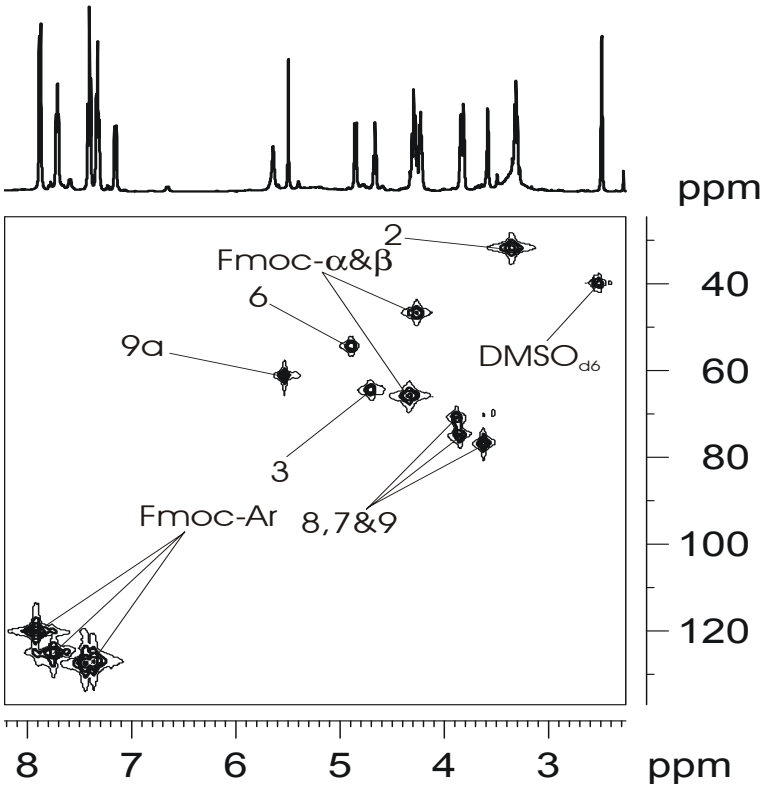

Figure 5 -5: HMQC spectrum of compound **9** Fmoc-Bic-COOH (500 MHz, DMSO-d_6). Assigned chemical shifts are marked to corresponding spin system with connecting lines. Projection of F2 (1H) axis is also give to elucidate the spectrum.

α and β protons belongs to Fmoc-group shows signal at 65.76 ppm and 46.42 ppm. The C-3 carbon appears at 61.04 ppm and C-9a carbon at 54.39 ppm. The C-6 and C-2 carbon atoms show signals at 64.46 ppm and 31.69 ppm, respectively.

*5.1.4. Compound **16** (Lys-Bic-Tyr)*

2D COSY spectrum of compound **16**, Lys-Bic-Tyr, (Figure 5 -6) shows signals at 7.03 ppm and 6.67 ppm with a coupling constant 8.0 Hz which corresponds to Tyr aromatic protons. A signal of Tyr-NH at 8.9 ppm, shows a crosspeak with Tyr-α appearing at 4.29 ppm. A coupling constant 7.22 Hz was observed in them. Quartet signal of Tyr-α show a crosspeak with Tyr-β (2.85ppm), with a coupling constant 6.87 Hz.

Proton signal for Bic-NH at 8.9 ppm and 6-H at 5.1 ppm show a correlation with a coupling constant 8.15 Hz. In addition to this 6-H shows a crosspeak with 8-H, 7-H and 9-H which appear at 3.85, 3.79 and 3.9 ppm, respectively. The triplet of 3-H at 4.76 ppm shows a correlation with 2-H (3.24 ppm) with a coupling constant 7.22 Hz. Two broad singlets of Lys-NH one is for Lys-NH-α at 8.90 ppm and second one for Lys-NH-ε at 8.31 ppm clearly show cross signals between

the Lys-NH-α and Lys-α (3.85 ppm) with a coupling constant 7.22 Hz and the cross signal between the Lys-NH-ε with Lys-CH_2-ε (2.73 ppm).

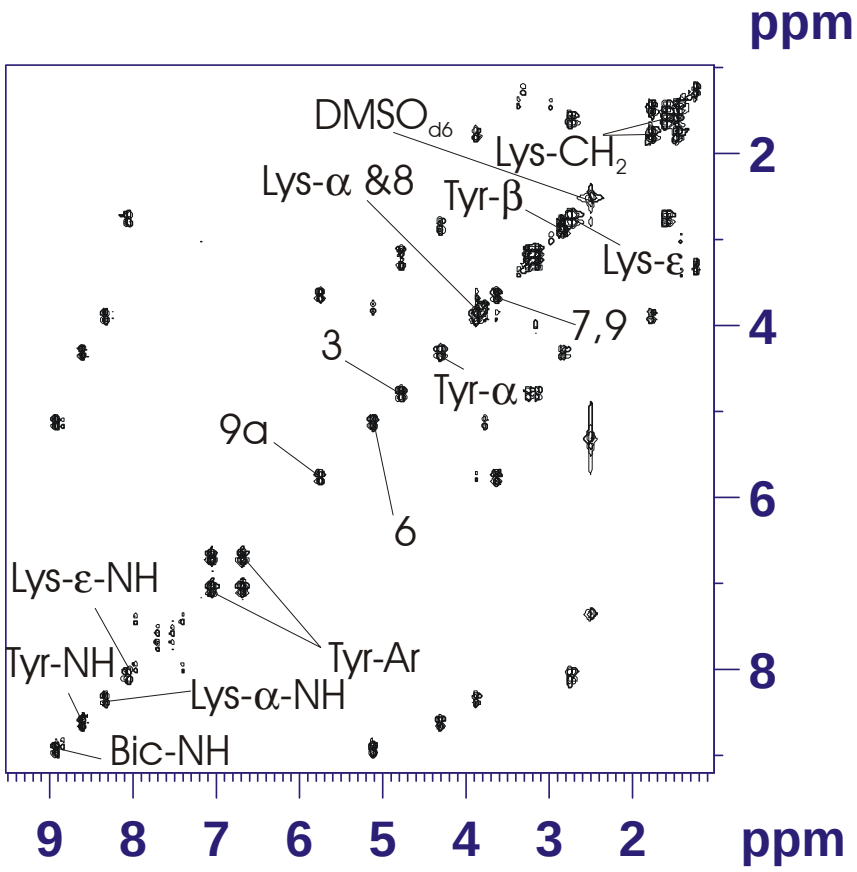

Figure 5 -6: COSY spectrum of compound **16**, Lys-Bic-Tyr, (500 MHz, DMSO-d_6). Assigned chemical shifts are marked to corresponding spin system with connecting lines.

The other CH_2 groups belonging to Lys appears at 1.76 ppm, 1.58 ppm and 1.45 ppm respectively.

*5.1.5. Compound **18** (NH_2-DOPA-Bic-Tyr-OMe)*

In a 2D COSY spectrum of compound **18**, NH_2-DOPA-Bic-Tyr-OMe, (see Figure 5 -7) aromatic protons of Tyr show two doublets at 6.98 ppm and 6.63 ppm with a coupling constant 8.47 Hz and 8.24 Hz. Aromatic protons of DOPA show two doublets and one doublet of doublet at 6.71 ppm and 6.66 ppm, respectively, with a coupling constant 2.06 Hz and 8.01 Hz whereas doublet of doublet shows a signal at 6.58 ppm with a coupling constant 8.01 Hz and 2.06 Hz. The doublet for proton Bic-NH gives a signal at 8.99 ppm. 2D COSY shows a correlation between the Bic-NH and 6-H proton (8.0 Hz) with a doublet at 5.11 ppm.

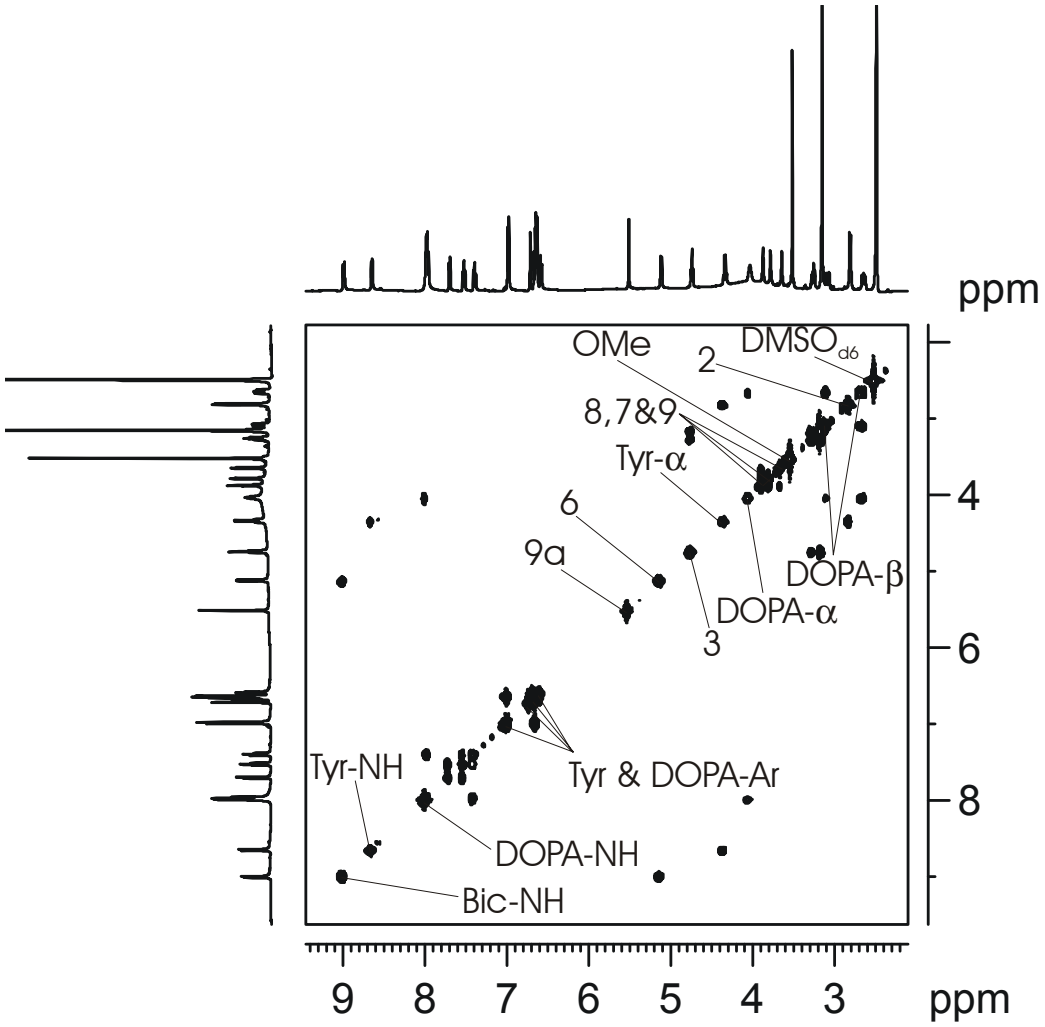

Figure 5 -7: 2D COSY spectrum of compound **18**, NH_2-DOPA-Bic-Tyr-OMe (500 MHz, DMSO-d_6). Assigned chemical shifts are marked to corresponding spin system with connecting lines and projections of both axes are given.

The triplet for proton 3-H appears at 4.74 ppm and shows a correlation with 2-H proton (3.08 ppm) with a coupling constant 7.33 Hz. Broad singlet for three protons of DOPA-NH_3^+ appears at 7.98 ppm and shows a correlation with DOPA-α (4.03 ppm).

A correlation of DOPA-α and multiplate DOPA-β can be also seen with its signal appearing at 3.08 ppm. Doublet of Tyr-NH at 8.65 ppm shows a correlation with Tyr-α (8.01 Hz) appearing as a quartet at 8.65 ppm. Tyr-α also shows a correlation with Tyr-β (7.1 Hz) and appears as a doublet at 2.80 ppm.

*5.1.6. Compound **23** (Lys-DOPA-Tyr-OMe)*

2D COSY of compound **23**, Lys-DOPA-Tyr-OMe is given in Figure 5 -8.

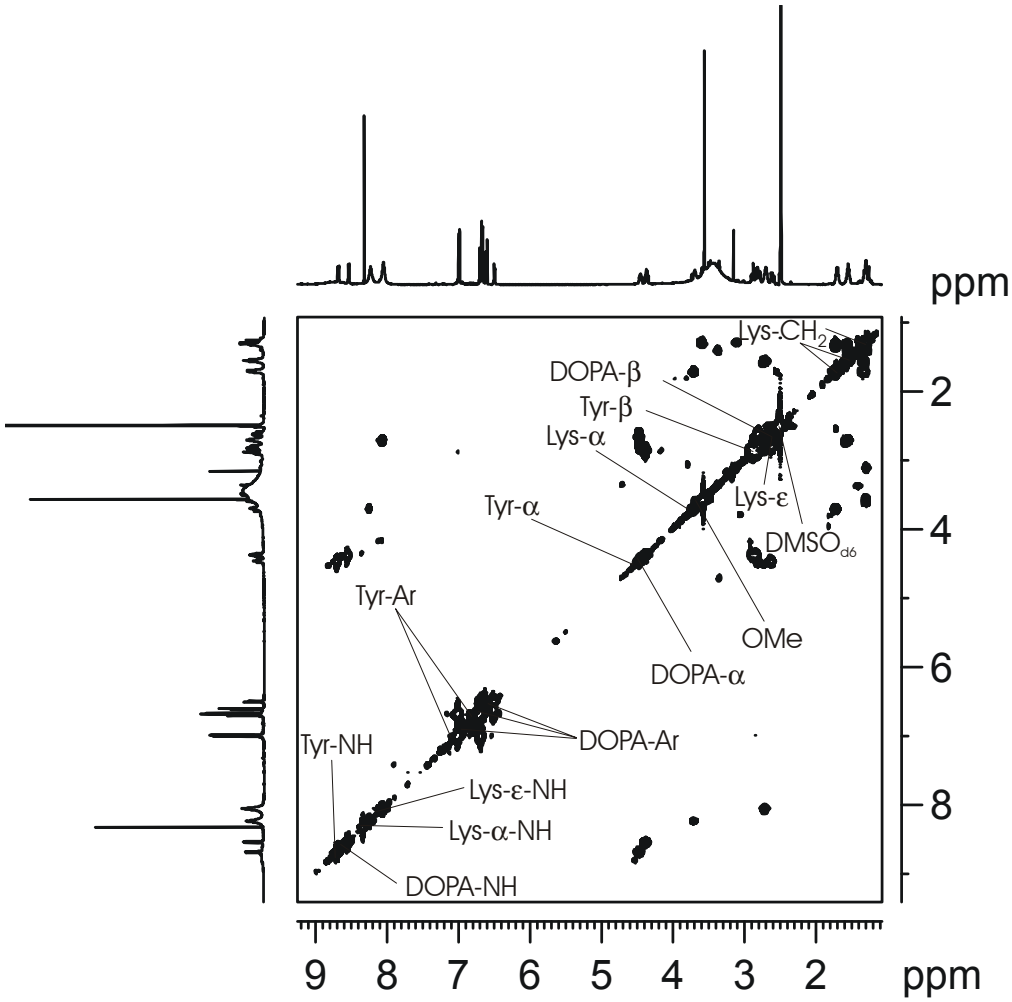

Figure 5 -8: 2D COSY spectrum of compound **23**, Lys-DOPA-Tyr-OMe (500 MHz, DMSO-d_6). Assigned chemical shifts are marked to corresponding spin system with connecting lines. Projections of F1 and F2 dimensions are also shown.

Two doublets of Tyr aromatic protons, appearing at 6.99 ppm and 6.67 ppm, show a correlation with a coupling constant 8.25 Hz and 8.43 Hz, respectively. Whereas, aromatic protons of DOPA show two doublets at 6.70 ppm (7.7 Hz) and 6.61 ppm (8.06 Hz) and one doublet of doublet at 6.49 ppm (8.06 Hz and 2.20 Hz). The doublet of DOPA-NH at 8.53 ppm shows a correlation with DOPA-α (4.36 ppm), with a coupling constant 7.70 Hz. 2D COSY also shows a correlation between DOPA-α and DOPA-β with a multiplet at 2.8 ppm. Doublet of Tyr-NH at 8.68 ppm, showing a correlation with Tyr-α (4.45 ppm) with a coupling constant 8.25 Hz can be also seen. Proton of Tyr-α show a correlation with proton of Tyr-β (2.61 ppm) as a doublet of doublet with a coupling constant 13.75 Hz and 9.7 Hz, respectively. Two broad singlets for Lys-NH-α and Lys-NH-ε appear at 8.23 ppm and 8.05 ppm. Lys-NH-α shows a correlation with Lys-α proton which appears at 3.69 ppm, and Lys-NH-ε shows a correlation with Lys-CH_2-ε (2.70 ppm). Other three Lys-CH_2 groups appear at 1.70 ppm, 1.54 ppm and 1.29 ppm.

5.1.7. Oligopeptides: poly-Tyr

2D HMQC spectrum of poly-Tyr (compound **30**) was taken in DMSO-d_6 at 500 MHz spectrometer (see Figure 5 -9 (A)). Tyr aromatic proton show signals at 6.58 and 6.45 ppm, respectively and the aromatic carbon signal appears at 114.81 and 119.6 ppm, respectively. The α-proton of poly-Tyr shows broad signal at 4.45 ppm corresponding to a carbon chemical shift at 54.62 ppm. Tyr-β protons appear at 2.79 ppm with a carbon signal at 45.3 ppm.

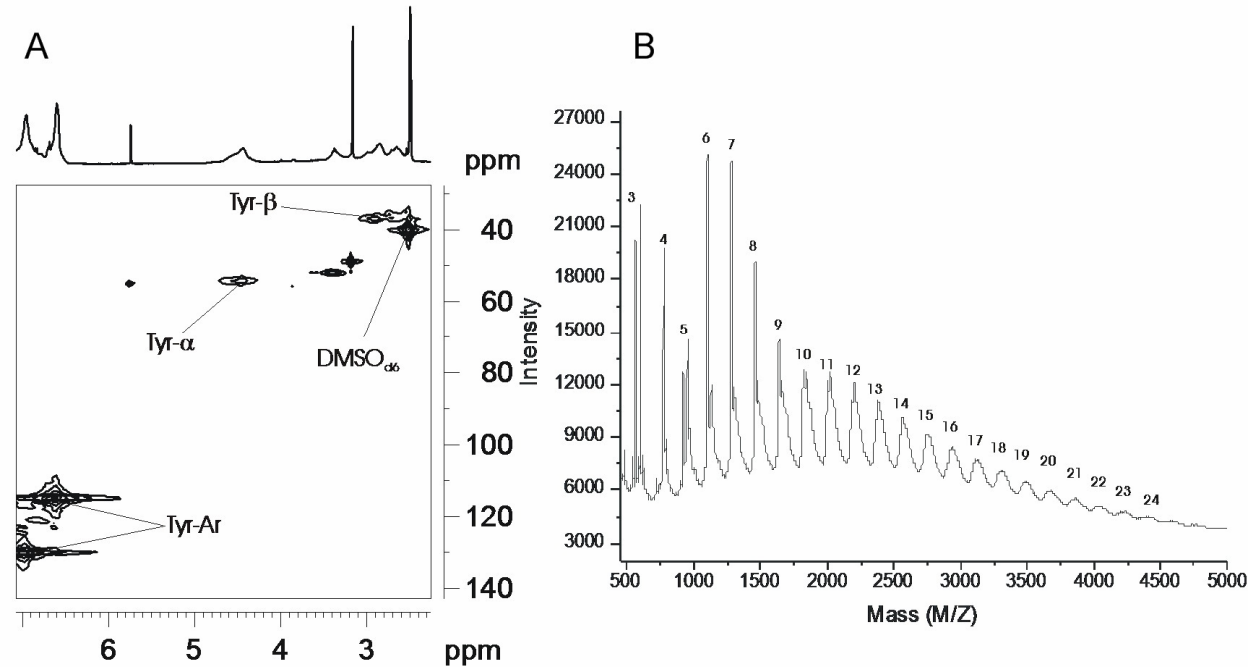

Figure 5 -9: 2D HMQC taken at a 500 MHz in DMSO-d_6 (A) and MALDI-TOF mass spectrum spectra (B) of poly-Tyr. Assigned chemical shifts are marked to corresponding spin system with connecting lines and proton plane projection is shown in A.

The MALDI-TOF mass spectrum of poly-Tyr was measured using matrices Caffic acid and α-cyano-4-hydroxy cinnamic acid. poly-Tyr shows different mixture of oligopeptides with masses ranging from 344 Da to 4256 Da with the highest amplitude around 1300 Da (see Figure 5 -9 B).

5.1.8. Oligopeptides: poly-DOPA

In 2D HMQC spectrum of poly-DOPA (see Figure 5 -10 (A)), DOPA aromatic protons show signals at 6.56 and 6.42 ppm with carbon chemical shifts at 115.05 and 119.84 ppm. The α-proton of poly-DOPA shows a signal at 4.33 ppm corresponding to its carbon chemical shift at 53.86

ppm. Whereas, β- carbon atom show a signal at 45.0 ppm with its proton chemical shift at 2.32 ppm.

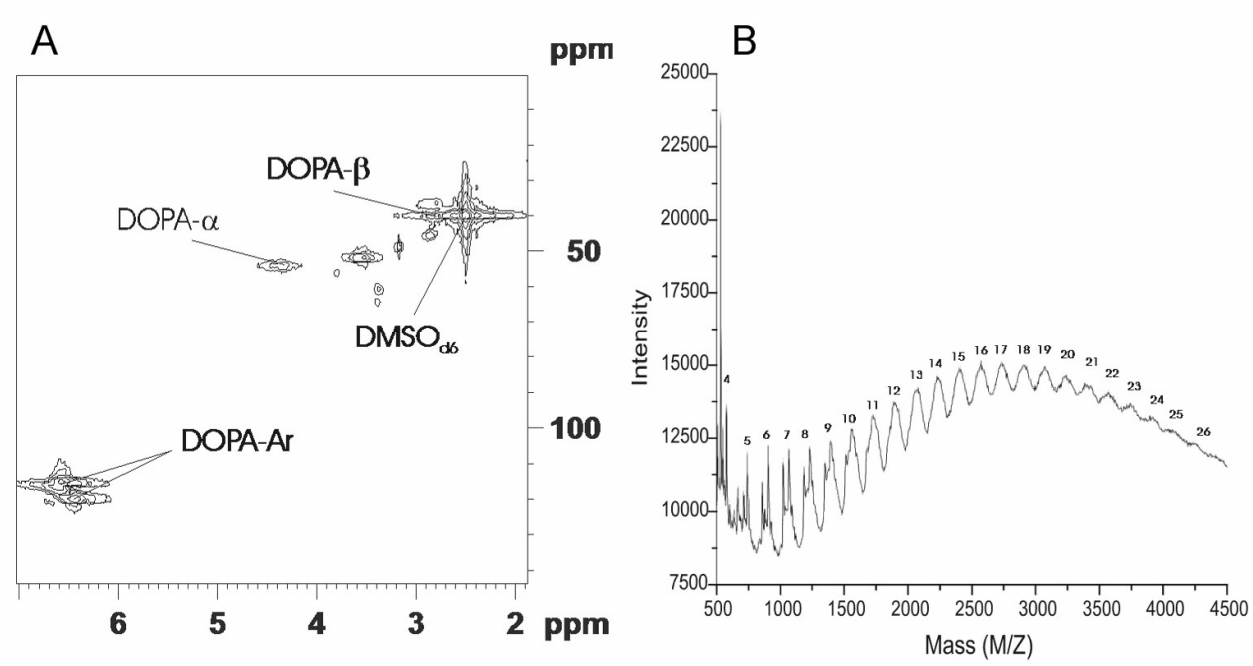

Figure 5 -10: 2D HMQC taken at a 500 MHz in DMSO-d_6 (A) and MALDI-TOF mass spectrum spectra (B) of poly-DOPA. Assigned chemical shifts are marked to corresponding spin system with connecting lines in A.

MALDI-TOF mass spectrum of poly-DOPA was carried out in caffic acid and α-cyano-4-hydroycinnamic acid. poly-DOPA shows different mixtures of oligomers with masses ranging from 376 Da to 4672 Da with a maximum intensity for mass 2750 Da.

5.1.9. Oligopeptides: poly-Lys(Z)

In a 2D HMQC of poly-Lys(Z), aromatic proton of the Z protecting group shows signals at 7.58 ppm and its carbon signals at 127.8 ppm. Protons belonging to CH_2-Z group appear at 4.9 ppm with a carbon chemical shift at 65.0 ppm. The Lys-α proton shows a chemical shift at 4.2 ppm and a corresponding carbon chemical shift at 52.1 ppm. Two protons belonging to ε carbon atom show a signal at 2.92 ppm and its carbon chemical shift appears at 40.0 ppm. Other CH_2 groups belonging to Lys show proton signals at 1.64, 1.35 and 1.2 ppm with corresponding carbon shifts at 29.8, 29.0 and 22.5ppm. This spectrum is shown in Figure 5 -11 (A).

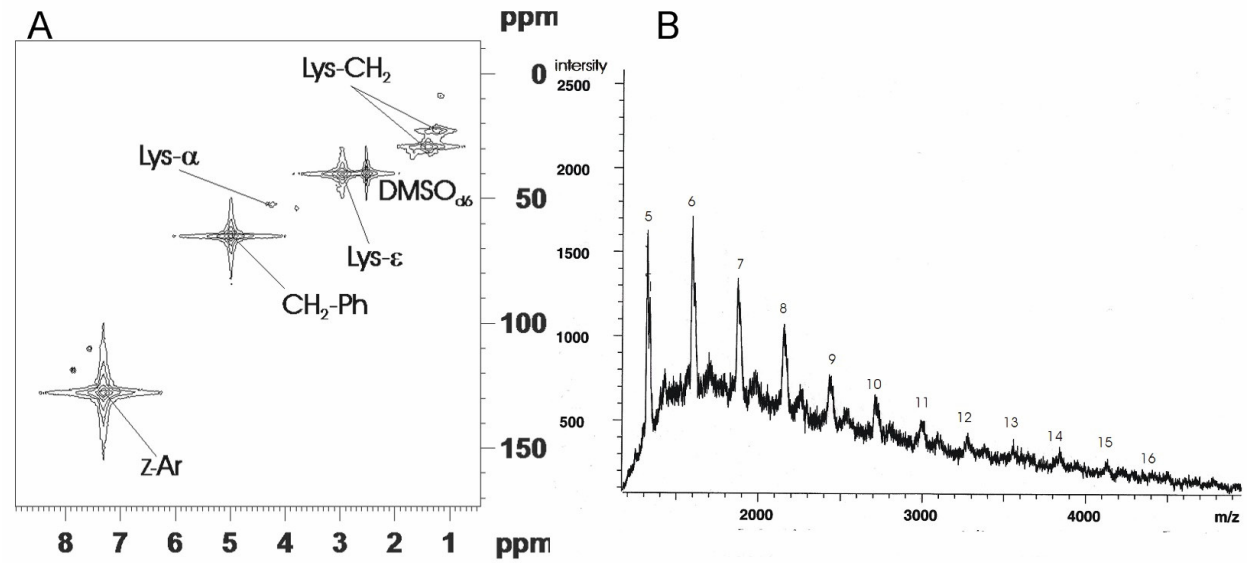

Figure 5 -11: 2D HMQC taken at a 500 MHz in DMSO-d_6 (A) and MALDI-TOF mass spectrum spectra (B) of poly-Lys (Z). Assigned chemical shifts are marked to corresponding spin system with connecting lines in A.

Caffic acid and α-cyano-4-hydroxy cinnamic acid were used as matrices measurement of MALDI-TOF mass spectrum of poly-Lys(Z). Poly-Lys (Z) shows different mixture of oligopeptides with masses ranging from 547 Da to 4498 Da with maximum intensity peak at 1750 Da as shown in Figure 5 -11 (B).

After the cleavage of Z-group, the α-proton of the Lys oligopeptide show a signal at 4.2 ppm and its carbon shift at 52.0 ppm (see Figure 5 -12 (A)).

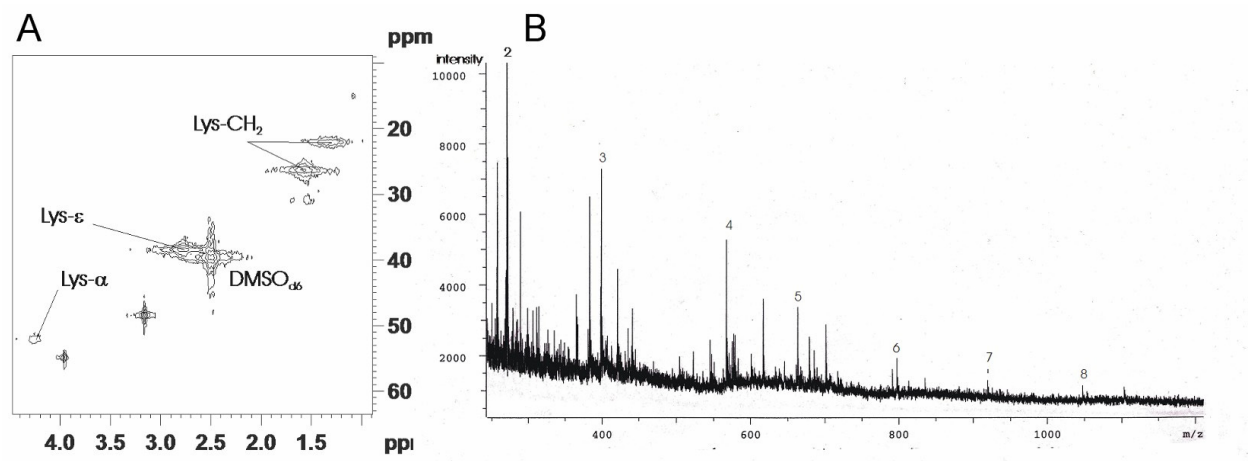

Figure 5 -12: 2D HMQC taken at a 500 MHz in DMSO-d_6 (A) and MALDI-TOF mass spectrum spectra (B) of poly-Lys. Assigned chemical shifts are marked to corresponding spin system with connecting lines in A.

Two ε-proton show signals at 2.7 ppm with their carbon signal appearing at 25.99 ppm. Other proton signals belonging to three CH_2 groups show at 1.56, 1.52 and 1.30 ppm, corresponding to their carbon shifts appearing at 25.99, 30.74 and 21.82 ppm, respectively.
The MALDI-TOF mass spectrum of poly-Lys (in caffic acid and α-cyano-4-hydroxycinnamic acid) resulted into mixture of different oligopeptides with masses ranging from 146 Da to 1012 Da (see Figure 5 -12 (B)).

5.1.10. Oligopeptides: poly-Bic

Chemical shift assignment of poly-Bic (compound **28**) was performed using 2D COSY, HSQC and HMQC spectra. HSQC shows that the three new broad signals appearing after the oligomerization at 6.03, 5.89 and 4.33 ppm belong to the CH or CH_3 group. 2D COSY spectrum shows that a signal at 6.03 ppm correlates with a signal at 4.01 ppm. Also, a signal appearing at 4.01 ppm shows a crosspeak with a signal at 4.33 ppm. A signal appearing at 6.03 ppm in 2D COSY is absent in HMQC as it belongs to hydroxyl protons.

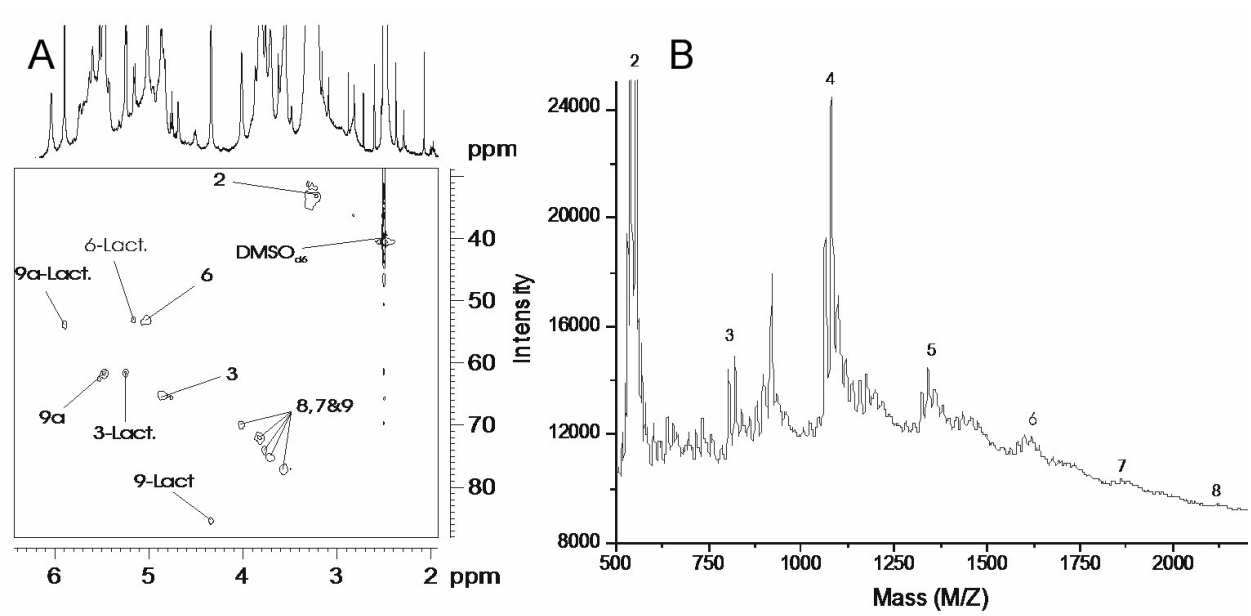

Figure 5 -13: 2D HMQC recorded at a 500 MHz in DMSO-d_6 (A) and MALDI-TOF mass spectrum spectra (B) of compound **28** poly-Bic. Assigned chemical shifts are marked to corresponding spin system with connecting lines and 1D projection of proton axis is shown in A.

2D COSY supplies evidences that the signal appearing at 6.03 ppm belongs to 8-OH. Peak appearing at 4.01 ppm belongs to 8-H and a signal appearing at 4.33 ppm belongs to 9-H. The peak appearing at 5.89 ppm corresponds to 9a-H (see Figure 5 -13 (A) and Figure 5 -14).

Based on these studies, it can be concluded that during the oligomerization of bicyclic molecules the terminal molecule of oligomer is converted to a lactone by utilizing 9-OH from the same residue.

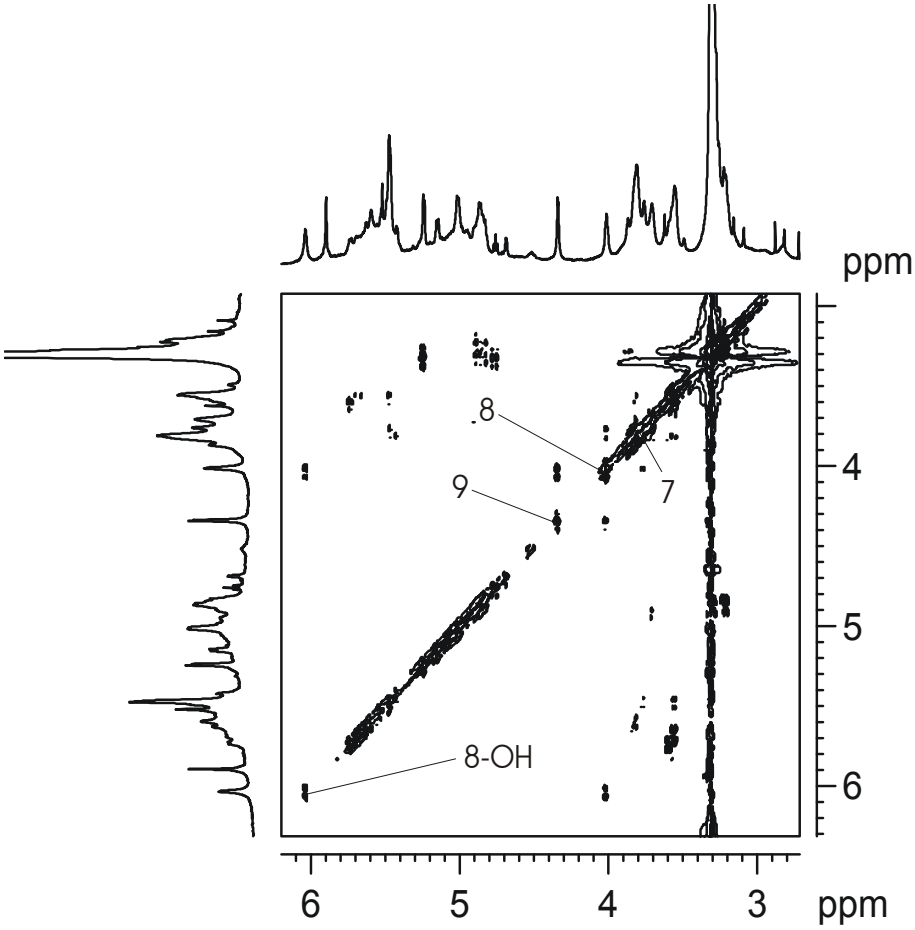

Figure 5 -14: 2D COSY spectrum of compound **28** poly-Bic taken at a 500 MHz in DMSO-d_6.Assigned chemical shifts are marked to corresponding spin system with connecting lines in A. Projections of both axis are also shown in figure.

The assignment of peaks belonging to oligopeptides is performed using 2D COSY (see Figure 5 - 14) and can be summarized as: 5.47 ppm (9a-H), 5.01 ppm (6-H), 4.85 (3-H), 3.81 (8-H), 3.76 (7-H), 3.71 (9-H), 3.39-3.22 (2-H).

The MALDI-TOF mass spectrum of poly-Bic, compound **28**, was measured in caffic acid and α-cyano-4-hydroxycinnamic acid. It shows mixtures different of oligomers with masses ranging from 538 Da to 2358 Da and with a peak of maximum intensity at 1125 Da as shown in Figure 5 - 13 (B).

After the hydrolysis, proton spectrum of compound **29** shows that peaks belonging to lactone (i.e., 9a-H, 3-H, 6-H, 8-H and 9-H) disappear.

2D HMQC shows a signal belonging to 9a-H at 5.46 ppm with a carbon chemical shift at 60.9 ppm. A peak at 5.01 ppm belongs to 6-H and two peaks at 4.85 and 4.6 ppm belongs to 3-H respectively. The carbon shift of 6-H is at 52.3 ppm and that of 3-H appears at 64.3 and 64.2 ppm. Three signals at 3.83, 3.75 and 3.58 ppm belong to 8-H, 7-H and 9-H protons with their carbon shifts corresponding to 71.04, 74.17 and 76.64 ppm. Proton signal for 2-H is seen at 3.28 ppm with its carbon resonance appearing at 32.1 ppm (see Figure 5 -15).

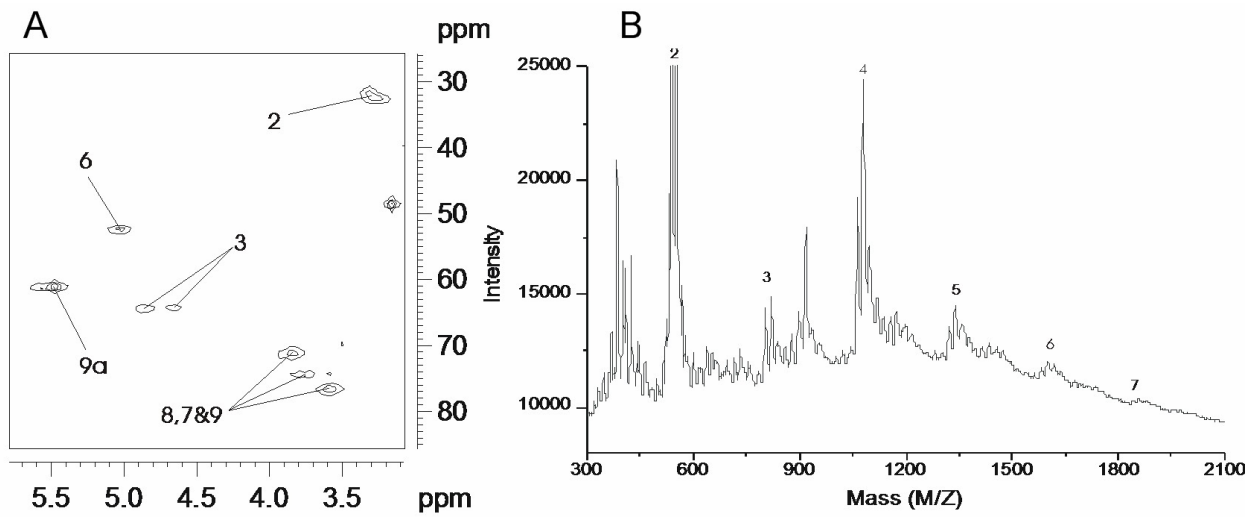

Figure 5 -15: 2D HMQC recorded at a 500 MHz in DMSO-d_6 (A) and MALDI-TOF mass spectrum spectra (B) of compound **29** poly-Bic. Assigned chemical shifts are marked to corresponding spin system with connecting lines in A.

MALDI-TOF mass spectrum of compound **29** (matrices: Caffic acid and α-cyano-4-hydroxy cinnamic acid) results into mixture of different oligopeptides with masses ranging from 538 Da to 1838 Da as shown in Figure 5 -15 (B).

5.1.11. Co-polymers: poly-Bic-Tyr

2D HMQC of poly-Bic-Tyr, compound **34**, gives two aromatic signals belonging to Tyr at 7.03 and 6.61 ppm. Signal belonging to 9a appears at 5.48 ppm. Two peaks at 5.0 and 4.66 ppm are from 6-H and 3-H respectively. The α-proton of Tyr appears at 4.49 ppm and three signals appearing at 3.85, 3.69 and 3.62 ppm belongs to 8-H, 7-H and 9-H protons, respectively. Tyr-β proton appears at 3.36 ppm. Broad peak at 3.10 ppm belongs to 2-H as seen in Figure 5 -16 (A).

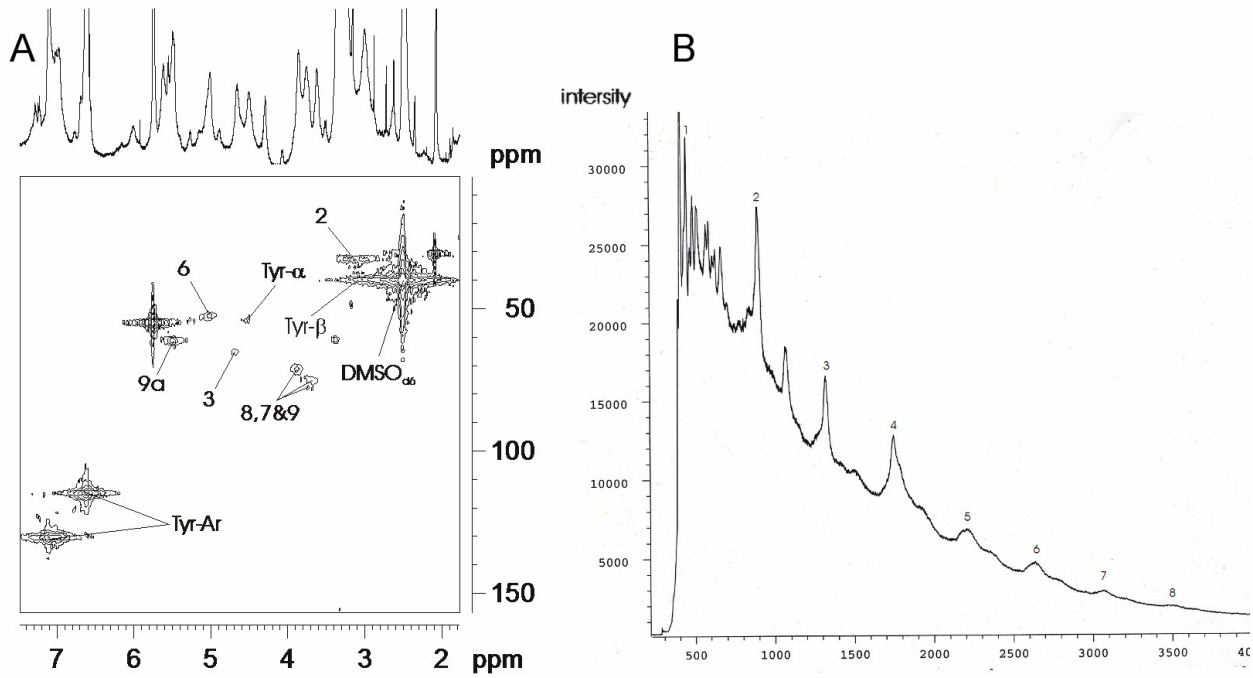

Figure 5 -16: 2D HMQC recorded at a 500 MHz in DMSO-d_6 (A) and MALDI-TOF mass spectrum spectra (B) of compound **34** poly-Bic-Tyr. Assigned chemical shifts are marked to corresponding spin system with connecting lines in A. A also shows 1D projection of proton axis.

Caffic acid and α-cyno-4-hydroxylcinnamic acid matrices were used to get molecular weight of poly-Bic-Tyr using MALDI-TOF mass spectroscopy. Masses with different oligomeric compositions in the range of 441 to 4671 Da are seen in Figure 5 -16 (B).

Molecular mass of poly-Bic-Tyr was also characterized using gel permission chromatography and has been shown in Figure 5 -17.

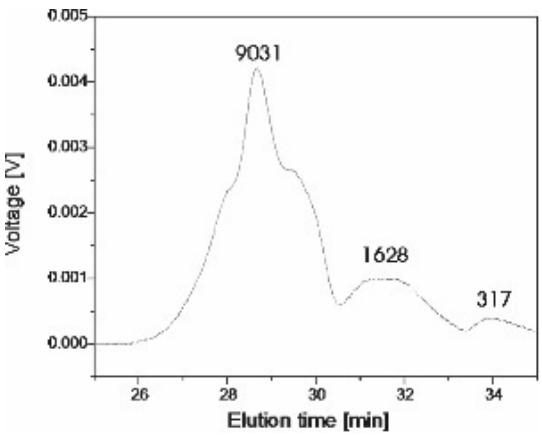

Figure 5 -17: Gel Permeation chromatography of poly-Bic-Tyr, compound **34**. Molecular weight of 9031 Da was observed although broad peaks suggest that the oligopeptide has a distribution of masses between 1628 to 9031 Da.

Polystyrene as a standard was used for these studies. GPC confirms presence of oligomeric mixture of higher molecular weight compound in the ranging of 1628 to 9031 Da. The high intensity of peak at 9031 Da suggests its high content in the oligometic mixture.
In addition to GPC and MALDI, molecular weight information of poly-Bic-Tyr was gained from running a polyacrylamide-SDS gel which is shown in Figure 5 -18.

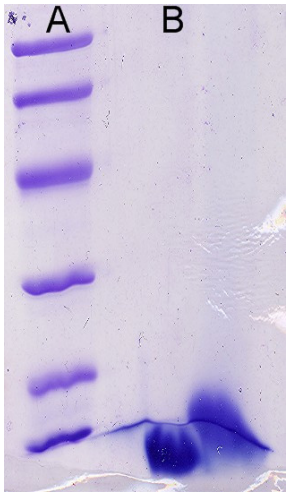

Figure 5 -18: Polyacrylamide-SDS gel of poly-Bic-Tyr (compound **34**). Panel A is a marker and bands in A corresponds to Phosphorylase b 97 kDa, Albumin 66 kDa, Ovalbumin 45 kDa, Carbonicanhydrase 30 kDa, Trypsin inhibitor 20.1 kDa, α-lactalbumin 14.4 kDa. Panel B is 10 μL load of poly-Bic-Tyr which runs little below 14.4 kDa band of α-lactalbumin proposing that poly-Bic-Tyr has a molecular weight of ca. 9 kDa.

After staining and destaining, SDS-PAGE of poly-Bic-Tyr gave a single band little below 14.4 kDa band corresponding to α-lactalbumin. An estimation of molecular weight has been performed as there was no available marker. This comes to be around 9000 kDa which is in good agreement with results obtained from GPC.

5.1.12. Co-polymers: poly-Lys(2-Cl-Z)-Tyr

Two dimensional HMQC of poly-Lys(2-Cl-Z)-Tyr, compound **34**, was recorded in DMSO-d_6 and is shown in Figure 5 -19 (A). The aromatic protons of *2-Cl-Z* protecting group appear at 7.40 ppm corresponding to carbon atom at 129.8 ppm. Protons belonging to CH_2-Z group show a signal at 5.3 ppm with a carbon chemical shift at 63 ppm. The aromatic protons of Tyr can be seen at 6.99 ppm and 6.64 ppm, respectively whereas their carbon shifts appear at 130 ppm and 114.7 ppm. The Lys-α group and Tyr-α shows proton signal at 3.68 ppm and at 4.25 ppm and related to their carbon signals at 51.8 ppm and 54.5 ppm respectively.

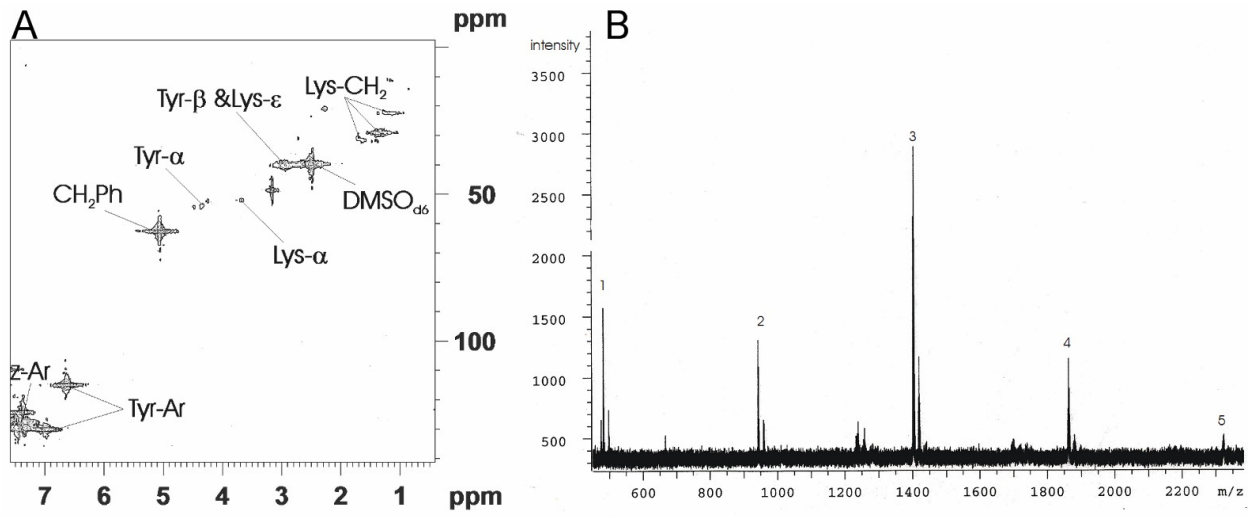

Figure 5 -19: 2D HMQC taken at a 500 MHz in DMSO-d_6 (A) and MALDI-TOF mass spectrum spectra (B) of compound **35** Lys(2-Cl-Z)Tyr. Assigned chemical shifts are marked to corresponding spin system with connecting lines in A.

Two protons belonging to ε-carbon atom and one proton belonging to Tyr-β appear at 2.94 and 2.8 ppm with their carbon chemical shift at 39.7 ppm. CH_2 groups belonging to Lys shows proton signals at 1.66, 1.38 and 1.19 ppm and carbon signals at 31.1, 29.0 and 22.0 ppm respectively.

The MALDI-TOF mass spectrum of compound **35** was measured using two different matrices Caffic acid and α-cyano-4-hydroxy cinnamic acid (see Figure 5 -19 (B)). The result shows that the different mixture of oligopeptides with masses ranging from 482 Da to 2323 Da is present.

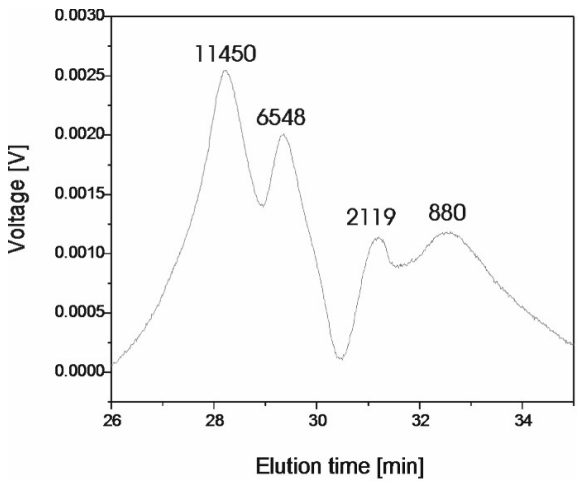

Figure 5 -20: Gel permeation chromatography of poly-Lys(2-Cl-Z)-Tyr, compound **35**. Molecular weight of 11450 Da was observed although broad peaks suggest that the oligopeptide has a distribution of masses between 880 to 11450 Da.

Gel permeation chromatography study of oligopeptide compound **35** shows that the product containing mixture of higher molecular weight compound, which are ranging from 880 to 11450 Da. It is shown in Figure 5 -20.

5.1.13. Co-polymers: poly-Lys(Z)-Bic-Tyr

In a 2D HMQC, the aromatic proton of the Z protecting group of compound **36**, poly-Lys(Z)-Bic-Tyr shows a signal at 7.34 ppm with its carbon signal at 127.5 ppm. The aromatic protons of the Tyr have been seen at 7.04 ppm and 6.6 ppm respectively, whereas their carbon shift appears at 130 ppm and 114.8 ppm. Proton belonging to CH_2-Z group shows a signal at 5.0 ppm and its carbon chemical shift appears at 64.9 ppm. Signal belonging to 9a appear at 5.5 ppm with carbon chemical shift at 70.1 ppm. Two peaks appearing at 5.13 ppm and 4.31 ppm belong to 6-H and 3-H respectively and their carbon shift come out at 64.8 and 52.1 ppm. Protons of Lys-α and Tyr-α group shows a signal at 3.85 ppm and 4.81ppm, respectively with carbon shifts at 51.77 ppm and 53.97 ppm. Two protons belonging to ε-carbon atom and one proton belongs to Tyr-β show a signal at 2.92, 2.83 ppm and 2.97 ppm and their corresponding carbon chemical shift appears at 34.4 ppm and 39.6 ppm.

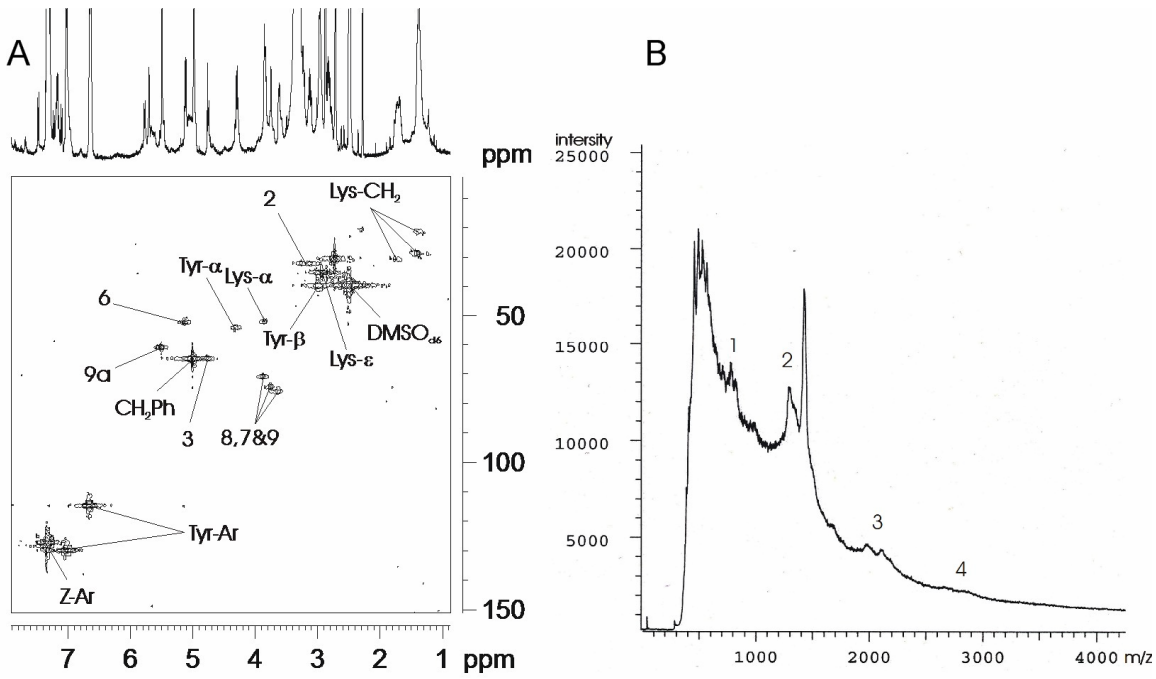

Figure 5 -21: 2D HMQC taken at a 500 MHz in DMSO-d_6 (A) and MALDI-TOF mass spectrum spectra (B) of compound **36** Lys(2-Cl-Z)Tyr. Assigned chemical shifts are marked to corresponding spin system with connecting lines in A. 1D projection of proton axis is also given in A.

Whereas, CH_2 groups belonging to Lys show proton signals at 1.73, 1.39 and 1.36 ppm and the carbon signals at 30.7, 28.4 and 21.4 ppm respectively. Proton signals at 3.87 ppm, 3.76 ppm and 3.62 ppm belongs to 8-H, 7-H and 9-H of the bicyclic ring, respectively with their carbon chemical shifts at 71.0 ppm, 74.5 ppm and 76.0 ppm. A signal at 3.17 belongs to 2-H of bicyclic ring with its carbon signal appearing at 32.0 ppm as shown in Figure 5 -21 (A).

MALDI-TOF mass spectrum of compound **36** was measured using two different matrices, Caffic acid and α-cyano-4-hydroxy cinnamic acid. Different mixtures of oligopeptides with masses in the range of 703 Da to 2758 Da were found as shown in Figure 5 -21 (B).

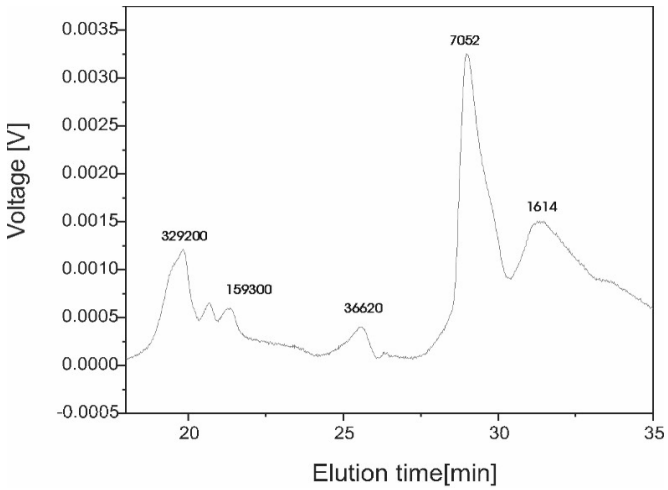

Figure 5 -22: Gel Permeation chromatography of poly-Lys(Z)-Bic-Tyr, compound **36**. Molecular weight of 329200 Da was observed although broad peaks suggest that the oligopeptide has a distribution of masses between 1614 to 329200 Da with the maximum amplitude at 7052 Da.

Gel permeation chromatography of oligopeptide compound **36**, poly-Lys(Z)-Bic-Tyr, suggests of a mixture of higher molecular weight compound in the range of 1614 Da to 329200 Da. The highest peak is seen at 7052 Da as shown in Figure 5 -22.

In addition to MALDI and GPC, molecular weight of compound **36**, poly-Lys(Z)-Bic-Tyr, was also determined using SDS-PAGE. After staining and destaining, SDS-PAGE of poly-Bic-Tyr gave a single band that appeared slightly below 14.4 kDa which correspond to α-lactalbumin. An estimation of molecular weight has been performed as there was no available marker in that range. It suggest that the molecular weight of poly-Lys(Z)-Bic-Tyr should be ca. 9000 kDa. This value is in good agreement with 7052 Da as obained from GPC.

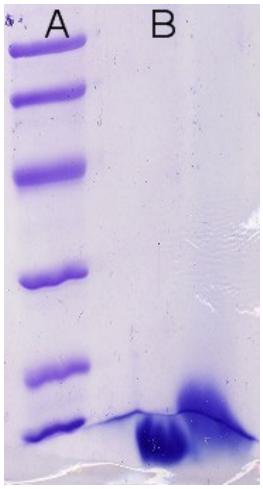

Figure 5 -23: Polyacrylamide-SDS gel of poly-Lys(Z)-Bic-Tyr (compound **36**). Panel A is a marker and bands in A corresponds to Phosphorylase b 97 kDa, Albumin 66 kDa, Ovalbumin 45 kDa, Carbonicanhydrase 30 kDa, Trypsin inhibitor 20.1 kDa, α-lactalbumin 14.4 kDa. Panel B is 10 □L load of poly-Bic-Tyr which runs little below 14.4 kDa band of α-lactalbumin proposing that poly-Bic-Tyr has a molecular weight of ca. 9 kDa.

The discrepancies in the masses of compound **34** and **36** arising from MALDI and GPC (and gel electrophoresis) could not be understood completely. One obvious reason could be the approach of detecting masses as MALDI is molecular weight based and GPC (and gel electrophoresis) is size based technique.

5.1.14. Co-polymers: poly-Lys-Bic-Tyr

After the cleavage of Z group from compound **36**, poly-Lys-Bic-Tyr was obtained and studied likewise, i.e. with the help of 2D HMQC. The chemical shifts of signals were very slightly affected from that of compound **36**.

The aromatic protons of the Tyr are seen at 7.00 and 6.78 ppm with their carbon shift appearing at 129.4 and 114.6 ppm. Signal belonging to 9a appear at 5.48 ppm and it shows a signal at 61.03 ppm in carbon dimension. Two peaks appearing at 5.03 ppm and 4.64 ppm belong to 6-H and 3-H, respectively with their carbon shifts appearing at 51.99 ppm and 64.45 ppm. Protons of Lys-α and Tyr-α group show a signal at 4.30 ppm and 4.3 ppm and appear at 53.9 ppm and 51.9 ppm on carbon chemical shift. Two protons belonging to ε-carbon atom and one proton belonging to Tyr-β show a signal at 2.69 and 3.15 ppm with their carbon chemical shifts appearing at 34.7 and 48.31 ppm, respectively. Three signals of proton 8-H, 7-H and 9-H appear at 3.88, 3.78 and 3.74 ppm and their carbon shift show at 71.1, 74.4 and 76.4 ppm. A signal for 2-H proton comes at 3.15 ppm with its carbon shift at 31.98 ppm. Remaining three CH_2 groups belonging to Lys

appear at 1.73, 1.39 and 1.36 ppm with their carbon shifts appearing at 30.7, 28.4 and 21.4 ppm. The 2D HMQC is shown in Figure 5 -24 (A).

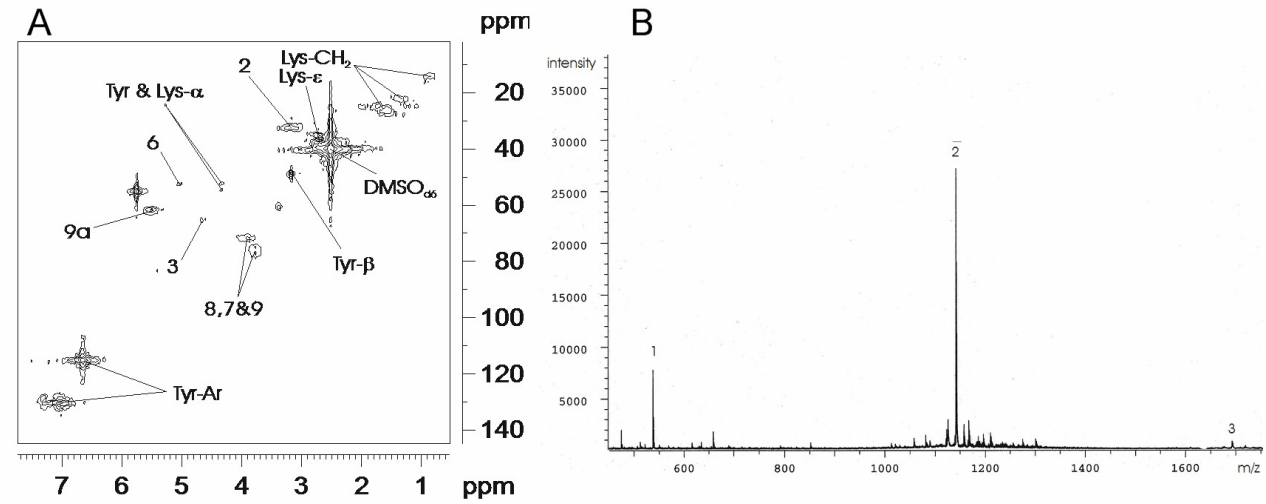

Figure 5 -24: 2D HMQC recorded at a 500 MHz in DMSO-d_6 (A) and MALDI-TOF mass spectrum spectra (B) of compound **37** poly-Lys-Bic-Tyr. Assigned chemical shifts are marked to corresponding spin system with connecting lines in A.

The MALDI-TOF mass spectrum of compound **37**, poly-Lys-Bic-Tyr was taken in Caffic acid and α-cyano-4-hydroxy cinnamic acid. Using both matrices compound **37** shows a mixture different oligopeptides with masses ranging from 569 Da to 1671 Da as shown in Figure 5 -24 (B) with maximum intensity peak around 1200 Da.

5.1.15. Comparison of Molecular Weights of Compounds

It should be noticed that a consistent discrepancy was seen in molecular weights obtained by MALDI and GPC for almost each synthesized oligomer and polymer. One obvious reason could be the approach of detecting masses in these two methods. MALDI is molecular weight based and GPC is size based technique.

One or more of the following reasons could be possible explanation for these discrepancies.

a) MALDI mass spectra from polydisperse polymers indicate that high-mass components are generally underrepresented with respect to lower mass oligomer peaks. This mass discrimination effect is caused by a combination of several factors, including sample preparation, mass-dependent desorption/ionization processes, and mass-dependent detection efficiency. Caution must be exercised when interpreting average molecular weights and molecular-weight distribution values from MALDI data, especially for highly polydisperse polymers. Although MALDI cannot

yet provide reliable molecular-weight parameters for polymers having large polydispersities, the combination of GPC and MALDI MS does provide a useful method for determining molecular-weight distributions of polydisperse polymers [257, 258].

b) MALDI can determine molecular weight independent of polymer structure. For example, rigid polymers are a challenge to analyze by GPC because these polymers have a linear sticklike geometry [259]. Although *mefp*-1 has a partially helical and partially random coil structural units, mimicked adhesive peptide might still be linear, rigid rod like chemical moiety. While, partially folded bio-polymers are readily analyzed by GPC methods, which are based on correlating the hydrodynamic volume of the coiled biopolymer chains with molecular weight. However, the hydrodynamic volume of rigid-rod-like polymers does not correlate with polymer molecular weight; hence, molecular weights determined by GPC analysis of these structures often deviate strongly from the true values.

c) Additional shortcomings of either method is proper calibration issue.

5.2. Techniques Used for Testing Adhesive Properties

5.2.1. Diffusion Ordered Spectroscopy

Diffusion-ordered 2D-NMR spectroscopy (DOSY) has generated significant interest because it allows the NMR spectroscopic observation of mixture on the basis of the size [260, 261]. As the gradient strength increases, in DOSY experiments, signals decay exponentially according to the translational diffusion coefficients of the molecule. It can be a very important experiment because it permits a noninvasive chromatographic separation of components in a mixture solution without need to any preliminary physical separation provided spectral resolution is retained [16, 262-269].

DOSY NMR can also be used as a powerful tool to distinguish between the complex and non complex forms in a mixture of host and guest compounds due to the differences in their diffusion coefficients. These will be reflected in the changes in their size and mass accompanied by complex formation. [265, 270-272].

DOSY NMR has been introduced to solve such kinds of problems in polymer mixture systems (e.g. polymer-polymer mixtures and polymer additives mixture) [16, 267, 273, 274]. 2D-DOSY technique for the analysis of graft copolymer solutions has been investigated by comparing the diffusion behavior of the target copolymer with the mixture of constituent polymers. By conventional ^{1}H NMR spectroscopy, some graft copolymers are not distinguished from the mixtures of their constituent polymers [275].

In order to check the adhesive properties of synthetic adhesive pepetides, DOSY spectrum was run with and without silicon nano beads. Silicon nano beads are bigger in size compared to

synthetic peptides. Therefore, if peptide would bind to silicon beads then it should affect translational diffusion of peptide. This would be expected either in the form of shift in the resoancnes in 1D DOSY or appearance of new signals in the 2D DOSY experiment. Nano beads which were used in this experiment had been synthesized by us using following protocol.

5.2.2. Synthesis of Silicon Beads

Mixture of water (82 mL) and ethanol (160 mL) was heated using an oil bath to 75°C. Simultaniously, tetraethylorthosilicate (TES) was placed in a flask in the same oil bath. At 75°C, ammonia was added into the mixture of solvents and stirred drastically so as to ensure very good mixing. After the addition of ammonia the temperature went down to 72.3°C. Once the temperature reached 75°C again, TES was poured into the mixture of solvents and ammonia using a funnel. The reaction was stirred for 15 s. Further, the reaction mixture was kept at 75°C for 2 h.
Size of nano beads was measured using electron microscope and was found to in the range of 55 nm to 75 nm.
For recording DOSY spectrum of adhesive peptides in presence of nano beads, 2 mg nano beads were used.

5.2.3. Atomic Force Microscopy

The atomic force microscope (AFM) [276] is a new type of scanning probe microscope which is capable of mapping forces near surfaces, or by means of these forces, mapping the topography of the surface it self. The AFM is an offshoot of the scanning tunneling microscope (STM) [276, 277]. Like the STM, the AFM is capable of extremely high spatial resolution in three dimensions. The AFM, however, can be used to study the surfaces of both electrically conducting and nonconducting samples, overcoming a major limitation of the STM.
AFM technology allowed single molecular analysis to become possible. The AFM probe has a sharp tip (5-50 nm radius of curvature) making the contact area of tip-substrate quite small and attractive forces between the AFM tip and the substrate at sub-nano Newton level can be monitored. Usually, for high resolution measurements, the sample is scanned instead of the tip as with the STM, because the AFM measures the relative displacement between the cantilever and few surfaces and any cantilever movement would add vibrations. For measurements of large samples, AFMs are available where the tip is scanned and the sample is stationary. As long as the AFM is operated in contact mode, little if any vibration is introduced.
The AFM combines the principles of the STM and the stylus profiler. In the AFM the force between the sample and the tip is detected, rather than the tunneling current, to sense the

proximity of the tip to the sample. The AFM can be used either in a static or dynamic mode. In the static mode, also referred to as repulsive mode or contact mode, a sharp tip at the end of a cantilever is brought in contact with a sample surface. During initial contact, the atoms at the end of the tip experience a very weak repulsive force due to the tip, electronic orbital overlap with the atoms in the sample surface. The force acting on the tip causes a cantilever deflection which is measured by tunneling, capacitive, or optical detectors. In the dynamic mode operation of the AFM, also referred to as attractive force imaging or non contact mode, the tip is brought in close proximity (within a few nm) to, and not in contact with sample. The cantilever is deliberately vibrated either in amplitude modulation (AM) mode or frequency modulation (FM) mode [278].

Very weak van der Waals attractive forces are present at the tip-sample interface. Although in this technique, the normal pressure exerted at the interface is zero (desirable to avoid any surface deformation), it is slow and is difficult to use and is rarely used outside research environments. In the two modes, surface topography is measured by laterally scanning the sample under the tip while simultaneously measuring the separation dependent force gradient between the tip and the surface. In contact mode, the interaction force between the tip and sample is measured by measuring the cantilever deflection. In the noncontact or dynamic mode, the force gradient is obtained by vibrating the cantilever and measuring the shift of resonance frequency of the cantilever. To obtaine topographic information, the interaction force is either recorded directly, or used as a control parameter for a feedback circuit that maintains the force or force derivation at a constant value.

The ability of the AFM to image at atomic resolution, combined with its ability to image a wide variety of samples under a wide variety of conditions, has created a great deal of interest in applying it to the study of biological structures. Images have appeared in the literature showing DNA, single proteins, structures such as gap junctions, and living cells [279].

The rupturing process of the single protein has been analyzed and the qualitative investigation regarding with secondary structure of both protein and peptides have been attempted by measuring force curves [280, 281]. AFM can also be utilized for analyzing peptide molecules. One can estimate hydrogen-bond energy, stiffness and α-helix content of a single α-helical peptide molecule from force curve analysis [282-284].

Molecular interactions can also be measured using AFM and unbinding forces from single molecular binding such as avidin and biotin, [285, 286] antigens and antibodies [287-289] and His-tag and nickel-nitrilo triacetic acid [290] have been accomplished.

The study of the interaction of oligopeptides on different surfaces like mica and graphite using contact mode AFM was performed for synthesized adhesive peptides. Additionally, the size of

oligopeptides was measured. The information on the size proves to be vital if oligopeptides show interaction with the surface (i.e., binding). In such case its size would change.

The briefly experimental study of the oligopeptides with different large surfaces is explained here. A Topometrix Explorer AFM equipped with a 2.5 μm scanner was used. Single-crystal silicon cantilever were used and all AFM imaging was conventional ambient non-contact mode AFM, with scan speeds of about 1-5 Hz and data collection at 400×400 pixels. Substrates used for oligopeptide adsorption were freshly cleaved mica, freshly cleaved graphite HOPG (high oriented pyrolytic graphite).

All experiments were performed by mixing of 1 mg oligomer compound in 0.1 ml dry DMF, 20-μL aliquot of the mixture was deposited on to bilayer like (mice and graphite). The sample was rapidly blow dried using a burst of compressed gas (Nitrogen or Argon).

5.3. Adhesiveness of Synthesized Peptides

5.3.1. DOSY of Lys-Bic-Tyr, Lys-DOPA-Tyr-OMe and DOPA-Bic-Tyr-OMe

In a 1D DOSY experiment of mixtures of compounds, one expects to see different lineshapes depending on the rotational correlation time [291]. The rotational correlation times of all the four tetrapeptide are bound to be very similar because of their relatively similar size and shape. However, in presence of nanobeads, as proposed, one or more tetrapeptide might bind due to adhesive property leading to a sudden decrease in the rotational correlation time. This would reflect in changed diffusion coefficient. A changed diffusion coefficient would then induce change in the lineshape or in the form of newly appearing signals.

Tetrapeptides like, compound **16** (Lys-Bic-Tyr), compound **23** (Lys-DOPA-Tyr-OMe) and compound **18** (DOPA-Bic-Tyr-OMe) were probed for adhesive properties using 1D DOSY which is shown in Figure 5 -25.

No change in shape of existing signal (broadening) or appearance of new signal has been observed for all four tetrapepetides. However, 1D DOSY is often limited with the spectral resolution partly due overecrowding of spectral resoanances arising from different compound in the mixture. The difficulty of extracting clean diffusion parameters from overlapping signal decays sets strict limits on the diffusion resolution of low resolution DOSY, but in the high resolution case, performed as 2D DOSY, relatively small differences (of the order of 1%) in diffusion coefficient can be resolved.

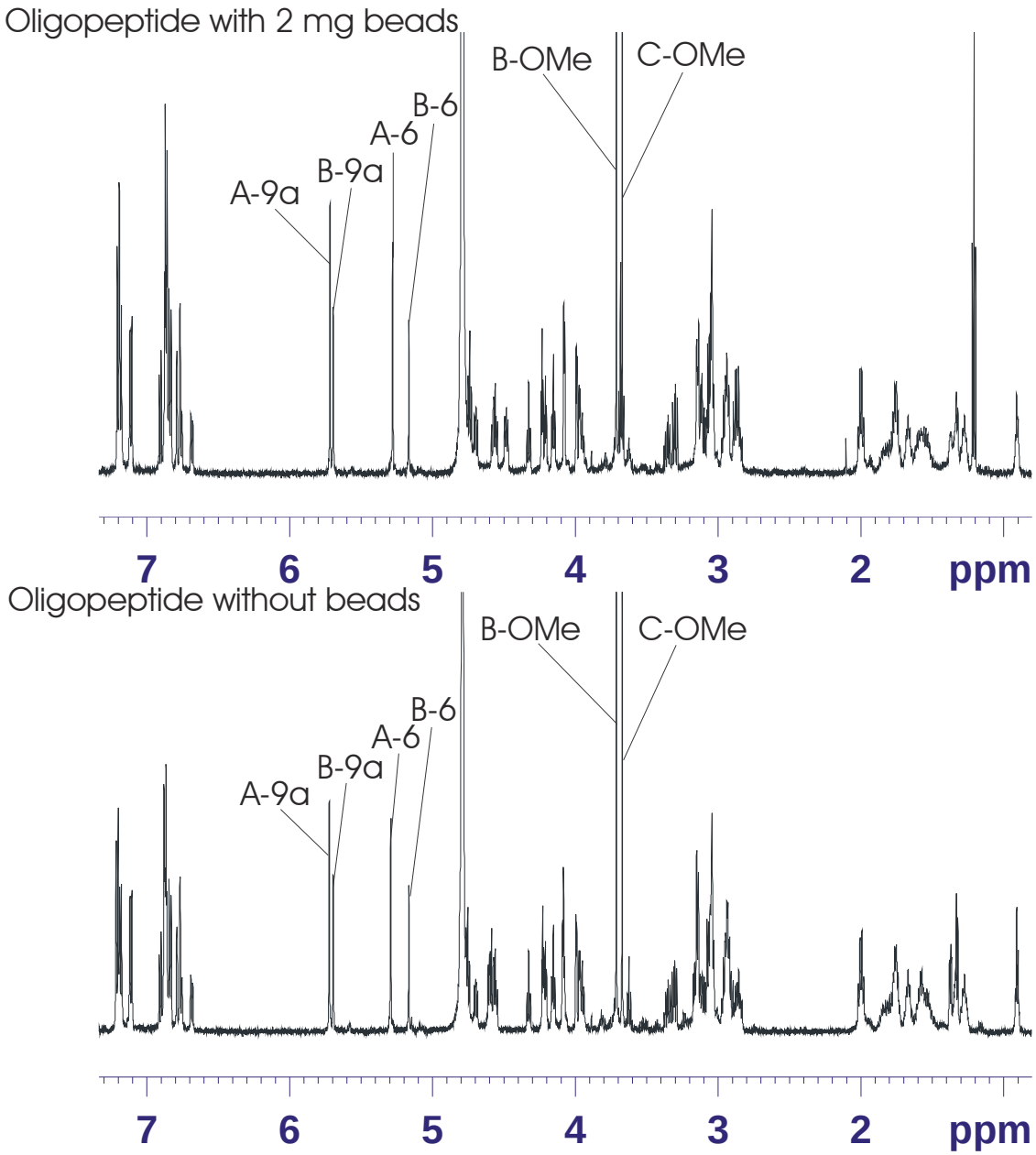

Figure 5 -25: 1D DOSY spectrum of mixtures of tetrapeptide (Lys-Bic-Tyr, Lys-DOPA-Tyr-OMe and DOPA-Bic-Tyr-OMe) recorded at 500 Mz in D_2O. Lower panel represents 1D DOSY without silicon nanobeads whereas upper panel is a 1D DOSY spectrum with 2 mg of silicon nanobeads. Signals corresponding to tetrapeptides are: (A) Lys-Bic-Tyr, (B) DOPA-Bic-Tyr-OMe, and (C) Lys-DOPA-Tyr-OMe.

A 2D DOSY of compound **16** (Lys-Bic-Tyr), compound **23** (Lys-DOPA-Tyr-OMe) and compound **18** (DOPA-Bic-Tyr-OMe) is shown in Figure 5 -26.

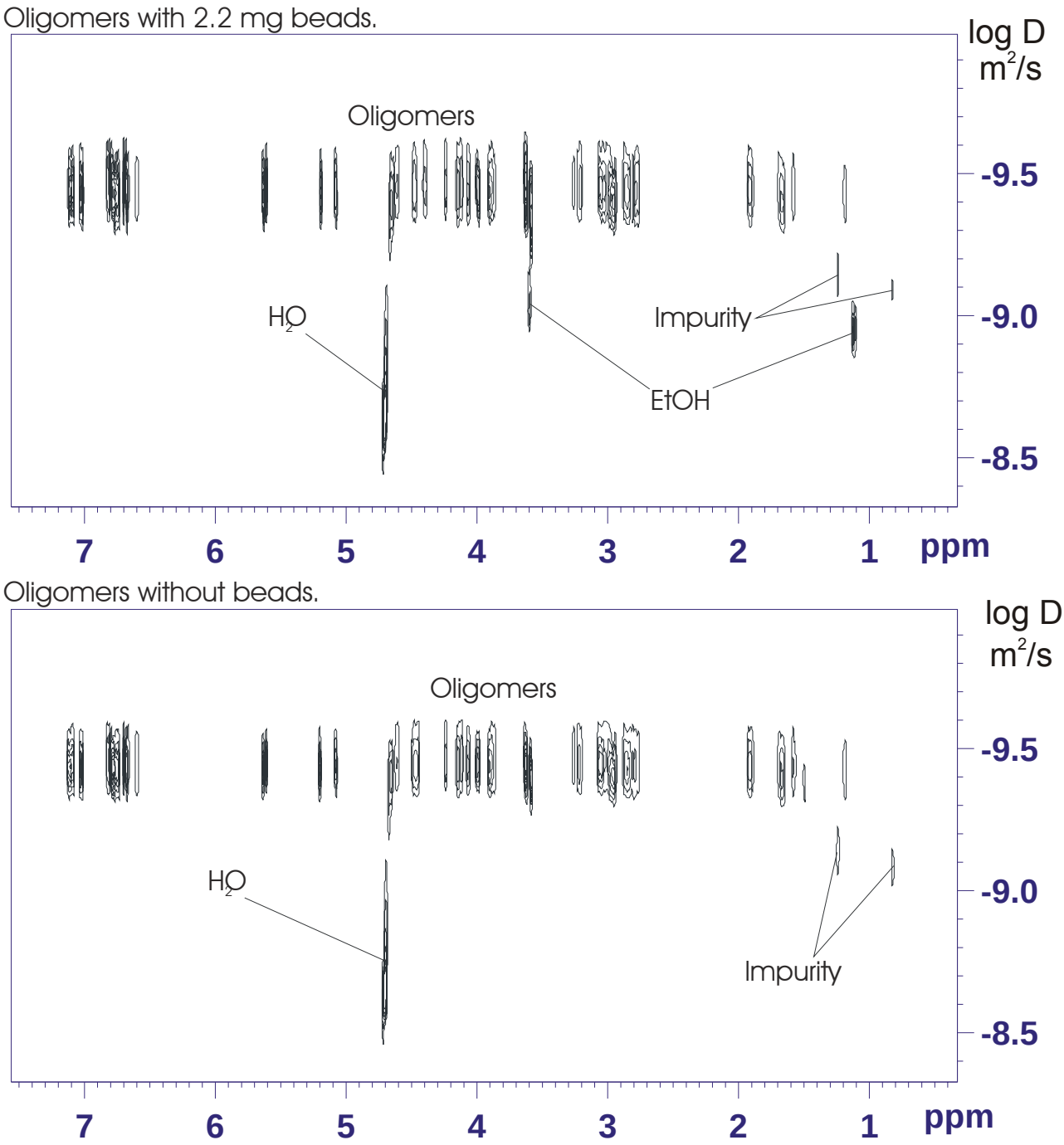

Figure 5 -26: 2D DOSY spectrum of the mixture of tetrapeptides (compound **16** (Lys-Bic-Tyr), compound **23** (Lys-DOPA-Tyr-OMe) and compound **18** (DOPA-Bic-Tyr-OMe)) recorded at 500 MHz with D_2Oas solvent. Upeer panel represents spectrum with 2.2 mg of silicon nanobeads whereas lower panel represents blank spectrum.

However, 2D DOSY spectrum of oligomers do not show binding with silicon nano beads. This is evident from unchanged spectral pattern and chemical shifts of oligomers with and without nanobeads.

5.3.2. DOSY of poly-Bic-Tyr

The adhesiveness property of the oligopeptide poly-Bic-Tyr (compound **34**) was measured using 1D and 2D diffusion order spectroscopy (DOSY).

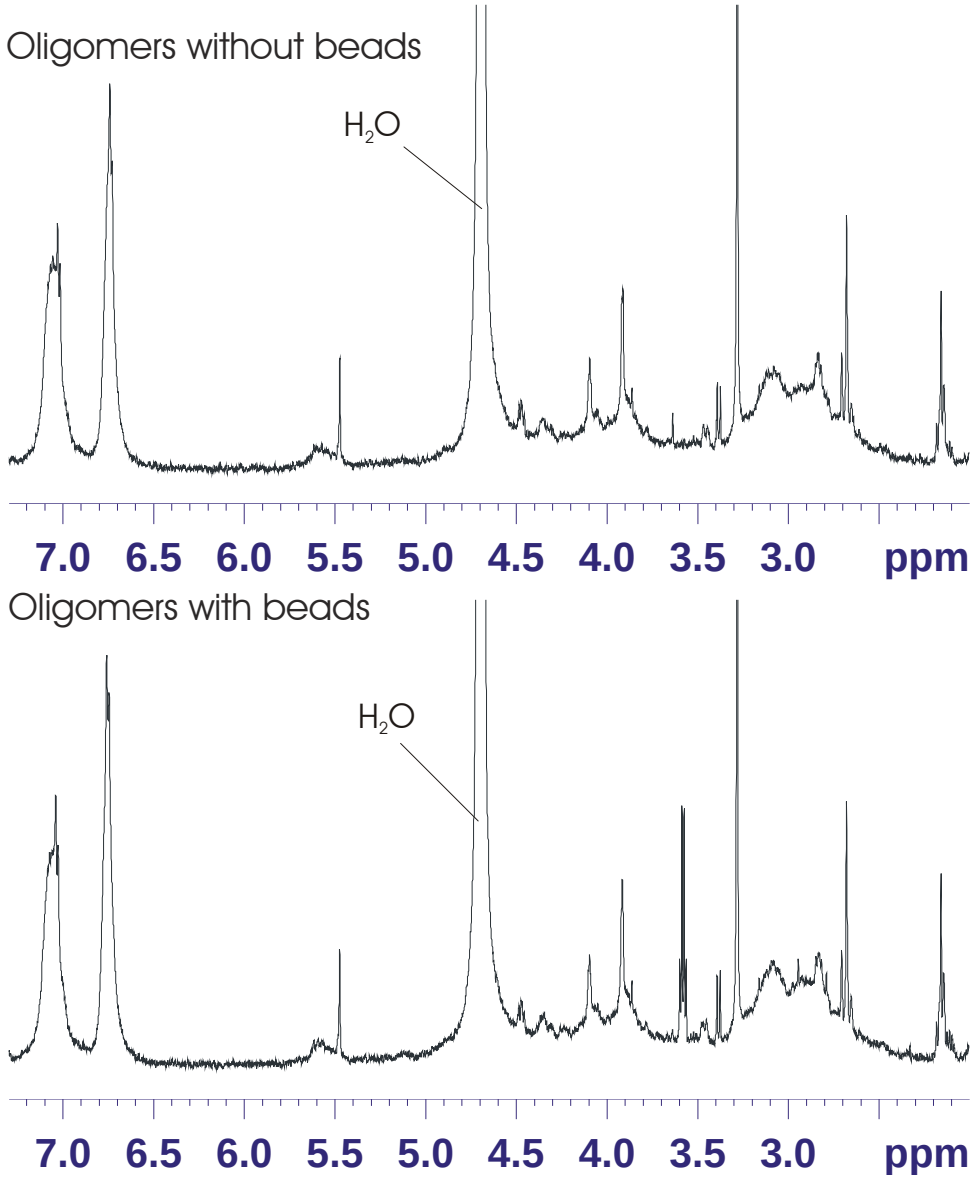

Figure 5 -27: 1D DOSY spectrum of poly-Bic-Tyr (compound **34**) without nano beads (lower panel) and with 2 mg nano beads (upper panel). Solvent signal is marked.

1D DOSY spectra of poly-Bic-Tyr (compound **34**), with and without silicon nanobeads are shown in Figure 5 -27. We see relatively broad signals from the oligomer. However, no change in the signal pattern and no appearance of new signal suggest that poly-Bic-Tyr does not bind to nanobeads. To gain futher insights into the binding of nanobeads with poly-Bic-Tyr, 2D DOSY spectra was measured and shown in Figure 5 -28.

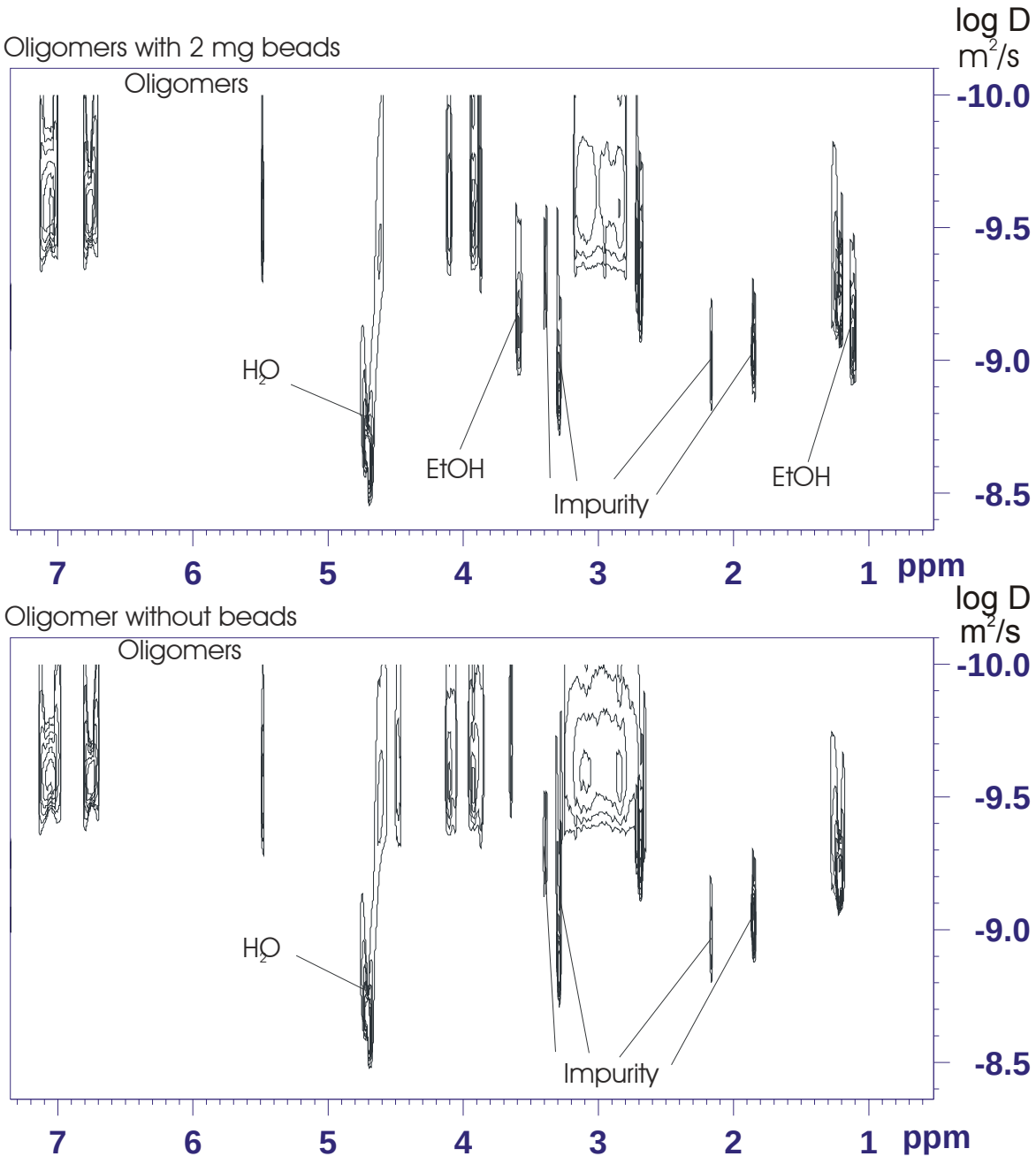

Figure 5 -28: 2D DOSY spectrum of poly-Bic-Tyr (compound **34**) recorded at 500 MHz with D_2O as solvent. Upper panel represents spectrum with 2.2 mg of silicon nanobeads whereas lower panel represents blank spectrum. No additionally appearing signal has been noticed in the upper panel. Impurities and solvent signals are marked in figure.

The measurement was performed in the absence and presence of silicon nanobeads. As stated previously, upon binding (interaction between two species), appearance of new signals is evident. However, 2D DOSY also shows exactly similar spectral pattern without any new signals in presence of silicon nanobeads suggesting that poly-Bic-Tyr does not bind to silicon nanobeads.

5.3.3. DOSY of poly-Lys(Z)-Bic-Tyr and poly-Lys-Bic-Tyr

The testing of adhesiveness was also performed in poly-Lys(Z)-Bic-Tyr (compound **36**) and poly-Lys-Bic-Tyr (copound **37**) using 1D and 2D DOSY.

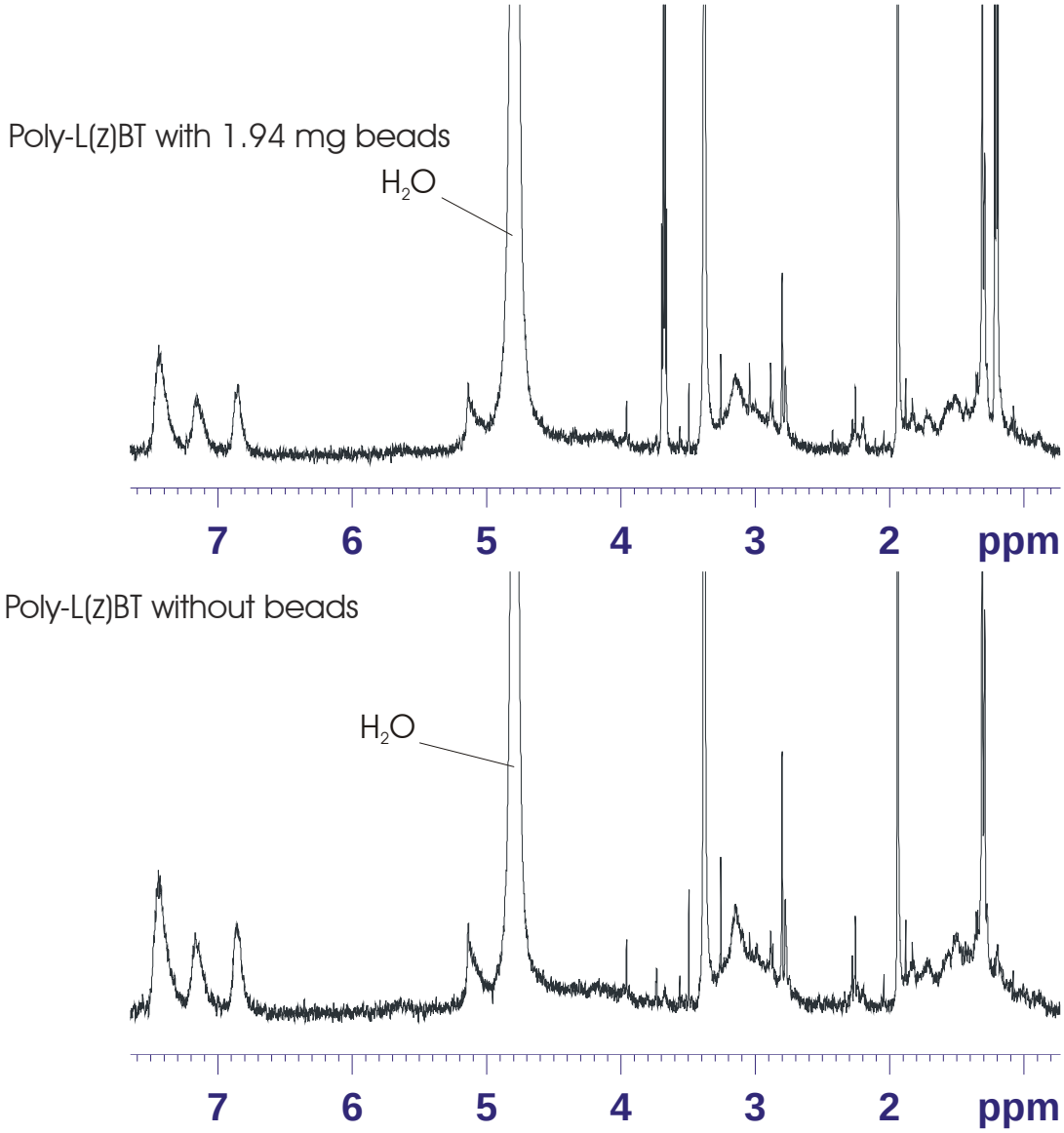

Figure 5 -29: 1D DOSY spectrum of poly-Lys(Z)-Bic-Tyr (compound **36**) without nano beads (lower panel) and with 1.94 mg nano beads (upper panel). Solvent signal is marked.

Figure 5 -29 represent 1D DOSY of poly-Lys(Z)-Bic-Tyr and Figure 5 -30 represnet 1D DOSY of poly-Lys-Bic-Tyr in presence and absence of silicon nanobeads. Appearance of no new signal suggests that there is no binding in both cases. However, both compounds give broad signals and therefore 2D DOSY was performed.

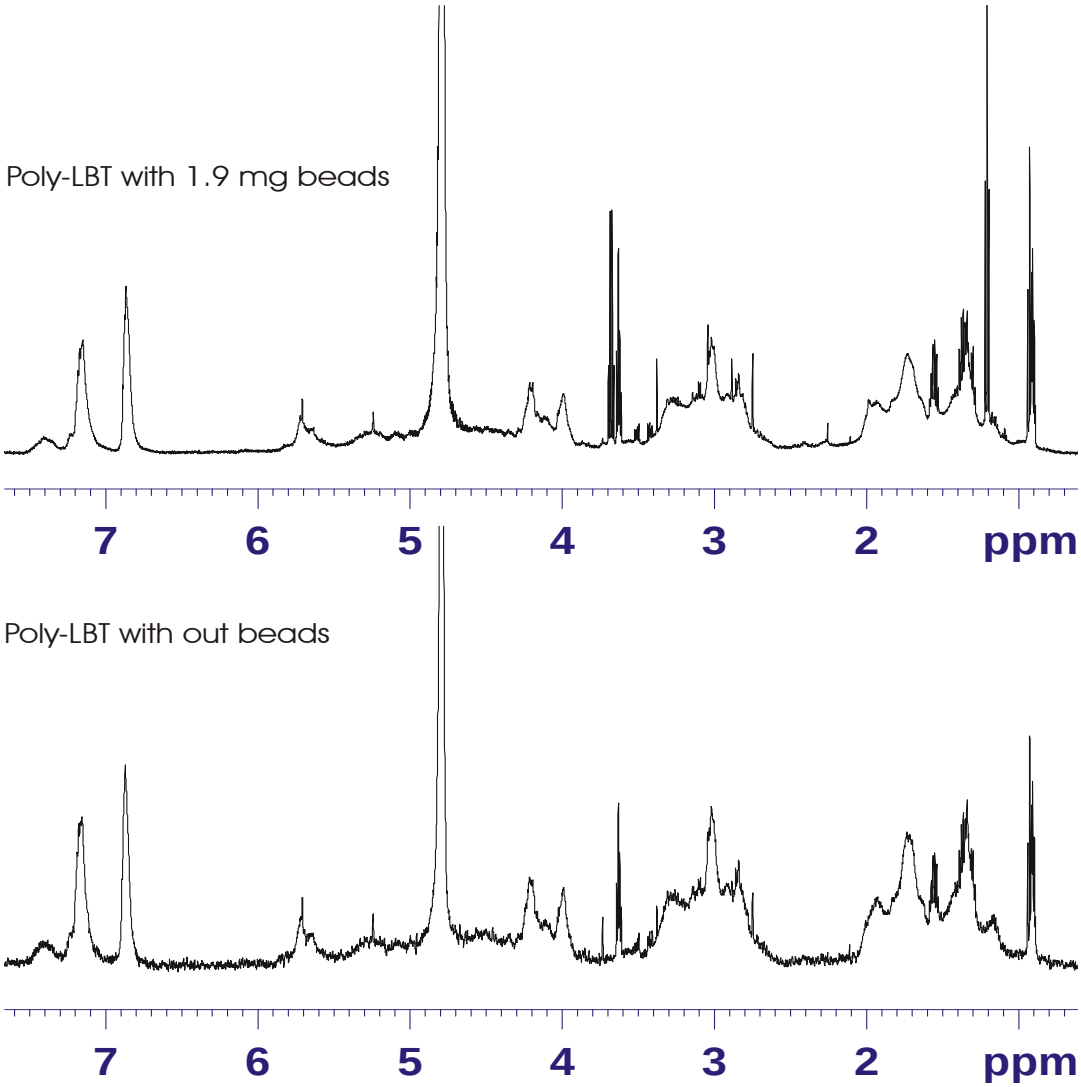

Figure 5 -30: 1D DOSY spectrum of poly-Lys-Bic-Tyr (compound **37**) without nano beads (lower panel) and with 1.9 mg nano beads (upper panel).

Figure 5 -31 and Figure 5 -32 represent 2D DOSY of poly-Lys(Z)-Bic-Tyr (compound **36**) and poly-Lys-Bic-Tyr (compound **37**).

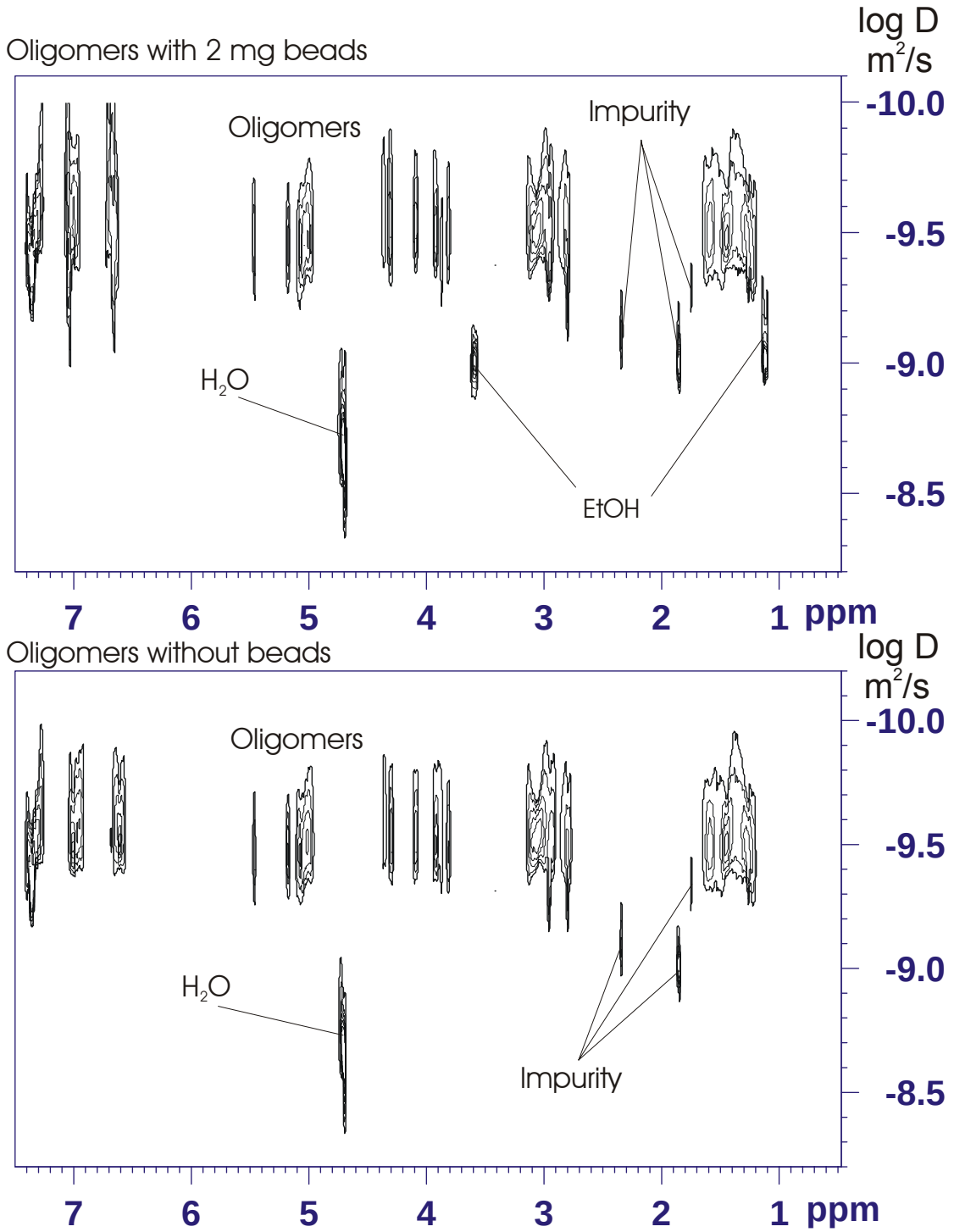

Figure 5 -31: 2D DOSY spectrum of poly-Lys(Z)-Bic-Tyr (compound **36**) recorded at 500 MHz with D_2O as solvent. Upper panel represents spectrum with 2 mg of silicon nanobeads whereas lower panel represents blank spectrum. No additionally appearing signal has been noticed in the upper panel. Impurities and solvent signals are marked in figure.

These spetra were recorded without silicon nanobeads in the first place and latter in the presence of nanobeads (2 and 1.9 mg respectively). Both spectra show no difference in the spectral pattern

and there was no newly appearing signal is seen. This strongly suggests that both poly-Lys(Z)-Bic-Tyr and poly-Lys-Bic-Tyr does not bind to silicon nano beads.

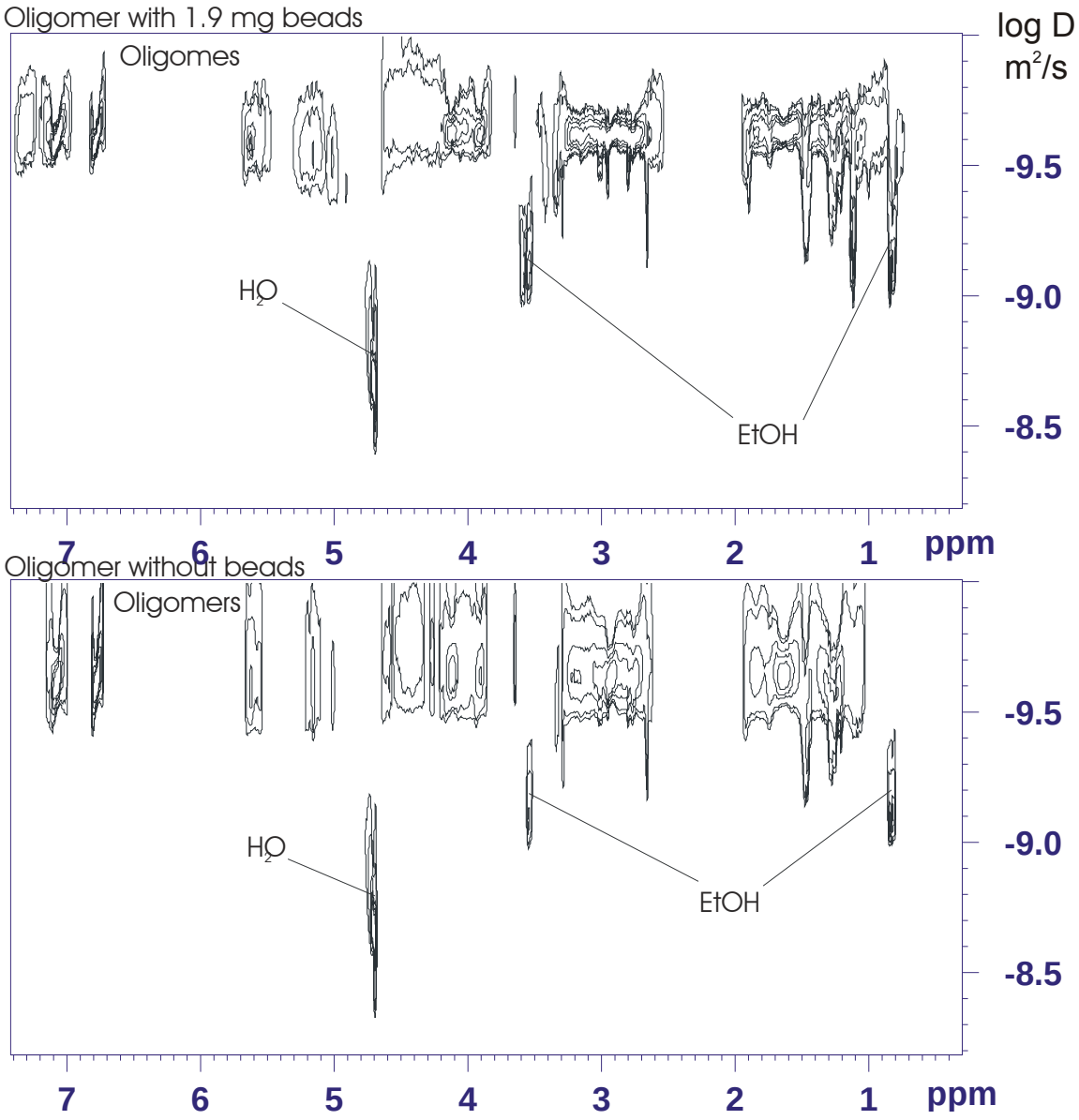

Figure 5 -32: 2D DOSY spectrum of poly-Lys-Bic-Tyr (compound **37**) recorded at 500 MHz with D_2O as solvent. Upper panel represents spectrum with 2.2 mg of silicon nanobeads whereas lower panel represents blank spectrum. No additionally appearing signal has been noticed in the upper panel. Impurities and solvent signals are marked in figure.

5.3.4. AFM Studies of poly-Bic-Tyr

Interaction of poly-Bic-Tyr (compound **34)** with large surfaces like mica and graphite was studded here. For all measurements 1 mg of compound **34** was dissolved in 0.1 mL dry DMF, a

20 µL aliquot of the mixture was deposited on to bilayer. The sample was rapidly blow dried using a burst of compressed gas (Nitrogen or Argon). To demonstrate the purity of the solvent used for sample preparation, 20 µL of the pure solvent was celebrated on the substrates blew dried, and AFM imaging was performed on these surfaces. No spots due to impurities of the solvent were found. The two AFM images of oligopeptide poly-Bic-Tyr (compound **34**) on mica and graphite surface were shown in Figure 5 -33.

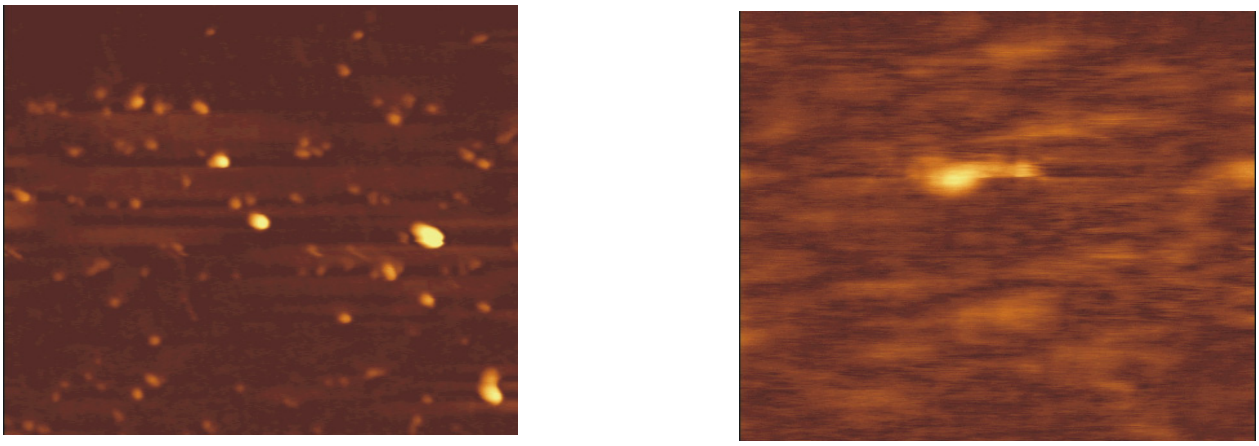

A B

Figure 5 -33: Image of the poly-Bic-Tyr (compound **34**) on (A) mica and (B) graphite. A number of bumps appear in the image, each presumably corresponding to a single oligomer. Different sizes of oligomers suggest that the mixture of different oligomeric species is present.

Using this concentration distinct oligomers of molecules were observed. Surface covered by a high density of dome like protrusion that emerges up to 8 nm from the substrate. Underneath these vesicular structures is a flat, defect-free surface. The simple interpretation of these images is that the oligopeptide have stably adsorbed to the substrate.

The mixture of oligomeric poly-Bic-Tyr contains some species which are smaller in height and some of the oligomers are higher in height. The mean diameter of this loop is 2.0 ± 0.5 nm, on mica surface; similar result is obtained for the studies performed using graphite surface. The distribution of the diameters of the loop formed at 0.5 µM on mica surfaces was shown in Figure 5 -34.

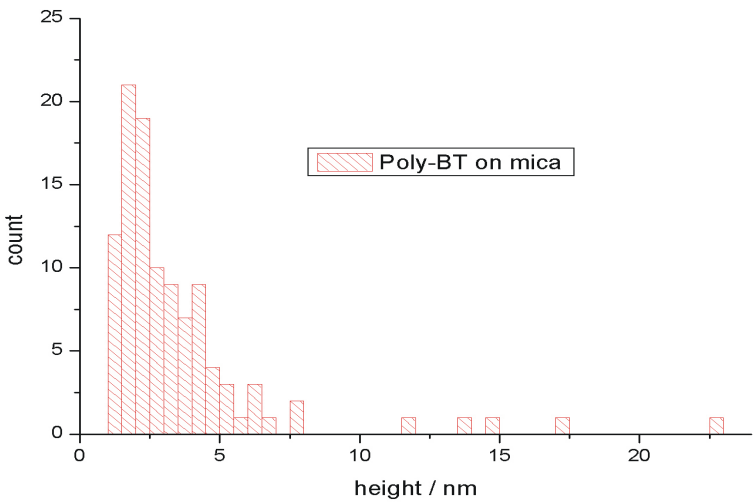

Figure 5 -34: Distribution of the diameters of the individual loops formed at 0.5 µM for the poly-Bic-Tyr (compound **34**).

This is a strong indication that the compound **34** (poly-Bic-Tyr) shows interactions (in terms of binding) on both mica and graphite surfaces suggesting that there is no adhesiveness.

5.3.5. AFM Studies of poly-Lys(Z)-Bic-Tyr

Interaction of compound **36** (poly-Lys(Z)-Bic-Tyr) with different large surfaces like mica and graphite is studied here and is shown in Figure 5 -35.

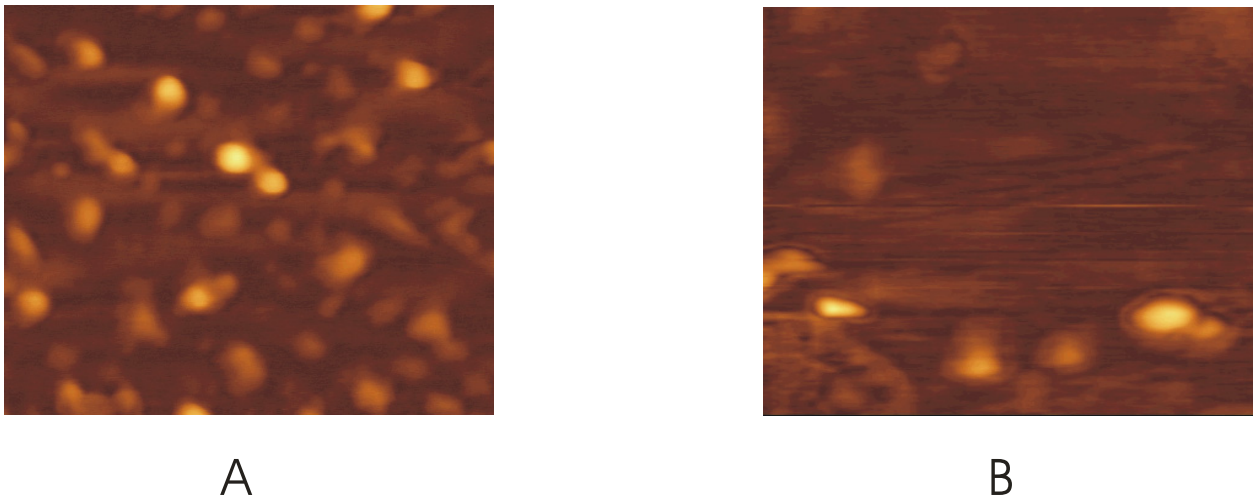

Figure 5 -35: Image of poly-Lys-(Z)-Bic-Tyr (compound **36**) on (A) mica and (B) graphite. A number of bumps appear in the image, each presumably corresponding to a single oligomer.

Using this concentration distinct oligomers of molecules are observed. Surface covered by a high density of dome like protrusion that emerges up to 8 nm from substrate. Underneath these vesicular structures is a flat, defect-free surface. The simple interpretation of these images is that the compound 36 adsorbes stably on the substrate.

Some of oligomers seen here are smaller in height while others are higher in height. The mean diameter of this loop is 2.7 ± 0.8 nm, on mica surface. Similar results of the mean diameter were obtained using graphite surfaces. The distribution of the diameters of the loop formed at 0.5 µM on different surfaces was shown in Figure 5 -36.

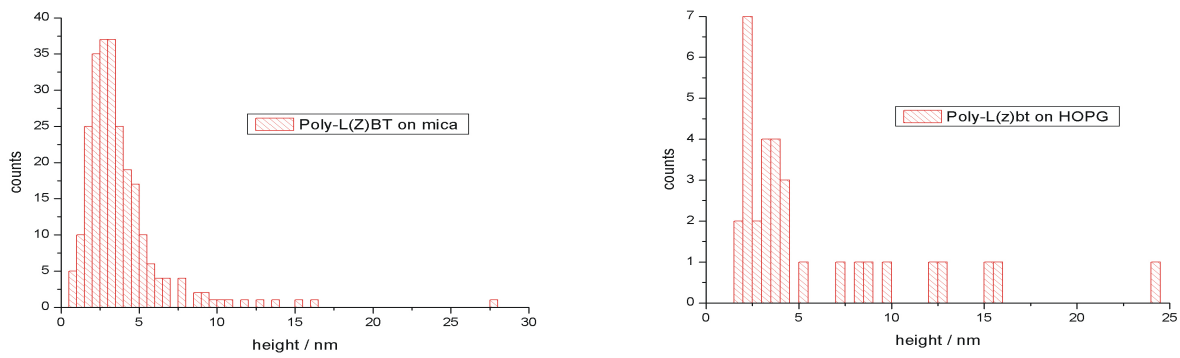

Figure 5 -36: Distribution of the diameter of the individual loops formed at 0.5 µM for poly-Lys-(Z)-Bic-Tyr (compound **36**).

This result indicates that compound **36** show interactions on both surfaces mica and graphite. It proves that compound **36** does not shows adhesion on mica as well as graphite surface.

5.3.6. AFM Studies of poly-Lys-Bic-Tyr

Similar AFM measurements were performed for compound **37** (poly-Lys-Bic-Tyr) and sample preparation was same like previous two compounds. Two AFM images of oligopeptide compound **37** on mica and graphite surfaces are shown in Figure 5 -37.

At this (1mg/0.1 mL) concentration distinct oilgomers of molecules were observed. Surface covered by a high density of dome like protrusion that emerges up to 7.5 nm from the surface. Underneath these vesicular structures is a flat, defect-free surface. A straightforward interpretation of these images is that the oligopeptides have stably adsorbed to the substrate surface. Distribution of smaller and higher heights of oligomers is seen here.

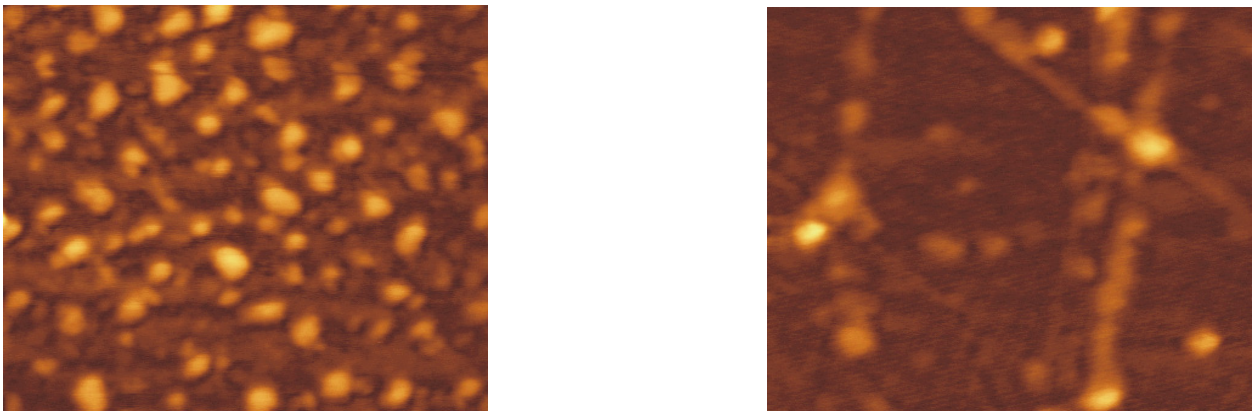

A B

Figure 5 -37: Image of the poly-Lys-Bic-Tyr (compound **37**) on (A) mica and (B) graphite. A number of bumps appear in the image, each presumably corresponding to a single oligomer.

The mean diameter of this loop is 2.8 ± 0.7 nm, on mica surface, the distribution of the diameters of the loop formed at 0.5 µM on different surfaces was shown in Figure 5 -38. Different result were obtained using graphite surface, in which case the mean diameter of this loop is 1.2 ± 0.3 nm. In the latter case, mean diameter of the loop is smaller.

Figure 5 -38: Distributation of the diameters of the individual loops formed at 0.5 µM for poly-Lys-Bic-Tyr (compound **37**).

These results indicate that compound **37** shows interactions on the both surfaces mica and graphite. Results obtained from Figure 5 -38 demonstrate that poly-Lys-Bic-Tyr shows stronger interaction on graphite (HOPG) compared to mica surface. It proves that compound **37** shows intra and/or inter molecular interactions on graphite surface clearly indiacating that it has adhesive characteristics.

6. Summary and Conclusions

Extensive studies revealed that mussel adhesion to underwater surfaces is mediated through a family of five proteins, named *mytilus edulis foot protein* (*mefp*-1 to 5). Presence of L-3,4-dihydroxyphenylalanine (DOPA), an post-transationally modified amino acid, is believed to be responsible for both adhesive and cross linking characteristics of MAPs. Despite extensive studies on MAPs, there remains an incomplete understanding of their adhesive and cohesive mechanisms. Possible commercial applications of synthetic analogues of MAPs would be its use as glue to stick organs or parts of it and use as environment friendly glue. Several research groups are involved in exploring various physical, mechanical and biological properties of MAPs, while others evaluated possible synthetic analogues that would mimick adhesive characteristics.

In this work, successful synthesis of a synthetic polypeptide has been carried out that shows adhesive properties.

The synthesis of oligomers and co-polymers were performed using polyhydroxylated bicyclic dipeptide buiding blocks. These dipeptides feature four hydroxyl groups (similar to DOPA which has two hydroxyl groups). Fmoc- and Boc- protection of one of the –OH was performed so that the oligomerization/polymerization reaction can be carried away at amide-carbonyl backbone. The course of synthesis was chosen such that oligomerization of bicyclic dipeptide (Bic), Tyr, Lys and DOPA was achieved first. Further copolymerization of Bic-Tyr, Lys-Tyr, and Lys-Bic-Tyr was carried out. Polymerization was accomplished using DCC and poly-DCC.

Structural features of these oligomers and copolymers were characterized using 1D and 2D NMR spectroscopy whereas molecular mass and size was determined using MALDI, GPC and gel electrophoretic techniques. Broad resoances in NMR and distribution of masses over a wide range suggested that a single species of a unique molecular weight was not present in any reaction. In other words, each oligomerization reaction produced a mixture of oligomer/co-polymer with wide mass distribution. It was found that oligomers and copolymers were mainly of the order of 1-2 kDa based on MALDI studies. At the same time, GPC and gel electrophoresis showed about ten fold higher size of the oligomer and copolymers. The reason for this descipency is still unresolved but one suggestion could be inability of MALDI to detect exact mass of polydisperse sample. In such cases, MALDI spetraof high-mass components are generally underrepresented with respect to lower mass oligomer peaks.

Adhesive properties of these copolymers/oligomers were accomplished using 1D and 2D diffusion ordered spectroscopy (DOSY) NMR experiment and AFM studies. DOSY relies on the translational diffusion coefficient of a molecule experiencing Brownian motions in an isotropic

solution. Binding of tetra, oligo and co-polymers with silicon nano beads was checked in this case. Upon binding with silicon nanobeads, one expects to see occurance of new peak and/or shifting of peak. However, none of the DOSY experiments recorded in presence of silicon nanobeads showed any difference from the ones which were recorded without nanobeads.

Atomic force microscopy can map topography of a surface and gives an exteremely high resolution image of the surface. Co-polymers like, poly-Bic-Tyr, poly-Lys(Z)-Bic-Tyr and poly-Lys-Bic-Tyr were probed for binding on mica and graphite surface. Results show that poly-Lys-Bic-Tyr adheres to graphite surface. Non binding of poly-Bic-Tyr and poly-Lys(Z)-Bic-Tyr on mica and/or graphite surface can be easily visualized as former misses long chain, positively charged and polar Lys whereas presence of Z group might be influencing adhesion of latter.

The adhesion of poly-Lys-Bic-Tyr suggests that the information gained in this study can be further used to probe several other synthetic peptides and polymers which mimic adhesive characteristics of MAPs. One approach could be to synthesize uniformely mass distributed polymer so that the activity can be correlated to minimum necessary length of the polymer. Also, Tyr and Lys could be replaced with other amino acids so that the polymer might gain further stability against proteolytic degredations. Mechanism to test the strength of the adhesion is also needed to be explored. At the same time, addition of other analogous amino acids to this polymer can be carried out so that the strength of the adhesion could be increased.

Overall, results obtained in this thesis suggest that the synthetic adhesive polymers based on peptidomimetics can be prepared. Further studies using this approach could lead to prepare synthetic MAPs which will have wide applications.

7. Experimental Section

This chapter presents the synthetic procedures and analytical data of the compounds those were synthesized during this Ph.D. work. The HPLC and GPC instruments used were as follows:

HPLC:

For the analytic separations the following equipment was used.

Column: Phenomex Luna C18 (2), 150 mm, 4.6, 5 um.

Equipment of the LC systems agilent 1100 G 1315A Bin pump, G1313A ALS, G1316A COLCOM, G1315B DAD, G1379 Degasser; as software "Chemstation for LC 3D Rev. A. 09.03" was used.

Gel permeation chromatography (GPC):

GPC measurements were performed versus polystyrene standards with a set of three columns with DMF as solvent (300 × 8 mm, type SDV, 10 µm from PSS) using a differential refractometer as detector at 25°C.

7.1. Compound 1: 9a(R)H-5-oxo-(6S,7S,8S,9R)-tetrahydroxy-octahydro-thiazolo-[3,2-a] azepin-3R-carboxilic acid-methyl ester.

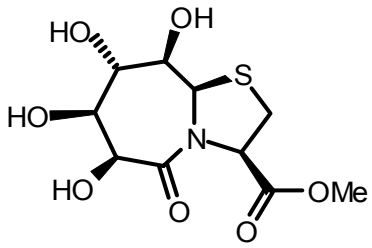

1

7.1.1. Procedure

Condensation of commercial D-glucurono-3,6-lactone (5 g, 28.4 mmol) with L-cysteine methyl ester (4.8 g, 28.4 mmol) using distilled water (100 mL) and pyridine (10 mL), gives bicyclic thiazolidinlactam 1. Yield obtained was 8.06 g. (27.4 mmol, 90%)

7.1.2. Analytical Data

^{1}H NMR (300 MHz, DMSO-d_6): δ = 5.55 (s, 1H, 7-OH), 5.41 (s, 1H, 9a-H), 5.27 (s, 1H, 8-OH), 4.73 (d, $^3J_{3,2}$ = 7.4Hz, 1H, 3-H), 4.67 (s, 1H, 6-H), 4.24 (d, $^3J_{8\text{-OH},8}$ = 10.3Hz, 1H, 8-OH), 3.79 (m, 2H, 7-H and 9-H), 3.62 (m, 1H, OMe), 3.52 (d, $^3J_{9\text{-H},9}$ = 5.77Hz, 1H, 9-H), 3.28 (m, 2H, 2-H).
^{13}C NMR (300 MHz, DMSO-d_6): δ = 170.55, 170.35 (CO-5, COMe), 31.39(C-2), 52.10 (OMe), 60.97 (C-9a), 63.78 (C-3), 70.86 (C-8), 76.00 (C-7), 76.87 (C-9).
ESI-MS (H_2O/MeOH + 10 mmole NH_4Ac) (m/z): 293.7 $[M-H]^+$, 310.8 $[M+NH_4]^+$, 315.8 $[M+Na]^+$, 604 $[2M+NH_4]^+$, 609 $[2M+Na]^+$.
Melting Point: 184°C.

7.2. Compound 2: 9a(R)H-5oxo-(6S)-trifluoromethansulfonyloxy-(7S,8S,9R)-trihydroxy-octahydro-thiazolo [3,2-a]azepin-3R-carboxilic acid-methyl ester.

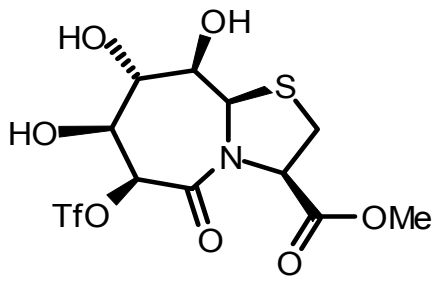

2

7.2.1. Procedure

Thiazolidinlactam **1** (8.2 g, 28 mmol) was dissolved in 250 mL DCM (abs) and 50 mL pyridine. After cooling with an ice-bath 6mL of triflic acid anhydride (36.4 mmol, 1.3 eq) in 7 mL of DCM (abs) were added. The ice-bath was removed after 20 minutes and the reaction mixture was kept at room temperature for another 10 min. Then 100 cm^3 ice were added and the product was extracted with DCM three times. The solvent was removed after drying with $NaSO_4$ and triflate **2** was purified by column chromatography ($CHCl_3$:MeOH in the ratio 5:1). Yield obtained was 10.9 g (24.6 mmol, 89%).

7.2.2. Analytical Data

^{1}H NMR (300 MHz, DMSO-d_6): δ = 6.60 (d, $^3J_{7\text{-OH},7}$ = 6.4 Hz, 1H, 7-OH), 5.98 (s, 1H, 6-H), 5.97 (d, $^3J_{8\text{-OH},8}$ = 2.40 Hz, 1H, 8-OH), 5.62 (s, 1H, 9a-H), 4.79 (pt, $^3J_{3,2}$ = 7.9 Hz, 1H, 3-H), 4.46 (d,

$^3J_{9\text{-}OH,9}$ = 10.6Hz, 1H, 9-OH), 4.04 (m, 1H, 7-H), 3.91 (m, 1H, 8-H), 3.64 (s, 3H, OMe), 3.61 (dd, $^3J_{9,9\text{-}OH}$ =10.8 Hz and $^3J_{9,8}$= 3.4Hz, 1H, 9-H), 3.33 (m, 2H).

^{13}C NMR (300 MHz, DMSO-d_6): δ = 169.88, 162.79 (CO-5, CO-Me), 86.01 (C-6), 76.55 (C-9), 73.90 (C-7), 70.17 (C-8), 64.18 (C-3), 60.93 (C-9a), 52.27 (OMe), 31.27 (C-2).

ESI-MS (CH_2Cl_2/MeOH + NH_4AC) (m/z): 443 $[M+NH_4]^+$, 867.7 $[2M+NH_4]^+$.

Melting Point: 55°C.

7.3. Compound 3: 9a(R)H-(6S)-azido-5-oxo-(7R,8S,9R)-trihydroxy-octahydro-thiazolo [3, 2-a]azepin-3R-carboxilic acid-methylester.

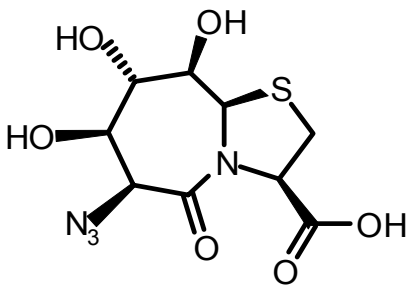

3

7.3.1. Procedure

Triflate **2** (10.6 g, 24.9 mmol) was dissolved in DMF (130 mL) and NaN_3 (2.5 g, 38.5 mmol) was added. After 40 h at room temperature and 8 h at 50°C, the solvent was removed and the residue extracted in EtOAc (400 mL) and H_2O (100 mL). The aqueous phase was extracted three times with EtOAc (200 mL) and the combined organic phase was dried over $NaSO_4$. Azide **3** was purified by column chromatography (EtOAc:toluene as 9:1). 6.5 g (20.4 mmol, 82%) of **3** were obtained as a colorless solid.

7.3.2. Analytical Data

^{1}H NMR (300 MHz, DMSO-d_6): δ = 5.65 (d, $^3J_{8\text{-}OH,8}$ = 3.57Hz, 1H, 8-OH), 5.56 (d, $^3J_{7\text{-}OH,7}$ = 6.31 Hz, 1H, 7-OH), 5.48 (s, 1H, 9a-H), 4.78 (s, 1H, 6-H) 4.74 (pt, $^3J_{3,2}$ = 3.84 Hz, 1H, 3-H), 4.42 (d, $^3J_{9\text{-}OH,9}$ = 10.43 Hz, 1H, 9-OH), 3.85 (m, 1H, 7-H), 3.80 (m, 1H, 8-H), 3.65 (s, 3H, OMe), 3.52 (dd, $^3J_{9\text{-}OH,9}$ = 10.43Hz, $^3J_{8,9}$ = 2.74Hz, 1H, 9-H), 3.29 (d, $^2J_{2,2}$ = 6.04 Hz, 2H, 2-H).

^{13}C NMR (300 MHz, DMSO-d_6): δ = 170.32 (CO_2Me), 166.55(C-5), 76.53 (C-9), 74.78 (C–7), 70.81 (C-8), 63.92 (C-3), 61.34 (C-6), 60.93 (C-9a), 52.19 (OMe), 31.39 (C-2).

ESI-MS (CH_2Cl_2/MeOH + NH_4AC) (m/z): 318 $[M]^+$.

Melting Point: 197°C.

7.4. Compound 4: 9a(R)H-(6S)-amino-5-oxo-(7R,8S,9R)-trihydroxy-octahydro-thiazolo[3,2-a]azepine-3R-carboxilic acid-methylester.

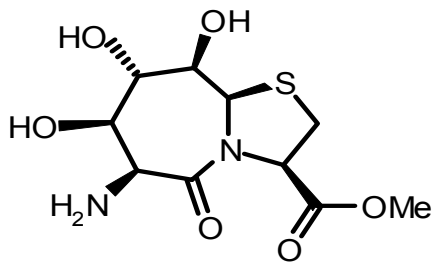

4

7.4.1. Procedure

A suspension of Pd/C (0.10 g) in MeOH (15 mL) was vigorous stirred under H_2 gas until the uptake of H_2 completed (10 min). Then Azide **3** (0.50 g, 1.57 mmol) in MeOH (5 mL) was added into the reaction mixture. The reaction mixture was stirred under H_2 atmosphere at room temperature up to 6 h. Reaction was monitored by TLC; yield obtained was 0.43g. (1.47 mmol, 94%).

Alternatively, this compound can be also prepared as:

Azide **3** (0.10 g, 0. 31 mmol) was dissolved in MeOH (5 mL). Pd/C (0.01 g) was added into reaction mixture. The reaction mixture was stirred for 6 h at room temperature under H_2 atmosphere. Reaction was monitored by TLC. Solvent was removed. Yield obtained was 0.086 g (29.5 mmol, 94%).

7.4.2. Analytical Data

^{1}H NMR (300 MHz, DMSO-*d*$_6$): δ = 8.38 (br, 3H, $NH_3^{+)}$, 5.95 (d, $^3J_{8\text{-OH},8}$ = 3.66 Hz, 1H, 8-OH), 5.78 (d, $^3J_{7\text{-OH},7}$ = 5.06 Hz, 1H, 7-OH), 5.61 (s, 1H, 9a-H), 4.75 (pt, $^3J_{3,2}$ = 7.6 Hz, 1H, 3-H), 4.66 (s, 1H, 6-H), 4.43 (d, $^3J_{9\text{-OH},9}$ = 10.7 Hz, 1H, 9-OH), 3.99 (s, 1H, 7-H), 3.90 (d, $^3J_{8,9}$ = 3.46Hz, 1H, 8-H), 3.65 (s, 3H, OMe), 3.65 (d, $^3J_{9,8}$ = 3.45 Hz, 1H, 9-H), 3.34 (d,$^2J_{2\text{-H}}$ =7.676 Hz, 2H, 2-H).

^{13}C NMR (300 MHz, DMSO-*d*$_6$): δ = 170.08 (CO-5), 165.51 (COOMe), 76.74 (C-9), 71.75 (C-7), 69.98 (C-8), 63.88 (C-3), 61.07 (C-9a), 53.08 (C-6), 52.27 (OMe), 31.52 (C-2).

ESI-MS (CH_2Cl_2/MeOH + NH_4AC) (m/z):293.1 $[M-H]^+$.

Melting Point: 175°C.

7.5. Compound 5: 9a(R)H-(6S)-tert-butyooxycarbonylamino-5-oxo-(7R,8S,9R)-trihydroxy-octahydro-thiazolo [3,2,-a]azepin-3R-carboxilic acid-methylester

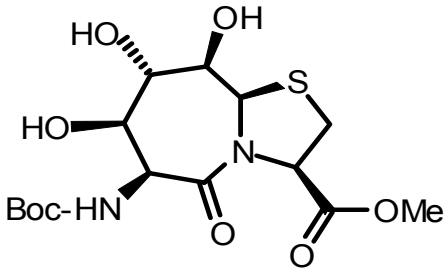

5

7.5.1. Procedure

Preparation of **5** from Azide **3**:

Azide **3** (1g, 3.14 mmol) was dissolved in MeOH (30 mL). Boc anhydride (0.82 g, 3.77 mmol) and Pd/C (0.20 g) were added into reaction mixture. The reaction mixture was stirred for 6 h under H_2 atmosphere. Reaction was monitored by TLC. Solvent was removed and reaction mixture was purified by column chromatography (MeOH:CH_3Cl as 1:9). Yield obtained was 1.18 g (3.01 mmol, 96%).

Preparation of **5** from amine **4**:

Amine **4** (0.01 g, 0.03 mmol) was dissolved in MeOH (5 mL). Boc anhydride (0.009g, 0.04 mmol) in MeOH (5 mL) was added slowly into stirring mixture. The reaction mixture was stirred at room temperature for 6 h. The solvent was removed and **5** was purified by column chromatography (MeOH:CH_3Cl as 1:9). Yield obtained was 0.012 g (0.030 mmol, 90%).

7.5.2. Analytical Data

^{1}H NMR (300 MHz, DMSO-d_6): δ = 5.54 (d, $^3J_{Boc\text{-}NH,6}$ = 9.05Hz, 1H, Boc-NH), 5.66 (d, $^3J_{8\text{-}OH,8}$ = 3.84Hz, 1H, 8-OH), 5.44(s, 1H, 9a-H), 5.33 (d, $^3J_{7\text{-}OH,7}$ = 4.12Hz, 1H, 7-OH), 4.78 (d, $^3J_{6\text{-}H,Boc\text{-}NH}$ = 9.06Hz, 1H, 6-H), 4.69 (t, $^3J_{3,2}$ = 7.68Hz, 1H, 3-H), 4.13 (d, $^3J_{9\text{-}OH,9}$ = 11.53 Hz, 9-OH), 3.81 (m, 1H, 8-H), 3.76 (m, 1H, 7-H), 3.62 (s, 3H, OMe), 3.55 (dd, $^3J_{9,8}$ = 3.1Hz and $^3J_{9\text{-}OH,9}$ = 8.5Hz, 1H, 9-H), 3.30 (m, 2H, 2-H).

^{13}C NMR (300 MHz, DMSO-d_6): δ = 170.66, 167.97 (CO-5, COOMe), 154.97 (Boc-CO), 78.0 (C-t-butyl), 77.23 (C-9), 74.96 (C-7), 70.31 (C-8), 63.97 (C-3), 60.90 (C-9a), 53.74 (C-6), 52.11 (OMe), 31.40 (C-2), 28.01 (3C, t-butyl).

ESI-MS (CH_2Cl_2/MeOH + NH_4AC) (m/z): 393 $[M-H]^+$, 415 $[M+Na]^+$, 807 $[2M+Na]^+$.

Melting Point: 145°C.

7.6. Compound 6: 9a(R)H-(6S)-Fmoc-amino-5-oxo-(7R,8S,9R)-trihydroxy-octahydro-thiazolo [3,2-a]azepin-3R-carboxilic acid-methylester.

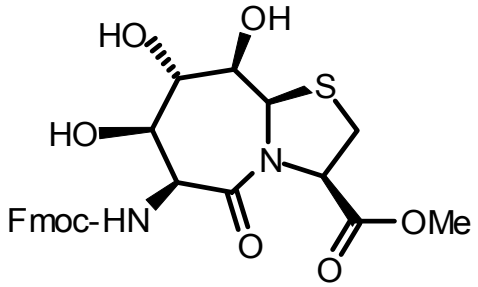

6

7.6.1. Procedure

Preparation of **6** from amine **4**:

Amine **4** (1 g, 3.4 mmol) and Fmoc-ONsu (1.38 g, 4.1 mmol) were dissolved in CH_3CN (30 mL) and MeOH (8 mL). The reaction mixture was stirred at room temperature for 6 h. The solvent was removed and **6** were purified by column chromatography (MeOH:CH_3Cl as 2:8). Yield obtained was 1.2 g (2.33 mmol, 68.18%). Same reaction was carried out using DMF as solvent where yield obtained was 62.5%.

Preparation of **6** from azide **3**:

Azide **3** (1 g, 3.14 mmol) was dissolved in MeOH (30 mL). Fmoc-ONsu (1.2 eq) in CH_3CN (30 mL) and Pd/C (0.200 g) were added into reaction mixture. The reaction mixture was stirred for 6 h under H_2 atm. Reaction was monitored by TLC. Solvent was removed and purified by column chromatography (MeOH/CH_3Cl 2/8). Yield obtained was 0.615 g (1.19 mmol, 38%).

7.6.2. Analytical Data

^{1}H NMR (300 MHz, DMSO-d_6): δ = 7.89 (d, $^3J_{Fmoc\text{-}Ar}$ = 7.41Hz, 2H, Fmoc-Ar), 7.72(d, $^3J_{Fmoc\text{-}Ar}$ = 7.14Hz, 2H, Fmoc-Ar), 7.41(t, $^3J_{Fmoc\text{-}Ar}$ = 7.14Hz, 2H, Fmoc-Ar), 7.32(t, $^3J_{Fmoc\text{-}Ar}$ = 7.14Hz, 2H, Fmoc-Ar), 7.20 (d, $^3J_{Bic\text{-}NH,6}$ = 8.78Hz, 1H, Fmoc-NH), 5.68 (d, $^3J_{8\text{-}OH,8}$ = 3.57Hz, 1H, 8-OH), 5.46 (s, 1H, 9a-H), 5.33 (d, $^3J_{7\text{-}OH,7}$ = 4.39Hz, 1H, 7-OH), 4.86 (d, $^3J_{6,Fmoc\text{-}NH}$ = 9.06Hz, 1H, 6-H), 4.69 (t, $^3J_{3,2}$ = 7.68Hz, 1H, 3-H), 4.54 (s, 1H, 9-OH), 4.25 (m, 3H, Fmoc-α and β), 3.81 (m, 2H, 7-H and 8-H), 3.63 (s, 3H, OMe), 3.56 (dd, $^3J_{9,8}$ = 3.20Hz and $^3J_{9\text{-}OH,9}$= 8.51Hz, 1H, 9-H), 3.30 (m, 2-H).

^{13}C NMR (300 MHz, DMSO-d_6): δ = 170.60 (CO-5), 167.73 (COOMe), 155.70 (Fmoc-CO), 143.67, 140.62, 127.55, 127.01, 125.13, 120.03 (Fmoc-Ar), 77.21 (C-9), 75.01 (C-8), 70.34 (C-7), 65.73 (Fmoc-CH_2), 64.01 (C-6), 60.93 (C-3), 54.16 (C-9a), 52.13 (OMe), 46.45 (Fmoc-CH), 31.41 (C-2).

ESI-MS (CH_2Cl_2/MeOH+ NH_4AC) (m/z): 515.2 $[M-H]^+$, 537.3 $[M+Na]^+$, 1051.4 $[2M+Na]^+$.

Melting Point: 118°C.

7.7. Compound 7: 9a(R)H-(6S)-amino-5-oxo-(7R,8S,9R)-trihydroxy-octahydro-thiazolo [3,2,a]azepin-3R-pottasium salt of carboxylic acid.

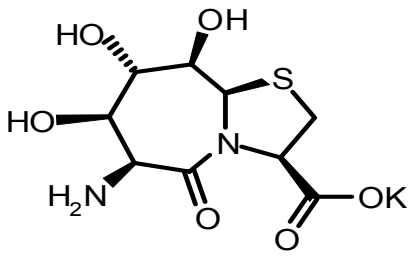

7

7.7.1. Procedure

Compound **4** (1.05 g, 3.6 mmol) was dissolved in (30 mL) water. 1N KOH (7.1 mL, 7.1 mmol) was added into reaction mixture. The reaction mixture was stirred for 30 minute at room temperature. Reaction was monitored by TLC (MeOH:EtOAC:H_2O as 2:2:1) and stopped after 30 minute with 1N HCl (3.59 mL). Solvent was removed and yield obtained was quantitative.

7.7.2. Analytical Data

^{1}H NMR (500 MHz, DMSO-d_6): δ = 5.58 (s, 1H, 9a-H), 4.58 (Pt. $^3J_{3,2}$ = 7.0 Hz, 1H, 3-H), 4.5173 (s, 1H, 6H), 3.865 (d, $^3J_{7,8}$ = 3.57 Hz, 1H, 7-H), 3.821 (d, $^3J_{8,9}$ = 4.086 Hz, 1H, 8-H), 3.512 (d, $^3J_{9,8}$ = 3.043Hz, 1H, 9-H), 3.21 (m, 2H, 2-H).

^{13}C NMR (300 MHz, DMSO-d_6): δ = 173.66, 165.55 (CO-5, COOK), 75.78 (C-9), 72.01 (C-7), 71.48 (C-8), 66.08 (C-3), 61.15 (C-9a), 53.13 (C-6), 32.73 (C-2).

ESI-MS (CH_2Cl_2/MeOH+NH_4AC) (m/z): 278.8 $[M-H]^+$, 316.9 $[M-H+K]^+$.

Melting Point: Decompose at 200°C.

7.8. Compound 8: 9a(R)H-(6S)-tetra-butyloxycarbonylamino-5-oxo-(7R,8S,9R)-trihydroxy-octahydro-thiazolo [3,2-a]azepin-3R-carboxilicacid

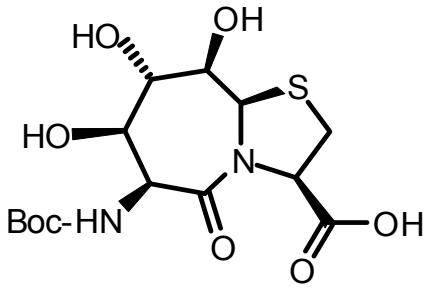

8

7.8.1. Procedure

Amine **7** (1.3 g, 4.67 mmol) was dissolved in water (20 mL), 1N Na_2CO_3 (9.0 mL, 9.02 mmol) was added into reaction mixture. Boc anhydride (1.18 g, 5.41 mmol) in 1,4-dioxane (20 mL) was added slowly into stirring mixture. The reaction mixture was stirred for 6 h at room temperature. Solvent was removed and **8** was purified by column chromatography (MeOH:CH_3Cl in the ratio of 2:8). Yield obtained was 1.5 g (3.9 mmol, 85%).

7.8.2. Analytical Data

^{1}H NMR (300 MHz, DMSO-d_6): δ = 7.17(s, 1H, OH), 6.49 (d, $^3J_{Boc\text{-}NH,6}$ = 8.23Hz, 1H, Boc-NH), 5.63 (s, 1H, OH), 5.48 (s, 1H, 9a-H), 5.12(s, 1H, OH), 4.74 (d, $^3J_{6\text{-}H,Boc\text{-}NH}$ = 8.51Hz, 1H, 6-H), 4.57 (t, $^3J_{3,2}$ = 6.59Hz, 1H, 3-H), 3.8 (d, $^3J_{8,9}$ = 3.84 Hz, 1H, 8-H), 3.68 (s, 1H, 7-H), 3.49 (s, 1H, 9-H), 3.21 (d, $^2J_{2\text{-}H}$ = 6.59Hz, 1H, 2-H), 3.15(d, $^2J_{2,3}$ = 4.94Hz, 1H, 2-H), 1.37 (s, 9H, t-butyl-CH_3).

^{13}C NMR (300 MHz, DMSO-d_6): δ = 174.51 (CO-5), 167.79 (COOH), 154.77 (Boc-CO), 78.05 (C-tbutyl$_{quart}$), 75.66 (C-9), 74.73 (C-7), 71.46 (C-8), 66.12 (C-3), 61.00 (C-9a), 53.52 (C-6), 32.48 (C-2), 28.05(3C, t-butyl).

ESI-MS (CH_2Cl_2/MeOH+NH_4AC) (m/z): 379 [M + H^+], 401 [M + Na]$^+$, 423.0 [M-H^+ + 2Na]$^+$.

Melting Point: Decompose at 210°C.

7.9. Compound 9: 9a(R)H-(6S)-Fmoc-amino-5-oxo-(7R,8S,9R)-trihydroxy-octahydro-thiazolo [3,2-a]azepin-3R-carboxilic acid.

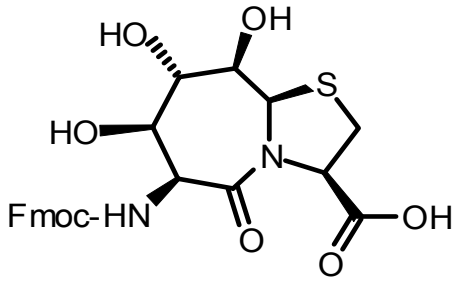

9

7.9.1. Procedure

Amine **7** (0.5 g, 1.7 mmol) was dissolved in water (20 mL), 1N $NaHCO_3$ (1.7 mL, 1.7 mmol) was added into reaction mixture. Fmoc-Cl (0.48 g, 1.88 mmol) in acetone (20 mL) was added slowly into stirring reaction mixture. Reaction mixture was stirred for 30 min. Reaction mixture was extracted three times with DCM. The solvent was removed and **10** were purified by column chromatography (MeOH:CH_3Cl in the ratio 2:8 and 2 drop acetic acid). Yield obtained was 0.35 g (0.71 mmol, 40%).

Alternatively, it was prepared as:

Fmoc protected amine **6** (0.50 g, 0.95 mmol) was dissolved in acetic acid (till amine was dissolved). 5M HCl (2 mL) was added into reaction mixture. The reaction mixture was stirred at room temperature for 5 days. The solvent was removed and **10** were purified by column chromatography (MeOH:CH_3Cl in the ratio 2:8 and 2 drop acetic acid). Yield obtained was 0.24 g (0.48 mmol, 50%).

7.9.2. Analytical Data

<u>^{1}H NMR (300 MHz, DMSO-d_6)</u>: δ = 7.88 (d, $^3J_{Fmoc\text{-}Ar}$ = 7.41 Hz, 2H, Fmoc-Ar), 7.72 (m, 2H, Fmoc-Ar), 7.40 (t, $^3J_{Fmoc\text{-}Ar}$ = 7.41Hz, 2H, Fmoc-Ar), 7.31 (t, $^3J_{Fmoc\text{-}Ar}$ = 7.41Hz, 2H, Fmoc-Ar), 5.74 (s, 1H, 8-OH), 5.47 (s, 1H, 9a-H), 4.81 (d, $^3J_{6,Fmoc\text{-}NH}$ = 8.78Hz, 1H, 6-H), 4.65 (t, $^3J_{3,2}$ = 7.4 Hz, 1H, 3-H), 4.24 (m, 2H, Fmoc α and β), 3.81 (s, 1H, 8-H), 3.57 (s, H, 7-H), 3.37 (s, 1H, 9H), 3.30 (m, 2H, 2-H).

<u>^{13}C NMR (300 MHz, DMSO-d_6):</u> δ = 171.87 (CO-5), 167.67 (COOH), 155.73 (Fmoc-CO), 143.68, 143.60, 140.54, 127.54, 127.02, 125.20, 119.98 (Fmoc-Ar), 76.37 (C-9), 74.40 (C-8),

70.66 (C-7), 65.76 (Fmoc-CH_2), 64.46 (C-6), 61.04 (C-3), 54.39 (C-9a), 46.42 (Fmoc-CH), 31.69 (C-2).

ESI-MS (CH_2Cl_2/MeOH+NH_4AC) (m/z): 501.2 $[M-H]^+$, 518.2 $[M+NH_4]^+$, 523.2 $[M+Na]^+$.

Melting Point: 180°C.

7.10. Compound 10: Boc-Bic-Tyr-OMe

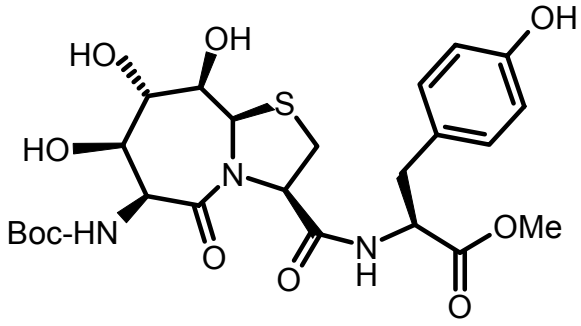

10

7.10.1. Procedure

Dipeptide **8** (0.20 g, 0.52 mmol) and Tyr methyl ester (0.09 g, 0.42 mmol) were dissolved in DMF (25 mL). Then HOBt (0.07 g, 0.52 mmol) and HBTU (0.20 g, 0.52 mmol) were added into reaction mixture and the pH of the reaction mixture was adjusted to 7-8 with DIPEA (0.09 mL). The reaction mixture was stirred for 6 h at room temperature. The solvent was removed and **9** was purified by flash chromatography ($CHCl_3$:MeOH in the ratio 4:1). Yield obtained was 0.36 g (0.66 mmol, 92%).

7.10.2. Analytical Data

^{1}H NMR (300 MHz, DMSO-d_6): δ = 9.20 (br, 1H, OH), 8.55 (d, $^3J_{Tyr\text{-}NH,Tyr\text{-}\alpha}$ = 7.37, Tyr-NH), 6.995 (d, $^3J_{Tyr\text{-}Ar}$ = 8.32Hz, 2H, Tyr-Ar), 6.64 (d, $^3J_{Tyr\text{-}Ar}$ = 8.56Hz, 2H, Tyr-Ar), 6.51 (d, $^3J_{Boc\text{-}NH,6}$ = 8.79Hz, 1H, Boc-NH), 5.55 (d, $^3J_{8\text{-}OH,8}$ = 3.33Hz, 1H, 8-OH), 5.44 (s, 1H, 9a-H), 5.4 (d, $^3J_{9\text{-}OH,9}$ = 9.27Hz, 1H, 9-OH), 5.03 (d, $^3J_{6\text{-}H}$ = 4.52Hz, 1H, 6-H), 4.73 (d, $^3J_{7OH,7}$ = 9.03Hz, 1H, 7-OH), 4.6 (t, $^3J_{3\text{-}H}$ = 7.58Hz, 1H, 3-H), 4.34 (qu, 1H, Tyr-α), 3.81 (d, $^3J_{8,9}$ = 3.57Hz, 1H, 8-H), 3.74 (t, $^3J_{7,6\text{ and }8}$ = 4.28Hz, 1H, 7-H), 3.55 (s, 1H, 9-H), 3.55 (s, 3H, Tyr-OMe), 3.21 (m, 1H, 2-H), 3.15 (m, 1H, 2H), 2.80 (d, $^3J_{Tyr\text{-}\beta,Tyr\text{-}\alpha}$ = 7.13 Hz, 2H, Tyr β), 1.38 (s, 9H, t-butyl-H).

^{13}C NMR (300 MHz, DMSO-d_6): δ = 171 (CO-NH), 170 (CO-5C), 168 (COOMe), 156 (Boc-CO), 155 (Try-Ar-PC), 130 (Tyr-Ar), 126.5 (Try-Ar), 115 (Tyr- Ar), 78 (Boc_{qut}), 77 (C-9), 74.8

(C-8), 71 (C-7), 65 (C-3), 61 (C-9a), 54 (C-6), 53.9 (Tyr-α), 51.5 (OMe), 36.9 (Tyr-β), 32.5 (C-2), 28 (t-butyl-CH_3).

ESI-MS (CH_2Cl_2/MeOH+NH_4AC) (m/z): 556 $[M-H]^+$, 573.2 $[M+NH_4]^+$, 574.2 $[M+Na]^+$.

Melting Point: 97°C.

7.11. Compound 11: Bic-Tyr-OMe

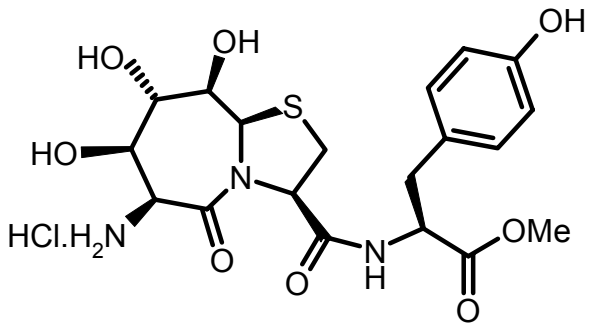

11

7.11.1. Procedure

Tetrapeptide **10** (0.10 g, 0.180 mmol) was treated with HCl (10 mL) in diethyl ether. The reaction mixture was stirred for 1 h at room temperature to yield the HCl salt of the free amine of **11**. Yield obtained was quantitative.

7.11.2. Analytical Data

^{1}H NMR (300 MHz, DMSO-d_6): δ = 9.33 (s, $NH_3^{+)}$, 8.66 (d, $^3J_{Tyr\text{-}NH,Tyr\text{-}\alpha}$ = 7.24Hz, 1H, Tyr-NH), 6.99 (d, $^3J_{Tyr\text{-}Ar}$ = 8.5Hz, 2H, Try-Ar), 6.66 (d, $^3J_{Tyr\text{-}Ar}$ = 8.54Hz, 2H, Try-Ar), 5.71 (s, 1H, 8-OH), 5.56 (d, $^3J_{9\text{-}OH,9}$ = 8.99Hz, 1H, 9-OH), 5.52 (s, 1H, 9a-H), 5.26 (s, 1H, 7-OH), 4.73 (t, $^3J_{3,2}$ = 7.4Hz, 1H, 3-H), 4.33 (q, $^3J_{Tyr\text{-}\alpha}$ = 7.15 Hz, 1H, Tyr α), 4.30 (s, 1H, 6-H), 3.52 (s, 3H, OMe), 3.59 (s_{br}, 2H, 8-H and 7-H), 3.59 (d, $^3J_{9,8}$ = 5.1 Hz, 1H, 9-H), 3.52 (s, 3H, Tyr-OMe), 3.22 (dd, $^2J_{2,2}$ = 11.0Hz and $^3J_{2,3}$ = 7.3Hz, 1H, 2-H), 3.13 (dd, $^2J_{2,2}$ = 11.05Hz and $^3J_{2,3}$ = 7.42 Hz, 1H, 2-H), 2.81 (dd, $^3J_{Tyr\text{-}\beta,Tyr\text{-}\alpha}$ = 6.96 Hz and $^3J_{Tyr\text{-}\beta,Tyr\text{-}\alpha}$ = 3.66 Hz, 2H, Tyr-β).

^{13}C NMR (300 MHz, DMSO-d_6): δ = 171.31 (CO-NH), 170.14 (CO-5C), 168.37 (COOMe), 156.09 (Tyr-Ar), 76.26 (C-9), 74.03 (C-8), 71.29 (C-7), 64.91 (C-6), 61.24 (C-9a), 54.24 (C-6), 53.37 (Tyr-α), 51.68 (OMe), 36.28 (Tyr-β), 32.30 (C-2).

ESI-MS (CH_2Cl_2/MeOH+NH_4AC) (m/z): 456 $[M-H]^+$, 911.4 $[2M+H]^+$.

Melting Point: Decompose at 190°C.

7.12. Compound 12: Bic-Tyr

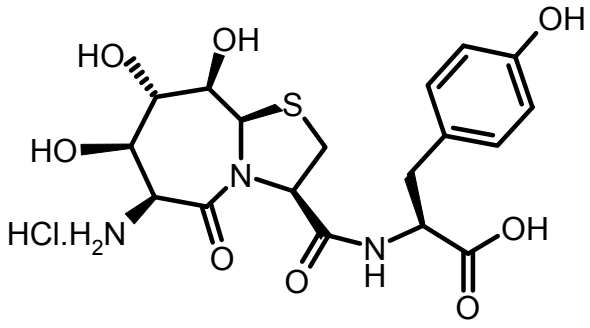

12

7.12.1. Procedure

Compound **11** (0.185 g, 0.49 mmol) was dissolved in minimum amount of H_2O (10 mL), 1N KOH (0.98 mL, 0.98 mmol) was added into reaction mixture. The reaction mixture was stirred for 7 h at room temperature. Reaction was monitored by TLC and stopped after 40 minute at room temperature with 1N HCl (0.49 mL). The solvent was removed, yield obtained was quantitative.

7.12.2. Analytical Data

^{1}H NMR (300 MHz, DMSO-d_6): δ = 8.62 (d, $^3J_{Tyr\text{-}NH,Tyr\text{-}\alpha}$ = 7.44 Hz, 1H, Tyr-NH), 7.04 (d, $^3J_{Tyr\text{-}Ar}$ = 8.3 Hz, 2H, Tyr-Ar), 6.67 (d, $^3J_{Tyr\text{-}Ar}$ = 8.5 Hz, 2H, Tyr-Ar), 5.59 (s, 1H, 9a-H), 4.78 (t, $^3J_{3,2}$ = 7.53 Hz, 1H, 3-H), 4.6 (q, $^3J_6$ = 5.3 Hz, 1H, 6-H), 4.29 (q, $^3J_{Tyr\text{-}\alpha,Tyr\text{-}\beta \text{ and NH}}$ = 6.84 Hz, 1H, Tyr-α), 3.93 (d, $^3J_{8,9}$ = 4.3 Hz, 1H, 8-H), 3.86 (t, $^3J_{7,6 \text{ and } 8}$ = 3.99 Hz, 1H, 7-H), 3.61 (d, $^3J_{9,8}$ = 3.2 Hz, 1H, 9-H), 3.26 (m, 1H, 2-H), 3.17 (m, 1H, 2-H), 2.87 (dd, $^2J_{Tyr\text{-}\beta,Tyr\text{-}\beta}$ = 13.98 Hz and $^3J_{Tyr\text{-}\beta,\ Tyr\text{-}\alpha}$ = 5.81 Hz, 1H, Tyr-β), 2.79 (dd, $^2J_{Tyr\text{-}\beta,Tyr\text{-}\beta}$ = 13.8 Hz and $^3J_{Tyr\text{-}\beta,Tyr\text{-}\alpha}$ = 7.3 Hz, 1H, Tyr-β).

^{13}C NMR (300 MHz, DMSO-d_6): δ = 172.00 (CO-NH), 170.00 (CO-5C), 165.32 (COOH), 159.09 (Tyr-Ar), 130.20 (Tyr-Ar), 126.98 (Tyr-Ar), 115.02 (Tyr-Ar), 76.63 (C-9), 71.75 (C-7), 71.01 (C-8), 64.67 (C-3), 61.34 (C-9a), 54.25 (Tyr-α), 53.25 (C-6), 36.07 (Tyr-β), 32.58 (C-2).

ESI-MS (CH_2Cl_2/MeOH+NH_4AC) (m/z): 442 $[M-H]^+$, 480 $[M+Na]^+$.

Melting Point: Decompose at 180°C.

7.13. Compound 13: Boc-Lys(Z)-Bic-Tyr-OMe

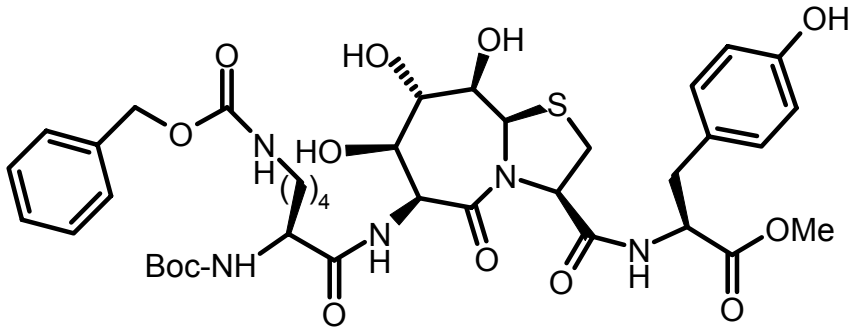

13

7.13.1. Procedure

The HCl salt of free amine **11** (0.59 g, 1.40 mmol) and Boc Lys (Z) (0.58 g, 1.54 mmol) were dissolved in DMF (15 mL). Then (1.02 g, 1.96 mmol) PyBOP was added into reaction mixture and the pH of the reaction mixture was adjust to 7-8 with DIPEA. The reaction mixture was stirred for 6 h at room temperature. The solvent was removed and **13** was purified by column chromatography ($CHCl_3$:MeOH in the ratio 4:1). Yield obtained was 0.859 g (1.03 mmol, 80%).

7.13.2. Analytical Data

^{1}H NMR (300 MHz, DMSO-d_6): δ = 8.59 (d, $^3J_{Tyr\text{-}NH,Tyr\text{-}\alpha}$ = 7.31 Hz, 1H, Tyr-NH), 7.84 (d, $^3J_{Bic\text{-}NH,6}$ = 8.10Hz, 1H, Bic-NH), 7.33 (m, 5H, Ar-z), 7.19 (t, $^3J_{Lys\text{-}NH\varepsilon,Lys\text{-}CH2}$ = 5.32 Hz, 1H, Lys-NHε), 6.98 (d, $^3J_{Tyr\text{-}Ar}$ = 8.26 Hz, 1H, Tyr-Ar), 6.94 (d, $^3J_{Lys\text{-}NH\alpha Lys\text{-}\alpha}$,= 8.26 Hz, 1H, Lys-NH-α), 6.64 (d, $^3J_{Tyr\text{-}Ar}$ = 8.42 Hz, 1H, Tyr Ar), 5.61 (d, $^3J_{8\text{-}OH,8}$ = 8.90 Hz, 1H, 8-OH), 5.56 (s_{br}, 1H, 9-OH), 5.48 (s, 1H, 9a-H), 5.06 (d, $^3J_{6,N\text{-}H}$= 8.4 Hz, 1H, 6-H), 5.04 (d, $^3J_{7\text{-}OH,7}$ = 6.6 Hz, 1H, 7-OH), 4.98 (s, 2H, CH_2), 4.70 (t, $^3J_{3,2}$ = 7.31 Hz, 1H, 3-H), 4.35 (q, $^3J_{Tyr\text{-}\alpha,Tyr\text{-}NH}$ = 7.15 Hz, 1H, Tyr-α), 3.89 (m, 1H, Lys-α), 3.82 (m, 1H, 8-H), 3.70 (m, 1H, 7-H), 3.59 (dd, $^3J_{9,9\text{-}OH}$ = 8.3 Hz and $^3J_{9,8}$ =2.9 Hz, 1H, 9-H), 3.51 (s, 3H, OMe), 3.22 (m, 1H, 2-H), 3.12 (m, 1H, 2-H), 2.95 (m, 1H, Lys-ε), 2.80 (d, $^3J_{Tyr\text{-}\beta,Tyr\text{-}\alpha}$= 6.99Hz, 1H, Tyr-β), 1.70 (m, 2H, Tyr-CH_2), 1.5 (m, 2H, Tyr-CH_2), 1.36 (s_{br}, 9H, t-butyl-CH_3), 1.3 (m, 2H, Tyr-CH_2).

^{13}C NMR (300 MHz, DMSO-d_6): δ = 173.32 (CO-HN: Lys-Bic), 171.28 (CO-NH: Tyr-Bic), 170.23 (CO-5C), 167.55 (COOMe), 156.01 (Boc-CO), 155.29 (Tyr-Ar), 142.81 (Z-Ar), 137.22 (Z-Ar), 130.00 (Tyr-Ar), 128.26 (Z-Ar), 127.64 (Z-Ar), 126.53 (Tyr-Ar), 5.01 (Tyr-Ar), 78.01 (C-t-butyl), 76.24 (C-9), 74.75 (C-7), 71.38 (C-8), 65.04 (CH_2-Z), 64.88 (C-3), 61.23 (C-9a), 54.41

(Tyr-α), 54.15 (Lys-α), 52.03 (C-6), 51.61 (C-OMe), 40.00 (Lys-ε), 36.37 (Tyr-β), 32.19 (C-2), 31.52 (Tyr-CH_2), 29.06 (Tyr-CH_2), 28.16 (t-butyl-CH_3), 22.78 (Tyr-CH_2).

ESI-MS (m/z): 840 $[M+Na]^+$, 856 $[M+K]^+$.

Melting Point: 96°C.

7.14. Compound 14: Boc-Lys(Z)-bic-Tyr

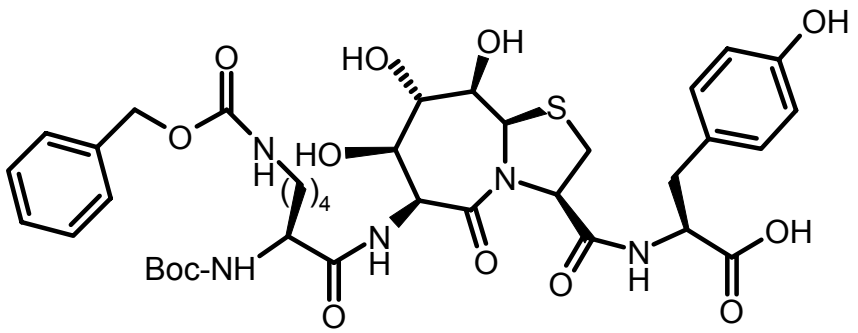

14

7.14.1. Procedure

Compound **13** (300 mg, 0.36 mmol) was dissolved in minimum amount of MeOH (10 mL). 1N KOH (0.73 mL, 0.73 mmol) was added into reaction mixture. The reaction mixture was stirred for 7 h at room temperature. Reaction was monitored by TLC and stopped with 1N HCl (0.36 mL). Then the solvent was removed, yield obtained was quantitative.

7.14.2. Analytical Data

^{1}H NMR (500 MHz, DMSO-*d*$_6$): δ = 9.22 (s, 1H, OH), 8.51 (d, $^3J_{Tyr\text{-}NH,Tyr\text{-}\alpha}$ = 7.38 Hz, 1H, Tyr-NH), 7.88 (d, $^3J_{Bic\text{-}NH,6}$ = 7.99 Hz, 1H, Bic-NH), 7.88 (m, 5H, Ar-Z), 7.19 (t, $^3J_{Lys\text{-}NH\varepsilon,Lys\text{-}CH2}$ = 4.99 Hz, 1H, Lys-NHε), 7.02 (d, $^3J_{Tyr\text{-}Ar}$ = 8.15 Hz, 2H, Tyr-Ar), 6.93 (d, $^3J_{Lys\text{-}NH\alpha,Lys\text{-}\alpha}$ = 8.15 Hz, 1H, Lys-NHα), 6.64 (d, $^3J_{Tyr\text{-}Ar}$ = 8.15 Hz, 2H, Tyr-Ar), 5.6 (d, $^3J_{8\text{-}OH,8}$ = 8.9 Hz, 1H, 8-OH), 5.59 (d, $^3J_{9\text{-}OH,9}$ = 3.3 Hz, 1H, 9-OH), 5.48 (s, 1H, 9a-H), 5.05 (d, $^3J_{6,Bic\text{-}NH}$ = 7.99Hz, 1H, 6-H), 4.98 (s, 2H, CH_2), 4.73 (t, $^3J_{3,2}$ = 7.22Hz, 1H, 3-H), 4.30 (q, $^3J_{Tyr\text{-}\alpha}$ = 6.81Hz, 1H, Tyr-α), 3.89 (m, 1H, Lys-α), 3.81 (d, $^3J_{8,9}$ = 3.2 Hz, 1H, 8-H), 3.68 (s_{br}, 1H, 7-H), 3.58 (d, $^3J_{9,8}$ = 5.8 Hz, 1H, 9-H), 3.22 (m, 1H, 2-H), 3.11 (m, 1H, 2-H), 2.95 (m, 1H, Lys-ε), 2.81 (m, 1H, Tyr-β), 1.65 (m, 2H, Lys-CH_2), 1.45 (m, 2H, Lys-CH_2), 1.36 (s, 11H, t-butyl-CH_3 and Lys-CH_2).

HMQC (500 MHz, DMSO-d_6): δ = 127.5 (Ar-Z), 130 (Tyr-Ar), 114.5 (Tyr-Ar), 60.5 (C-9a), 51.5 (C-6), 64.8 (CH_2-C), 64.5 (C-3), 53.8 (Tyr-α), 54.1 (Lys-α), 70.9 (C-8), 74.5 (C-7), 75.7 (C-9), 32.0 (C-2), 39.7 (Lys-ε), 35.8 (Tyr-β), 30.5 (Tyr-CH_2), 27.5 (t-butyl-CH_3 and Tyr-CH_2), 18.15 (Tyr-CH_2).

ESI-MS (m/z): 826 $[M+Na]^+$, 842 $[M+K]^+$.

Melting Point: Decompose at 195°C.

7.15. Compound 15: Lys(Z)-Bic-Tyr

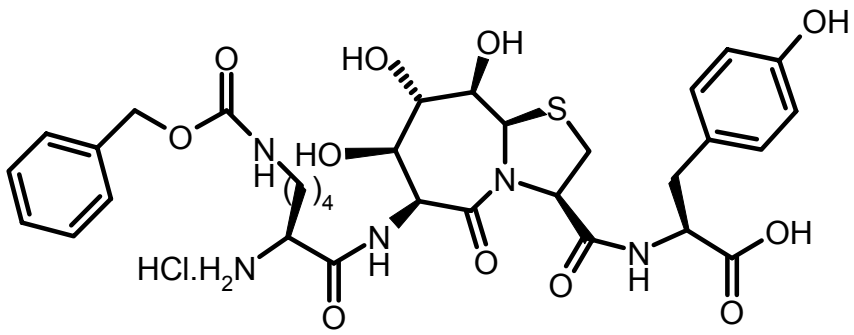

15

7.15.1. Procedure

Tetrapeptide **14** (200 mg) was treated with 10 mL HCl in diethyl ether. The reaction mixture was stirred for 40 min at room temperature to yield the HCl salt of the free amine of **15**. Yield obtained was quantitative.

7.15.2. Analytical Data

^{1}H NMR (500 MHz, DMSO-d_6): δ = 9.25 (s, 1H, OH), 8.83 (d, $^3J_{Bic\text{-}NH,6}$ = 8.41Hz, 1H, Bic-NH), 8.54 (d, $^3J_{Tyr\text{-}NH,Tyr\text{-}\alpha}$ = 7.71Hz, 1H, Tyr-NH), 8.21 (d, $^3J_{NH3+,Lys\text{-}\alpha}$ = 4.56 Hz, 3H, Lys-NH_3^+), 7.32 (m, 5H, Ar-H), 7.17 (t, $^3J_{Lys\text{-}NH\varepsilon,Lys\text{-}CH2}$ = 5.26 Hz, 1H, Lys-NHε), 7.02 (d, $^3J_{Tyr\text{-}Ar}$ = 8.0 Hz, 2H, Tyr-Ar), 6.65 (d,$^3J_{Tyr–Ar}$ = 8.06 Hz, 1H, Tyr–Ar), 5.72 (m**,** 2H, 8 and 9- OH), 5.49 (s, 1H, 9a-H), 5.12 (d, $^3J_{6\text{-}H,NH}$ = 8.4 Hz, 1H, 6-H), 5.0 (s, 1H, 7-OH), 4.98 (s, 2H, CH_2-Z), 4.76 (t, $^3J_{3,2}$ = 7.19 Hz, 1H, 3-H), 4.30 (q, $^3J_{Tyr\text{-}\alpha,Tyr\text{-}\beta \text{ and NH}}$ = 6.8 Hz, 1H, Tyr-α), 3.85 (s_{br}, 2H, Lys-α and 8-H), 3.75 (s_{br}, 1H, 7-H), 3.62 (s_{br}, 1H, 9-H), 3.23 (m, 1H, 2-H), 3.11 (m, 1H, 2-H), 2.96 (m, 1H, Lys-ε), 2.81 (m, 1H, Tyr-β), 1.72 (m, 1H, Lys-CH_2), 1.58 (m, 1H, Lys-CH_2), 1.38 (m, 1H, Lys-CH_2).

HMQC (500 MHz, DMSO-d_6):δ = 127.5 (Ar-Z), 129.8 (Tyr-Ar), 114.8 (Tyr-Ar), 61.0 (C-9a), 52.1 (C-6), 54.82 (C-CH_2), 64.5 (C-3), 53.8 (Tyr-α), 51.5 (Lys-α), 70.7 (C-8), 74.4 (C-7),

75.8 (C-9), 31.85 (C-2), 39.6 (Tyr-β), 36.2 (Lys-ε), 30.1 (Lys-CH_2), 28.6 (Lys-CH_2), 22 (Lys-CH_2).

ESI-MS (m/z): 704 $[M-H]^+$, 726 $[M+Na]^+$, 742 $[M+K]^+$.

Melting Point: Decompose at 280°C.

7.16. Compound 16: Lys-Bic-Tyr

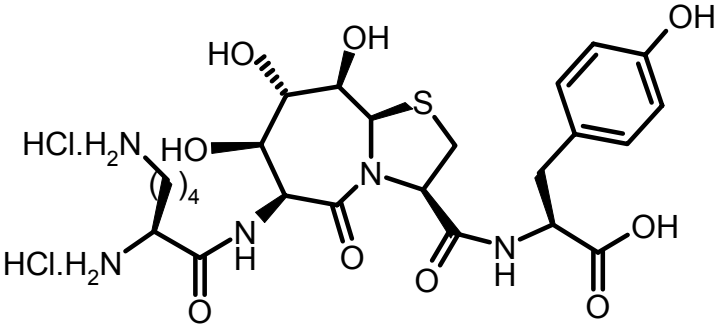

16

7.16.1. Procedure

Compound **15** (30 mg, 0.042 mmol) was dissolved in MeOH (5 mL). Pd/C (10 mg) was added into reaction mixture. The reaction mixture was stirred for 2 h at room temperature under H_2 atmosphere. Reaction was monitored by TLC. Solvent was removed, yield obtained was quantitative.

7.16.2. Analytical Data

^{1}H NMR (500 MHz, DMSO-d_6): δ = 9.32 (s, 1H, OH), 8.90 (d, $^3J_{Bic\text{-}NH,6}$ =7.22 Hz, 1H, Bic-NH) 8.60 (d, $^3J_{Tyr\text{-}NH,Tyr\text{-}\alpha}$ = 7.7 Hz, 1H, Tyr-NH), 8.31 (s_{br}, 3H, NH_3^+), 8.04 (s_{br}, 3H, NH_3^+), 7.03(d, $^3J_{Tyr\text{-}Ar}$ = 7.99 Hz, 1H, Tyr-Ar), 6.67 (d, $^3J_{Tyr\text{-}Ar}$ = 8.15 Hz, 1H, Tyr-Ar), 5.73 (d, $^3J_{8\text{-}OH,8}$ = 8.9 Hz, 1H, 8-OH), 5.49 (s, 1H, 9a-H), 5.10 (d, $^3J_{6,NH}$ = 8.15 Hz, 1H, 6-H), 4.76 (t, $^3J_{3,2}$ = 7.22 Hz, 1H, 3-H), 4.29 (q, $^3J_{Tyr\text{-}\alpha,NH\ and\ Tyr\text{-}\beta}$ = 6.87 Hz, 1H, Tyr-α), 3.85 (s_{br}, 2H, Lys-α and 8-H), 3.79 (s_{br}, 1H, 7-H), 3.6 (d, $^3J_{9,8}$ = 5.99 Hz, 1H, 9-H), 3.24 (m, 1H, 2-H), 3.12 (m, 1H, 2-H), 2.85 (dd, $^2J_{Tyr\text{-}\beta,Tyr\text{-}\beta}$ = 13.68 Hz and $^3J_{Tyr\text{-}\beta Tyr\text{-}\alpha}$= 6.15 Hz, 1H, Tyr-β), 2.78 (dd, $^2J_{Tyr\text{-}\beta Tyr\text{-}\beta}$ = 14.15 Hz and $^3J_{Tyr\text{-}\beta,Tyr\text{-}\alpha}$ = 7.5 Hz, 1H, Tyr-β), 2.73 (s_{br}, 2H, Lys-ε), 1.76 (m, 2H, Lys-CH_2), 1.58 (m, 2H, Lys-CH_2), 1.45 (m, 2H, Lys-CH_2).

^{13}C NMR (500 MHz, DMSO-d_6): δ = 172.29 (CO-NH), 170.33 (CO-5C), 167.84 (COOH), 167.19 (CO-NH), 155.99 (Tyr-Ar), 130.11 (Tyr-Ar), 126.98 (Tyr-Ar), 114.96 (Tyr-Ar), 76.24 (C-9),

74.47 (C-7), 71.08 (C-8), 64.8 (C-3), 61.18 (C-9a), 54.18 (Tyr-α), 52.56 (C-6), 51.62 (Lys-α), 38.21 (Tyr-β), 3619 (Lys-ε), 32.22 (C-2), 30.28 (Lys-CH_2), 26.13 (Lys-CH_2), 20.82 (Lys-CH_2).
ESI-MS (m/z): 570 $[M-H]^+$.
Melting Point: Decompose at 210°C.

7.17. Compound 17: Boc-DOPA-Bic-Tyr-OMe

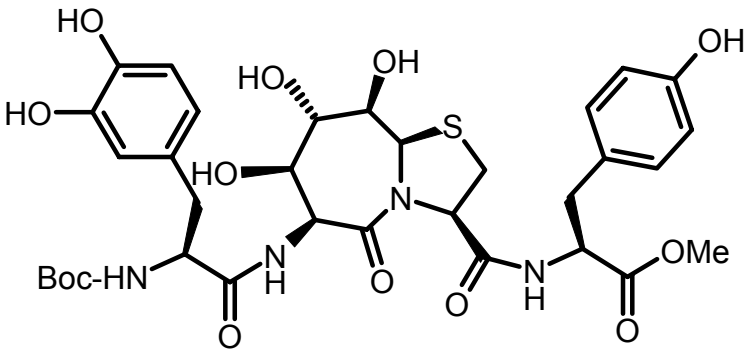

17

7.17.1. Procedure

The HCl salt of the free amine **11** (0.150 g, 0.32 mmol) and Boc-DOPA (0.117 g, 0.39 mmol) were dissolved in DMF (15 mL). HOBt (0.053 g, 0.39 mmol) and HBTU (0.149 g, 0.39 mmol) were added and the pH of the reaction mixture was adjusted to 7-8 with DIPEA. The reaction mixture was stirred for 6 h at room temperature. The solvent was removed and **17** was purified by column chromatography (CHCl3:MeOH as 4:1). Yield obtained was 0.191 g (0.26 mmol, 79%).

7.17.2. Analytical Data

^{1}H NMR (500 MHz, DMSO-d_6): δ = 8.62 (d, $^3J_{Tyr\text{-}NH,Tyr\text{-}\alpha}$ = 7.08 Hz, 1H, Tyr-NH), 8.01 (d, $^3J_{Bic\text{-}NH,6}$ = 8.3 Hz, 1H, Bic-NH), 6.98 (d,$^3J_{Tyr\text{-}Ar}$ = 8.54 Hz, 1H, Tyr-Ar), 6.90 (d, $^3J_{DOPA\text{-}Ar}$ = 8.54 Hz, 1H, DOPA-Ar), 6.63 (d, $^3J_{Tyr\text{-}Ar}$ = 8.30 Hz, 1H, Tyr-Ar), 6.58 (d, $^3J_{DOPA\text{-}Ar}$ = 7.81 Hz, 1H, DOPA-Ar), 6.49 (dd, $^3J_{DOPA\text{-}Ar}$ = 8.05 Hz and $^3J_{DOPA\text{-}Ar}$ = 1.95 Hz, 1H, Dopa-Ar), 5.63 (d, $^3J_{8\text{-}OH,8}$ = 9.03 Hz, 1H, 8-OH), 5.50 (s_{br}, 1H, 9a-H), 5.09 (s_{br}, 1H, 6-H), 5.07 (d, $^3J_{7\text{-}OH,7}$ = 4.15 Hz, 7-OH), 4.70 (t, $^3J_{3,2}$ = 7.44 Hz, 1H, 3-H), 4.34 (q, $^3J_{Tyr\text{-}\alpha,NH\ and\ Tyr\text{-}\beta}$= 699 Hz, 1H, Tyr-α), 4.07 (m, 1H, DOPA-α), 3.83 (m, 1H, 8-H), 3.73 (m, 1H, 7-H), 3.60 (dd, 1H, $^3J_{9,9\text{-}OH}$ = 8.78 Hz, and $^3J_{9,8}$ = 3.4 Hz, 9-H), 3.51 (s, 3H, OMe), 3.23 (dd, $^2J_{2,2}$ = 11.23 and $^3J_{2,3}$ = 7.31 Hz, 1H, 2-H), 3.13 (dd, $^2J_{2,2}$ = 11.10 Hz and $^3J_{2,3}$ = 7.4 Hz, 1H, 2-H), 2.89 (dd, $^2J_{DOPA\text{-}\beta,DOPA\text{-}\beta}$ = 13.91 Hz and $^3J_{DOPA\text{-}}$

$_{\beta,DOPA-\alpha}$ = 2.92 Hz, 2H, DOPA-β), 2.80 (d, $^3J_{Tyr\beta,Tyr\alpha}$ = 7.08 Hz, 2H, Tyr-β), 1.29 (s, 9H, t-butyl-CH_3).

^{13}C NMR (500 MHz, DMSO-d_6): δ = 171.32, 171.16 (CO-NH), 170.29 (CO-5C), 167.57 (COOMe), 156.04 (Boc-CO), 155.17 (Tyr-Ar), 144.74, 143.547 (DOPA-Ar), 130.03 (Tyr-Ar), 129.05 (DOPA-Ar), 126.53 (Tyr-Ar), 119.80 (DOPA-Ar), 116. 57 (DOPA-Ar), 115.95 (DOPA-Ar), 115.04 (Tyr-Ar), 78.01 (t-butyl-quat), 76.30 (C-9), 74. 74 (C-7), 71. 41 (C-8), 64.91 (C-3), 61.26 (C-9a), 56.16 (DOPA-α), 54.20 (Tyr-α), 52.17 (C-6), 51.64 (OMe), 36.81 (DOPA-β), 36.38 (Tyr-β), 32.22 (C-2), 28.14 (t-butyl-CH_3).

ESI-MS (m/z): 735 $[M+H]^+$, 757 $[M+Na]^+$, 773 $[M+K]^+$.

Melting Point: 185°C.

7.18. Compound 18: DOPA-BiC-Tyr-OMe

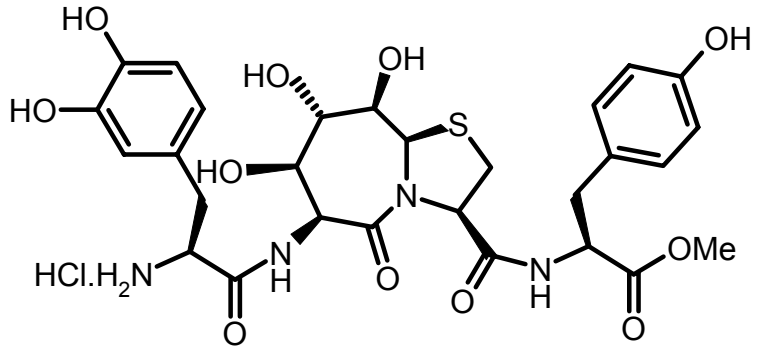

18

7.18.1. Procedure

Tetrapeptide **17** (275 mg) was treated with HCl (20 mL) in diethyl ether. The reaction mixture was stirred for 1 h at room temperature to yield the HCl salt of the free amine of **18**. Yield obtained was quantitative.

7.18.2. Analytical Data

^{1}H NMR (500 MHz, DMSO-d_6): δ = 8.99 (d, $^3J_{Bic-NH,6}$ = 7.10 Hz, 1H, Bic-NH), 8.65 (d, $^3J_{Tyr-NH,Tyr-\alpha}$ = 8.01 Hz, 1H, Tyr-NH), 7.98 (s, 3H, NH_3^+), 6.98 (d, $^3J_{Tyr-Ar}$ = 8.47 Hz, 1H, Tyr-Ar), 6.63 (d, $^3J_{Tyr-Ar}$ = 8.24 Hz, 2H, Tyr-Ar), 6.71 (d, $^3J_{DOPA-Ar}$ = 2.06Hz, 1H, DOPA-Ar), 6.66 (d, $^3J_{DOPA-Ar}$ = 8.01 Hz, 1H, DOPA-Ar), 6.63 (d, $^3J_{Tyr-Ar}$ = 8.47 Hz, 2H, Tyr-Ar), 6.58 (dd, $^3J_{DOPA-Ar}$ = 8.01 Hz and $^3J_{DOPA-Ar}$ = 2.06 Hz 1H, DOPA-Ar), 5.51 (s, 1H, 9a-H), 5.11 (d, $^3J_{6,NH}$ = 8.4 Hz, 1H, 6-H), 4.74 (t, $^3J_{3,2}$ = 7.33 Hz, 1H, 3-H), 4.33 (q, $^3J_{Tyr-\alpha,NH\ and\ Tyr-\beta}$= 7.10 Hz, 1H, Tyr-

α), 4.03 (m, 1H, DOPA-α), 3.87 (t, $^3J_{8,9}$ = 4.12 Hz, 1H, 8-H), 3.78 (d, 1H, $^3J_{7,8}$ = 4.35Hz, 7-H), 3.64 (d, $^3J_{9,8}$ = 3.66 Hz, 1H, 9-H), 3.51 (s, 3H, OMe), 3.25 (m, 1H, 2-H), 3.08 (m, 3H, 2-H and DOPA–β), 2.80 (d, $^3J_{Tyr\text{-}\beta,Tyr\text{-}\alpha}$= 7.1 Hz, 2H, Tyr-β).

HMQC (500 MHz, DMSO-*d*$_6$): δ = 129.8 (Tyr-Ar), 116.7 (DOPA-Ar), 114.6 (Tyr-Ar), 120.1 (DOPA-Ar), 120.2 (DOPA-Ar), 61 (C-9a), 52.2 (C-6), 64.3 (C-3), 54.1 (Tyr-α), 53.3 (DOPA-α), 71.1 (C-8), 74.3 (C-7), 76. 1(C-9), 51.4 (OMe), 32 (C-2), 35.8 (DOPA-β), 36.2 (Tyr-β).

ESI-MS (m/z): 635 $[M+H]^+$, 657 $[M+Na]^+$, 673 $[M+K]^+$,

Melting Point: 245°C.

7.19. Compound 19: Boc-DOPA-Tyr-OMe

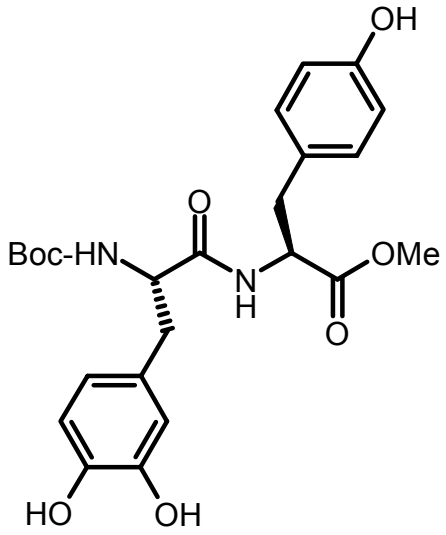

19

7.19.1. Procedure

Boc-DOPA (1.53 g, 5.17 mmol) and Tyr methyl ester (1 g, 4.3 mmol) were dissolved in DMF (20 mL). Then HOBt (0.69 g, 5.17 mmol) and HBTU (1.96 g, 5.17 mmol) were added and pH of the reaction mixture was adjusted to 7-8 with DIPEA. The reaction mixture was stirred for 6 h at room temperature. The solvent was removed and **19** was purified by column chromatography ($CHCl_3$:MeOH as 4:1). Yield obtained was 2.26 g (4.79 mmol, 93%).

7.19.2. Analytical Data

^{1}H NMR (500 MHz, DMSO-*d*$_6$): δ = 9.19 (s, 1H, OH), 8.10 (d, $^3J_{Tyr\text{-}NH,Tyr\text{-}\alpha}$ = 7.54Hz, 1H, Tyr-NH), 6.977 (d, $^3J_{Tyr\text{-}Ar}$ = 8.20 Hz, 2H, Tyr-Ar), 6.70 (d, $^3J_{DOPA\text{-}Ar}$ = 8.64Hz, 1H, DOPA-Ar), 6.64 (d, $^3J_{Tyr\text{-}Ar}$ = 8.4 Hz, 2H, Tyr-Ar), 6.57 (d, $^3J_{DOPA\text{-}Ar}$ = 7.98Hz, 1H, DOPA-Ar), 6.43 (dd,

$^3J_{DOPA\text{-}Ar}$ = 7.9Hz and $^3J_{DOPA\text{-}Ar}$ = 1.99Hz, 1H, DOPA-Ar), 4.39 (q, $^3J_{Tyr\text{-}\alpha,NH\ and\ Tyr\text{-}\beta}$ = 7.17 Hz, 1H, Tyr-α), 4.04 (m, 1H, DOPA-α), 3.55 (s, 1H, OMe), 2.85 (m, 2H, Tyr-β), 2.69 (dd, $^2J_{DOPA\text{-}\beta,DOPA\text{-}\beta}$ = 13.5 Hz and $^3J_{DOPA\text{-}\beta,DOPA\text{-}\alpha}$ = 3.32 Hz, 2H, DOPA-β), 1.29 (s, 3H, t-butyl-CH_3).

^{13}C NMR (500 MHz, DMSO-d_6): δ = 171.93, 171.89 (CO-NH, COMe), 156.01 (Tyr-Ar), 155.10 (Boc-CO), 144.73,143.61 (DOPA-Ar), 130.03 (Tyr-Ar), 128.78 (DOPA-Ar), 126.89 (Tyr-Ar), 119.89, 116.61, 115.03 (DOPA-Ar), 115.03 (Tyr-Ar), 78.00 (t-butyl-quart), 55.92 (DOPA-α), 53.75 (Tyr-α), 51.74 (OMe), 36.79 (DOPA-β), 36.09 (Tyr-β), 28.13 (3C, t-butyl-CH_3).

ESI-MS (m/z): 473.2 $[M\text{-}H^+]^-$; 947.5 $[2M\text{-}H^+]^-$.

Melting Point: 118°C.

7.20. Compound 20: DOPA-Tyr-OMe

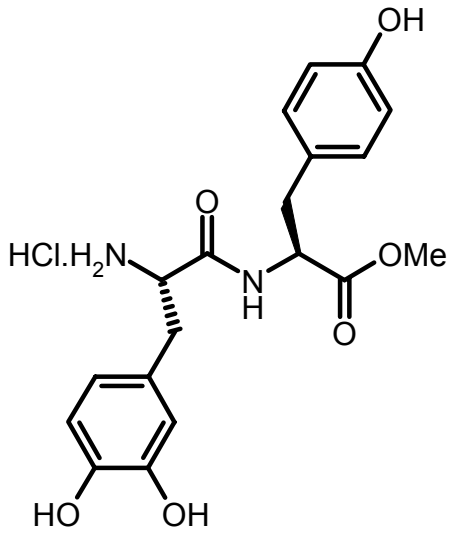

20

7.20.1. Procedure

Dipeptide **14** (1.6 g, 3.38 mmol) was treated with HCl (20 mL) in diethyl ether. The reaction mixture was stirred for 1 h at room temperature to yield the HCl salt of the free amine of **15**. Yield obtained was quantitative.

7.20.2. Analytical Data

^{1}H NMR (500 MHz, DMSO-d_6): δ = 9.31 (s, 1H, OH), 8.96 (d, $^3J_{Tyr\text{-}NH,Tyr\text{-}\alpha}$ = 7.78 Hz, 1H, Tyr-NH), 8.07 (d, $^3J_{NH3,DOPA\text{-}\alpha}$ = 8.07 Hz, 3H, NH_3^+), 7.00 (d, $^3J_{Tyr\text{-}Ar}$ = 8.69 Hz, 2H, Tyr-Ar), 6.67 (d, $^3J_{Tyr\text{-}Ar}$ = 8.54 Hz, 2H, Tyr-Ar), 6.675 (d, $^3J_{DOPA\text{-}Ar}$ = 4.57Hz, 1H, DOPA-Ar), 6.65 (d, $^3J_{DOPA\text{-}Ar}$ = 8.08 Hz, 1H, DOPA-Ar), 6.50 (dd, $^3J_{DOPA\text{-}Ar}$ = 8.01 Hz and $^3J_{DOPA\text{-}Ar}$ = 2.21 Hz, 1H,

DOPA-Ar), 4.44 (q, $^{3}J_{Tyr-\alpha, NH\ and\ Tyr-\beta}$ = 7.22 Hz, 1H, Tyr-α), 3.89 (m, 1H, DOPA-α), 3.58 (s, 3H, OMe), 3.2 (m, 1H, DOPA-β), 2.92 (m, 2H, Tyr-β), 2.82 (m, 1H, DOPA-β).

^{13}C NMR (500 MHz, DMSO-d_6): δ = 171.21, 168.24 (CO-NH, COMe), 156.14 (Tyr-Ar), 145.17,144.51 (DOPA-Ar), 129.98 (Tyr-Ar), 126.61 (DOPA-Ar), 125.29 (Tyr-Ar), 120.30, 116.96, 115.14 (DOPA-Ar), 115.14 (Tyr-Ar), 54.16 (Tyr-α), 53.48 (DOPA-α), 51.91 (OMe), 36.31 (Tyr-β), 35.95 (DOPA-β).

ESI-MS (m/z): 375 $[M + H]^+$, 397 $[M + Na]^+$.

Melting Point: 82°C.

7.21. Compound 21: Boc-Bic-DOPA-Tyr-OMe

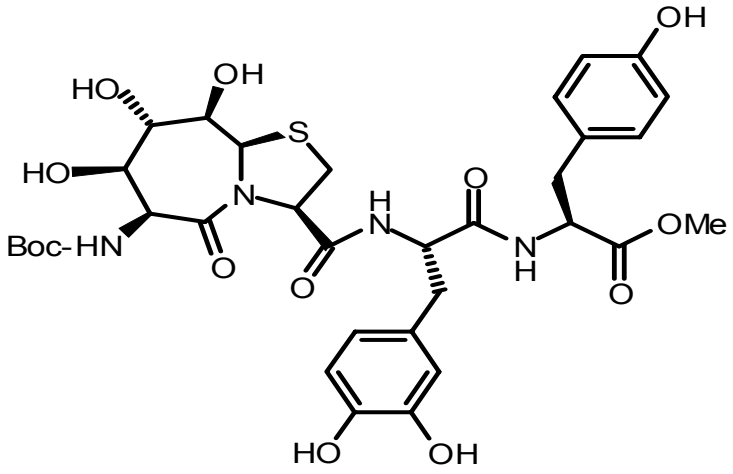

21

7.21.1. Procedure

The HCl salt of free amine **20** (0.30 g, 0.73 mmol) and Boc-Bic (0.30 g, 0.80 mmol) was dissolved in DMF (30 mL). HOBt (0.10 g, 0.80 mmol) and HBTU (0.30 g, 0.80 mmol) were added and the pH of the reaction mixture was adjusted to 7-8 with DIPEA. The reaction mixture was stirred for 6 h at room temperature. Solvent was removed and **21** was purified by column chromatography ($CHCl_3$:MeOH as 4:1). Yield obtained was 0.47 g (0.64 mmol, 80%).

7.21.2. Analytical Data

^{1}H NMR (400 MHz, DMSO-d_6): δ = 8.18 (d, $^{3}J_{DOPA-NH,DOPA-\alpha}$ = 8.45Hz, 1H, DOPA-NH), 7.74 (d, $^{3}J_{Tyr-NH,Tyr-\alpha}$ = 7.83Hz, 1H, Tyr-NH), 6.98 (d, $^{3}J_{Tyr-Ar}$ = 8.63Hz, 2H, Tyr-Ar), 6.65 (d, $^{3}J_{Tyr-Ar}$ = 8.51Hz, 2H, Tyr-Ar), 6.58 (m, 2H, DOPA-Ar), 6.44 (m, 2H, DOPA–Ar and Bic-NH), 6.01 (d, $^{3}J_{8-OH,8}$ = 6.66Hz, 1H, 8-OH), 5.55 (s, 1H, 7-OH), 5.48 (s,1H, 9a-H), 4.81 (d, $^{3}J_{6,Bic-NH}$ = 8.45Hz,

1H, 6-H), 4.44 (t, $^3J_{3,2}$ = 8.4Hz, 1H, 3-H), 4.2 (m, 2H, Tyr-α and DOPA-α), 3.85 (s, 2H, 7-H and 8-H), 3.70 (s, 1H, 9-H), 3.45 (s, 3H, OMe), 3.14 (d, $^3J_{2,3}$ = 8.86 Hz, 2H, 2-H), 2.94 (m, 2H, DOPA-β), 2.84 (m, 2H, Tyr-β), 1.267 (s, 9H, t-butyl-CH_3).

^{13}C NMR (400 MHz, DMSO-d_6): δ = 171.59 (CO-5C), 170.57 (Tyr-CONH), 169.51 (DOPA-CONH), 169.07 (COOMe), 155.97 (Boc-CO), 154.91, 130.09, 126.93, 114.99 (Tyr-Ar), 144.88, 143.63, 129.00, 119.81, 115.26, 116.14 (DOPA-Ar), 78.18 (t-butyl-quart), 77.27 (C-9), 74.69 (C-8), 71.83 (C-7), 66.46 (C-3), 61.48 (C-9a), 54.83 (DOPA-α), 54.77 (Tyr-α), 53.78 (C-6), 51.43 (OMe), 36.79 (DOPA-β), 36.41 (C-Tyr-β), 32.32 (C-2), 27.96 (t-butyl-3 CH_3).

ESI-MS (m/z): 735.2 $[M-H]^+$, 752 $[M+NH_4]^+$, 757.2 $[M+Na]^+$.

Melting Point: 154°C.

7.22. Compound 22: Boc-Lys(Z)-DOPA-Tyr-OMe

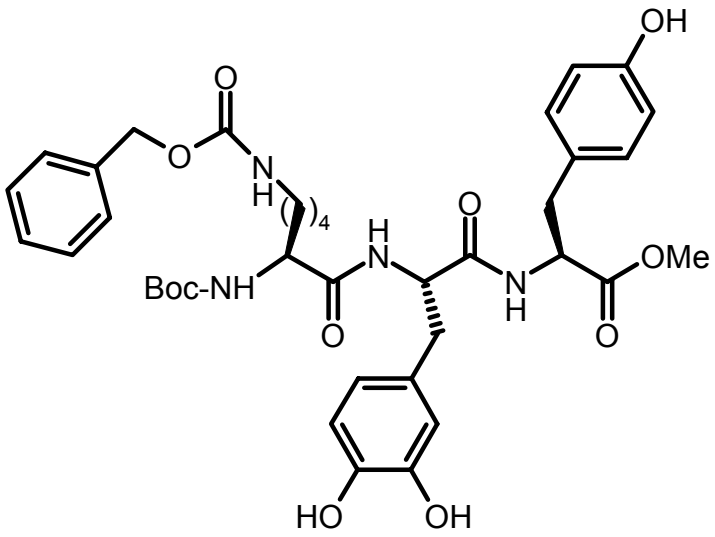

22

7.22.1. Procedure

The HCl salt of free amine **20** (0.59 g, 1.57 mmol) and Boc(Z)Lys (0.50 g, 1.31 mmol) were dissolved in DMF (20 mL). HOBt (0.21 g, 1.57 mmol) and HBTU (0.59 g, 1.57 mmol) were added and the pH of the reaction mixture was adjusted to 7-8 with DIPEA. The reaction mixture was stirred for 7 h at room temperature. The solvent was removed and **22** was purified by column chromatography ($CHCl_3$:MeOH in the ratio 4:1). Yield obtained was 0.99 g (1.26 mmol, 80%).

7.22.2. Analytical Data

^{1}H NMR (500 MHz, DMSO-d_6): δ = 8.29 (d, $^3J_{Tyr\text{-}NH,Tyr\text{-}\alpha}$= 7.8Hz,1H, Tyr-NH), 7.73 (d, $^3J_{DOPA\text{-}NH\text{-}DOPA\text{-}\alpha}$= 7.57 Hz, 1H, DOPA-Ar), 6.85 (d, $^3J_{Lys\text{-}\alpha,NH}$ = 8.36Hz, 1H, Lys-α,NH), 6.78 (d, $^3J_{DOPA\text{-}Ar}$ = 8.36Hz, 2H, DOPA-Ar), 6.64 (m, 2H, DOPA-Ar), 6.62 (d, $^3J_{Tyr\text{-}Ar}$= 6.62 Hz, 2H, Tyr-Ar), 6.29(dd, $^3J_{DOPA\text{-}Ar}$ = 5.2 Hz and $J_{DOPA\text{-}Ar}$ = 1.82Hz, 1H, DOPA-Ar), 4.98 (s, 2H, CH_2-Z), 4.43 (s, 1H, DOPA-α), 4.31 (q, $^3J_{Tyr\text{-}\alpha,\ NH\ and\ Tyr\text{-}\beta}$= 7.05 Hz, 1H, Tyr-α), 3.80 (s, 1H, Lys-α), 3.52 (s, 3H, OMe), 2.96 (s, 2H, Lys-ε), 2.92 (m, 2H, DOPA-β), 2.82 (s, 2H, Tyr-β), 1.46 (s, 2H, Lys-CH_2), 1.34 (s, 3H, t-butyl-CH_3), 1.22 (s, 2H, Lys-CH_2), 1.12 (s, 2H, Lys-CH_2).

HMQC-NMR (500 MHz, DMSO-d_6): δ = 127.8 (C-Z), 115.19, 130.2 (C-Tyr-Ar), 118.55, 121.04, 123.54 (DOPA-Ar), 64.7 (CH_2-Z), 53.0 (DOPA-α), 53.6 (Tyr-α), 54.0 (Lys-α), 51.1 (OMe), 35.5 (Lys-ε), 39.7 (DOPA-β), 35.8 (Tyr-β), 30.9 (Lys-CH_2), 27.7 (t-butyl-3 CH_3), 22.0 (Lys-CH_2), 23.4 (Lys-CH_2).

ESI-MS (m/z): 830 [M+K]$^+$.

Melting Point: 88°C.

7.23. Compound 23: Lys(Z)-DOPA-Tyr-OMe

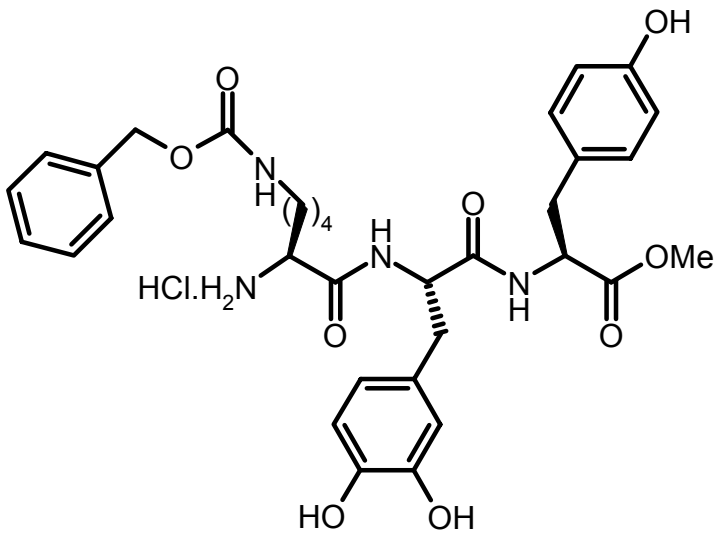

23

7.23.1. Procedure

Tetrapeptide **22** (0.20 g, 0.25 mmol) was treated with HCl (10 mL) in diethyl ether. The reaction mixture was stirred for 40 minute at room temperature to yield the HCl salt of the free amine of **23**. Yield obtained was quantitative.

7.23.2. Analytical Data

^{1}H NMR (500 MHz, DMSO-d_6): δ = 7.32 (m, 5H, Z), 6.96 (d, $^3J_{Tyr-Ar}$ = 8.2 Hz, 2H, Tyr-Ar), 6.69 (m, 1H, DOPA-Ar), 6.64 (d, $^3J_{Tyr-Ar}$ = 8.50 Hz, 2H, Tyr-Ar), 6.60 (d, $^3J_{DOPA-Ar}$ = 7.99 Hz, 1H, DOPA-Ar), 6.49 (dd, $^3J_{DOPA-Ar}$ = 7.9 Hz and $^3J_{DOPA-Ar}$ = 2.31 Hz, 1H, DOPA-Ar), 4.98 (s, 2H, CH_2-Ar), 4.47 (m, 1H, DOPA-α), 4.38 (m, 1H, Tyr-α), 3.67 (m, 1H, Lys-α), 3.55 (s, 3H, OMe), 2.95 (DOPA-β), 2.86 (Tyr-β), 2.71 (Lys-ε), 1.66 (Lys-CH_2), 1.36 (Lys-CH_2), 1.3 (Lys-CH_2).
^{13}C NMR (500 MHz, DMSO-d_6): δ = 128.0 (C-Z), 130.0 (Tyr-Ar), 119.9 (DOPA-Ar), 117.0 (DOPA-Ar), 114.7 (Tyr-Ar), 114.8 (DOPA-Ar), 65.0 (CH_2-Ar), 54.4 (DOPA-α), 53.9 (Tyr-α), 51.9 (Lys-α), 51.7 (OMe), 39.9 (DOPA-β), 38.0 (Lys-ε), 35.1 (Tyr-β), 30.2 (Lys-CH_2), 28.4 (Lys-CH_2), 21.0 (Lys-CH_2).
ESI-MS (m/z): 637 $[M-H]^+$, 659 $[M+Na]^+$.
Melting Point: 128°C.

7.24. Compound 24: Lys-DOPA-Tyr-OMe

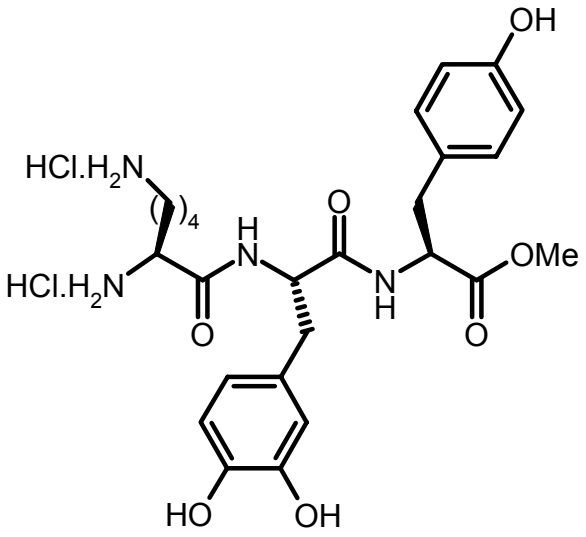

24

7.24.1. Procedure

Compound **23** (30 mg, 0.047 mmol) was dissolved in MeOH. Pd/C (10 mg) was added into reaction mixture. The reaction mixture was stirred for 3 h at room temperature under H_2 atmosphere. Reaction was monitored by TLC. Solvent was removed, yield obtained was quantitative.

7.24.2. Analytical Data

^{1}H NMR (500 MHz, DMSO-d_6): δ = 8.68 (d, $^3J_{DOPA\text{-}NH,DOPA\text{-}\alpha}$ = 8.25 Hz, 1H, DOPA-NH), 8.53 (d, $^3J_{Tyr\text{-}NH,Tyr\text{-}\alpha}$ = 7.70 Hz, 1H, NH), 8.23 (s_{br}, 2H, NH_3^+, Lys-ε), 8.05 (sbr, 2H, NH_3^+), 6.99 (d, $^3J_{Tyr\text{-}Ar}$ = 8.25 Hz, 2H, Tyr-Ar), 6.70 (d, $^3J_{DOPA\text{-}Ar}$ = 7.07 Hz, 1H, DOPA-Ar), 6.67 (d, $^3J_{Tyr\text{-}Ar}$ = 8.43 Hz, 2H, Tyr- Ar), 6.61 (d, $^3J_{DOPA\text{-}Ar}$ = 8.06 Hz, 1H, DOPA-Ar), 6.49 (dd, $^3J_{DOPA\text{-}Ar}$ = 8.06 Hz and $^3J_{DOPA\text{-}Ar}$= 2.20 Hz, 1H, DOPA-Ar), 4.45 (m, 1H, DOPA-α), 4.36 (m, 1H, Tyr-α), 3.69 (m, 1H, Lys-α), 3.56 (s, 3H, OMe), 2.88 (m, 2H, DOPA-β), 2.70 (m, 2H, Lys-ε), 2.61 (dd, $^2J_{Tyr\text{-}\beta,Tyr\text{-}\beta}$ = 13.75 Hz and $^3J_{Tyr\text{-}\beta,Tyr\text{-}\alpha}$ = 9.7 Hz, 2H, Tyr-β), 1.70 (m, 2H, Lys- CH_2), 1.54 (qu, $^2J_{Lys\text{-}CH2,CH2}$ = 7.42 Hz, 2H, Lys-CH_2), 1.29 (m, 2H, Lys-CH_2).

^{13}C NMR (300 MHz, DMSO-d_6): δ = 171.76, 171.06 (CO-NH), 168.30 (COOMe), 156.03 (Tyr-Ar), 144.85, 143.79 (DOPA-Ar), 129.92 (Tyr-Ar), 128.24 (DOPA-Ar), 126.96 (Tyr-Ar), 119.95, 116.70, 115.34 (DOPA-Ar), 115.04 (Tyr-Ar), 54.57 (DOPA-α), 53.98 (Tyr-α), 51.76 (Lys-α and OMe), 38.19 (DOPA-β), 36.76 (Tyr-β), 35.88 (Lys-ε), 30.25 (Lys-CH_2), 26.13 (Lys-CH_2), 20.83 (Lys-CH_2).

ESI-MS (m/z): 525 $[M + H]^+$, $[M+2Na]^+$.

Melting Point: remains semi-solid.

7.25. Compound 25: Boc-Lys(2-Cl-Z)-Tyr-OMe

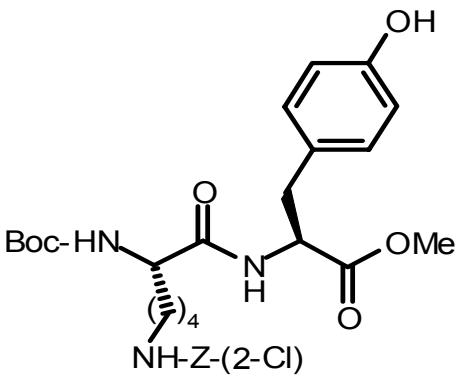

25

7.25.1. Procedure

Tyrosine methyl ester (0.50 g, 2.76 mmol) and Boc(2-Cl-Z) Lys (1.26 g, 3.03 mmol) were dissolved in **20** mL DMF. Then HOBt (0.48 g, 3.59 mmol) and HBTU (1.36 g, 3.59 mmol) were added and pH of the reaction mixture was adjusted to 7-8 with DIPEA. The reaction mixture was

stirred for 6 h at room temperature. The solvent was removed and **25** was purified by column chromatography ($CHCl_3$:MeOH as 4:1). Yield obtained was 1.39 g (2.35 mmol, 92%).

7.25.2. Analytical Data

^{1}H NMR (500 MHz, DMSO-d_6): δ = 7.39 (m, 2H, 2-Cl-Z), 7.24 (m, 2H, 2-Cl-Z), 6.9 (d, $^3J_{Tyr\text{-}Ar}$ = 8.41 Hz, 2H, Tyr-Ar), 6.74 (d, $^3J_{Tyr\text{-}Ar}$ = 8.41 Hz, 2H, Tyr-Ar), 6.65 (d, $^3J_{Boc\text{-}NH,\ Lys\text{-}\alpha}$= 8.06 Hz, 1H, Boc-NH), 5.20 (s, 2H, CH_2), 4.81 (m, 1H, Tyr-α), 4.03 (s_{br}, 1H, Lys-α), 3.70 (s_{br}, 3H, OMe), 3.11 (m, 3H, Lys-ε and Tyr-β), 2.93 (m, 1H, Tyr-β), 1.42 (s_{br}, 13H, t-butyl-CH_3 and Lys-CH_2),1.21 (s, 2H, Lys-CH_2).
^{13}C NMR (500 MHz, DMSO-d_6): δ = 129.5 (Ar–Z), 129.4 (Ar-Z), 130.2 (Tyr-Ar), 115.2 (Tyr-Ar), 64.0 (CH_2), 52.9 (Tyr-α), 54.0 (Lys-α), 52.4 (OMe), 40.1 (Lys-ε), 37.2 (Tyr-β), 28.1 (Lys-CH_2), 22.3 (Lys-CH_2), 23.4 (Lys-CH_2), 28.0 (t-butyl-3CH_3).
ESI-MS (m/z): 614 [M+Na$^+$], 630 [M+K$^+$].
Melting Point: 60°C.

7.26. Compound 26: Boc-Lys(2-Cl-Z)-Tyr

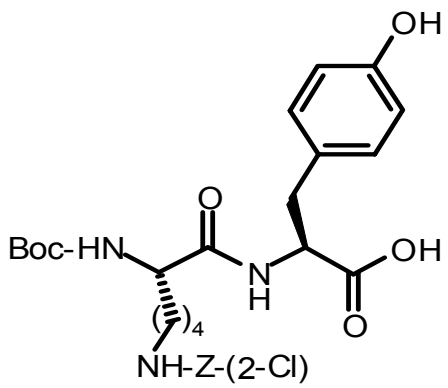

26

7.26.1. Procedure

Compound **25** (0.077 g, 0.15 mmol) was dissolved in minimum amount of MeOH (5 mL). 1N KOH (0.30 mL, 0.30 mmol) was added into reaction mixture. The reaction mixture was stirred for 7 h at room temperature. Reaction was monitored by TLC and stopped with 1N HCl (0.15 mL). Then the solvent was removed, yield obtained was quantitative.

7.26.2. Analytical Data

^{1}H NMR (400 MHz, DMSO-d_6): δ = 9.20 (s, 1H, OH), 7.45 (m, 2H, 2-Cl-Z), 7.34 (m, 3H, 2-Cl-Z), 7.24 (d, $^3J_{Tyr–NH,Tyr-\alpha}$ = 7.0 Hz, 1H, Tyr–NH), 6.98 (d, $^3J_{Lys–NH,Lys-\alpha}$ = 7.71 Hz, 1H, Lys–NH),6.90 (d, $^3J_{Tyr-Ar}$ = 8.41 Hz, 2H, Tyr-Ar), 6.54 (d, $^3J_{Tyr-Ar}$ = 8.4 Hz, 2H, Tyr-Ar), 5.07 (s, 2H, CH_2), 4.02 (m, 1H, Tyr-α), 3.73 (m, 1H, Lys-α), 2.94 (m, 3H, Lys-ε and Tyr β), 2.82 (dd, $^2J_{Tyr-\beta,Tyr-\beta}$ = 13.3 Hz and $^3J_{Tyr-\beta,Tyr-\alpha}$ = 5.61 Hz, 1H, Tyr-β), 1.56 (m, 2H, Lys CH_2), 1.3 (m, 2H, Lys-CH_2), 1.35 (s, 9H, Boc-CH_3), 1.21 (m, 2H, Lys-CH_2).
^{13}C NMR (500 MHz, DMSO-d_6): δ = 129.5 (Ar-Z), 128.2 (Ar-Z), 130.2 (Tyr-Ar), 114.2 (Tyr-Ar) 62.2 (CH_2-Z), 54.82 (Tyr-α), 54.6 (Lys-α), 38.2 (Lys-ε), 36.1 (Tyr-β), 30.2 (Lys-CH_2), 28.1 (Lys-CH_2), 25.6 (t-butyl-3CH_3), 22.5 (Lys-CH_2).
ESI-MS (m/z): 600 $[M+Na]^+$, 616 $[M+K]^+$.
Melting Point: 196°C.

7.27. Compound 27: Lys(2-Cl-Z)-Tyr

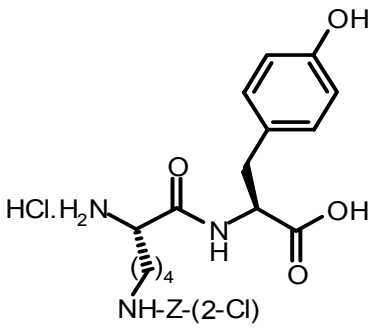

27

7.27.1. Procedure

Dipeptide **26** (280 mg, 0.48 mmol) was treated with HCl (10 mL) in diethyl ether. The reaction mixture was stirred for 6 h at room temperature to yield the HCl salt of the free amine of **27**. Yield obtained was quantitative.

7.27.2. Analytical Data

^{1}H NMR (500 MHz, DMSO-d_6): δ = 12.84 (s, 1H, OH), 9.31 (s, 1H, OH), 8.75 (d, $^3J_{Tyr-NH,Tyr-\alpha}$ = 7.62 Hz, 1H, Tyr-NH), 8.18 (s, 3H, NH_3^+), 7.45 (m, 2H, Ar-H), 7.35 (m, 3H, Ar-H and Lys-NHε), 7.04 (d, $^3J_{Tyr–Ar}$ = 8.62 Hz, 2H, Tyr–Ar), 6.66 (d, $^3J_{Tyr-Ar}$ = 8.62 Hz, 2H, Tyr-Ar),

5.06 (s, 2H, CH_2), 4.37 (m, 1H, Tyr-α), 3.7 (m, 1H, Lys-α), 2.95 (m, 2H, Lys-ε), 2.82 (m, 2H, Tyr-β), 1.71 (m, 2H, Lys-CH_2), 1.56 (m, 2H, Lys-CH_2), 1.36 (m, 1H, Lys CH_2).

^{13}C NMR (500 MHz, DMSO-d_6): δ = 129.2 (Ar-Z), 127.2 (Ar-Z), 129.9 (Tyr-Ar), 62.2 (CH_2-Z), 53.9 (Tyr-α), 51.5 (Lys-α), 39.9 (Tyr-β), 35.2 (Lys-ε), 30.2 (Lys-CH_2), 28.2 (Lys-CH_2), 20.8 (Lys-CH_2).

ESI-MS (m/z): 478 $[M-H]^+$, 500 $[M+Na]^+$, 516 $[M+K]^+$.

Melting Point: 124°C.

7.28. Compound 28: Poly-Bic

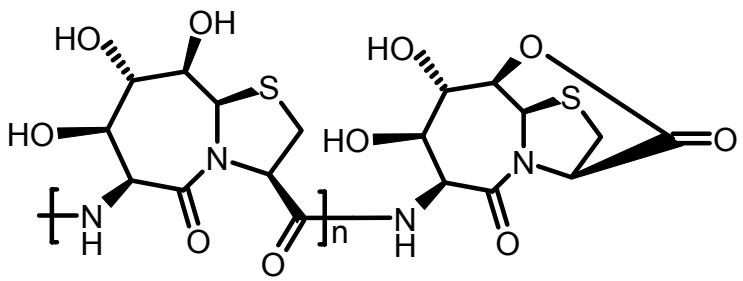

28

n = 1,2,3….7.

7.28.1. Procedure

Polyhydroxylated dipeptide (0.25 g, 0.89 mmol) was dissolved in DMF (10 mL). Then HOBt (0.60 g, 4.4 mmol) and of Poly DCC [*N*-Cyclohexylcarbodiimide, *N′*-methyl polystyrene] (1.38 g, 1.79 mmol) were added and the pH of the reaction mixture was adjusted to 7-8 with triethylamine (0.25 mL, 1.79 mmol). The reaction mixture was stirred for 48 h at room temperature. The reaction was monitored by TLC (MeOH:EtOAC:H_2O as 2:2:1). The solvent was removed. Reaction mixture was washed with 10% MeOH in $CHCl_3$ to remove excess HOBt. Yield obtained was quantitative.

Alternatively, this compound was also synthesized as:

Polyhydroxylated dipeptide (0.10 g, 0.36 mmol) was dissolved in (5 mL) DMF. Then HOBt(0.24 g, 1.8 mmol) and DCC (0.148 g, 0.72 mmol) were added and the pH of the reaction mixture was adjusted to 7-8 with triethylamine (0.10 mL, 0.72 mmol). The reaction mixture was stirred for 48 h at room temperature. The reaction was monitored by TLC (MeOH:EtOAC:H_2O as 2:2:1). The solvent was removed. Reaction mixture was washed with 10% MeOH in $CHCl_3$ to remove the excess HOBt and DCU. Yield obtained was quantitative.

7.28.2. Analytical Data

^{1}H NMR (300 MHz, DMSO-d_6): ^{1}H NMR spectra in these solvent showed only numerous unassignable peaks. Therefore, experiments like 2D COSY (Correlated Spectroscopy) and HMQC (Heteronuclear Multiple Quantum Correlation Spectroscopy) were used to assign terminal lactones peaks and some peaks which belong to oligomers mixtures.

^{1}H NMR (600 MHz, DMSO-d_6): δ = 6.03 (s_{br}, 8-OH), 5.89 (s_{br}, 9a-H), 5.47 (7-OH), 5.24 (3-H), 4.33 (d, $^3J_{9H,9}$ = 3.2 Hz, 9H), 4.01 (8-H), 3.80 (7-H), 3.28 (2-H).

^{13}C NMR (600 MHz, DMSO-d_6): δ = 84.5 (C-9), 76.3 (C-8), 69(C-7), 60.7 (C-3), 52.9 (C-9a), 52.2 (C-6), 33.5 (C-2).

Oligomer mixtures:

^{1}H NMR (600 MHz, DMSO-d_6): δ = 5.47 (s, 9a-H), 5.01 (s, 6-H), 4.85 (s, 3-H), 3.81 (s, 8-H), 3.76 (s, 7-H), 3.71 (s, 9-H), 3.39 (s, 2-H), 3.22 (s, 2-H).

^{13}C NMR (600 MHz, DMSO-d_6): δ = 74.2 (C-9), 73 (C-7), 71.2 (C-8), 64.1 (C-3), 60.8 (C-9a), 52.1 (C-6), 32.2 (C-2).

MALDI–TOF: A series of polyhydoxylated dipeptide oligomers were observed with masses ranging from 538 to 2358 Da. (n = 2; 538), (n = 3; 798), (n = 3; 1058), (n = 4; 1318), (n = 5; 1578), (n = 6; 1838), (n = 7; 2098), (n = 8; 2358).

GPC: GPC shows the mixture of different molecular weight compounds ranging from 2962 to 36950 Da.

HPLC: It shows the mixture of different peaks, while the retention time ranging from 6.58 min to 14.65 min.

7.29. Compound 29: Poly-Bic

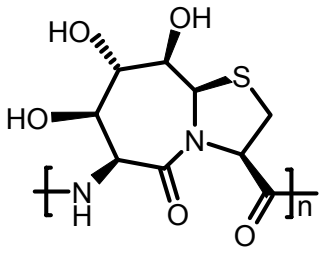

29

n = 1,2…..8.

7.29.1. Procedure

Compound **28** (0.02 g) was dissolve in minimum amount of DMF (3 mL). 1N KOH in MeOH was added into reaction mixture till pH was about 9 to 10. The reaction mixture was stirred for 30 min at room temperature and stopped with 1N HCl in MeOH till pH was about 6 to 7. Solvent was removed, yield obtained was quantitative.

7.29.2. Analytical Data

^{1}H NMR (600 MHz, DMSO-d_6): δ = 5.46 (s_{br}, 9a-H), 5.01 (6-H), 4.85 and 4.6 (3-H), 3.83 (8-H), 3.75 (7-H), 3.58 (9-H), 3.28 (2-H).
^{13}C NMR (600 MHz, DMSO-d_6): δ = 76.64 (C-9), 74.17 (C-7), 71.04 (C-8), 60.9 (C-9a), 52.3 (C-6), 64.3 and 64.2 (C-3), 32.1 (C-2).
MALDI–TOF: A series of polyhydixylated dipeptide oligomers were observed with masses ranging from 538 to 2358 Da. (n = 2; 538), (n = 3, 798), (n = 3; 1058), (n = 4; 1318), (n = 5; 1578), (n = 6; 1838), (n = 7, 2098), (n = 8; 2358).

7.30. Compound 30: Poly-Tyr

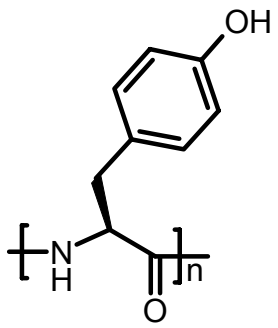

30

7.30.1. Procedure

Tyrosine methyl ester (0.10 g, 0.55 mmol) was dissolved in DMF (8 mL). Then HOBt (0.37 g, 2.75 mmol) and DCC (0.22 g, 1.10 mmol) were added and the pH of the reaction mixture was adjusted to 7-8 with triethylamine (0.15 mL, 1.10 mmol). The reaction mixture was stirred for 48 h at room temperature. Reaction was monitored by TLC (MeOH:EtOAC:H_2O as 2:2:1). The solvent was removed. Reaction mixture was washed with $CHCl_3$ to remove excess HOBt and DCU. Yield obtained was quantitative.

7.30.2. Analytical Data

(Based on 2D HMQC experiment)

^{1}H NMR (500 MHz, DMSO-d_6): δ = 6.58 (s, Ar-H), 6.45 (s, Ar-H), 4.65-3.78 (s, Tyr-α), 2.79 (s, Tyr-β).

^{13}C NMR (500 MHz, DMSO-d_6): δ = 114.81 (Tyr-Ar), 119.6 (Tyr-Ar), 55.62-53.6 (Tyr-α), 45.3 (Tyr-β).

MALDI–TOF: A series of Tyr oligomers were observed with masses ranging from 344 to 4256 Da.

7.31. Compound 31: Poly-DOPA

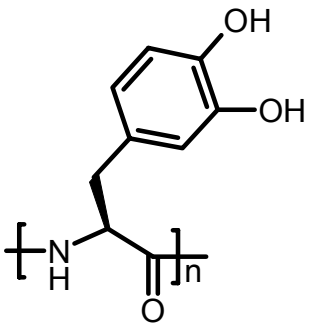

31

7.31.1. Procedure

DOPA (0.10 g, 0.50 mmol) was dissolved in minimum amount of DMF (5 mL). Then HOBt (0.34 g, 2.52 mmol) and DCC (0.20 g, 1.01 mmol) were added and the pH of the reaction mixture was adjusted to 7-8 with triethylamine (0.14 mL, 1.01 mmol). The reaction mixture was stirred for 48 h at room temperature. Reaction was monitored by TLC (MeOH:EtOAC:H_2O as 2:2:1). The solvent was removed. Reaction mixture was washed with $CHCl_3$ to remove excess HOBt and DCU. Yield obtained was quantitative.

7.31.2. Analytical Data

(Based on 2D HMQC experiment)

^{1}H NMR (500 MHz, DMSO-d_6): δ = 6.56 (DOPA-Ar), 6.42 (DOPA-Ar), 4.33 (DOPA-α), 2.85 (DOPA-β).

^{13}C NMR (500 MHz, DMSO-d_6): δ = 115.05 (DOPA-Ar), 119.84 (DOPA-Ar), 53.86 (DOPA-α), 45.0 (DOPA-β).

MALDI–TOF: A series of DOPA oligomers were observed with masses ranging from 376 to 4672 Da.

7.32. Compound 32: Poly-Lys(Z)

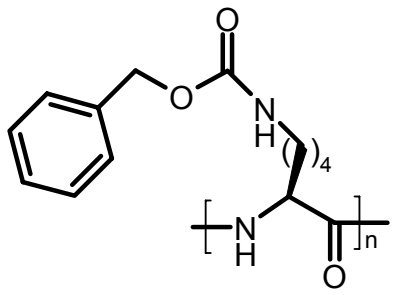

32

7.32.1. Procedure

Lys(Z) (0.50 g, 1.78 mmol) was dissolved in DMF (10 mL). Then of HOBt (1.2 g, 8.9 mmol) and DCC (0.73 g, 3.56 mmol) were added and the pH of the reaction mixture was adjusted to 7-8 with triethylamine (0.49 mL, 3.56 mmol). The reaction mixture was stirred for 48 h at room temperature. Reaction was monitored by TLC (MeOH:EtOAC:H_2O as 2:2:1). The solvent was removed. Reaction mixture was washed with $CHCl_3$ to remove excess HOBt and DCU. Yield obtained was quantitative.

7.32.2. Analytical Data

(Based on 2D HMQC experiment)

^{1}H NMR (500 MHz, DMSO-d_6): δ = 7.58 (s, Ar-H), 4.9 (s, CH_2-Z), 4.2 (s, Lys-α), 2.92 (s, Lys-ε), 1.64, 1.35, 1.2 (Lys-CH_2).

^{13}C NMR (500 MHz, DMSO-d_6): δ = 127.8 (C-Ar), 65.0 (C-CH_2), 52.1 (C-Lys-α), 40.0 (C-Lys-ε), 29.8, 29.0, 22.5 (Lys-CH_2).

MALDI–TOF: A series of Lys (Z) oligomers were observed with masses ranging from 547 to 4498 Da.

7.33. Compound 33: Poly-Lys

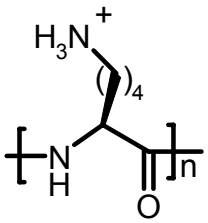

33

7.33.1. Procedure

Compound **32** (15 mg) was dissolved in 60% TFA in DMF (2 mL), and then of 33% HBr (0.5 mL) in acetic acid were added into reaction mixture. The reaction mixture was stirred for 20 minute. The product was precipitated by addition of ether and then dried. The crud polymer was dissolved in a small amount of methanol, precipitated out by addition of ether, and dried in vacuum. Yield obtained was 10 mg.

7.33.2. Analytical Data

(Based on 2D HMQC experiment)

^{1}H NMR (500 MHz, DMSO-d_6): δ = 7.85 (s_{br}, NH), 4.2 (Lys-α), 2.7 (Lys-ε), 1.56 (Lys-CH_2), 1.52 (Lys-CH_2), 1.30 (Lys-CH_2).

^{13}C NMR (500 MHz, DMSO-d_6): δ = 52.0 (Lys-α), 38.23 (Lys-ε), 25.99 (Lys-CH_2), 30.74 (Lys-CH_2), 21.82 (Lys-CH_2).

MALDI-TOF: A series of Lys (Z) oligomers were observed with masses ranging from 146 to 1042 Da.

7.34. Compound 34: Poly-Bic-Tyr

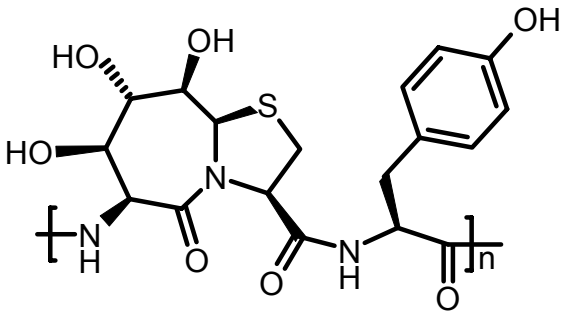

34

7.34.1. Procedure

Compound **12** (0.05 g, 0.11 mmol) was dissolved in DMF (5 mL). Then HOBt (0.07 g, 0.56 mmol) and Poly DCC [*N*-Cyclohexylcarbodiimide, *N′*-methyl polystyrene] (0.17 g, 0.22 mmol) were added and the pH of the reaction mixture was adjusted to 7-8 with triethylamine (0.03 mL, 0.22 mmol). The reaction mixture was stirred for 48 h at room temperature. Reaction was monitored by TLC (MeOH:EtOAC:H_2O as 2:2:1). The solvent was removed. Reaction mixture was washed with 10% MeOH in $CHCl_3$ to remove excess HOBt. Yield obtained was quantitative.

Alternatively, this compound was prepared as:

Compound **12** (0.10 g, 0.22 mmol) was dissolved in DMF (5 mL). Then HOBt (0.15 g, 1.13 mmol) and DCC (0.09 g, 0.45 mmol) were added and the pH of the reaction mixture was adjusted to 7-8 with triethylamine (0.07 mL, 0.45 mmol).The reaction mixture was stirred for 48 h at room temperature. The solvent was removed. Reaction was monitored by TLC (MeOH:EtOAC:H_2O as 2:2:1). Reaction mixture was washed with 10% MeOH in $CHCl_3$ to remove excess HOBt and DCU. Yield obtained was quantitative.

7.34.2. Analytical Data

(Based on 2D HMQC experiment)

^{1}H NMR (500 MHz, DMSO-d_6): δ = 7.03 (s, Tyr-Ar), 6.61 (s, Tyr-Ar), 5.48 (s, 9a), 5.0 (s, 6-H), 4.66 (s, 3-H), 4.49 (Tyr-α), 3.85 (8-H), 3.69 (7-H), 3.62 (9-H), 3.36 (s, Tyr-β), 3.22-2.97 (s, 2H).

^{13}C NMR (500 MHz, DMSO-d_6): δ = 129.3 (Tyr-Ar), 114.6 (Tyr-Ar), 75.1 (C-9H), 74.5 (C-7), 70.7 (C-8), 60.6 (C-9a), 52.0 (C-6), 64.7 (C-3), 53.3 (Tyr-α), 32.3-32.1 (C-2H), 48.2 (Tyr-β).

MALDI–TOF: A series of oligomers were observed with masses ranging from 441 to 4671 Da. (n = 1; 441), (n = 2; 864), (n = 3; 1287), (n = 4; 1710), (n = 5; 2133), (n = 6; 2556), (n = 7; 2979), (n = 8; 3402), (n= 9; 3825), (n = 10; 4248).

GPC: GPC shows the mixture of different molecular weight compounds ranging from 1628 to 9031 Da.

7.35. Compound 35: Lys(2-Cl-Z)-Tyr

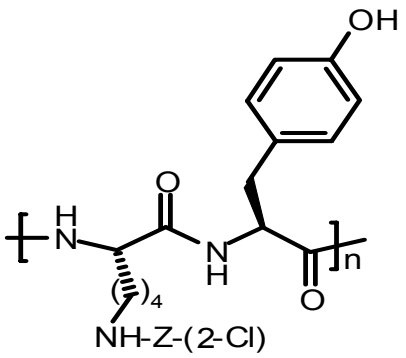

35

7.35.1. Procedure

Compound **27** (0.05 g, 0.104 mmol) was dissolved in DMF (2 mL). Then HOBt (0.07 g, 0.52 mmol) and Poly DCC [*N*-Cyclohexylcarbodiimide, *N′*-methyl polystyrene] (0.16 g, 0.20 mmol) were added and the pH of the reaction mixture was adjusted to 7-8 with triethylamine (0.03 mL, 0.209 mmol). The reaction mixture was stirred for 48 h at room temperature. Reaction was monitored by TLC ((MeOH:EtOAC:H_2O as 2:2:1). The solvent was removed. Reaction mixture was washed with 10% MeOH in $CHCl_3$ to remove excess HOBt. Yield obtained was quantitative.

Alternative, compound **35** was synthesized as:

Compound **27** (0.05 g, 0.104 mmol) was dissolved in DMF (5 mL). Then HOBt (0.07 g, 0.52 mmol) and DCC (0.04 g, 0.20 mmol) were added and the pH of the reaction mixture was adjusted to 7-8 with triethylamine (0.03 mL, 0.209 mmol). The reaction mixture was stirred for 48 h at room temperature. Reaction was monitored by TLC (MeOH:EtOAC:H_2O as 2:2:1). The solvent was removed. Reaction mixture was washed with 10% MeOH in $CHCl_3$ to removed excess HOBt and DCU. Yield obtained was quantitative.

7.35.2. Analytical Data

(Based on 2D HMQC experiment)

^{1}H NMR (500 MHz, DMSO-d_6): δ = 7.45, 7.34 (br, Ar-Z), 6.99 (Tyr-Ar), 6.64 (Tyr-Ar), 5.3 (CH_2-Ar), 4.8-4.25 (Tyr-α), 3.68 (Lys-α), 2.94-2.8 (Tyr-β and Lys-ε), 1.66 (Lys-CH_2), 1.38 (Lys-CH_2), 1.19 (Lys-CH_2).

^{13}C NMR (500 MHz, DMSO-d_6): δ = 130.0 (Tyr-Ar), 129.8 (Ar-Z), 114.7 (Tyr-Ar), 63.0 (CH_2-Ar), 54.5 (Tyr-α), 51.8 (Lys-α), 39.9-39.6 (Tyr-β and Lys-ε), 31.1 (Lys-CH_2), 29.0 (Lys-CH_2), 22.0 (Lys-CH_2).

MALDI–TOF: A series of Lys (2-Cl-Z) oligomers were observed with masses ranging from 482 to 2323 Da. (n = 1; 482), (n = 2; 941.6), (n = 3; 1403), (n = 4; 1862.5), (n = 5; 2323.9).

GPC: GPC shows the mixture of different molecular weight compounds ranging from 880 to 11450 Da.

7.36. Compound 36: Poly-Lys(Z)-Bic-Tyr

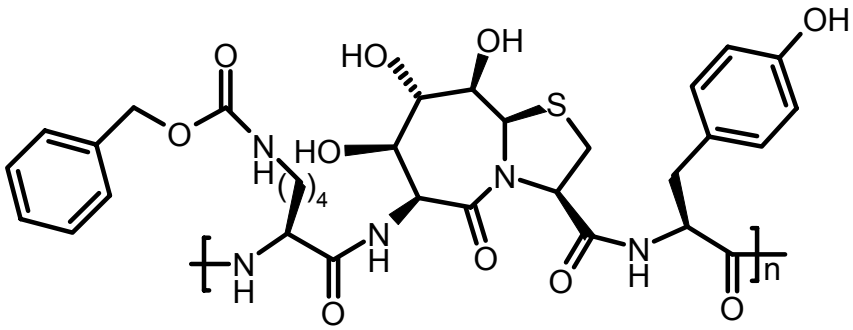

36

7.36.1. Procedure

Compound **15** (0.050 g, 0.071 mmol) was dissolved in DMF (5 mL). Then HOBt (0.048 g, 0.35 mmol) and Poly DCC [*N*-Cyclohexylcarbodiimide, *N′*-methyl polystyrene] (0.109 g, 0.142 mmol) were added and the pH of the reaction mixture was adjusted to 7-8 with triethylamine (0.02 mL, 0.142 mmol). The reaction mixture was stirred for 48 h at room temperature. Reaction was monitored by TLC (MeOH:EtOAC:H_2O as 2:2:1). The solvent was removed. Reaction mixture was washed with 10% MeOH in $CHCl_3$ to remove excess HOBt. Yield obtained was quantitative.

Alternatively, this product was synthesized as:

Compound **15** (0.050 g, 0.071 mmol) was dissolved in DMF (5 mL). Then HOBt (0.048 g, 0.35 mmol) and DCC (0.029 g, 0.142 mmol) were added and the pH of the reaction mixture was adjusted to 7-8 with triethylamine (0.02 mL, 0.142 mmol). The reaction mixture was stirred for 48 h at room temperature. Reaction was monitored by TLC (MeOH:EtOAC:H_2O as 2:2:1). The solvent was removed. Reaction mixture was washed with 10% MeOH in $CHCl_3$ to remove excess HOBt and DCU. Yield obtained was quantitative.

7.36.2. Analytical Data

(Based on 2D HMQC experiment)

^{1}H NMR (500 MHz, DMSO-d_6): δ = 7.34 (Ar-Z), 7.04 (Tyr-Ar), 6.66 (Tyr-Ar), 5.5 (9a-H), 5.13 (6-H), 5.0 (CH_2-Ar), 4.31 (Tyr-α), 4.77 (3-H), 3.87 (8-H), 3.85 (Lys-α), 3.76 (7-H), 3.62 (9-H), 3.11-3.25 (2-H), 2.97 (Tyr-β), 2.92-2.83 (Lys-ε), 1.73 (Lys-CH_2), 1.39 (Lys-CH_2), 1.36 (Lys-CH_2).

^{13}C NMR (500 MHz, DMSO-d_6): δ = 130.0 (Tyr-Ar), 127.5 (Ar-Z), 114.8 (Tyr-Ar), 76.0 (C-9), 74.5 (C-7), 71.0 (C-8), 70.1 (C-9a), 64.9 (CH_2-Ar), 64.8 (C-3), 53.97 (Tyr-α), 51.77 (Lys-α), 52.1 (C-6), 32.0 (C-2), 39.6 (Tyr-β), 34.4 (Lys-ε), 30.7 (Lys-CH_2), 28.4 (Lys-CH_2), 21.4 (Lys-CH_2).

MALDI–TOF: A series of oligomers were observed with masses ranging from 742 to 2783 Da. (n = 2; 1410), (n = 3; 2096.8), (n = 4; 2783.2).

GPC: GPC shows the mixture of different molecular weight compounds ranging from 1614 to 32920 Da.

7.37. Compound 37: Poly-Lys-Bic-Tyr

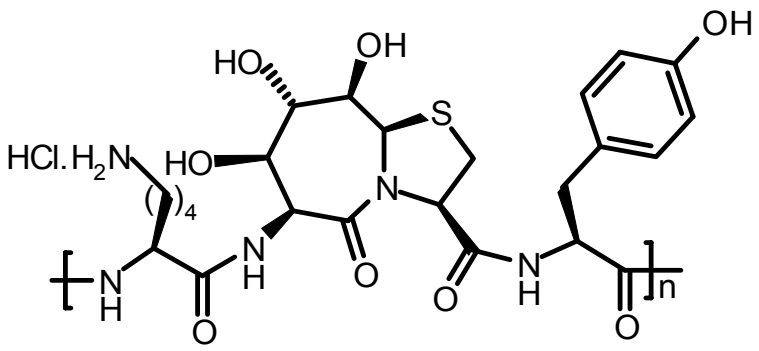

37

7.37.1. Procedure

Compound **36** (25 mg) was treated with HCl (10 mL) in diethyl ether. The reaction mixture was stirred for 8 h at room temperature to yield the HCl salt of the free amine of **37**. Yield obtained was quantitative.

7.37.2. Analytical Data

(Based on 2D HMQC experiment)

^{1}H NMR (500 MHz, DMSO-d_6): δ = 7.30-7.0 (Tyr-Ar), 6.88-6.28 (Tyr-Ar), 5.48 (9a-H), 5.03 (6-H), 4.64-4.59 (3-H), 4.30 (Tyr-α), 4.30 (Lys-α), 3.98-3.77 (8-H), 3.78 (7-H), 3.74 (9-H), 3.15 (Tyr-β),2.69 (Lys-ε), 3.22-3.07 (2-H), 1.55 (Lys-CH_2), 1.32 (Lys-CH_2), 0.83 (Lys-CH_2).
^{13}C NMR (500 MHz, DMSO-d_6): δ = 129.4 (Tyr-Ar), 114.76-114.58 (Tyr-Ar), 61.03 (C-9a), 51.99 (C-6), 64.59-64.3 (C-3), 53.9 (Lys-α), 51.9 (Tyr-α), 71.1 (C-8), 75.4 (C-7), 76.4 (C-9), 48.31 (Tyr-β), 34.7 (Lys-ε), 31.98 (C-2), 26.08 (Lys-CH_2), 21.41 (Lys-CH_2), 13.49 (Lys-CH_2).
MALDI-TOF: A series of oligomers were observed with masses ranging from 569 to 1671 Da.

7.38. Compound 38: Saponification Reaction

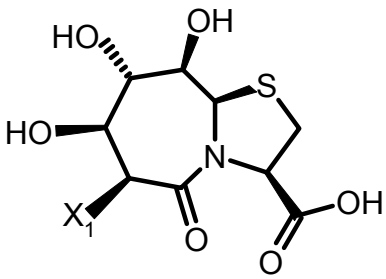

38

X_1 = OH, N_3, NH_2, Boc-NH.
XOH = KOH, NaOH, LiOH.

7.38.1. Procedure

Methyl ester of X_1 (where X_1 could be either acid or azide or amine or Boc-NH) (1 g, 1 eq) was dissolved in H_2O till ester was soluble. XOH (2 eq, 1N) was added into reaction mixture. Reaction was monitored by TLC and stopped after 30 min with (1 eq, 1N) HCl. Solvent was removed, yield obtained was quantitative. Saponification reaction did not work for azide as the 6-H atom is more acidic.

7.38.2. Analytical Data

(a) For X_1 = acid,
^{1}H NMR (300 MHz, DMSO-d_6): δ = 7.94 (s, 1H, COOH), 5.45 (s, 1H, 9a-H), 4.59 (pt, $^{3}J_{3,2}$ = 7.96 Hz, 1H, 3-H), 4.32 (s_{br}, 1H, 6-H), 3.39 (s_{br}, 1H, 7-H), 3.62 (d, $^{3}J_{8,9}$ = 5.49 Hz, 1H, 8-H), 3.44 (dd, $^{3}J_{9,9\text{-OH}}$ = 8.78Hz and $^{3}J_{9,8}$ = 3.29 Hz, 1H, 9-H), 3.16 (m, 2H, 2-H).
^{13}C NMR (300 MHz, DMSO-d_6): δ = 170.55, 170.35 (CO-5, COMe), 31.39(C-2), 52.10 (OMe), 60.97 (C-9a), 63.78 (C-3), 70.86 (C-8), 76.00 (C-7), 76.87 (C-9).

ESI-MS (H_2O/MeOH + 10 mmole/NH_4Ac) (m/z): 293.7 $[MH]^+$, 310.8 $[M+NH_4]^+$, 315.8 $[M+Na]^+$, 604 $[2M+NH_4]^+$, 609 $[2M+Na]^+$.

Melting Point: Decompose at 208°C.

(b) For X_1 = amine,

^{1}H NMR (300 MHz, DMSO-d_6): δ = 5.58 (s, 1H, 9a-H), 4.58 (pt. $^3J_{3,2}$ = 7.0 Hz, 1H, 3-H), 4.51 (s, 1H, 6H), 3.86 (d, $^3J_{7,8}$ = 3.57 Hz, 1H, 7-H), 3.82 (d, $^3J_{8,9}$ = 4.086 Hz, 1H, 8-H), 3.51 (d, $^3J_{9,8}$ = 3.043Hz, 1H, 9-H), 3.21 (m, 2H, 2-H).

^{13}C NMR (300 MHz, DMSO-d_6): δ = 173.66, 165.55 (CO-5, CO-OH), 75.78 (C-9), 72.01 (C-7), 71.48 (C-8), 66.08 (C-3), 61.15 (C-9a), 53.13 (C-6), 32.73 (C-2).

ESI-MS (CH_2Cl_2/MeOH+NH_4AC) (m/z): 278.8 $[M-H]^+$.

Melting Point: Decompose at 200°C.

(c) for X_1 = Boc-NH,

^{1}H NMR (500 MHz, DMSO-d_6): δ = 7.17 (s, 1H, OH), 6.49 (d, $^3J_{Boc\text{-}NH,6}$ = 8.23Hz, 1H, Boc-NH), 5.63 (s, 1H, OH), 5.48 (s, 1H, 9a-H), 5.12 (s, 1H, OH), 4.74 (d, $^3J_{6\text{-}H,Boc\text{-}NH}$ = 8.51Hz, 1H, 6-H), 4.57 (t, $^3J_{3,2}$ = 6.59Hz, 1H, 3-H), 3.8 (d, $^3J_{8,9}$ = 3.84 Hz, 1H, 8-H), 3.68 (s, 1H, 7-H), 3.49 (s, 1H, 9-H), 3.21 (d, $^3J_{2,3}$ = 6.59Hz, 1H, 2-H), 3.15 (d, $^3J_{2,3}$ = 4.94Hz, 1H, 2-H), 1.37 (s, 9H, t-butyl-CH_3).

^{13}C NMR (300 MHz, DMSO-d_6): δ = 174.51 (CO-5), 167.79 (COOH), 154.77 (Boc-CO), 78.05 (C-t-butyl$_{quart}$), 75.66 (C-9), 74.73 (C-7), 71.46 (C-8), 66.12 (C-3), 61.00 (C-9a), 53.52 (C-6), 32.48 (C-2), 28.05(3C, t-butyl CH_3).

ESI-MS (CH_2Cl_2/MeOH+NH_4AC) (m/z): 379 $[M + H^+]$, 401 $[M + Na]^+$, 423.0 $[M-H^+ + 2Na]^+$.

Melting Point: Decompose at 210°C.

8. References

[1] T. Crutius, *J Prakt Chem*, 24, 239, **1881**.

[2] E. Fischer, *Ber Dtsch Chem Ges*, 35, 1095, **1902**.

[3] M. Bergmann, L. Zervas, *Ber Dtsch Chem Ges*, 65, 1192-1201, **1932**.

[4] R. B. Merrifield, *J Am Chem Soc*, 85, 2149-2154, **1963**.

[5] J. H. Waite, T. J. Housley, M. L. Tanzer, *Biochemistry*, 24, 5010-5014, **1986**.

[6] L. M. Rzepecki, K. M. Hansen, J. H. Waite, *Biol Bull*, 183, 123-137, **1992**.

[7] J. H. Waite, X. Qin, *Biochemistry*, 40, 2887-2893, **2001**.

[8] S. Haemers, G. M. Koper, G. Frens, *Biomacromolecules*, 4, 632-640, **2003**.

[9] J. H. Waite, *J Biol Chem*, 258, 2911-2915, **1983**.

[10] K. A. Resing, B. A. Dale, K. A. Walsh, *Biochemistry*, 24, 4167-4175, **1985**.

[11] D. R. Filpula, S. M. Lee, R. P. Link, S. L. Strausberg, R. L. Strausberg, *Biotechnol Prog*, 6, 171-177, **1990**.

[12] P. I. Nagy, H. C. Patel, W. Dreyer, A. J. Hopfinger, *Int J Pep Prot Res*, 38, **1991**.

[13] P. Matt, S. S. Deacon, J. Davis, W. Herbert, S. E. Harding, *Biochemistry*, 37, 14108-14112, **1998**.

[14] K. Yamada, T. Chen, G. Kumar, O. Vesnovsky, L. D. Topoleski, G. F. Payne, *Biomacromolecules*, 1, 252-258, **2000**.

[15] H. Yamamoto, Y. Sakai, K. Ohkawa, *Biomacromolecules*, 1, 543-551, **2000**.

[16] A. Jerschow, N. Müller, *Macromolecules*, 31, 6573-6578, **1998**.

[17] B. P. Lee, J. Dalsin, P. B. Messersmith, *Biomacromolecules*, 3, 1038-1047, **2002**.

[18] J. M. Berg, L. Stryer, J. L. Tymoczko *Biochemistry*, 5th ed., W. H. Freeman, New York, **2005**.

[19] R. K. Harrison, R. L. Stein, *Biochemistry*, 29, 3813-3816, **1990**.

[20] M. L. Moore, G. A. Grant, *Peptide Design Considerations in Synthetic Peptides: A User's Guide*, Freeman, New York, **1992**.

[21] J. W. Payne, R. Jakes, B. S. Hartley, *Biochem J*, 117, 757-766, **1970**.

[22] R. C. Pandey, J. C. Cook, K. L. Rinehart, *J Am Chem Soc*, 99, 8469-8483, **1977**.

[23] H. Morishima, T. Takita, T. Aoyagi, T. Takeuchi, H. Umezawa, *J Antibiot*, 23, 263-265, **1970**.

[24] G. Barany, R. B. Merrifield, *J Am Chem Soc*, 99, 7363-7365, **1977**.

[25] M. Bodanszky, V. du Vigneaud, *Nature*, 183, 1324-1325, **1959**.

[26] E. Atherton, R. C. Sheppard, *Solid Phase Peptide Synthesis: A Practical Approach*, Oxford University Press, London, **1989**.

[27] G. B. Fields, R. L. Noble, *Int J Pept Protein Res*, 35, 161-214, **1990**.

[28] C. Chan, D. White, *Fmoc Solid Phase Peptide Synthesis: A Practical Approach*, Oxford University Press, New York, **2000**.

[29] L. A. Carpino, G. Y. Han, *J Am Chem Soc*, 92, 5748-5749, **1970**.

[30] L. A. Carpino, G. Y. Han, *J Org Chem*, 37, 3404-3409, **1972**.

[31] L. A. Carpino, D. Sadat-Aalaee, H. G. Chao, D. R. H., *J Am Chem Soc*, 112, 9651-9652, **1990**.

[32] H. Chantrenne, *Nature*, 160, 603-604, **1947**.

[33] J. Kovacs, L. Kisfaludy, M. Q. Ceprini, *J Am Chem Soc*, 89, 183-184, **1967**.

[34] M. Bodanszky, Principles of Peptide Synthesis, Springer Verlag, Berlin, pp. 36-44, **1984**.

[35] D. Hudson, *J Org Chem*, 53, 617-624, **1988.**

[36] A. Fournier, C. T. Wang, A. M. Felix, *Int J Pept Protein Res*, 31, 86-97, **1988**.

[37] L. D. Short, A. B. Borkovec, W. A. Knapp, *Toxicol Appl Pharmacol*, 499-509, **1971**.

[38] K. S. Hermann, K. Hartke, *Tet Lett*, 18, 1269-1272, **1978**.

[39] H. Gausepohl, *12th American Peptide Symposium (Peptide Chemistry and Biology)*, 523, Leiden, **1992**.

[40] G. Sabatino, G. Sabatino, B. Mulinacci, M. C. Alcaro, M. Chelli, P. Rovero, A. M. Papini1, *Lett Pept Sci*, 9, 119-123, **2002**.

[41] M. Gude, S. Barthelemy, *Proceedings of the 27th European Peptide Symposium*, 122, Naples, **2002**.

[42] K. Horiki, *Tet Lett*, 22, 1897-1900, **1977**.

[43] K. Horiki, *Tet Lett*, 22, 1901-1904, **1977**.

[44] F. Albericio, S. A. Kates, Coupling Methods, in *Solid Phase Peptide Synthesis: A Practical Guide* (Eds.: F. Albericio, S. A. Kates), Marcel Dekker, New York, pp. 273-328, **2000**.

[45] J. C. Sheehan, G. P. Hess, *J Am Chem Soc*, 77, 1967-1968, **1955**.

[46] F. Albericio, R. Chinchilla, D. J. Dodsworth, C. Nájera, *Org Prep Proc Int*, 33, 202-303, **2001**.

[47] C. J. Branden, J. Tooze *Introduction to Protein Structure*, 1st ed., Garland Publishing Agency, New York, **1991**.

[48] http://xray.bmc.uu.se/~kenth/bioinfo/structure/secondary.

[49] D. Eisenberg, *Annu Rev Biochem*, 53, 595-623, **1984**.

[50] W. T. Wickner, H. F. Lodish, *Science*, 230, 400-407, **1985**.

[51] L. Pauling, R. B. Corey, *Proc Natl Acad Sci*, 37, 251-256, **1951**.

[52] http://employees.csbsju.edu/hjakubowski/classes/ch331/protstructure.

[53] J. A. Smith, L. G. Pease, *Crit Rev Biochem*, 8, 315-399, **1980**.

[54] J. E. Rivier, M. R. Brown, *Biochemistry*, 17, 1766-1771, **1978**.

[55] R. Walter, C. W. Smith, P. K. Mehta, S. Boonjarern, J. A. L. Arruda, N. A. Kurtzman, Conformational Considerations of Vasopressin as a Guide to Development of Biological Probes and Theapeutic Agents, in *Disturbances in Body Fluid Osmolality, Vol. 1* (Eds.: T. E. Andreoli, J. J. Grantham, F. C. Rector), American Physiological Society, Bethesda, MD, pp. 1-76, **1977**.

[56] C. Chotia, *Annu. Rev. Biochem.*, 53, **1984**.

[57] W. R. Gray, L. B. Sandberg, J. A. Foster, *Nature*, 246, 461-466, **1973**.

[58] A. Bennick, *Mol Cell Biochem*, 45, 83-99, **1982**.

[59] T. J. Deming, *Curr Opin Chem Biol*, 3, 100-105, **1999**.

[60] L. H. Rzepecki, J. H. Waite, *Bioorganic Marine Chemistry, Vol. 4*, 4 ed., Springer Verlag, New York, **1991**.

[61] J. H. Waite, *Comp Biochem Physiol*, 97, 19-29, **1990**.

[62] S. G. George, B. J. S. Pirie, T. L. Coombs, *J Exp Mar Biol Ecol*, 23, **1976**.

[63] T. L. Coombs, P. J. Keller, *Aquat Toxicol*, 1, 291-300, **1981**.

[64] J. R. Donat, K. W. Bruland, *Trace Elements in Natural Waters*, CRC, Ann Arbor, **1995**.

[65] A. M. Baty, P. K. Leavitt, C. A. Siedlecki, B. J. Tyler, P. A. Suci, R. E. Marchant, G. G. Geesey, *Langmuir*, 13, 5702-5710, **1997**.

[66] J. B. Robin, P. Picciano, R. S. Kusleika, J. Salazar, C. Benedict, *Arch Ophthalmol*, 106, 973-977, **1988**.

[67] M. P. Olivieri, K. H. Rittle, K. S. Tweden, R. E. Loomis, *Biomaterials*, 13, 201-208, **1992**.

[68] J. P. Fulkerson, L. A. Norton, G. Gronowicz, P. Picciano, J. M. Massicotte, C. W. Nissen, *J Orthop Res*, 8, 793-798, **1990**.

[69] J. Schnurrer, C. M. Lehr, *Int J Pharm*, 141, 251-256, **1996**.

[70] I. Fiebrig, S. S. Davis, S. E. Harding, *Biopolymer Mixtures*, Nottingham University Press, Nottingham, **1995**.

[71] J. M. Gosline, M. Lillie, E. Carrington, P. A. Guerette, C. S. Ortlepp, K. N. Sabage, in *Philos Trans, Vol. B357*, **2002**, pp. 121-132.

[72] M. J. Sever, J. T. Weisser, J. Monahan, S. Srinivasan, J. J. Wilker, *Angew Chem Int Ed Engl*, 43, 448-450, **2004**.

[73] K. M. Rudall, *Symp Soc Exp Biol*, 9, **1955**.

[74] E. H. Mercer, *Austr J Mar Freshwater Res*, 3, 199-204, **1952**.

[75] S. C. Melnick, *Nature*, 181, 1483, **1958**.

[76] C. V. Benedict, P. T. Picciano, *ACS Symp Ser*, 385, 465-483, **1989**.

[77] D. P. deVore, G. H. Engebretson, C. F. Schactele, J. J. Sauk, *Comp Biochem Physiol*, 77B, 529-531, **1984**.

[78] J. P. Pujol, J. Bocquet, J. P. Borel, *Acad Sci Hebd Seances*, 283, 555-558, **1976**.

[79] J. Pikkarainen, J. Rantanen, M. Vastamaki, K. Lapiaho, A. Kari, E. Kulonen, *Eur J Biochem*, 4, 555-560, **1968**.

[80] C. H. Brown, *Quat J Microsc Sci*, 91, 331-339, **1950**.

[81] L. J. Gathercole, A. Keller, Light Microscopic Waveforms in Collagenous Tissues and Their Structural Implications, in *Structure of Fibrous Biopolymers* (Eds.: E. D. Atkins, A. Keller), Butterworths, London, pp. 153-167, **1975**.

[82] H. A. Price, *J Zool Lond*, 194, 245-255, **1981**.

[83] J. M. Mascolo, J. H. Waite, *J Exp Zool*, 240, 1-7, **1986**.

[84] J. H. Waite, *Results Probl Cell Differ*, 19, 27-54, **1992**.

[85] J. H. Waite, H. C. Lichtenegger, G. D. Stucky, P. Hansma, *Biochemistry*, 7653-7662, **2004**.

[86] A. Kornberg, *Trends Biochem Sci*, 28, **2003**.

[87] F. Vollrath, D. P. Knight, *Nature*, 410, 541-548, **2001**.

[88] X. Qin, J. H. Waite, *J Exp Biol*, 198, 633-644, **1995**.

[89] C. Sun, J. M. Lucas, J. H. Waite, *Biomacromolecules*, 3, 1240-1248, **2002**.

[90] H. S. Mason, *Adv Enzymol*, 16, 105-184, **1955**.

[91] J. G. Cory, E. Frieden, *Biochemistry*, 6, 116-120, **1967**.

[92] C. Mays, T. L. Rosenberry, *Biochemistry*, 20, 2810-2817, **1981**.

[93] S. N. Bhattacharyya, *Biochem J*, 193, 447-457, **1981**.

[94] J. H. Waite, *Biochemistry of Mollusca*, Academic Press, New York, **1983**.

[95] M. P. Soriaga, A. T. Hubbard, *J Am Chem Soc*, 104, 2735-2742, **1982**.

[96] R. Davies, J. L. Frahn, *J Chem Soc*, 20, 2295-2297, **1977**.

[97] J. Monahan, J. J. Wilker, *Chem Comm*, 1672-1673, **2003**.

[98] C. H. Brown, *Quat J Microsc Sci*, 487-502, **1952**.

[99] J. D. Smyth, *Q J Microsc Sci*, 95, 139-152, **1954**.

[100] L. Vitellaro-Zuccarello, *Tissue & Cell*, 13, 701-713, **1981**.

[101] M. Kitamura, K. Kawakami, N. Nakamura, K. Tsumoto, H. Uchiyama, Y. Ueda, I. Kumagai, T. Nakaya, *J Poly Sci Part A: Poly Chem*, 37, 729-736, **1999**.

[102] S. W. Taylor, C. J. Hawkins, D. J. Winzor, *Inorg Chem*, 32, 422-427, **1993**.

[103] S. W. Taylor, J. Cashion, D., L. J. Brown, C. J. Hawkins, G. R. Hanson, *Inorg Chem*, 34, 1487-1497, **1995**.

[104] S. W. Taylor, G. W. Luther, J. H. Waite, *Inorg Chem*, 33, 5819-5824, **1994**.

[105] S. W. Taylor, D. B. Chase, M. H. Emptage, M. J. Nelson, J. H. Waite, *Inorg Chem*, 35, 7572-7577, **1996**.

[106] S. Sato, H. Nakamura, Y. Ohizumi, J. Kobayashi, Y. Hirata, *FEBS Lett*, 155, 277-280, **1983**.

[107] B. M. Olivera, J. M. McIntosh, *Biochemistry*, 23, 5087-5090, **1984**.

[108] J. W. Catt, G. J. Hills, K. Roberts, *Planta*, 131, 165-171, **1976**.

[109] K. J. Tautvydas, *Planta*, 140, **1978**.

[110] D. Ashford, A. Neuberger, *Trends Biochem Sci*, 5, 245-248, **1980**.

[111] K. Usui, K. Yoshida, C. L. San Clemente, *Can J Microbiol*, 27, 955-958, **1981**.

[112] M. Tanaka, K. Sato, T. Uchida, *J Biol Chem*, 256, 11397-11400, **1981**.

[113] Y. H. Chen, J. T. Yang, K. H. Chau, *Biochemistry*, 13, 3350-3359, **1974**.

[114] J. T. Yang, C. S. Wu, H. M. Martinez, *Methods Enzymol*, 130, 208-269, **1986**.

[115] P. Y. Chou, G. D. Fasman, *Adv Enzymol*, 47, 45-148, **1978**.

[116] R. W. Henkens, *Arch Biochem and Biophy*, 2, 415-422, **1989**.

[117] S. Haemers, M. C. van der Leeden, G. Frens, *Biomaterials*, 26, 1231-1236, **2005**.

[118] S. E. Harding, *Biochem Soc Trans*, 31, 1036-1041, **2003**.

[119] V. Rodrigues, M. Chaudhri, M. Knight, H. Meadows, A. E. Chambers, W. R. Taylor, C. Kelly, A. J. Simpson, *Mol Biochem Parasitol*, 32, 7-13, **1989**.

[120] V. Vreeland, J. H. Waite, *J Phycol*, 34, 1-8, **1998**.

[121] V. V. Papov, T. V. Diamond, K. Biemann, J. H. Waite, *J Biol Chem*, 270, 20183-20192, **1995**.

[122] S. W. Taylor, J. H. Waite, M. M. Ross, J. Shabanowitz, D. F. Hunt, *J Am Chem Soc*, 116, 10803-10804, **1994**.

[123] A. Batey, P. A. Suci, B. J. Tyler, G. G. Geesey, *J Coll Interface Sci*, 177, 307-315, **1996**.

[124] C. L. Borders, J. A. Broadwater, P. A. Bekeny, J. E. Salmon, A. S. Lee, A. M. Eldridge, V. B. Pett, *Protein Sci*, 3, 541-548, **1994**.

[125] M. M. Flocco, S. L. Mowbray, *J Mol Biol*, 235, 709-717, **1994**.

[126] K. M. Meek, J. B. Weiss, *Biochim Biophys Acta*, 587, 112-120, **1979**.

[127] K. Inoue, Y. Takeuchi, D. Miki, S. Odo, S. Harayama, J. H. Waite, *Eur J Biochem*, 239, 172-176, **1996**.

[128] H. Nielsen, J. Engelbrecht, S. Brunak, G. von Heijne, *Protein Eng*, 10, 1-6, **1997**.

[129] J. R. Long, J. L. Dindot, H. Zebroski, S. Kiihne, R. H. Clark, A. A. Campbell, P. S. Stayton, G. P. Drobny, *Proc Natl Acad Sci*, 95, 12083-12087, **1998**.

[130] H. Meisel, C. Olieman, *Anal Chim Acta*, 372, 291-297, **1998**.

[131] M. Yu, T. J. Deming, *Macromolecules*, 31, 4739-4745, **1998**.

[132] M. Yu, J. Hwang, T. J. Deming, *J Am Chem Soc*, 121, 5825-5826, **1999**.

[133] J. H. Waite, M. L. Tanzer, *Biochem Biophys Res Commun*, 96, 1554-1561, **1980**.

[134] O. A. Akemi, R. L. Garrell, *Biopolymers*, 57, 92-102, **2000**.

[135] M. J. Sever, J. J. Wilker, *Tetrahedron*, 57, 6139-6146, **2001**.

[136] B. F. Matzanke, G. Müller-Matzanke, K. N. Raymond, Iron Carriers and Iron proteins (Ed.: T. M. Loher), VCH, New York, **1989**.

[137] L. Que, *Coord Chem Rev*, 50, 73-108, **1983**.

[138] K. K. Anderson, D. D. Cox, L. Que, T. Flatmark, J. Haavik, *J Biol Chem*, 263, 18621-18626, **1988**.

[139] M. J. Nelson, *Biochemistry*, 27, 4273-4278, **1988**.

[140] S. P. Gieseg, J. A. Simpson, T. S. Charlton, M. W. Duncan, R. T. Dean, *Biochemistry*, 32, **1993**.

[141] Y. Kato, T. Nishikawa, S. Kawakishi, *Photochem. Photobiol.*, 61, **1995**.

[142] A. Aberg, M. Ormo, P. Nordlund, B. M. Sjoberg, *Biochemistry*, 32, 9845-9850, **1993**.

[143] J. H. Waite, *Int J Adhes Adhesit*, 7, 9-14, **1987**.

[144] J. H. Waite, *Methods Enzymol*, 258, 1-20, **1995**.

[145] K. Ohkawa, K. Fujii, A. Nishida, T. Yamauchi, H. Ishibashi, H. Yamamoto, *Biomacromolecules*, 2, 773-779, **2001**.

[146] L. I. Smith-Mungo, H. M. Kagan, *Matrix Biol*, 16, 387-398, **1998**.

[147] J. H. Waite, X. X. Qin, K. J. Coyne, *Matrix Biol*, 17, 93-106, **1998**.

[148] U. Nagai, R. Nakamura, K. Kato, S. Y. Ying, Synthesis of an LH-RH Analog with Restricted Conformation by Incorporation of a Bicyclic β- turn Dipeptide Unit, in *Peptide Chemistry* (Ed.: R. Miyazawa), Protein Research Foundation, Osaka, p. 295, **1987**.

[149] U. Nagai, R. Kato, K. Sato, R. Nakrmura, *Tetrahedron*, 3577-3592, **1993**.

[150] N. L. Subasinghe, R. J. Bontems, E. McIntee, R. K. Mishra, R. L. Johnson, *J Med Chem*, 36, 2356-2361, **1993**.

[151] P. J. Belshaw, S. D. Meyer, D. D. Johnson, D. Roma, Y. Ikeda, M. Andrus, D. G. Alberg, L. W. C. Schultz, J. Clardy, S. L. Schreiber, *Synlett*, 381-392, **1994**.

[152] J. E. Baldwin, E. Lee, *Tetrahedron*, 6551-6555, **1986**.

[153] F. A. Etzkorn, T. Guo, M. A. Lipton, S. D. Goldberg, P. A. Bartlett, *J Am Chem Soc*, 10412-10425, **1994**.

[154] A. Nagai, H. Yamamoto, *Bull Chem Soc Jpn*, 62, 2410-2412, **1989**.

[155] D. M. Ferguson, W. A. Glausr, D. J. Raber, *J Comp Chem*, 10, 903-910, **1989**.

[156] D. M. Ferguson, D. J. Raber, *J Am Chem Soc*, 111, 4371-4378, **1989**.

[157] G. D. Rose, L. M. Gierasch, J. Smith, *Adv Protein Chem*, 37, 1-109, **1985**.

[158] U. Nagai, K. Sato, Synthesis and Properties of Some Peptides Containing a Bicyclic Dipeptide Unit with Semi-rigid β-turn Conformation, in *Peptide Structure and Function Proceedings of the 9th Am Peptide Symp, Vol. III* (Eds.: C. M. Dever, V. J. Hruby, K. D. Kopple), Pierce Chem Company, Rockford, p. 465, **1985**.

[159] U. Nagai, K. Sato, N. Ling, T. Matsuzaki, Y. Tomotake, Synthesis and properties of some peptides related to the bicyclic β-turn dipeptide (BTD), in *Peptides, Chemistry and Biology* (Ed.: G. R. Marshall), ESCOM, Leiden, p. 129, **1988**.

[160] A. C. Bach, J. A. Markwalder, W. C. Ripka, *Int J Pept Protein Res*, 38, 314-323, **1991**.

[161] K. Sato, U. Nagai, *J Chem Soc Perkin Trans I*, 1231-1234, **1986**.

[162] P. M. Doyle, J. C. Harris, C. M. Moody, P. J. Sadler, M. Sims, J. M. Thornton, J. Uppenbrink, J. H. Viles, *Int J Pept Protein Res*, 47, 427-436, **1996**.

[163] W. A. Slusarchyk, J. A. Robl, P. C. Taunk, M. M. Asaad, J. E. Bird, J. DiMarco, Y. Pan, *Bioorg Med Chem Lett*, 753-758, **1995**.

[164] S. Hanessian, G. McNaughton-Smith, H.-G. Lombart, W. D. Lubell, *Tetrahedron*, 53, 12789-12854, **1997**.

[165] J. Royer, M. Bonin, L. Micouin, *Chem Rev*, 104, 2311-2352, **2004**.

[166] M. Canle, A. Lawley, E. C. McManus, R. A. More O'Ferrall, *Pure Appl Chem*, 68, 813-818, **1996**.

[167] A. Geyer, D. Bockelmann, K. Weissenbach, H. Fischer, *Tet Lett*, 40, 477-478, **1999**.

[168] A. Geyer, F. Moser, *Eur J Org Chem*, 1113-1120, **2000**.

[169] P. Tremmel, A. Geyer, *J Am Chem Soc*, 124, 8548-8549, **2002**.

[170] V. Avetisov, V. I. Goldanskii, V. V. Kuz'min, *Phys Today*, 44, 33-41, **1991**.

[171] B. M. Wallace, J. S. Lasker, *Science*, 912-913, **1993**.

[172] H. Yamamoto, T. Hayakawa, *Polymer*, 18, 979-982, **1977**.

[173] H. Yamamoto, T. Hayakawa, *Biopolymers*, 21, 1137-1151, **1982**.

[174] H. Yamamoto, T. Hayakawa, *Biopolymers*, 18, 3067-3076, **1979**.

[175] H. Yamamoto, *J Chem Soc Perkin Trans I*, 613-618, **1987**.

[176] H. Yamamoto, T. Hayakawa, *Macromolecules*, 16, 1058-1063, **1983**.

[177] H. Yamamoto, A. Nagai, *Marin Chem*, 37, 131-143, **1992**.

[178] H. Yamamoto, A. Nagai, T. Okada, A. Nishida, *Marin Chem*, 26, 331-338, **1989**.

[179] H. Yamamoto, S. Kuno, A. Nagai, A. Nishida, S. Yamauchi, K. Ikeda, *Int J Biol Macromol*, 12, 305-310, **1990**.

[180] H. R. Kricheldorf, L- Amino Acid -*N*-carboxyanhydrides and Related Heterocycles, Springer Verlag, Berlin, **1987**.

[181] M. J. Grourke, J. H. Gibbs, *Biopolymers*, 5, 795-808, **1971**.

[182] G. Seipke, H. A. Arfmann, K. G. Wagner, *Biopolymers*, 13, 1621-1633, **1974**.

[183] G. Seipke, H. A. Arfmann, K. G. Wagner, *Biopolymers*, 19, 189-201, **1980**.

[184] S. S. Pierre, R. T. Ingwall, M. S. Verlander, M. Goodman, *Biopolymers*, 17, 1837-1848, **1978**.

[185] Y. Trudelle, *Polymer*, 16, 9-15, **1975**.

[186] H. Yamamoto, T. Hayakawa, *Polymer*, 19, 1115-1117, **1978**.

[187] V. J. Hruby, W. Wang, J. Yang, J. Ying, C. Xiong, J. Zhang, C. Cai, *J Org Chem*, 67, 6353-6360, **2002**.

[188] H. Kessler, E. G. V. Roedern, E. Lohof, G. Hessler, M. Hoffmann, *J Am Chem Soc*, 118, 10156-10167, **1996**.

[189] J. Gante, *Angew Chem Int Ed Engl*, 33, 1699-1720, **1994**.

[190] A. E. P. Adang, P. H. H. Hermkens, J. T. M. Linders, H. C. J. Ottenheijm, C. J. van Staveren, *Rec Trav Chim Pays Bas*, 113, 63-78, **1994**.

[191] G. L. Olson, D. R. Bolin, M. P. Bonner, M. Bos, C. M. Cook, D. C. Fry, B. J. Graves, M. Hatada, D. E. Hill, M. Kahn, V. S. Madison, V. K. Rusiecki, R. Sarabu, J. Sepinwall, G. P. Vinent, M. E. Voss, *J Med Chem*, 36, 3039-3049, **1993**.

[192] D. C. Horwell, *Bioorg Med Chem Lett*, 3, 797, **1993**.

[193] A. Giannis, T. Kolter, *Angew Chem Int Ed Engl*, 32, 1244-1267, **1993**.

[194] B. A. Morgan, J. A. Gainor, *Annu Rep Med Chem*, 24, 243-252, **1989**.

[195] J. Rizo, L. M. Giersach, *Annu Rev Biochem*, 61, 387-418, **1992**.

[196] M. Kahn, *Synlett*, 821-826, **1993**.

[197] M. Kahn, *Tetrahedron*, 49, 3433, **1993**.

[198] G. Hölzemann, *Kontakte (Dramstadt)*, 1, 3-12, **1991**.

[199] G. L. Olson, M. E. Voss, D. E. Hill, M. Kahn, V. S. Madison, C. M. Cook, *J Am Chem Soc*, 112, 323-333, **1990**.

[200] J. B. Ball, P. F. Alewood, *J Mol Recogn*, 3, 55-64, **1990**.

[201] H. Yamamoto, S. Kuno, A. Nagai, A. Nishida, S. Yamauchi, K. Ikeda, *Int J Biol Macromol*, 12, 305-310, **1990**.

[202] M. Goodman, G. W. Kenner, *Adv Prot Chem*, 12, 465-468, **1957**.

[203] W. Grassmann, E. Wunsch, *Fortschr Chem Org Naturstoffe*, 13, 444-459, **1956**.

[204] M. Frankel, E. Katchalski, *Nature*, 144, 330-331, **1939**.

[205] M. Frankel, E. Katchalski, *J Am Chem Soc*, 64, 2264-2269, **1942**.

[206] T. Wieland, H. A. Bernhard, 1953, 582, 218, *Ann*, 218, 582-584, **1953**.

[207] M. Frankel, Y. Liwschitz, A. Zilkha, *Experi*, 9, 179-180, **1953**.

[208] M. Frankel, Y. Liwschitz, A. Zilkha, *Bull Res Council Israel*, 9, 37-40, **1954**.

[209] M. Frankel, Y. Liwschitz, A. Zilkha, *J Am Chem Soc*, 76, 2814-2815, **1954**.

[210] S. Pascual, D. M. Haddleton, D. M. Heywood, E. Khoshdel, *Eur Poly J*, 39, 1559-1565, **2003**.

[211] R. Liu, L. E. Orgel, *Evol Biosphere*, 28, **1998**.

[212] J. V. Staros, *Biochemistry*, 21, 3950-3955, **1982**.

[213] G. W. Anderson, J. E. Zimmerman, F. M. Callahan, *J Am Chem Soc*, 86, 1839-1842, **1964**.

[214] D. Sehgal, I. K. Vijay, *Anal Biochem*, 218, 87-91, **1994**.

[215] T. K. Sawyer, Structure Based Design: Diseases, Targets, Techniques and Developments (Ed.: P. Verrapandian), Marcel Dekker, New York, pp. 559-634, **1977**.

[216] R. M. Freidinger, *Trends Pharmacol Sci*, 10, 270-274, **1989**.

[217] R. Hirschmann, *Angew Chem Int Ed Engl*, 30, 1278-1301, **1991**.

[218] R. Hirschmann, K. C. Nicolaou, S. Pietranico, E. Leahy, M., J. Salvino, B. Arison, A. Maria, P. Cichy, G. Spoors, W. C. Shakespeare, P. A. Sprengeler, P. Hamley, A. B. Smith, T. Reisine, K. Raynor, L. Maechler, C. Donaldson, W. Vale, R. M. Freidinger, M. R. Cascieri, C. D. Strader, *J Am Chem Soc*, 115, 12550-12568, **1993**.

[219] P. S. Farmer, *Drug Design, Vol. 10*, Academic Press, New York, **1980**.

[220] N. Avraham, B. Khaykovich, Y. Myasoedov, M. Rappaport, H. Shtrikman, D. E. Feldman, T. Tamegai, P. H. Kesk, M. Lik, M. Konczykowski, K. Beek, E. Zeldov, *Nature*, 411, 451-454, **2001**.

[221] C. S. Tutton, J. W. Crayton, *J Addict Dis*, 12, 109-112, **1993**.

[222] W. T. Astbury, C. E. Dalgliesh, S. E. Darmon, K. T. Sutherland, *Nature*, 162, 596-600, **1948**.

[223] J. Noguchi, *Chem Abstr*, 46, **1952**.

[224] J. Noguchi, *Chem High Poly Jpn*, 6, 196-198, **1949**.

[225] E. Katchalski, M. Sela, *Res Council Israel*, 2, 315-320, **1952**.

[226] E. Katchalski, M. Sela, *J Am Chem Soc*, 75, 5284-5289, **1953**.

[227] B. G. Overell, V. Petrow, *J Chem Soc*, 232-236, **1955**.

[228] R. Longo, P. Castellani, M. Tibolla, *Phytochemistry*, 13, 167-171, **1974**.

[229] E. Tolosa, M. J. Marti, F. Valldeoriola, J. L. Molinuevo, *Neurology*, 50, 2-10, **1998**.

[230] R. A. Laurson, Reflections on the Structure of Mussel Adhesive Proteins, in *Structure, Cellular Synthesis and Assembly of Biopolymers* (Ed.: S. T. Case), Spring Verlag, Berlin, pp. 55-74, **1992**.

[231] A. C. Rice-Ficht, Composition and Design of Fasciola Hepatica Eggshells, in *Structure, Cellular Synthesis and Assembly of Biopolymers* (Ed.: S. T. Case), Springer Verlag, Berlin, pp. 75-95, **1992**.

[232] K. E. Wells, J. S. Cordingly, The Cell and Molecular Biology of Eggshell Formation in Schistosoma Mansoni, in *Structure, Cellular Synthesis and Assembly of Biopolymers* (Ed.: S. T. Case), Springer Verlag, Berlin, pp. 96-114, **1992**.

[233] H. J. Harwood, H. G. Cassidy, *J Am Chem Soc*, 79, 4360-4365, **1957**.

[234] M. Sela, A. Berger, *J Am Chem Soc*, 77, 1893-1898, **1955**.

[235] A. Berger, M. Sela, E. Katchalaski, *Anal Chem*, 25, 1553-1555, **1953**.

[236] K. Champney, H. B. Levy, A. M. Lerner, *Clin Res*, 24, 451-454, **1976**.

[237] H. B. Levy, G. Baer, S. Baron, C. E. Buckler, C. J. Gibbs, M. J. Ladarola, W. T. London, J. Rice, *J Infact Dis*, 132, 434-437, **1975**.

[238] P. Calabresi, R. F. Parks, *Pharmacological Basis of Therapeutics*, 5th ed., MacMillan, New York, **1975**.

[239] H. J. Ryser, W. C. Shen, *Proc Natl Acad Sci*, 75, 3867-3870, **1978**.

[240] H. J. Ryser, W. C. Shen, *Cancer*, 45, 1207-1211, **1980**.

[241] M. Frankel, E. Katchalski, *J Am Chem Soc*, 66, 763-724, **1944**.

[242] E. Katchalski, I. Grossfeld, F. M., *J Am Chem Soc*, 70, 2094-2101, **1948**.

[243] R. R. Becker, M. A. Stahmann, *J Am Chem Soc*, 74, 38-41, **1952**.

[244] E. Katchalski, *Methods in Enzymology, Vol. III*, Academic Press, New York, **1957**.

[245] D. Ben-Ishai, A. Berger, *J Org Chem*, 17, 1564-1570, **1952**.

[246] S. Akabori, H. Tani, J. Noguchi, *Nature*, 167, 159-160, **1951**.

[247] H. Yuki, *J Chem Soc Jpn*, 77, 44-50, **1956**.

[248] H. G. Khorana, *J Chem Soc*, 386, 2076-2081, **1952**.

[249] M. Bodanszky, *Nature*, 175, 685-686, **1955**.

[250] J. A. Farrington, G. W. Kenner, J. M. Turner, *Chemistry and Industry*, London, **1955**.

[251] R. Schwyzer, M. Feurer, B. Iselin, *Helv Chim Acta*, 38, 83-87, **1955**.

[252] R. Schwyzer, M. Feurer, B. Iselin, H. Keegi, *Helv Chim Acta*, 38, 80-85, **1956**.

[253] C. Saez, J. Pardo, E. Gutierrez, M. Brito, L. O. Burzio, *Comp Biochem Physiol*, 98b, 569-572, **1991**.

[254] M. Atreyi, V. R. Rao, S. Kumar, *Biopolymers*, 22, 747-753, **1983**.

[255] J. P. Vollmer, S. G., *Biopolymers*, 5, 337-349, **1967**.

[256] U. K. Laemmli, *Nature*, 227, 680-685, **1970**.

[257] D. C. Schriemer, L. Li, *Anal Chem*, 69, 4169-4176, **1997**.

[258] D. C. Schriemer, L. Li, *Anal Chem*, 69, 4176-4182, **1997**.

[259] H. J. Räder, J. Spickermann, M. Kreyenschmidt, K. Müllen, *Macromol Chem Phys*, 197, 3285-3288, **1996**.

[260] C. S. Johnson, *Prog Nucl Magn Reson Spect*, 34, 203-256, **1999**.

[261] K. F. Morris, C. S. Johnson, *J Am Chem Soc*, 114, 3139-3141, **1992**.

[262] P. Groves, M. O. Rasmussen, M. D. Molero, E. Samain, F. J. Canada, H. J. Driguez, J. imenerz-Barbero, *J Glycobiology*, 14, 451-456, **2004**.

[263] M. J. Stchedroff, A. M. Kenwright, G. A. Morris, M. Nilsson, R. K. Harris, *Phys Chem Chem Phys*, 6, 3221-3227, **2004**.

[264] M. Nilsson, I. F. Duarte, C. Almeida, I. Delgadillo, B. J. Goodfellow, A. M. Gil, G. A. Morris, *J Agric Food Chem*, 52, 3736-3743, **2004**.

[265] A. Chen, D. Wu, C. S. Johnson, *J Phys Chem*, 99, 828-834, **1995**.

[266] K. E. Price, L. H. Lucas, C. K. Larive, *Anal Bioanal Chem*, 378, 1405-1407, **2004**.

[267] T. Zhao, H. W. Beckham, *Macromolecules*, 36, 9859-9865, **2003**.

[268] G. S. Kapur, M. Findeisen, S. Berger, *Fuel*, 79, 1347-1351, **2000**.

[269] H. U. Kim, K. H. Lim, *Bull Korean Chem Soc*, 25, 382-388, **2004**.

[270] S. Viel, L. Mannina, A. Segre, *Tet Lett*, 43, 2515-2519, **2002**.

[271] E. M. de Carvalho, M. H. Velloso, L. W. Tinoco, J. D. Figueroa-Villar, *J Magn Reson*, 164, 197-204, **2003**.

[272] M. D. Diaz, S. Berger, *Carbohydr Res*, 329, 1-5, **2000**.

[273] F. Rittig, J. Kärger, M. C. Papadakis, G. Fleischer, P. Stepanek, K. Almdal, *Phys Chem Chem Phys*, 1, 3923-3931, **1999**.

[274] D. A. Jayawickrama, C. K. Larive, E. F. McCord, D. C. Roe, *Magn Reson Chem*, 36, 755-760, **1998**.

[275] S. Ahn, E. H. Kim, C. Lee, *Bull Korean Chem Soc*, 26, 331-333, **2005**.

[276] G. Binnig, C. H. Gerber, C. F. Quate, *Quat Phys Rev Lett*, 56, 930-933, **1986**.

[277] P. K. Hansma, J. Tersoff, *J Appl Phys*, 61R, 1-24, **1987**.

[278] B. Bhushan, *Scanning Probe Microscopy: Principle of Operation, Instrumentation, and Probes*, Springer Verlag, London, **2004**.

[279] J. H. Hoh, P. K. Hansma, *Trends Cell Biol*, 2, 208-213, **1992**.

[280] M. Rief, M. Gautel, F. Oesterhelt, J. M. Fernandez, H. E. Gaub, *Science*, 276, 1109-1112, **1997**.

[281] K. Mitsui, M. Hara, A. Ikai, *FEBS Lett*, 385, 29-33, **1996**.

[282] M. A. Lantz, S. P. Jarvis, H. Tokumoto, T. Martynski, T. Kusumi, C. Nakamura, M. J., *Chem Phys Lett*, 315, 61-68, **1999**.

[283] M. Kageshima, M. A. Lantz, S. P. Jarvis, H. Tokumoto, S. Takeda, A. Ptak, C. Nakamura, J. Miyake, *Chem Phys Lett*, 343, 77-82, **2001**.

[284] S. Takeda, A. Ptak, C. Nakamura, J. Miyake, M. Kageshima, S. P. Jarvis, H. Tokumoto, *Chem Pharam Bull*, 49, 1512-1516, **2001**.

[285] E. L. Florin, V. T. Moy, H. E. Gaub, *Science*, 266, 257-259, **1994**.

[286] C. Yuan, A. Chen, P. Kolb, V. T. Moy, *Biochemistry*, 39, 10219-10223, **2000**.

[287] P. Hinterdorfer, W. Baumgartener, H. Gruber, J., K. Schilcher, H. Schindler, *Proc Natl Acad Sci*, 93, 3477-3481, **1996**.

[288] S. Allen, X. Chen, J. Davies, M. C. Davies, A. C. Dawkes, J. C. Edwards, C. J. Roberts, J. Sefton, S. J. Tendler, P. M. Williams, *Biochemistry*, 36, 7457-7463, **1997**.

[289] F. Schwesinger, R. Ros, T. Strunz, D. Anselmentti, H. J. Guntherodt, L. Honegger, L. Jermutus, L. Tiefenauer, A. Pluckthun, *Proc Natl Acad Sci*, 9972-9977, **2000**.

[290] L. Schmitt, M. Ludwig, H. E. Gaub, R. Tampe, *Biophys J*, 78, 3275-3285, **2000**.

[291] J. Michael, N. Thrippleton, M. Loening, J. Keeler, *Magn Reson Chem*, 41, 441-447, **2003**.